OBESITY-RELATED FACTORS INVOLVED IN ENDOPLASMIC RETICULUM STRESS INDUCTION IN ADIPOCYTES

MIHAI, ADINA,DANIELA

OBESITY-RELATED FACTORS INVOLVED IN ENDOPLASMIC RETICULUM STRESS INDUCTION IN ADIPOCYTES

Adina Daniela Mihai

This thesis is submitted as a part of the requirements for the award of

Degree of Doctor of Philosophy

School of Biological and Biomedical Sciences

Durham University

November 2015

ABSTRACT

Obesity is the most common nutritional disorder in the developed world and represents a major risk factor for associated diseases like type 2 diabetes mellitus, cardiovascular diseases and hypertension. The condition affects the whole body homeostasis but mainly the adipose tissue and is characterised by low grade inflammation, insulin resistance and hyperlipidemia. In adipocytes, it has been associated with endoplasmic reticulum stress (ER stress) induction and activation of the unfolded protein response (UPR).

ER stress has been shown to play a central role in the molecular events leading to inflammation and insulin resistance in obese adipocytes, but the physiological triggers of ER stress are still unknown. The aim of my thesis was to investigate the role of obesity-related factors such as high concentrations of saturated fatty acids, cholesterol, proinflammatory cytokines or tissue remodelling-induced hypoxia and glucose starvation in ER stress induction

My results indicate for the first time that glucose starvation and hypoxia, two markers of adipose tissue remodelling in obesity, represent physiological triggers of ER stress in *in vitro* differentiated 3T3-F442A and 3T3-L1 adipocytes. High concentrations of saturated fatty acid palmitic acid, cholesterol or proinflammatory cytokines (TNFα, IL-6 and IL-1β), although shown to be potent inducers in other cell lines, do not induce ER stress in my model of *in vitro* differentiated adipocytes.

In conclusion, my results suggest that the adipose tissue remodelling process in obesity could play a central role in ER stress induction in adipocytes.

Table of Contents

LIST OF FIGURES AND TABLES

Table no	Title	Page no
1.1	Prevalence of obesity in adults in developed European countries in 2010-2014	**25**
1.2	Gender distribution of obesity prelevance in adult population in the UK between 1993 and 2013	**26**
1.3	Adipokines produced and secreted by the white adipose tissue	**43**
2.1.	Chemicals.	**76**
2.2	List of reagents used in tissue culture work	**78**
2.3.1.	List of enzymes used in the study.	**79**
2.3.2.	List of antibodies used in the study	**80**
2.4.	List of commercially available kits used in the study	**81**
2.5.	Oligonucleotides sequences.	**82**
2.6.	Buffers and solutions used in the study.	**86**
2.7	Special equipment used in the study	**90**
2.8	Reverse transcription reaction reagents and conditions	**105**
2.9.	The general protocol of the PCR reaction	**106**
2.10.	PCR conditions for of *XBP1* mRNA splicing	**107**
2.11	Reaction mix per sample using 2xqPCR MasterMix or FAST 2xqPCR MasterMix (Primer Design)	**109**

LIST OF ABBREVIATIONS

5'-UTR	5' untranslated region
A.U.	Arbitrary units
A230	Absorbance 230 nm
A260	Absorbance 260 nm
A280	Absorbance 280 nm
ACAT	Acyl-CoA:cholesterol acyltransferase
ACAT1	Acetyl-coenzyme A acetyltransferase 1
AcLDL	Acetylated low density lipoprotein
AGPAT	1-acylglycerol-3-phosphate acyltransferase
Akt/PKB	Protein kinase B
AMP	Adenosine monophosphate
AMPK	AMP-activated protein kinase
AP-1	Activator protein 1
aP2	Adipocyte protein 2
ASK1	Apoptosis signal-regulating kinase 1
ATF4	Activating transcript factor 4
ATF6	Activating transcription factor 6
ATGL	Adipose triglyceride lipase
ATP	Adenosine triphosphate
BAFF	lymphotoxin B and B cell activating factor
BAT	Brown adipose tissue
bFGF	Basic fibroblast growth factor

BiP/GRP78	Binding protein 1
BMI	Body mass index
BSA	Bovine serum albumin
bZIP	Basic-leucine zipper
C/EBP α	CCAAT enhancer binding protein α
Ca^{2+}	Calcium
CaMK2	Calcium/calmodulin-dependent kinase 2
cAMP	Cyclic AMP
CCR 2	C-C motif chemokine receptor 2
CD 36	Cluster of differentiation 36
CD36	Cluster of differentiation 36
CD40	Cluster of differentiation 40
CE	Cholesteryl ester
CHOP	C/EBP homologous protein
ChREBP	Carbohydrate response element binding protein
cIAP	Cellular inhibitor of apoptosis
CoA	Coenzyme A
CREBH	cAMP responsive element-binding protein, hepatocytes specific
CRP	C reactive protein
Ct	Cycle threshold
dATP	Deoxyadenosine triphosphate
dCTP	Deoxycytidine triphosphate
DEPC	Diethyl pyrocarbonate
DGAT	Acyl-CoA: diacylglycerol acyltransferase

dGTP	Deoxyguanine triphosphate
DMEM	Dulbecco's Modified Eagle Medium
DMSO	Dimethyl sulphoxide
dNTP	deoxiribonucleotides
DTT	Dithiothreitol
dTTP	Deoxythymidine triphosphate
EDEM	Endoplasmic reticulum degradation enhancing α-mannoside-like protein
EDTA	Ethylenediamine tetraacetic acid
eIF2α	Eukaryotic initiation factor 2α
ER	Endoplasmic reticulum
ERAD	Endoplasmic reticulum-associated degradation
ERO1	Endoplasmic reticulum oxidation 1
ERSE	ER stress response element
FAs	Fatty acids
FAS	Fatty acid synthase
FAT	Fatty acid translocase
FC	Free (unesterified) cholesterol
FL-1	Fluorescence 1
FSC	Forward scatter
GADD34	Growth arrest and DNA damage-inducible protein
GAPDH	Glyceraldehyde-3-phosphate dehydrogenase
GLUT4	Glucose transport protein 4
GPAT	Glycerol-3-phosphat acyltransferase

GRP/94	Glucose regulated protein 94
HCl	Hydrochloric acid
HepG2	Hepatocytes
HIF-1α	Hypoxia inducible factor 1
HIF-1α	hypoxia inducible factor 1 α
HPA	Hypothalamic-pituitary-adrenal
HRD1	HMG-CoA reductase degradation protein
HRP	Horseradish peroxydase
HSE	Health Survey for England
HSL	Hormone-sensitive lipase
IBMX	3-Isobutyl-l-methylxanthine
IC_{50}	Half maximal inhibitory concentration
IKK	I kappa B kinase
IL-10	Interleukin 10
IL-12	Interleukin 12
IL-1β	Interleukin 1 β
IL-1β	Interleukin 1β
IL-6	Interleukin 6
IL-6	Interleukin 6
IL-R1	Interleukin 1 receptor 1
IL-Ra	Interleukin-1 receptor agonist
iPLA2	Calcium-independent phospholipase A2
IR	Insulin receptor
IRE1α	Inositol requiring 1α

IκB	Inhibitory kinase B
JNK	c-jun N-terminal kinase
LD	Lipid droplet
LRP1	Low density lipoprotein-related receptor 1
MAPKs	mitogen-activated kinases
MC4-R	Melanocortin-4 receptor
MCP-1	Macrophage chemotactic protein 1
MEFs	Mouse embryonic fibroblasts
MGL	Monoacylglycerol lipase
MIF 1	Macrophage migration inhibitory factor 1
mRNA	Messenger RNA
MTT	Thiazolyl blue tetrazolium bromide
MUFA	Monounsaturated fatty acid
MyD88	myeloid differentiation factor 88
NADPH	Nicotinamide adenine dinucleotide phosphate
Nck	Non-catalytic region of a tyrosine kinase adaptor protein
NF-Y	Nuclear factor Y
NFκB	Nuclear factor κB
NKT	Natural killer T
NO	Nitric oxide
Nrf2	Nuclear factor (erythroid-derived 2)like-2
O_2	Oxygen
OxLDL	Oxydated low density lipoprotein
P	Pearson's coeficient

p38 MAPK	P38 mitogen activate protein kinase
PAI 1	Plasminogen activator 1
PAPs	Phosphatidic acid phosphohydrolases
PBS	Phosphate buffer saline
PC1	Prohormone convertase 1
PCR	Polymerase chain reaction
Pcyt2	Phosphate cytidyltransferase 2, ethanolamine
PDI	Protein disulfide isomerase
PDI-P5	Protein disulfide-isomerase P5
PERK	Double-stranded RNA-dependent protein kinase (PKR)-like ER kinase
PHDs	Prolyl hydroxylase enzymes
PKA	Protein kinase A
PKC θ	Protein kinase teta
PL	Phospholipid
PMA	Phorbol 12-myristate 13-acetate
POMC	Pro-opiomelanocortin
PPARγ2	Peroxisome proliferator-activated receptor γ 2
PPi	Pyrophosphate
pre-mRNA	Pre-messenger RNA
PVDF	Polyvinylidene difluoride
RelA	V-rel avian reticuloendotheliosis viral oncogene homolog A
RelB	V-rel avian reticuloendotheliosis viral oncogene homolog B
RIP	Regulated intramembrane proteolysis

RIPA	Radioimmunoprecipitation buffer
ROI	Intermediate reactive oxygen species
ROS	Reactive oxygen species
Rpm	Rotations per minute
RPMI	Roswell Park Memorial Institute medium
RT	Room temperature
RT-qPCR	Real-Time polymerase chain reaction
S1P	Site protease 1
S2P	Site protease 2
SAP	Serum amyloid P component
SCD1	Stearoyl-CoA desaturase 1
SDS	Sodium dodecyl sulphate
Ser-63	Serine 63
Ser-73	Serine 73
SERCA	Sarcoplasmic reticulum calcium transport ATPase
SFA	Saturated fatty acids
SOCS-3	Suppresor of cytokine signalling 3
SR-B1	Scavenger receptor class B1
SREBP1	Sterol regulatory element-binding protein 1
SREBP1-c	Sterol regulatory element-binding protein 1c
SSC	Side scatter
TAE	Tris-acetic acid-EDTA
TAG	Triacylglycerol
TBS	Tris-buffered saline

TE	Tris-EDTA
Tg	Thapsigargin
TGFβ	Transforming growth factor β
TIR	Toll/IL-1 receptor
TLR 2	Toll-like receptor 2
TLR4	Toll-like receptor 4
TMP-153	N-[4-(2-chlorophenyl)-6,7-dimethyl-3-quinolinyl]-N'-(2,4-difluorophenyl)-urea
TNFR	Tumour necrosis factor α receptor
TNFR 1	Tumour necrosis factor α receptor 1
TNFα	Tumor necrosis factor α
TRAF2	TNFR-associated factor 2
TRAF6	TNF-receptor associated factor 6
Tris	Tris (hydroxymethyl) methylamine
UCP1	Uncoupling protein 1
uORF	Upstream open reading frame
UPR	Unfolded protein response
UV	Ultra violet radiation
v/v	Volume/volume
VEGF	Vascular endothelial growth factor
VEGFA	Vascular endothelial factor 1 A
w/v	Weight/volume
WAT	White adipose tissue
WHO	Worlds Health Organisation

XBP1	X box protein 1
$XBP1^{s}$	XBP1 spliced
$XBP1^{u}$	XBP1 unspliced

STATEMENT OF COPYRIGHT

ACKNOWLEDGEMENTS

I would like to express my deepest gratitude to my supervisor Dr. Martin Schroeder, who has been a great mentor for me. I would like to thank you for your continuous support, guidance, encouragement and especially for your tremendous patience. Your advice on both research as well as on my career have been priceless.

I would also like to express my gratitude to my second supervisor Dr. Adam Benham for all the kind support and endless advice during my work in the laboratory.

I would also like to also thank my Thesis Committee members, Professor Keith Lindsey, Dr. Heather Knight and Dr. Ari Sadanandom for the all the scientific support and encouragement during my PhD years.

A heartfelt thank you to my dear friends Sid Narayanan, Andrei Constantinescu and Zoe Papagiannouli for being my "UK family" throughout the last years, for all the help, friendship and encouragement. I could not have done this without you!!

Many thanks to my lab colleagues Max Brown and Jamie Watson for all the help, scientific support, friendship and the never ending good time in the lab during my PhD. I really hope we will have the chance to work together again.

Finally, I would like to give a special thanks to my family. Words cannot express how grateful I am to my mother, father and sister for all the love and support during the last years.

I would like to dedicate this thesis to the loving memory of my grandmother

CHAPTER 1

INTRODUCTION

1.1. Obesity – a growing epidemic

1.1.2. Definition and causes

Obesity is the most common nutritional disease in the developed countries and though *per se* is not considered a life threatening disease, its association with morbidities such as type 2 diabetes, cardiovascular diseases and cancer [1-3] have made it one of the world's leading public health issues in the last decades. Defined as accumulation of excess body fat that leads to health impairment, obesity is a complex multifactorial disease that affects the whole body homeostasis and leads to profound pathological changes in general metabolism [4].

The onset and increased prevalence of the disease is caused by various factors including life style, medication, pre-existent diseases, genetic factors and alterations in the gut microbiome. The most prevalent though, is the sedentary life style characterised by reduced physical activity associated with high caloric intake [5]. Its major effects and role in the growing incidence of obesity are correlated with the increasing technological progress and quality of life in developed countries. The continuously growing urban communities and increase in population have facilitated the introduction and excessive usage of processed, high fat and sugar-containing foods that further affect the metabolic balance of the body. This results in an imbalance between the caloric intake and expenditure that is balanced by progressive storage of energy as lipid deposits in the adipose tissue. Due to the plasticity of the tissue, the imbalance does not rapidly affect the general metabolism but prolonged excess intake associated with minimal expenditure of the energy deposits will finally lead to overexertion of the adipose tissue and subsequent dysfunction. This is reflected also in the statistics showing correlation of increased obesity prevalence and high urbanisation rates and establishment of fast food restaurant chains [5]. This correlation have been described

also in *in vivo* studies on animal models, exposure of C57BL/6J mice [6] and rat models (Wirstar or DIO rat) to food high in fat and sucrose [6] or carbohydrates (eg "cafeteria food") leads to similar increased adiposity, hyperinsulinemia and hyperglycaemia phenotypes as in humans [7]. These effects could be reversed by switching to normal chow-diet suggesting that the phenotype is strictly related to the diet used.

Other factors that can lead to obesity are: emotional distress (stress, depression), age, pregnancy, reduced sleep and usage of medication that can induce adipose tissue development or hormonal imbalance (eg. corticosteroids, epilepsy drugs, antidepressants or schizophrenia medicines). Pre-existent diseases such as hypothyroidism that affects general metabolism [8], Cushing's syndrome characterized by increased secretion of adipogenic hormone cortisol [9] and polycystic ovarian syndrome that induce high secretion of androgens [10] can also contribute to the development of obesity. In the recent years a large number of studies have also suggested that a shift in the gut microbial population in obese individuals could play a causal role in development of obesity [11]. These observations have been confirmed by the results obtained in the investigation of microbial populations in obese *ob*/*ob* mice versus lean animals. A population shift towards microbial species with greater energy extraction capacity was observed in the obese animals possibly contributing to increased fatty acid absorption at cecum level [12]. Furthermore, transfer of gut microbiota or cecum contents from obese animals to lean or germ-free recipients showed an increased weight gain and adiposity in the recipients [13] while diet-induced obese animals with transplanted microbiota from lean animals showed a reversion of the obese phenotype [12]. This suggests that the gut microbiota may indeed represent a key factor in the development of the obese phenotype in mice.

There are no clear evidences so far for the involvement of gut microbiota in obesity in humans but considering the important role of gut bacteria in fatty acids absorption,

regulation of intestinal permeability, gut-hormone production and inflammatory lipopolysaccharide (LPS) production, future studies may provide a better insight on the role of this possible inducing factor of obesity.

Another important factor involved in the onset of the disease is the genetic predisposition, though the number of cases determined by it is reduced compared to the other factors. In humans, one of the most common genetic factors inducing obesity is the Prader-Willi syndrome, an autozomal dominant disorder resulting from deletions in paternal chromosomal segment 15q11-q13 or the deletion of the entire paternal chromosome 15 leading to expression of only the maternal chromosomes [14]. The syndrome has multiple physiological, neurological and metabolic effects and causes morbid obesity in affected children [15]. Few other monogenic causes of obesity have been described, all mutated genes encoding for central proteins that are part of the adipose tissue - hypothalamic leptin axis that controls food intake and satiety [16]. These monogenic diseases include mutations in the genes encoding for leptin [17], the leptin receptor [16] [18], prohormone convertase 1 (PC1) [19], pro-opiomelanocortin (POMC) [20], melanocortin-4 receptor (MC4-R) [21] and peroxizome proliferator-activated receptor γ 2 (PPARγ2) [16]. Except for MC4-R that presents dominant inheritance but no apparent insulin or hormonal imbalance, mutations in these genes cause rare and recessive forms of morbid obesity, associated with multiple endocrine abnormalities [19, 22, 23]. The identification of the genetic alterations involved in obesity onset allowed the development of new animal models of obesity that can be used for molecular and pharmacological research and lead to development of new strategies to minimize the pathological burden. These models, depending on the number of mutated genes have been categorised as: monogenetic or polygenic models of obesity and present phenotypic characteristics similar to the ones induced by genetic factors in humans. The monogenic models include: models of defective genes for molecules involved in leptin

signalling (POMC $^{-/-}$, MC4-R $^{-/-}$ mice) [24], lethal yellow mutant (KK-A^{y}) mouse that presents an adipose tissue-specific agouti gene overexpression and an overgrowth of adipose tissue without alteration of food intake [25], defective leptin receptor rats (Zucker rat) [24] and the leptin deficient *ob*/*ob* [26] and *db*/*db* [7] mice that both present impaired leptin signalling, hyperphagia, reduced energy expenditure, increased adiposity on normal chow diet compared to control animals, hyperglycaemia (severe in *db*/*db* model) and increased insulin levels [24]. Although single mutations are very rare in humans, the monogenic models are providing a deep insight into the role of different molecules and molecular mechanisms involved in the pathological progress of the disease.

Polygenic models include animal models obtained by selective breeding in order to present obesity phenotypes at different onset of the disease allowing investigation of the pathological process in different stages of animal development. This category is best represented by the obesity-prone (DIO) and diet-resistant (DR) rats that initially become obese only after feed on high-fat diet and that after selective breeding can become obese without the necessity of the high fat diet [27]. Other models are the New Zeeland obese (NZO) mouse that presents several genetic susceptibility loci including the leptin receptor and the age-related obesity mice (LOO) [24].

1.1.3. Prevalence

During the last decades, a steep increase in the number of overweight and obese individuals was observed. An extensive study spanning 33 years (1980-2013) investigating the prevalence of overweight and obese (defined as body mass index, BMI > 25 kg/m^2) individuals in the global population showed a worldwide increase of ~ 16 % in the adult population representing 8.1 % increase in men and 8.2 % increase in women and ~ 13 %

increase in children and young population with an 6.2 % increase in boys and 6.9 % increase in girls [28]. Whereas in the US the high prevalence of obesity (34.9 % or 78.6 million individuals in 2013 [29]) has been in the public attention for a long time and numerous efforts have been made to limit its expansion, in Europe the disease has become an increasing problem only in the last two decades [4]. The prevalence of obesity has followed similar trends with the increase in the US though the percentage of the population affected is significantly lower, with an average prevalence of obesity in total population in European countries of 21.3 % in 2014 [4] (Table 1).

Table 1.1. Prevalence of obesity in adults in developed European countries in 2010-2014. Prevalence is presented as percentage of total adult population, according to gender distribution.

Country	**Prevalence (%) men (aged 18 +)**			**Prevalence (%) women (aged 18 +)**			**Prevalence (%) in both genders**	
Year	**2010**	**2014**	**%increase**	**2010**	**2014**	**%increase**	**2010**	**2014**
Germany	19.9	21.9	2	17.2	18.5	1.3	18.5	20.1
France	21.8	23.8	2	22.3	24	1.7	22	23.9
Spain	21.1	22.8	1.7	23.1	24.7	1.6	22.1	23.7
UK	24.1	26.9	2.8	26.8	29.2	2.4	25.5	28.1

According to the World Health Organisation (WHO) report for 2014 UK has the highest obesity prevalence in a European country, the number of obese individuals (both genders) amounting for 28.1 % of the total population [4]. The gender distribution indicated also the highest number of obese individuals for each gender than in any other European country investigated, with an increase in prevalence between 2012 and 2014 of 2.8 % in men and 2.4 % in women (Table 1). The high prevalence presented in the WHO reports corresponds to the previous national reported data by the Health and Social Care Info Centre report for the

year 2013 [30] showing that 24.7 % of the population in the UK can be classified as obese and are in accordance (0.7 % *vs* 1.28 % in men and 0.6 % *vs* 0.7 % in women) with the relatively stable annual increase trend data described in the Health Survey for England (HSE) report for 2013 [31] (Table 2)

Table 1.2. Gender distribution of obesity prelevance in adult population in the UK between 1993 and 2013. Data presented according to Health Survey for England report for 2013.

Prelevance (%)	Year		Average % increase/year
	1993	2013	
Men (aged 18 +)	13.2	26	1.28
Women (aged 18+)	16.4	23.8	0.74

Globally, the most recent WHO reported data indicate that in 2014 more than 1.9 billion people aged over 18 years (39 % of world population) were overweight out of which more than 600 million were obese (13 % of world population). The extent of the disease in the world population, the continuous increase in prevalence and the medical and economic implications have made obesity one of the major health issues of the century. Although various local and global strategies have been developed in order to decrease or slow the extent of the problem, most of them are fighting the existing health complications of the disease but not its causes. Life style and diet changes have become urgent for disease control as the health and economic burden of obesity and associated complications are continuously increasing.

1.1.4. Health and economic implications

Though obesity is not a life-threatening disease, through its associated morbidities, it can affect the quality of life and can be disabling or even affect life expectancy. In 2010 obesity was shown to be responsible for more than 3.4 million deaths [28] and a 4 % decrease of in life expectancy worldwide [17, 32].

Various studies have shown that obesity represents a major risk factor for various diseases, with the most important being type 2 diabetes [33-36], cardiovascular diseases [2, 35] and various types of cancer [1, 37]. According to WHO reports, 44 % of type 2 diabetes cases, 23 % of ischemic heart condition and 7 – 41 % of different type of cancers could be attributed to overweight and obesity [4]. Renehan *et al* [37] showed that for every additional 5 kg/m² in BMI there is an increase of 52% in the risk for development of oesophageal cancer and 24 % for development of colon cancer suggesting a central role for obesity in the pathological onset of these diseases. But the health burden of obesity is not only represented by the association with pathologies as cancer and diabetes. Numerous studies have revealed that obesity is also an important risk factor for depression, with an 55 % higher risk of development in obese subjects [38], Alzheimer's disease [39] and obstructive sleep apnoea [40]. It was also associated with diseases like disabiliting osteoarthritis [41] and fertility reduction [42]. Therefore, obesity is associated with virtually every aspect of health, from the contribution to chronic conditions such as diabetes, cardiovascular diseases and cancer, to interfering with cognitive functions, breathing, mood stability and reproduction. Taking into consideration the continuing increase in the prevalence of the disease, its effects will affect more than half of the world population by 2050 [4] and will become the largest health burden globally.

In order to minimize the health burden associated with obesity, numerous approaches have been developed in recent years. Some of the strategies implemented worldwide for reducing the effects of obesity are increased obesity research, development of new drugs that block lipid absorption eg. Orlistat) and gastric surgeries (bariatric surgeries). But all these strategies along with health care expenses of the already existent morbidities have become a huge economic burden globally [4].

In the US, the area with the highest prevalence of obesity in the world, it was estimated that the annual cost of obesity for 2008 was $ 147 billion, with the cost for general health care being increased with $ 1.429 per obese individual compared to normal weight due to associated morbidities [29].

In Europe, a McKinsey Global Institute report indicates that the health-care system uses for obesity up to 2-7 % of the total health-care budget in the developing countries to which up to 20 % of the cost of treatment for associated diseases is added [43]. In the UK, the European country with the highest prevalence of obesity, it was estimated that in 2007 the heath care cost for overweight and obese related morbidities amounted to £ 15.8 billion, with obesity alone representing £4.2 billion, approximately 6 % the NHS costs [44]. Considering the prediction in the increase in prevalence of obesity in the next years, the economic burden in UK alone will amount to £ 5.2 billion for health-care for obesity alone by 2025 and £ 7.1 billion by 2050 [44].

Globally, the cost of obesity pandemic represents ~ $ 2.0 trillion (2.8 % of global GDP) [43] indicating the extension of the health and economic burden of the disease.

1.2. Cellular and molecular implications of adipose tissue in obesity

Obesity is a disease defined as abnormal accumulation of fat that can affect the body homeostasis and can contribute to metabolic dysfunction. It is characterised by dysregulation in glucose and lipid metabolism as a result of excessive accumulation of fat due to sustained imbalance between the energy intake and energy expenditure. As the main organ involved in the fat storage, the adipose tissue dysfunction in obesity is one of the key pathological events leading to lipotoxicity, inflammation and insulin resistance. Due to its role, the study of the anatomy and physiology of the adipose tissue in normal and pathological states has become central in the study of obesity.

1.2.1. Composition and function of adipose tissue

In mammals, the adipose tissue is represented by a connective tissue organised in numerous depots distributed throughout the body and that together form the adipose organ [45]. The depots size and localisation are strictly related to the function served and can present distinct tissue composition [46]. According to the cell composition, anatomical and physiological functions, two different types of adipose tissue have been described: the brown adipose tissue and the white adipose tissue. The brown adipose tissue is specialised in thermoregulation and is widely extended in small mammals and human newborns [47] but relatively low represented in adults [48, 49]. The white adipose tissue is specialised in lipid storage and metabolism and forms the majority of the fat depots in adult life contributing to both physical protection (subcutaneous) and metabolic homeostasis of the near organs

(visceral) [46]. While both type of tissues present similar cell type composition, the cell type ratio, adipocyte cell phenotype and metabolic functions are very different.

1.2.1.1. The brown adipose tissue (BAT)

BAT is a tissue especially abundant in newborns and hibernating mammals [50] and is mainly involved in both basal and inducible energy expenditure in the form of non-shivering thermogenesis [47]. It is a highly vascularised tissue formed mainly of brown adipocytes, preadipocytes and vascular cells. The brown adipocyte presents two unique characteristics: an increased number of intracellular lipid droplets and numerous mitochondria which uniquely express uncoupling protein 1 (UCP1) essential for its thermogenesis function [45, 51]. This mitochondrial inner membrane protein uncouples the rates of substrate oxidation and adenosine triphosphate (ATP) production by favouring a loss of protons in the intermembrane space and accumulation of protons in the matrix resulting in release of energy in the form of heat. The process is highly regulated by the sympathetic nervous system via secretion of norepinephrine and is dependent of the fatty acid deposits in the brown adipose cell that are used as substrate [47].

BAT distribution and abundance is highly related to its function in thermogenesis. In small mammals and hibernating animals, the BAT tissue is maintained throughout the adult life as a result of increased needs for thermoregulation in cold environments [52]. In humans, it is found primarily in foetuses and newborns [47] and decreases shortly after birth, remaining present only in small depots throughout adult life [49]. Its role in young organisms is essential due to reduced capacity of the newly formed body to protect itself against cold [53]. Increased differentiation of white adipose tissue (WAT) with age ensures the “insulating”

necessities of the body, and the role of BAT becomes almost non-existent in adults and related only to thermoregulation in case of long-term exposure to cold or hyperadrenergic stimulation in pheochromocytoma [54]. However, the reduced role of BAT in adult humans have become questionable when an increased number of studies [55-57] have identified that BAT deposits are maintained in adult in a higher number than previously believed suggesting that the role of BAT may not limited to thermoregulation. Studies on animal models have brought evidence on BAT involvement in the body energy expenditure and metabolic efficiency. In 1979, Rothwell *et al* [58] study using rats fed with different types of "cafeteria food" showed that BAT could play an important role in improving the body general metabolic efficiency suggesting that diet-induced thermogenesis could represent a mechanism of defence against caloric overload, or survival in case of exposure to low nutritional diets. Lowell et al [59] brought more evidence that BAT is involved regulation of metabolic efficiency by showing that transgenic toxigene UCP-1-ablated mice that exhibit reduced BAT develop obesity in the absence of hyperphagia suggesting increased metabolic efficiency in BAT deficient mice. Their observations were further consolidated by observations that in the mouse model where the UCP1 expression was restored, the obese phenotype was lost. The role of BAT and UCP1 in obesity was further consolidated by the study of Feldman *et al* [60] that showed development of obesity in UCP1-ablated mice irrespective of the diet used compared to wild-type mice. Later observations investigating the role of BAT in metabolic efficiency and obesity in human adults showed, decreased BAT activity in obese individuals compared to lean [61, 62] and an inverse correlation between BAT and BMI values [54] and increased energy expenditure in cold-induced BAT activity [57]. These observations have brought new perspectives in the fight against obesity and different approaches have been studied since. Increasing BAT mass or activity via low temperature, genetic or pharmacological compounds represent some of these approaches that

are continuously studied in present. Though progress has been made using low temperature exposure [63], chemical uncouplers that mimic the actions of UCP1 [64], epinephrine or adrenergic agonists [54, 65], none of these approaches yet has been successful. The discovery of beige adipocytes [52] that present mixed brown and white adipocyte phenotype represent also possible new strategies. The cells localised in the adult human WAT are considered induced non-classical induced brown cells (from a precursor that is not common for brown cells) or transdifferentiated white-to-brown cells [52, 66]. New research focused on fatty acid uptake and metabolism and glucose utilisation by BAT are considered possible strategies in tackling obesity but further understanding of the mechanisms involved is needed in order to develop optimal strategies.

1.2.1.2. The white adipose tissue (WAT)

WAT is the most common type of adipose tissue representing, in the healthy adult, 20-25 % of body weight. It is composed primarily of large unilocular adipocytes that represent more than 50% of the tissue cells and also preadipocytes, fibroblasts, stem cells, endothelial cells, vascular muscle cells, macrophages and other infiltrating immune cells. The tissue is supported by a dense network of capillaries and numerous sympathetic nerve fibres that accompany the arteries and arterioles [67] (Figure 1.1)

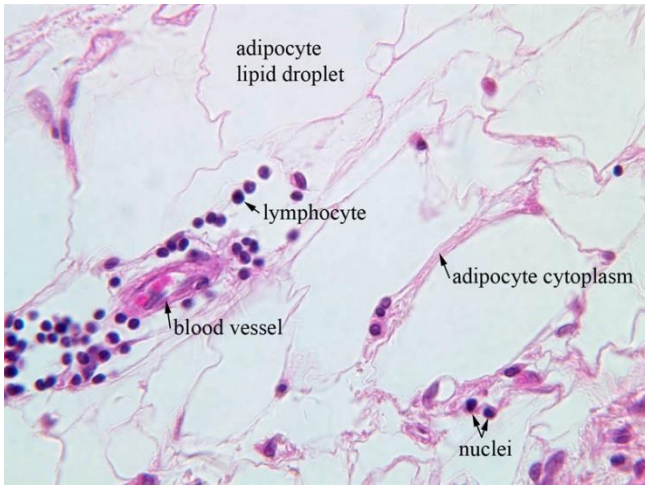

Figure 1.1. White human adipose tissue composition, haematoxylin and eosin staining, 40X (with permission from A. Pistorio, www.medicalhistology.us/wiki/Main/AdipocyteImages)

The size of white adipocytes varies in relation to the lipid content of the cell, ranging from 30-130 μm in diameter in normal conditions [46] and being considerably bigger than brown adipocytes (25-40 μm) [68]. Compared to the brown adipocyte, the white adipocyte presents a single lipid droplet that can fill almost all the cell volume while the number of mitochondria is reduced and the nucleus is pushed towards the periphery of the cell [69]. The plasma membrane presents numerous receptors for lipids (low density lipoprotein-related receptor 1, LRP1, fatty acid translocase FAT/CD36, scavenger receptor class B1, SR-B1), hormones, cytokines and other signalling molecules involved in cellular homeostasis, lipid metabolism, glucose and insulin uptake [70].

There are various WAT depots distributed throughout the human body that according to their local function can present different protein expression profiles and responsiveness to endocrine stimuli. Three types of WAT depots have been described: the subcutaneous, the visceral and the dermal adipose tissue. The first two types have been extensively studied in the last decades and their origin, cellular composition and functions are largely known. The

dermal adipose tissue was initially considered subcutaneous WAT and has only recently been revealed to be a distinct type of adipose tissue generated from a common precursor with the mesodermal fibroblasts but different from one of subcutaneous adipocytes [71]. The dermal adipocytes were shown to form early in development, during embryonic day 14 of development for mice [71] and second trimester of gestation for humans [72] and their function was linked to epidermal homeostasis during hair follicle regeneration and wound healing [71].

The subcutaneous tissue forms an insulating and protection layer under the skin while the visceral tissue surrounds the inner organs contributing to local energy homeostasis. The differences between the two types of WAT vary from cellular composition and gene expression to metabolic responsiveness and hormonal regulation. The subcutaneous WAT, corresponding to its protection function, presents a higher preadipocytes to adipocytes differentiation rate [73], increased vascularisation and angiogenic capacity [74]. The adipocyte cells size is smaller than the visceral one [75] while the secretion of adipocyte specific factors adiponectin [76] and leptin [77] have also been shown to be increased compared to the visceral counterpart. The visceral adipocyte cells, due to their role in maintaining the lipid homeostasis of neighbouring organs present a higher insulin sensitivity [78], lipolytic activity [75], fatty acids up-take [79] and lipid metabolism rate. Secretion of proinflammatory cytokines is also increased in the visceral adipocytes in response to cellular dysfunction and due to the tissue proximity to the major organs, represents one of the most important cause of the general inflammation and lipotoxicity in obesity [80].

1.2.1.2.1 WAT functions

There are three main functions of the tissue which influence whole body homeostasis: lipid storage and metabolism and the regulatory endocrine function [46].

A. Lipid storage and metabolism

Fatty acids (FAs) are essential molecules for cell structure, function and signalling. They act as building blocks in the synthesis of membrane phospholipids [81], energy source via β-oxidation [82] and signalling messengers [83, 84]. Due to their important functions, it is essential that the blood concentration of FAs is maintained within the physiological range in order to assure the cellular homeostasis. Decreased FAs levels could be, as previously described, associated with impaired cellular homeostasis and signalling whereas excess concentrations can lead to lipid overload, cellular toxicity and general dysfunction [85, 86]. Although FAs can be synthesised in mammalian cells with the involvement of fatty acids synthase [87], a major source is represented by the dietary lipids (esterified long-chain FAs or triacylglycerols) [81] that are hydrolysed by the pancreatic lipase in the lumen of the small intestine and absorbed in the blood stream as free fatty acids [88]. Via blood circulation they are distributed to the cells in need and the excess is taken up by the adipocytes and stored for times of demand. As the central energy storage organ of the body, the main function of the adipose tissue is to maintain the circulatory FAs concentration optimal in both postprandial and fasting states [89] In order to accomplish this function, the adipocytes have developed cell-specific mechanisms that allow them to uptake high amounts of FAs and glucose in time of energy excess and store them as triacylglycerol (TAG) in the lipid droplet. In fasting periods or increased energy requirements (exercise, thermoregulation) the

adipocytes release the stored FAs via hydrolysis of TAG (lipolysis) and restore the circulating concentrations needed [81]. These two metabolic processes of adipocytes are highly regulated and the balance between the two is responsible for the general homeostasis of lipids. Cellular dysfunction can cause imbalance between the two processes leading to release of a high amount of FAs in the blood stream and, via systemic circulation, contributes to general lipotoxicity [90].

Triacylglycerol biosynthesis

The synthesis of triacylglycerol (TAG) was described more than 40 years ago by Weiss *et al* [91] and it is a complex metabolic process that involves multiple steps catalysed by specific enzymes. Regulation of the TAG biosynthesis involves numerous hormonal and nutritional factors including insulin, carbohydrates and fatty acids, along with transcription factors as sterol regulatory element-binding protein 1c (SREBP-1c), carbohydrate response element binding protein (ChREBP) and PPARγ [92].

The process takes place mostly at the endoplasmic reticulum though it has been suggested that mitochondrial enzymes could be also involved [93]. In short, after the FA cellular uptake, TAG biosynthesis involves five steps (Figure 1.2):

1. Formation of FA-CoA by esterification of FA with coenzyme A (CoA) in the cytoplasm. The process involves hydrolysis of adenosine triphosphate (ATP) to adenosine monophosphate (AMP) and pyrophosphate (PP_i) and it is catalysed by the enzyme acetyl-CoA synthetase.

$$FA + ATP \rightarrow FA\text{-}AMP + PPi$$

$$FA\text{-}AMP + \text{Coenzyme A} \rightarrow FA\text{-}CoA + AMP$$

2. Acylation of glycerol-3-phosphate with fatty acyl-CoA and formation of 1-acyl-glycerol-3-phosphate (lysophosphatidic acid). The reaction takes place at the ER or mitochondria and is catalysed by glycerol-3-phosphate acyltransferases 3 and 4 (GPAT 3 and 4) [92].
3. Further acylation of lysophosphatidic acid resulting in formation of 1,2-diacylglycerol-3-phosphate (phosphatidic acid). The reaction is catalysed by 1-acylglycerol-3-phosphate acyltransferase (AGPAT) and takes place at the ER. At this step, the phosphatidic acid can be shunted into the synthesis of various phospholipids or into the synthesis of TAG, the two separate branches of glycerolipid synthesis.
4. Dephosphorylation of phosphatidic acid to the intermediate 1,2-diacylglycerol by the phosphatidic acid phosphohydrolases (PAPs) [94].
5. Acylation of 1,2-diacylglycerol to triacylglycerol (TAG) is catalysed by acyl-CoA: diacylglycerol acyltransferases 1 and 2 (DGAT 1 and 2) [95].

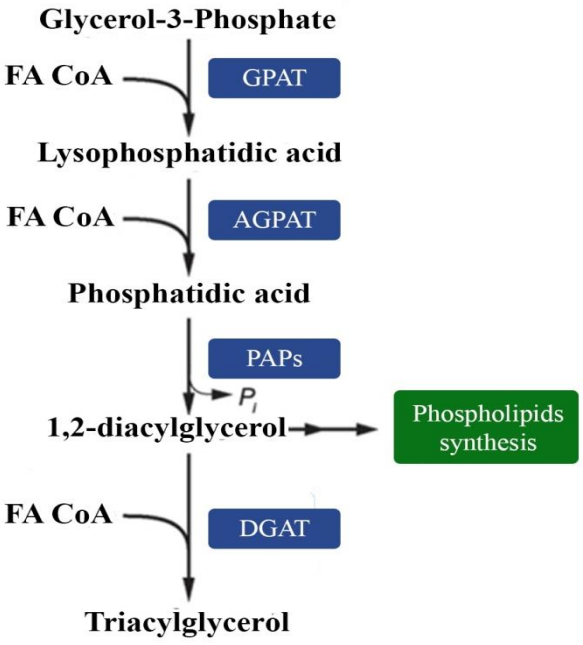

Figure 1.2. Biosynthesis of triacylglycerol in adipocytes (modified after Yen *et al* [96])

According to the nature of the dietary FAs uptaken from the circulation and substrate affinities of the enzymes involved in TAG biosynthesis, the process is more often including an additional step of desaturation of the FAs in the acyl-CoA thiolesters. It was observed that GPAT enzymes 3 and 4 exhibits marked specificity for saturated acyl-CoA thiolesters, AGPAT for mono- and dienoic fatty acyl-CoA thioesters [97] and DGAT 1 and 2 for unsaturated substrates [98], suggesting that the mono- and polyunsaturated fatty acids are preferred substrates in TAG biosynthesis. As the major part of the dietary FAs in processed food are represented by saturated long chain fatty acids, e.g. palmitic and stearic acid, the FAs desaturation have become a very important step in the TAG synthesis. The reaction is catalysed by stearoyl-CoA desaturase 1 (SCD1), an endoplasmic reticulum-resident Δ^9 desaturase and involves insertion of a *cis* double bond in the Δ-9 position of the FA. The enzyme can use different chain length fatty acids from C12:0 to C19:0 but has higher affinity for substrates such as palmitoyl-CoA (C16:0) and stearoyl-CoA (C18:0) that are converted to palmitoleoyl-CoA (C16:1) and oleoyl-CoA (C18:1), respectively [99]. These products are the most abundant monounsaturated FAs (MUFAs) and serve as substrates for the synthesis of various kinds of lipids, including phospholipids, TAG, cholesteryl esters and wax esters [100].

The important role of the desaturation step in TAG biosynthesis is indicated by up-regulation of *SCD1* mRNA during adipocyte differentiation [101] and up-regulation of mRNA levels and protein activity in animals subjected to high saturated fat diets [102]. As desaturation represents a rate-limiting step in TAG biosynthesis and it is strictly regulated by the dietary FAs, expression and the activity of SCD1 have been investigated in the context of FA overloading of obese adipocytes. The onset of obesity have been shown to correlate with increased SCD1 expression and activity [103, 104]. Via desaturation of dietary saturated

fatty acids SCD1 increases the intracellular levels of MUFAs. Taking into consideration that MUFAs can be used as substrate for TAG synthesis, this process allows storage of the increased circulating FAs in the lipid droplet and protects the adipocytes against accumulation of toxic intracellular fatty acids in obesity [105, 106]. Also, by increasing the intracellular MUFAs, the enzyme indirectly contributes to increased biosynthesis of phospholipids that maintain the membrane structure integrity and fluidity during adipocyte hypertrophy as a result of lipid overload in obesity [107]. All these evidences indicate a protective role for SCD1 against adipocyte FAs overload-induced cellular stress. Other studies though, indicated that SCD1 deficiency protects against obesity. Ntambi *et al* [108] have shown that *scd1*$^{-/-}$ mice present generally reduced body adiposity in both chow and high fat diet and increased insulin sensitivity compared to the wild-type counterpart. The increased insulin sensitivity observed may be related to reduced adiposity and reduced levels of leptin in the plasma. Also, in *scd1*$^{-/-}$ mice hepatic expression of genes encoding for enzymes involved in lipid oxidation is up-regulated whereas lipid synthesis genes *SREBP-1*, *FAS* and *GPAT* are down-regulated, suggesting that lipid oxidation is activated by *scd1* deficiency and to the oxidative pathway will be favoured to TAG synthesis and storage [108, 109]. Similar evidences have shown that *scd1* deficiency reduces ceramide synthesis in skeletal muscle of *ob/ob* mice [110]. In cultured 3T3-L1 adipocytes, Kim *et al* [111] also show that chemical inhibition of SCD1 decreases expression of lipogenic genes without altering the genes for enzymes involved in lipid oxidation suggesting a potential beneficial effect against cellular lipid accumulation in response to high lipid intake. But, according to the SCD1 described role in desaturation [100, 112], deficiency of *scd1* in adipocytes should lead to accumulation of intracellular cytotoxic fatty acids and decreased TAG synthesis [104] and thus reduced postprandial circulating FA clearance resulting in possible systemic lipotoxicity. Considering its various effects SCD1 remain under investigation as a possible

candidate in tackling obesity but further research is needed to better understand the tissular and systemic effects of SCD1 modulation.

TAG lipolysis

During periods of energy demand, TAG stored in the adipocytes lipid droplets can be rapidly mobilised by the hydrolytic action of lipases and released as free FAs into the circulation in order to adjust the energy requirements of the organism [113]. By the hydrolysis, in the lipolytic process, one molecule of glycerol and three molecules of FAs are produced from one molecule of TAG. The resulting FAs can be either released into the circulation to be taken up by other tissues or used for re-esterification in adipocytes to produce TAG [114].

For many years, hormone-sensitive lipase (HSL) has been considered to be the regulatory enzyme of the lipolytic process and the only one involved in the three successive hydrolysis reactions (Figure 1.3). HSL activity is regulated by hormones such as catecholamine and insulin that are under nutritional regulation [115, 116]. Catecholamine hormones induce HSL via activation of protein kinase A (PKA) due to increase intracellular concentrations of cyclic AMP (cAMP). PKA activation of HSL can be either directly via serine phosphorylation of the protein [117], or indirect via phosphorylation of the lipid droplet-associated protein perilipin A [118]. In contrast, insulin inhibits HSL phosphorylation by inducing hydrolysis of cAMP [119, 120]

Recent work though has revealed existence of a novel adipocyte triglyceride lipase. HSL-deficient mice fed a high-fat diet have been found to exhibit normal body weight and decreased fat mass, but their white adipose tissue still retained ~ 40 % of TAG lipase activity compared with wild type mice [121]. Detailed analysis identified a novel TAG lipase as lipid-droplet associated adipose triglyceride lipase (ATGL or desnutrin) [115] in mice and calcium-independent phospholipase A_2 ($iPLA_2$) ζ in humans [122]. *In vitro* experiments

indicated that desnutrin expression is up-regulated during adipocyte differentiation [123] while in mice ablation of ATGL increased adipose tissue mass and caused lipid deposition in other tissues [124]. ATGL activity is regulated by glucocorticoids and insulin, being induced by glucocorticoids during fasting [123] and down-regulated by re-feeding and insulin [125].

Therefore, in the current proposed model of the lipolytic cascade, lipolysis is catalysed by at least three enzymes: ATGL, HSL and monoacylglycerol lipase, which is abundant and not regulated. The hydrolysis steps in lipolysis and regulation are (Figure 1.3.):

1. TAG hydrolysis to 1,2-diacylglycerol and FA catalysed by adipose triglyceride lipase (ATGL) and hormone sensitive lipase (HSL).
2. Hydrolysis of 1,2-diacylglycerol to 2-monoacylglycerol and FA catalysed by HSL.
3. Hydrolysis of 2-monoacylglycerol to glycerol and FA catalysed by HSL and monoacylglycerol lipase.

In obesity, decreased lipolysis leading to TAG and cholesteryl esters accumulation induces cellular lipotoxicity and dysfunction and has been associated with decreased HSL expression and catecholamine-induced lipolysis in adipocytes [116].

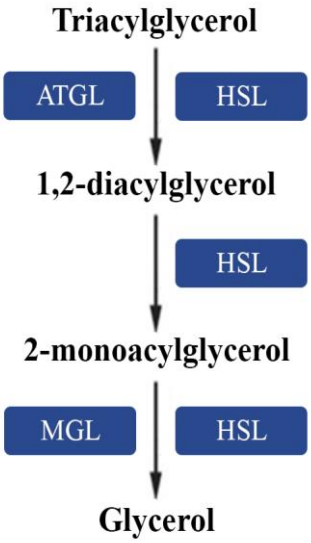

Figure 1.3. Lipolysis in adipocytes

B. Adipose tissue - an endocrine organ

For many decades it was believed that the adipose tissue represents only a passive energy storage organ. It was only in the last 30 years that adipose tissue was identified as a major site for secretion of a large variety of bioactive factors such as leptin [126] , adiponectin [127], adipsin [128] and pro- and anti-inflammatory cytokines [129]. These adipocyte factors that can act both locally (autocrine/paracrine) and systemic (endocrine) coordinating regulate multiple processes including energy metabolism, neuro-endocrine and immune functions.

The importance of the endocrine function of adipose tissue became evident with the pathologies associated with its dysfunction. Obesity characterised by hypertrophy and hyperplasia of adipose tissue is associated with profound both local and systemic effects including dyslipidemia, insulin resistance, inflammation, hyperglycaemia and hypertension

[129]. Adipose tissue deficiency has also been associated with dyslipidemia, insulin resistance and other features of metabolic syndrome in both humans and animals [130].

The complexity of the endocrine function is reflected by the various adipokines secreted and their multiple roles in general homeostasis (Table 1.3).

Biological effect	**Protein**
Metabolic regulators	Adiponectin
	Leptin
	Resistin
	Visfatin
Pressure regulators	Angiotensinogen
Coagulation regulators	Plasminogen activator 1 (PAI 1)
Mediators of inflammation	Tumor necrosis factor α (TNF α)
	Interleukin 6 (IL-6)
	Interleukin 1 β (IL-1β)
	Macrophage migration inhibitory factor 1 (MIF 1)
Growth factors	Transforming growth factor β (TGF β)
Angiogenesis factors	Vascular endothelial growth factor (VEGF)
Proteins of the alternative complement pathway	Adipsin

Table 1.3. Adipokines produced and secreted by the white adipose tissue

Taking into consideration the increased variety of factors secreted by adipocytes, I have focused on the two major hormones, leptin and adiponectin whose function and imbalance is highly related to the pathological process in obesity.

Leptin

Leptin was identified by Zhang *et al* [26] in 1994 as the product of the obese gene (*ob*) in *ob/ob* mice. It is a 16 kDa polypeptide containing 167 amino acids [125] secreted by adipocytes in response to the nutritional status and that presents with differences in secretion between the two type of WAT (increased secretion in subcutaneous compared to visceral depots) [131]. Leptin expression and protein secretion is regulated by a variety of factors including insulin [132], glucocorticoids, TNFα and estrogens [129] that positively correlates with both mRNA induction and protein levels, while β3-adrenergic stimulation [133], and FA [134], decrease its expression.

The main function of leptin is regulation of general energy homeostasis as a rate limiting factor between the energy intake and expenditure. Leptin action on the neurons localised in the hypothalamic arcuate nucleus regulates hunger and satiety in accordance to the energy stores [135]. Studies on *ob/ob* mice have brought evidence of the role of leptin in food intake regulation. The leptin-deficient animals were shown to exhibit hyperphagia, obesity and insulin resistance and administration of leptin reversed their conditions [126]. The administration of leptin to lipoatrophic mice (which lack subcutaneous adipose tissue and thus have low levels of leptin) was also shown to improve metabolic abnormalities, including insulin resistance and hyperlipidemia [136]. Thus, leptin levels are correlated with both nutritional intake and the adipose tissue mass, the hormone levels being maintained decreased in case of caloric restriction [137] and increase in case of increased food intake or

high caloric diet [138]. In obesity though, the increased adipose tissue mass is associated with increased leptin levels indicating that the leptin-hypothalamic signalling axis is affected by the condition [126]. This suggests a possible leptin resistance state in obesity and though the mechanisms are still largely unknown, it is believed that it may result from defects in leptin signalling or transport across the blood-brain barrier [139].

In addition to this important energy regulator function, leptin modulates neuroendocrine functions involved in reproduction and regulates other processes such as angiogenesis, immune response, blood pressure control and osteogenesis [129]. In *ob/ob* mice leptin deficiency is associated with activation of the hypothalamic-pituitary-adrenal (HPA) axis and suppression of the hypothalamic-pituitary-thyroid and -gonadal axes that leads to hypogonadism and reduced to absent fertility [140]. Leptin is also involved in immune system regulation by increases cytokine production, macrophage adhesion and phagocytosis, and proliferation of T cells [135, 141]. Leptin also promotes angiogenesis, and accelerates wound healing [142].

Adiponectin

The protein adiponectin was first described in 1995 [129] and represents the most abundant adipose tissue-secreted hormone into the blood stream [135]. It is an adipocyte-specific protein highly induced during differentiation process [143] and that similar to leptin is expressed more in subcutaneous WAT then the visceral depot [131]. Structurally, the 30 KDa protein containing a collagen-like domain and a C-terminal globular domain is exposed to posttranslational modification (hydroxylation and glycosylation) resulting in formation of multiple isoforms that assemble through collagen-like domain interactions into trimers

and further stable multimeric oligomers [144]. All these forms along with proteolytic cleavage products containing the globular domain can be found in the circulation [145]

Roles for adiponectin have been identified mostly from evidence related to obesity and metabolic disorders. Plasma levels of adiponectin have been shown to decline at the onset of obesity and are maintained low throughout the development of insulin resistance [146] while improvement of insulin sensitivity restore the secretion [147] suggesting involvement of the protein in insulin sensitivity and possible effects of adipose tissue expansion on its expression. Studies using adiponectin-deficient mice show that absence of the hormone is correlated with premature diet-induced glucose intolerance, insulin resistance and increased serum non-esterified FAs supporting the previous hypothesised role of adiponectin [148]. Along with the role in insulin sensitivity and glucose homeostasis adiponectin is also an important anti-atherosclerotic factor by stimulating angiogenesis and endothelial vasodilatation while inhibiting proinflammatory cytokine secretion and monocytes adhesion on the endothelial layer [135].

1.2.2. Adipose tissue pathology in obesity

The pathological onset of obesity, when non-genetic, is caused by a chronic imbalance between the energy intake in form of nutrients and energy expenditure. As the major energy storage organ, the adipose tissue is the primarily affected tissue by the pathological effects of this imbalance. Increasing energy intake leads to adipocytes increase in size (hypertrophy) and number (hyperplasia) and is associated with structural and metabolic alterations [149]. Due to the rapid progression of cellular alterations, the cells begin to display markers of cellular dysfunction, especially mitochondrial and endoplasmic reticulum stress [150].

Altered glucose transport and metabolism, insulin resistance and inflammation become evident in the lipid-burdened dysfunctional adipocyte and contribute, via the endocrine function of the cell, to tissue inflammation, remodelling and lipotoxicity.

Though the molecular mechanisms leading to adipose tissue dysfunction in obesity and their role in the pathological progress are still not fully understood, the adipose tissue remodelling, inflammation, cellular stress adipocyte insulin resistance and glucose metabolism impairment have been described to be the main factors affecting the progress and extent of the disease [149, 151-153].

Adipose tissue remodelling

Adipose tissue remodelling is a continuous and often discrete process that reflects the tissue capacity to rapidly and dynamically respond to variations in nutrient intake. It is influenced by the high plasticity of the adipocytes and turnover of the different adipose tissue cells, and plays a very important role in the normal development of the body and metabolic homeostasis [149, 154]. Adipose tissue remodelling, though an adaptative ongoing process throughout the life, it is pathologically accelerated in obesity and associated with adipocyte dysfunction, increased macrophage infiltration and reduced angiogenic remodelling [149].

In obesity, adipocyte hypertrophy, hyperplasia and subsequent dysfunction represent the starting point of the pathological process affecting the homeostasis of this tissue. Overloaded adipocytes exhibit mitochondrial and endoplasmic reticulum (ER) stress [150] that activate proinflammatory pathways and lead to secretion of inflammatory cytokines (TNFα, IL-6, IL-1β) [70, 155] and chemotactic proteins (MIF). Accumulation of reactive oxygen species (ROS) as a result of increased metabolic processes contributes to the inflammatory status of the cell and secretion of proinflammatory adipokines. This proinflammatory adipokine

secretion initiates macrophage recruitment and infiltration in the adipose tissue and the inflammatory status of the tissue [156, 157].

Macrophage infiltration

In obesity, an increase in macrophage population of the adipose tissue has been described, leading from 10 % in lean mice and humans to 50 % in obese, leptin-deficient mice and 40 % in obese humans [152]. This increase in macrophage recruitment was shown to be multifactorial and positively correlated with the adipose tissue mass and insulin resistance [152]. It is a process highly induced and regulated by adipose tissue remodelling via multiple effects that are closely connected with adipocyte dysfunction: adipokine-induced chemotaxis, apoptosis, low vascular supply and dysregulation of fatty acid fluxes [158]. Though most of the adipose tissue cells secrete proinflammatory cytokines, macrophage infiltration is the major factor involved in the inflammatory status of the obese adipose tissue, being considered the second major event in obesity progression and the major determinant of the adipose tissue low grade inflammation specific to the obesity pathology [154, 159].

Adipocyte dysfunction is associated with activation of proinflammatory signalling pathways and secretion of proinflammatory cytokines (TNFα, IL-6, IL-1β) and chemokines (MIF and MCP-1) [153, 160]. Kanda *et al* [160] have shown that MCP-1 expression and secretion in adipocytes plays an important role in the inflammatory process. Using genetically modified mouse models that present either loss or gain of MCP-1 expression, they have shown that adipose tissue induced expression of MCP-1 transgene was sufficient to induce macrophage infiltration and insulin resistance in mice. Furthermore, they have shown that following disruption of the *MCP-* gene these effects were reverted suggesting that MCP-1 is directly involved in macrophage recruitment and inflammation in the adipose tissue. Adipocyte apoptosis or necrosis resulting from lipid overload was also associated with macrophage

recruitment into the adipose tissue. Cinti *et al* [161] have shown that in advanced obesity macrophages surround the necrotic adipocytes in crown-like structures, fuse to phagocytose the residual lipid droplet and form a large lipid-laden multinucleated syncytia specific for tissular chronic inflammation. These observations are supported also by evidence of increased macrophage recruitment in the adipose tissue in transgenic models of lipoatrophy [162] or adipocyte inducible apoptosis [163].

Another important aspect of macrophage infiltration is the phenotypic switch of macrophages from a "alternative activated" phenotype (M 2) that secretes anti-inflammatory cytokines such as IL-10, to a "classically activated" phenotype (M 1) which secretes proinflammatory cytokines such as IL-1, IL-6, TNF α and MCP-1 [164]. Though both types of macrophages are normally resident in the tissue, the M 1/M 2 ratio is very small in normal conditions, with the M 2 population being predominant. This is due to the different functions of the two types of macrophages: the M 2 macrophages are involved in general adipose tissue remodelling and secrete anti-inflammatory and angiogenic factors [165] while M 1 have a predominantly inflammatory function, secreting high levels of proinflammatory cytokine, ROS and NO [164]. In high fat diet and obesity, the M 1/M 2 ratio has been shown to switch towards the M 1 population [154]. Due to the proinflammatory phenotype of M 1 this switch in polarisation is correlated with systemic inflammation and insulin resistance [164, 166]. These observations are sustained by evidence showing that deletion of M 1 marker genes such as TNF α [167] or C-C motif chemokine receptor 2 (CCR 2) [168] resulted in normalisation of insulin sensitivity. Exercise training in mice with high fat-induced obesity [169] and gastric surgery in humans [170] have been also shown to promote the M 1 to M 2 shift, consolidating the evidence showing the role of adipose tissue expansion and insulin resistance in obesity and the macrophage polarisation.

Increased fatty acids released from dysfunctional adipocytes also contribute to macrophage infiltration. Accumulation of intracellular FAs can act as ligands for the tool-like receptor 4 (TLR4) in the plasma membrane of macrophages and activate the classical inflammatory response leading to proinflammatory cytokine secretion and signalling for macrophage recruitment [171-173].

Vascular remodelling in obesity

Most of the organs in the healthy human body stop growing in adult life and thus the vascular network remains quiescent after the body reaches maturity [174]. The adipose tissue, due to its plasticity and dynamics under different nutritional conditions, retains the capacity of blood vessel formation (angiogenesis) throughout the entire life [149]. The angiogenic capacity is essential for the tissue in assuring the necessary nutrient and O_2 supply, hormonal regulation, molecular signalling and general homeostasis. Thus, it can be affirmed that angiogenesis represents a rate-limiting factor of adipose tissue expansion [175]. Though during tissue remodelling in development, adipogenesis and angiogenesis are temporally and spatially coupled [176], in obesity ,during the tissue rapid expansion the angiogenic process seems to be slower than the rate of adipose remodelling [177]. Blood flow studies in obese *vs* lean rats showed that the blood supply remained similar in both lean and obese animals independent of the size of the adipose tissue[177]. This suggests that the blood flow per adipocyte declines with obesity leading to possible nutrient and O_2 deficits. Both preadipocytes and adipocytes are known to secrete pro-angiogenic factors such as basic fibroblast growth factor (bFGF) and vascular endothelial growth factors (VEGF) [149]. These factors are induced by various stimuli, with leptin and adiponectin levels being some of the most important in adipose tissue remodelling [178]. In obesity, angiogenesis induction is multifactorial. Claffey *et al* [179] showed that *VEGFA* mRNA and protein are expressed

in a differentiation-dependent manner in 3T3-F442A adipocytes suggesting that increased differentiation of preadipocytes in obesity could indirectly lead to angiogenesis induction. Furthermore, the rapid overexpansion of the adipose tissue can lead to low blood supply in distal adipocyte clusters, exposing the cells to hypoxia and nutrient starvation[180, 181]. HIF-1α is an oxygen-sensing transcription factor induced by hypoxia and the key regulator of oxygen homeostasis in the cell [182]. In normoxic conditions HIF-1α is hydroxylated by prolylhydrolase enzymes in the presence of oxygen and subjected to degradation. In hypoxia, due to inactivation of the hydrolase enzymes, An increase in HIF-1α protein expression in adipocytes is increased and was shown to induce *VEGFA* mRNA contributing to the angiogenic signalling [183]. In addition, VEGFA expression has been shown to be induced by various proinflammatory cytokines such as TNF α, IL-1β, and IL-6 [184] secreted by both dysfunctional adipocytes and infiltrating macrophages.

Adipose tissue inflammation in obesity

Accumulating evidence show that chronic inflammation plays a crucial role in the pathogenesis of obesity-related insulin resistance [157, 185] and metabolic dysfunction [151] and it is one of the first responses of the adipose tissue to adipocyte lipid overloading. The first evidence of inflammation in obese adipose tissue was brought by Hotamisligil *et al* [186] who showed increased expression and production of TNF α in adipose tissue of obese mice compared with lean controls. Since then increasing number of studies confirmed the up-regulation of genes encoding inflammatory factors and increased secretion of cytokines and chemokines in the enlarged adipocyte [70, 155]. It is considered that adipocyte lipid overloading represents the first step in the inflammatory drift in obesity [70, 187]. Increased metabolic burden of the cell leads to cellular stress and subsequent activation of proinflammatory pathways that induce synthesis and secretion of proinflammatory cytokines

(TNF α, IL-6, IL-1β) and chemokines (MCP-1 and MIF). Accumulation of proinflammatory cytokines and chemokines in the intracellular space and the capillary blood flow leads to recruitment of macrophages in the affected tissue. The process is augmented also by increased adipocyte apoptosis in the tissue as result of progressive cellular stress and dysfunction [161]. Macrophage infiltration and polarisation from the adaptative M 2 type to the proinflammatory M 1 type is increasing the local inflammatory status via increased secretion of proinflammatory molecules such as TNF α, IL-1β, IL-6, IL-12, and MCP-1. This increased inflammatory state recruits not only macrophages but also other immune cells as mast cells and natural killer T (NKT) cells [188] that contribute to the progress of inflammation via further secretion of proinflammatory factors.

Molecular aspects of the inflammation in adipocytes

At the molecular level, inflammation in adipocytes is mediated via two major pro-inflammatory signalling pathways: nuclear factor κB (NFκB) and c-jun N-terminal kinase (JNK). Though in obesity both signalling pathways are activated by similar triggers, the downstream effects can vary. If NFκB activation leads mostly to proinflammatory cytokine secretion and can be involved in apoptosis induction, JNK activation is also a central player in insulin resistance induction in overloaded adipocytes.

The NFκB pathway is one of the most important intracellular signalling pathways involved in the regulation of inflammation In mammals, NFkB represents a group of structurally related and evolutionarily conserved proteins with five members in mammals: Rel (c-Rel), RelA (p65), Rel B, NFkB1 and NFkB2 involved in key cellular responses that modulates the outcome of cells exposed to stress stimulation [189]. In normal physiological state, NF-κB (p65/p50 heterodimer) is maintained inactive in the cytoplasm by inhibitory subunit IκB. In the presence of inflammatory stimuli IκB is phosphorylated by the IκB kinase (IKK)

complex and subsequently degradated allowing NFκB to translocate to the nucleus and induce transcription of numerous inflammatory genes such cytokines, immunoreceptors and adhesion molecules [190]. In mammalian cells, according to the activation pattern, there are two described NFκB pathways: the canonical (classical) pathway and the non-canonical (alternative) pathway [191]. Both pathways involve the IKK dependent phosphorylation of IκBα and translocation of the NFκB dimmers to the nucleus, the difference between the two pathways consisting of the catalytic IKK kinase that activates the pathway. The canonical pathway is the most commonly activated NFκB pathway and is depending on the activity of IKKβ and NEMO kinases of the IKK complex leading mainly to phosphorylation of IκBα and nuclear translocation of mostly p65-containing heterodimers [190]. This pathway is activated by ligands binding to cytokines receptors, antigen receptors and pattern-recognition receptors and Toll-like receptor 4 (TLR 4) [190]. The non-canonical pathway is responsible for activation of p100/RelB complexes by the IKKα subunits of the IKK complex, partial processing and generation of p52-RelB complexes [190]. The non-canonical pathway activation is involved in development of lymphoid organs and induced by specific members of the TNF cytokine family, such as CD40 ligand, lymphotoxin B and B cell activating factor (BAFF) and lymphotoxin-β [189].

JNK kinases family represents a group of mitogen-activated kinases (MAPKs) activated by a variety of exogenous stimuli such growth factors deprivation, FAs or TNFα treatments and UV irradiation and plays an important role in regulation of the inflammatory status of the cell. Initially identified as kinases that phosphorylate c-Jun at Ser-63 and Ser-73 [192], the group was shown to be able to bind as homo- and heterodimeric complexes to the transcription factor activating protein 1 (AP-1) [190] [193].

The JNK protein kinases are encoded by three genes: *Jnk1*, *Jnk2* and *Jnk 3*, with *Jnk1* and *Jnk2* ubiquitously expressed and *Jnk3* with an expression pattern limited to brain, heart and testis [194]. The transcripts derived from all three genes are subjected to two series of alternative splicing. The first alternative splicing can remove the C-terminal domain leading to formation of different size isoforms with unknown functional significance leads to isoforms. The second one is restricted to the *Jnk1* and *Jnk2* genes and involves the selection of one of two alternative exons that encodes part of the kinase domain and influences the substrate specificity of the JNK isoforms to bind to substrates [194]. Via activation of the AP-1 complex, JNK signalling is involved in regulation of important cellular processes including inflammation, proliferation and apoptosis [195].

Both canonical NFκB and JNK pathway activation have been described in the adipose tissue of obese animals in response to various obesity-related triggers such as increased levels of FAs, cytokines and nutrient and energy starvation. The pathways can also be induced by cellular stress components such as ROS and are mainly involved in the initiation and expansion of inflammation [151, 196, 197].

FAs have been described to be one of the most important factors contributing to adipocyte dysfunction in obesity. High concentrations of FAs have been shown to activate the proinflammatory pathways in two ways: a direct one involving TLR4 downstream signalling and an indirect one via induction of cellular stress and subsequent activation of the inflammatory NFκB and JNK.

The direct pathway including activation of TLR 4 was recently described after numerous observations indicating expression of the receptor on the adipocyte membrane [198] and activation of the receptor by FA binding, though normally the receptor is an innate immune system receptor activated by LPS binding [171, 173, 199]. The signalling cascade activated by FA binding to TLR 4 includes recruitment of the adaptor protein myeloid differentiation

factor 88 (MyD88) to the Toll/IL-1 receptor (TIR) domain of the receptor and activation of downstream signalling cascade leading to proinflammatory pathways activation [200] (Figure 4).

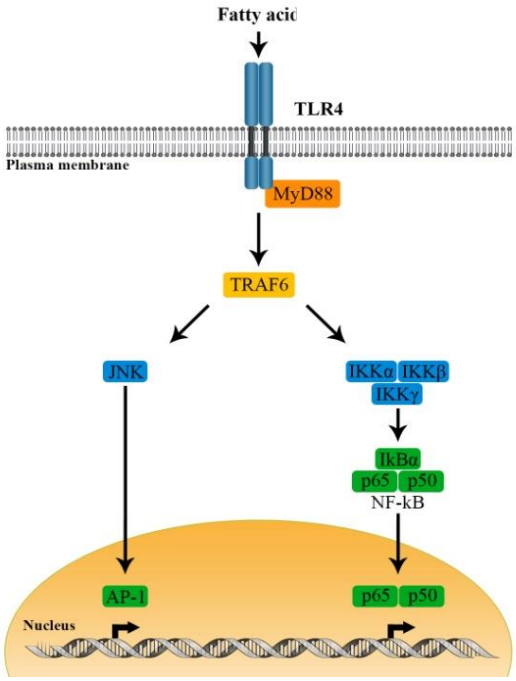

Figure 1.4. Fatty acids-induced direct activation of JNK and NFκB pathways in adipocytes

(modified after Akira *et al* [201])

Numerous studies have shown alsoa possible involvement of TLR 2 in direct induction of inflammatory pathways by FAs but the role of TLR 2 is still not clear. Similar to TLR 4, TLR2 has been identified on the membrane of adipocytes [199] and is known to be activated primarily by cytokines but also by FAs and other lipid molecules [202]. TLR 2 expression was shown to be increased in WAT and muscle of diet-induced obese mice inhibition of TLR 2 was associated with decreased inflammation and improved insulin signalling [203]. Also, it was reported that activated TLR 2 interacts with the CD 36 transporter of FAs [204] and TLR2 knockdown has been associated with reduced adiposity [205] supporting its possible role in FA's activation of proinflammatory pathways. There is no direct evidence though for its involvement in the FA-induced inflammation in adipocytes it's activation of

proinflammatory pathways being more related to the binding of inflammatory cytokines, especially TNF α [199].

Indirect activation of the proinflammatory pathways by FAs is mediated by lipid accumulation, metabolic burden and cellular stress induction (mitochondrial and endoplasmic reticulum stress) [206-208]. Accumulation of DAG and ceramide in obese adipocytes was shown to induce NFκB and JNK pathways via PKC θ activation [209]. Increased concentrations of FA have been shown to induce oxidative stress via NADPH oxidase activation [208] and accumulation of oxygen species (ROS) leads to activation of proinflammatory signalling pathways.. Increased catabolism in the mitochondria of hypertrophic adipocytes leads also to oxidative stress and production of free radicals [210] while metabolic induced ER stress represents also a source of ROS induction via PDI activity[211]. Thus, ER stress induction contributes to inflammatory state via the PERK-eIF2α- Iκβ pathway [212] or IRE1- TRAF2 -IKK [213] for NFκB and IRE1α- TRAF2- JNK pathway [214] described in detail in the subchapter dedicated to ER (section 1.2.2.1)

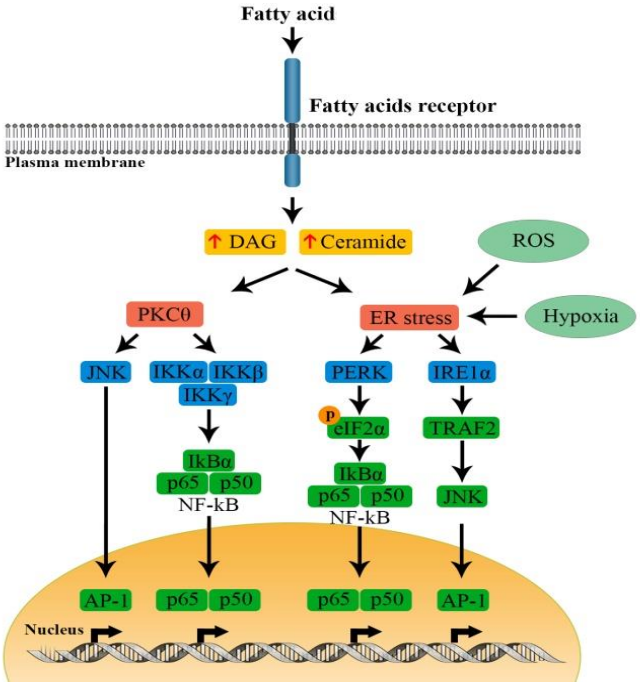

Figure 1.5. Indirect FAs-induced activation of JNK and NFκB pathways in obese adipocytes

(modified after Gao *et al* [209])

Another important factor involved in activation of the proinflammatory pathways is the accumulation of inflammatory cytokines in the adipose tissue and their autocrine and paracrine actions. Macrophage infiltration and activation in the adipose tissue leads to increased proinflammatory cytokine secretion including TNF α, IL-6 and IL-1β. Similar cytokines are secreted also by the dysfunctional adipocytes as a response to both metabolic inflammation and the macrophage cytokine action. The inflammatory response becomes a vicious cycle: the cells secrete proinflammatory cytokines as a result of the inflammatory signalling and the secreted molecules trigger an inflammatory response in both a paracrine and autocrine way. Thus, the initial inflammation becomes a self-sustaining and expanding process involving both the adipocytes as the macrophages and other immune cells in the tissue. The inflammatory response in adipocytes induced by the increased levels of cytokines is mediated mostly via the TNF α receptor 1 (TNFR 1), TLR 2 and TLR 4. TNFR activation and downstream induction of NFκB and JNK pathways is mediated via TNF receptor-associated factor 2 (TRAF 2)/cIAP protein complex, the cIAP proteins being mediators of the anti-apoptotic TNF α signalling [215] (Figure 6).

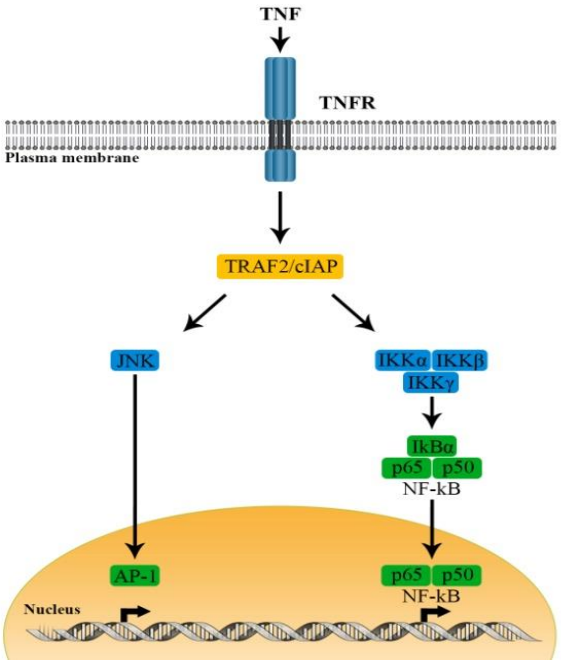

Figure 1.6. TNFα inductions of JNK and NFκB via TNF receptor (modified after Faustman *et al* [216])

The interleukin 1 receptor 1 (IL-1R1) involvement in inflammation in adipocytes is still under debate as numerous studies have revealed increased expression and secretion of interleukin-1 receptor agonist (IL-1Ra) in the adipose tissue of obese individuals [217]. The IL-1Ra is a member of IL-1 family that binds to IL-1 receptor without inducing a cellular response and thus having antagonizing effect with IL-1α and IL-1β [218]

Hypoxia was shown also to contribute to the activation of the two inflammatory signalling pathways. Culver *et al* [219] have demonstrated that hypoxia activates NFκB via calcium/calmodulin-dependent kinase 2 (CaMK2)- TAK1- IKK pathway while Koong and collaborators [220] shown that activation can also be mediated by phosphorylation at a tyrosine residue on IκBα but through an IKK-independent mechanism. Activation of ER stress in hypoxic conditions is another mechanism of hypoxia for inflammatory pathways induction as previously described in this subchapter.

1.2.2.1. Endoplasmic reticulum stress in obesity

The endoplasmic reticulum (ER) is a cytoplasmic membranous network of branching tubules and flattened sacs that is present in all eukaryotic cells. It is the principal site of lipid and protein biosynthesis and together with the Golgi apparatus it facilitates the transport and release of correctly folded proteins to their proper target sites [221]. It also represents the cellular Ca^{2+} storage organ and key organelle involved in detoxification of xenobiotics. Nascent polypeptides translated by the ribosomes are directed to the ER luminal space for proper folding. Within the ER lumen chaperone proteins as binding protein 1 (BiP or GRP78), calnexin and calreticulin assist the proper folding of nascent proteins and prevent the aggregation of unfolded or misfolded proteins [150]. The correctly folded proteins are then transported to the Golgi apparatus for final modification and then to their cellular destination. Unfolded or misfolded proteins are retained in the ER and then retrotranslocated to the cytosol by the machinery of ER-associated degradation (ERAD) and degraded by the proteasome [222].

In physiological states when the cellular demand for protein synthesis exceeds the capacity of the folding apparatus of the ER and the ERAD machinery, unfolded or misfolded proteins accumulate in the ER lumen leading to a condition referred to as ER stress. To prevent such accumulation of unfolded proteins and to ensure a high fidelity in protein folding, eukaryotic cells have evolved a self-defence mechanism - the unfolded protein response (UPR) [221-223].

The UPR consists of five adaptative mechanisms that work together to ensure the return of the ER to its normal physiological state: (1) attenuation of protein synthesis which prevents

any further accumulation of unfolded proteins; (2) up-regulation of ER chaperone gene expression to increase the folding capacity and (3) increased phospholipid synthesis to expand the ER; (4) transcriptional induction of genes encoding the ERAD component to increase the rate of unfolded protein degradation and (5) induction of apoptosis to safely dispose of cells injured by ER stress and to ensure the survival of the organism [222].

In mammalian cells the UPR signalling cascades are initiated by three ER transmembrane protein sensors: PERK (double-stranded RNA-dependent protein kinase (PKR)-like ER kinase), IRE1 (inositol requiring 1) and ATF6 (activating transcription factor 6) (Figure 1.7).

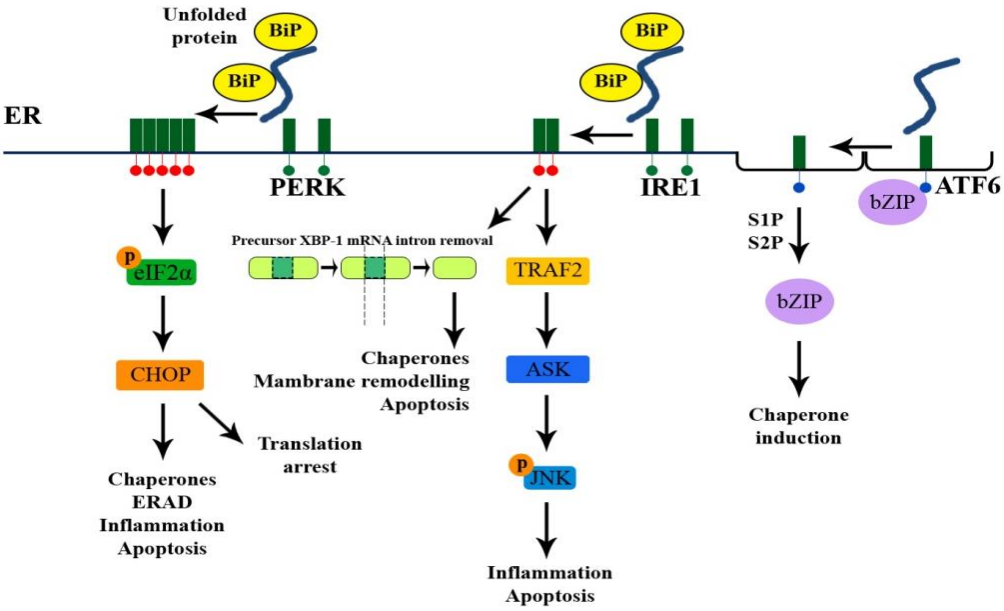

Figure 1.7. The UPR response pathways (modified after Schroeder *et al* [224])

PERK

PERK is an ER type I transmembrane protein serine/threonine protein kinase that has a luminal domain which acts as a sensor for unfolded proteins, a transmembrane domain enclosed in the ER membrane and a cytosolic domain that transmits signals to downstream effectors [224]. In an inactive state the luminal domain of the protein is associated with the ER chaperone BiP [225](reference). BiP release due to the accumulation of unfolded proteins leads to activation through oligomerisation and autophosphorylation [225]. Once activated, PERK phosphorylates substrate proteins such as eIF2α (eukaryotic initiation factor 2 α) and the transcription factor Nrf2 [nuclear factor (erythroid-derived 2)like-2] [150, 222, 226]. eIF2α is the α subunit of the heterotrimeric eukaryotic translation initiation factor eIF2. Phosphorylation of eIF2α at serine 51 leads to general attenuation of translation which represents the first step in preventing further protein loading of the ER [227] and induces clearance of short-lived proteins. Interestingly, the phosphorylation of eIF2α up-regulates the ATF4 transcription factor through preferential mRNA translation [222, 228]. This escape from translational attenuation is due to a mechanism referred to as reinitiation after a short upstream open reading frame (uORF) and is based on the existence of one or more short uORFs in the 5'-UTR region of the mRNA. In normal conditions when eIF2α is active (unphosphorylated) the ribosome first binds to a 5'-cap structure, slides on the *ATF4* mRNA in 5' to 3' direction and starts translation at the first small ORFs. After reaching the stop codon the ribosome detaches from the RNA before the ATF4 ORF can be translated. This process is repeated at each following uORF. By contrast, in ER stress when eIF2α is inactivated (phosphorylated), the translation rarely starts at the small uORFs. The ribosome scans further through the mRNA and through the last uORF resulting in initiation of translation at the ATF4 ORF (Figure 1.8) [222, 228-230].

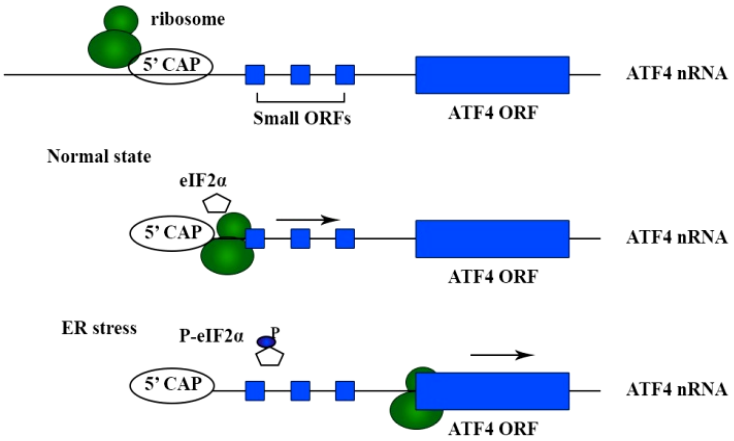

Figure 1.8. Escape mechanism of ATF4 mRNA from translational repression mediated by eIF2α phosphorylation (modified after Yoshida *et al* [222]**)**

Translation of *ATF4* is an important step in deciding cell fate as a result of endoplasmic reticulum stress. This is reflected by the main target genes of ATF4. Once translated, ATF4 translocates to the nucleus and induces expression of genes such as ERO1 (ER oxidation 1) involved in disulphide bond formation in the protein folding process, CHOP (C/EBP homologous protein) involved in apoptosis, and GADD34 (growth arrest and DNA damage-inducible protein) that limits the inhibitory effect of PERK activation on eIF2α [224] ATF4 is also required for expression of genes involved in amino acid transport, glutathione biosynthesis and resistance to oxidative stress [226].

Beside eIF2α, PERK also phosphorylates Nrf2, a transcription factor that acts as a crucial regulator of cellular redox homeostasis through its capacity to induce expression of enzymes such glutathione *S*-transferase, NAD(P)H:quinine oxidoreductase and γ-glutamylcysteine synthetase which contributes to clearance of oxygen reactive species [223, 229].

IRE1

IRE1, the second sensor in the ER membrane, is a serine/threonine protein kinase endoribonuclease that, similarly to PERK, consists of an ER luminal domain, a transmembrane domain and two cytosolic domains: a kinase domain and a endoribonuclease domain [229, 231]. The protein is highly conserved in all eukaryotes and in mammals is present in two copies: IRE1α and IRE1β. IRE1α is a ubiquitous protein. Deletion of IRE1α results in an embryonic lethal phenotype in mice [232]. IRE1β expression is limited to the epithelial cells of the gastrointestinal tract. Knock-out of IRE1β induces a viable but susceptible to colitis phenotype in mice [233].

The inactive state of IRE1 is also maintained by binding of BiP to the luminal domain. Release of BiP protein in ER stress leads to IRE1 homooligomerization. Close contacts between two cytosolic domains result in *trans*-autophosphorylation and activation of the ribonuclease domain [231]. The activated IRE1α ribonuclease domain cleaves the constitutively transcribed *XBP1* (X box protein 1) pre-mRNA into mature mRNA by un unconventional splicing mechanism [222]. *XBP1* mRNA has two conserved overlapping ORFs. On activation of the UPR, IRE1α removes a 26 nucleotide intron from unspliced *XBP1* mRNA, which leads to a translational frame shift and produces a fusion protein encoded from the two ORFs. The new carboxyl-terminus of the product from spliced *XBP1* mRNA *($XBP1^s$)* converts *$XBP1^u$* (the product from the unspliced mRNA) into a potent active transcription factor [229] (Figure 1.9)

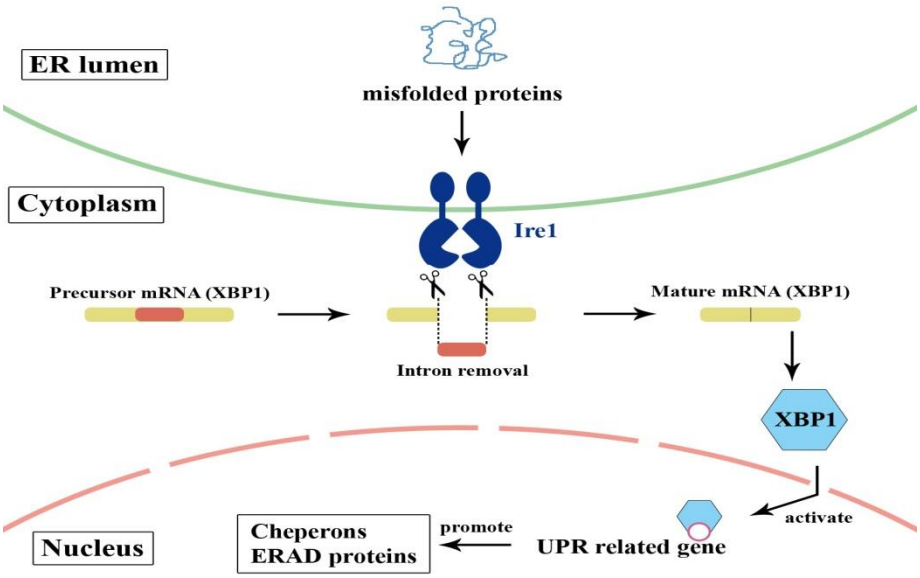

Figure 1.9. XBP1 mRNA splicing (modified after Lee *et al.* 2008)

The *XBP1*^{s} transcription factor then translocates into the nucleus and activates the transcription of ERAD component genes such as EDEM (endoplasmic reticulum degradation enhancing α-mannoside-like protein), HRD1 (HMG-CoA reductase degradation protein) and genes for ER chaperones such BiP and PDI-P5 involved in the quality control of protein folding in the ER. Thus, IRE1α promotes adaptation via *XBP1*^{s} [222].

Another important aspect of atypical splicing of *XBP1* is the cellular compartment where the mRNA is processed. Conventional splicing takes place in the nucleus whereas *XBP1* splicing takes place in the cytoplasm [234]. The biological significance of cytoplasmic splicing is that pre-mRNA used for translation in the cytoplasm can be spliced when it is necessary to change the nature of the protein translated from the mRNA in response to extracellular or intracellular signalling. This is not the case of nuclear splicing were cleaved mRNA once exported cannot be modified again so another pre-mRNA must be *de novo* transcribed and spliced. Recently it was shown that *XBP1*^{u} encoded in *XBP1* pre-mRNA is a negative feedback regulator of *XBP1*^{s} [234]. Thus, in the case of *XBP1*, pre-mRNA and mature

mRNA encode negative and positive regulators, and their expression is switched by cytoplasmic splicing in response to the situation in the ER [222] [233].

In mammals, besides the role in *XBP1* mRNA processing, IRE1α has additional functions in cell signalling. Recent evidence suggests that the activated kinase domain of IRE1α binds to the adaptor protein TNFR-associated factor 2 (TRAF 2) triggering activation of the apoptosis signal-regulating kinase 1 (ASK1) and c-Jun-N terminal kinase (JNK) pathway [232]. IRE1α is also involved in modulation of "alarm genes" such p38 MAPK [235] and NFκB pathway [213] possibly by binding of the non-catalytic region of a tyrosine kinase adaptor protein (Nck) and the protein complex IKK/TRAF2. Thus, IRE1α is involved in both protection via adaptation through XBP1 splicing, and cellular injury via JNK, p38 MAPK and NFκB activation processes triggered by endoplasmic reticulum stress.

ATF6

ATF6, the third ER membrane stress sensor, is a type II transmembrane protein containing an ER luminal domain responsible for sensing unfolded proteins and two cytosolic domains: a DNA-binding domain containing a basic-leucine zipper (bZIP) motif and a transcriptional activation domain [222].

In mammals, there are two homologous proteins, ATF6α and β. Both are expressed ubiquitously and with similar functions [236]. In the absence of ER stress, the ATF6 luminal domain is bound to the BiP chaperone that inhibits translocation of ATF6 to the Golgi apparatus. Accumulation of unfolded proteins in the ER lumen leads to dissociation of BiP from the complex and translocation of ATF6 to the Golgi apparatus [226]. Here ATF6 is sequentially cleaved by two proteases: site 1 protease (S1P) that cleaves in the luminal

domain and the metalloprotease site 2 protease (S2P) that cleaves the N-terminal membrane-anchored fragment of ATF 6 [224, 226]. This proteolytic activation process takes place in the membrane of the Golgi apparatus and is called regulated intramembrane proteolysis (RIP). The same mechanism is responsible also for cleavage of sterol response element-binding proteins (SREBPs) which are activated when cholesterol is depleted [237]. SREBPs act as regulators of sterol biosynthesis. In the case of ATF6 cleavage, the proteolytic reactions release the cytosolic N-terminal region encoding the bZIP transcription factor. Once translocated to the nucleus, this active transcription factor binds to a *cis*-acting element, the ER stress response element (ERSE) and together with nuclear factor Y (NF-Y) induces the transcription of ER chaperone genes such BiP, GRP/94 and calreticulin [221, 222, 229]. Nevertheless, if the unfolded protein burden exceeds the ER capacity to adapt, ATF6 cleavage can induce activation of ER-associated degradation process (ERAD) proteins and also of pro-apoptotic CHOP [221].

ER stress and inflammation

Increasing number of studies suggest that the signalling pathways in the UPR and inflammation are connected through various mechanisms including production of ROS, release of Ca^{2+} from the ER, activation of the proinflammatory NFκB and JNK signalling pathways and induction of an acute-phase response [221]. Prolonged activation of the UPR could lead to accumulation of ROS as a result of UPR-stimulated up-regulation of chaperone proteins involved in disulfide bond formation in the ER lumen [150]. The enzyme responsible for this process is ER oxidoreductin 1 (ERO1) [229] protein that perform redox reactions using molecular oxygen as the final electron acceptor [150]. Accumulation of ROS

during ER stress can become toxic and initiate an inflammatory response. In order to limit this possible ROS toxicity the cells have evolved an antioxidant response involving Nrf2 activation regulated by the PERK signalling pathway. This adaptative mechanism allows the cell to reduce the increasing toxic ROS and prevent a further toxic burden on the cell. In progressive chronic induction of ER stress ROS accumulation can exceed the buffering induced by Nrf2 and result in activation of the proinflammatory NFκB pathway, a key regulator in the onset of inflammation [221]. There are a few proposed mechanisms for ER stress-associated NFκB activation. The first one is related to ROS accumulation as a result of excessive protein folding and involves the ER enzymes responsible for disulphide bond formation and ERO1 that use molecular oxygen as a terminal electron acceptor in their redox reactions [238]. Additional oxidative stress can also result from the depletion of reduced glutathione consumed in reactions that reduce unstable and improperly formed disulphide bonds. Therefore, an increase in the protein-folding load in the ER can lead to accumulation of ROS and initiate an inflammatory response.

The second proposed mechanism is activation of NFκB as a result of ER stress-mediated leakage of calcium into the cytosol [239]. Pahl *et al* [240] showed that ER overload leads to increased efflux of Ca^{2+} into the cytosol and subsequent generation of intermediate reactive oxygen species (ROI). Experiments showed that NFκB induction by ER stress is prevented by pre-incubation of cells with intracellular Ca^{2+} chelators and antioxidants suggesting that both these signals are required for NFκB activation in response to ER stress [240]

The third mechanism proposed is that UPR response *per se* can directly promote NFκB activation through PERK-induced eIF2α phosphorylation. Unlike canonical signalling pathways that promote IκB phosphorylation and degradation, eIF2α phosphorylation is not affecting the phosphorylation status of IκB but, due to general attenuation of translation induce proteasomal degradation of the kinase whose half-life is relative short and release of

the proinflammatory NFκB complex [241]. This effect has been observed in cells treated with ER stress-inducing reagents and in UV-irradiated cells, both of which activate the PERK pathway. Also recent studies found that ER stress-mediated NFκB activation is attenuated both in *perk*$^{-/-}$ and cells bearing two mutant allele of *EIF2A* in which serine 51 (the substrate of the stress-inducible kinases) has been mutated to an alanine suggesting an important regulatory role of eIF2α phosphorylation in NFκB activation under stress conditions [242].

The last mechanism proposed for NFκB activation in response to ER stress involves the IRE1α signalling pathway. ER stress-induced *trans*-autophosphorylation of IRE1α was proposed to induce conformational changes in the cytosolic domain of the protein that allows the binding of the adaptor protein TRAF2 [232]. The IRE1α-TRAF2 complex recruits IκB kinase (IKK) that phosphorylates IκB leading to proteasomal degradation of the inhibitory IκB subunit α and NFκB translocation to the nucleus [213]. Though described here, the mechanism is still not fully understood and needs further investigation. A similar mechanism was proposed also for JNK activation. Activation of JNK in response to ER stress is mediated also by formation of IRE1-TRAF2 complex, as shown in studies using truncated TRAF2 in the N-terminal RING effector domain that leads to inhibition of JNK activation in response to ER stress signals and by experimental evidence that showed that JNK activation in response to ER-stress is impaired in mouse embryonic fibroblasts that lack IRE1α [232].

Recently it has been indicated that the UPR response can also induce inflammation by up-regulation of an acute-phase response through an ER-resident transcription factor CREBH in the liver [243]. CREBH is an ATF6 homologous protein expressed in hepatocytes and highly induced by inflammatory cytokines. In ER stress, CREBH is activated by translocation to the Golgi complex where it is cleaved by S1P and S2P. An N-terminal fragment of CREBH is released into the cytosol and translocates to the nucleus inducing

transcription of acute phase genes such serum amyloid P component (SAP) and C-reactive protein (CRP) [232, 243].

ER stress induced inflammation and insulin resistance in obesity

In the last decade an increased number of studies suggest a positive association between ER stress, inflammation and insulin resistance in obesity, mainly through UPR-induced activation of pro-inflammatory signalling pathways such JNK and NFκB [221]. In response to metabolic dysfunction, IRE1α activation as result of ER stress leads to conformational changes in the cytosolic domain that allows recruitment of adaptor protein TRAF 2 and activates inflammatory MAP kinases JNK and IKK. IKK activation induces IκB phosphorylation and degradation, leading to NFκB translocation to the nucleus and transcriptional activation of proinflammatory genes [213]. JNK activation on the other side induces serine phosphorylation of insulin receptor-1 substrate (IRS-1) inhibiting phosphorylation of tyrosine residues and functional activation of the receptor [244]. Also, activation of JNK leads to phosphorylation of activator protein-1 (AP-1) and transcription of proinflammatory genes. This mechanism is supported by data showing that tissue specific deletion of JNK1 in adipose tissue decreased IL-6 expression in adipose tissue and improved hepatic insulin sensitivity in mice fed a high fat diet [245]. These observations suggest that IRE1α could be the link between ER stress and JNK activation leading to increased cellular inflammation and insulin resistance. Consistent with this model is also the observation that mice lacking one allele of *XBP1* (*xbp1*$^{+/-}$ mice) display increased activation of PERK, IRE1α, JNK and dysregulated phosphorylation of IRS-1 when fed a high-fat diet [221]. In addition, activation of PERK and IRE1α could lead to NFκB activation via IκB phosphorylation and

attenuation of general translation, leading to increased transcription of proinflammatory genes. Similar activation was found in the case of hepatocytes [246, 247], cardiomyoblasts, pancreatic β-cells [248, 249], macrophages and 3T3 L1 preadipocytes [221, 250] incubated with free fatty acids or cholesterol. Although the mechanisms by which the FAs are inducing ER stress are still unknown, there is an increased amount of data suggesting that high levels of saturated fatty acids (SFA) induce activation of the UPR and subsequently activation of proinflammatory pathways including NFκB and JNK. This activation leads to insulin resistance either via direct inhibition of insulin receptor Tyr phosphorylation through the IRE1-TRAF2-JNK pathway [251] or to increased expression of proinflammatory cytokines through the PERK- eIF2α-IκB-NFκB pathway [34, 224]. Attenuation of FA-induced ER stress by chemical chaperones effectively reduced FA-induced expression of proinflammatory cytokines and improved insulin signalling which was accompanied by reduced IKKβ and JNK phosphorylation [206]. Also activation of the UPR in response to FAs increases the expression of the ER chaperone BiP and by its interaction with Akt, decreases phosphorylation of Ser-473 and general Akt phosphorylation leading to impaired insulin signaling [252]. By inhibition of general translation ER stress decrease the total level of Akt leading to subsequent decreased insulin signalling [253].

Recent evidence shows also that inflammatory cytokines produced by hypertrophic adipocytes or macrophages recruited into inflamed adipose tissue [254], can itself elicit ER stress in L929 cells and hepatocytes [243, 255] suggesting that UPR activation triggers a self-sustaining vicious inflammatory cycle in adipose tissue leading to peripheral insulin resistance, adverse effects on the cardiovascular system and type II diabetes. Several studies have documented a role of proinflammatory cytokines such as TNFα, IL-6 and IL-1β in insulin resistance in both rodents and human subjects [213, 256-260]. TNFα exposure has been shown to induce insulin resistance by both inactivation of the insulin receptor as a

consequence of increase Ser 307 phosphorylation of IRS-1 through JNK activation [261, 262] and down-regulation of *IRS-1* and *GLUT 4* gene expression and decrease *GLUT 4* mRNA stability [263, 264]. IL-6 on the other hand have been reported to modulate the insulin signaling pathway in tissue specific manner: it transiently activate SOCS-3 and induces a reduction in IRS-1 phosphorylation and PI3K activation in hepatocytes [265] and reduced expression of *IRS-1, GLUT4* genes decreasing insulin-stimulating transport of glucose in adipocytes.

Although in the last years considerable progress has been made towards understanding the molecular events that underlie the pathological onset and progress of obesity, many mechanisms involved remain still unknown. The adipose tissue and mainly the adipocyte dysfunction have been shown to play a central role in the development of the condition leading to lipotoxicity, inflammation and insulin resistance. Though increasing data have shown involvement of various mechanisms in the cellular dysfunction, little is known about the factors that trigger the dysfunction.

1.3. Aims and objectives

In the last years, multiple pieces of evidence have shown that ER stress induction in the adipose tissue [266] and mainly in the adipocytes from obese subjects (or mice) [267, 268] mediates part of the inflammatory response and insulin resistance in dysfunctional cells, contributing to the pathological onset and progression of obesity. Although the molecular events that ER stress coordinates have been extensively studied, the physiological triggers of this ER stress are still unknown. In order to answer this question, the aim of my thesis was to investigate whether physiological alterations in obesity, such as elevated plasma fatty acids, cholesterol levels, inflammation and adipose tissue remodelling can induce ER stress in adipocytes.

Therefore, the objectives of this thesis can be summarised as follows:

- To characterise whether high concentrations of saturated fatty acids commonly found in obese individuals are inducing ER stress in obesity (Chapter 4). Recent evidence have showed that exposure to high concentrations of fatty acids, especially palmitate, leads to development of ER stress in different cell lines such as preadipocytes [221, 250], β-pancreatic cells [248, 249]**,** and hepatocytes [246, 247]

- To investigate if hypercholesterolemia, another hallmark of obesity and a major risk factor for development of cardiovascular and metabolic diseases [269] is able to induce UPR in adipocytes (Chapter 5). High cholesterol concentrations were shown

to induce ER stress in macrophages [270] and smooth muscle cells [271] but there are no studies investigating the effect on adipocytes.

- To investigate if increased levels of proinflammatory cytokines as TNF α, IL-6 and IL-1β can induce ER stress in adipocytes (Chapter 6). These cytokines commonly found in the blood of obese patients are the most abundant cytokines in the dysfunctional adipose tissue and have been shown to induce UPR in hepatocytes [255] and β-cells [272-274].

- To study if glucose starvation can represent a trigger for ER stress in adipocytes (Chapter 7). Adipose tissue remodelling has been shown to play a central role in obesity dysfunction due to formation of low vascularised areas as result of rapid overexpansion. The low nutrient intake have been associated with cellular dysfunction and especially ER stress in cancer cells [275] and β-pancreatic cells [276] but few data are known about the effect on adipocytes.

- To investigate if hypoxia can induce UPR in adipocytes (Chapter 8). Adipose tissue remodelling and low vascularisation affect not only the nutrient supply of the adipocyte but also the O_2 intake. Hypoxia has been previously shown to induce inflammation [277, 278] and insulin resistance [279, 280] in adipocytes But the mechanisms underlying these effects are still not fully understood.

The summary of my thesis aim and objectives are represented in the flow chart below (Figure 1.10)

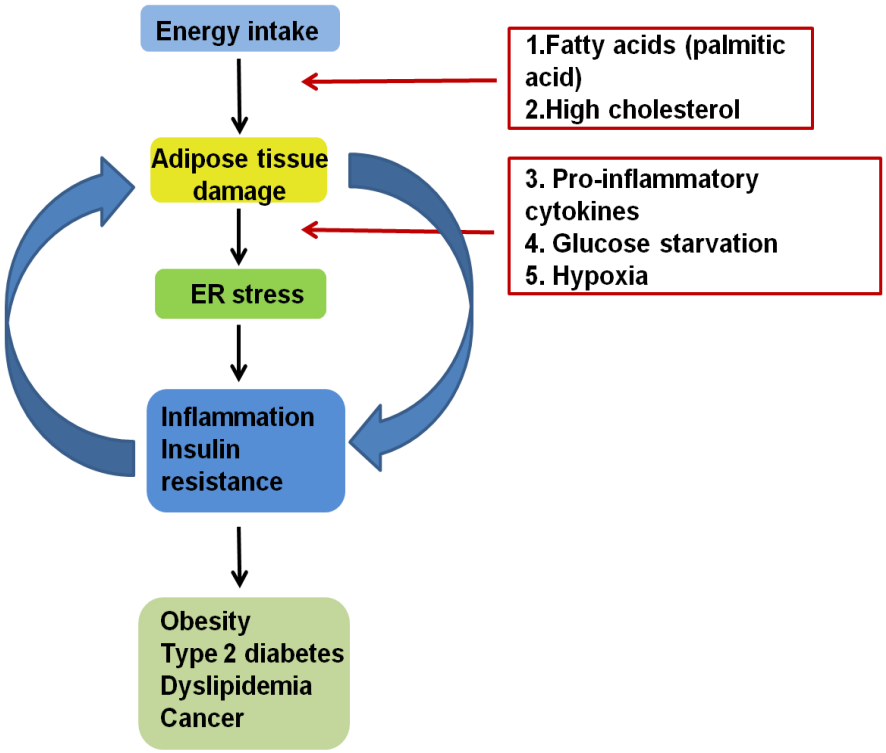

Figure 1.10. The flow chart of the pathological progress of obesity in the adipose tissue with proposed stages of ER stress induction in response obesity-related factors investigated in the study

CHAPTER 2

MATERIALS AND METHODS

2.1. Materials

2.1.1. General chemicals

Table 2.1. Chemicals.

Chemical	**Company and catalogue number (cat. no.)**
3-Isobutyl-l-methylxanthine (IBMX)	Sigma-Aldrich, # I5879
37% (w/v) formaldehyde	Fisher Scientific, #P/0840/53
Agarose (electrophoresis grade**)**	Bioline, BIO-41025
Acetic acid (HOAc)	Fisher Scientific, A/0360/PB17
Bovine serum albumin	Sigma-Aldrich, # A2153
Bovine serum albumin**,** fatty acid free	Sigma-Aldrich, # A3803
β-Mercaptoethanol	Sigma-Aldrich, M6250
Bromophenol blue	Sigma-Aldrich, #11439
Complete mini protease inhibitors	Roche, #11836 153 001
Coomassie Brilliant Blue R	Sigma-Aldrich, # B0149
Diethyl pyrocarbonate (DEPC**)**	Acros Organics, # A0300574
Dexamethasone	Sigma-Aldrich, # D4902
Dimethyl sulphoxide	Sigma-Aldrich, #D5879
Ethylenediamine tetraacetic acid (EDTA)	Fisher Scientific, # D/0700/53
Ethanol	Fisher Scientific, # E/0650DF/25

Ethidium Bromide (10 mg/ml)	Sigma-Aldrich, # E1510
Glycerol	Fisher Scientific, # G/0650/17
Glycine	Fisher Scientific,# BP381-1
Hydrochloric acid	Fisher Scientific, # H/1100/PB17
Insulin from bovine pancreas	Sigma-Aldrich, # I0516
Interleukin 1β	Thermo Fisher, # RIL1B1
Interleukin 6	Life Technologies, # PHC0066
Methanol	Fisher Scientific, # M/4000/PC17
Native human acetylated LDL	AbD Serotec, # 5685-3404
Nile red	Sigma-Aldrich, # N3013
Nonidet-P40	Fluka, #74385
Oil red O	Sigma-Aldrich, # O0625
Palmitic acid	Sigma-Aldrich, # P5585
Phorbol 12-myristate 13-acetate (PMA)	Sigma-Aldrich, # P1585
Propanol	Fisher Scientific, # P/7490/17
Potassium chloride	Fisher Scientific, # P/4240/53
Potassium dehydrogenate phosphate	Fisher Scientific, # 7778-77-0
Ponceau S	Sigma-Aldrich, #P3504
Sodium chloride	Fisher Scientific, # S/3120/65
Sodium deoxycholate	Sigma-Aldrich, # D6750
Sodium dodecyl sulphate (SDS)	Fisher Scientific, # BPE116-500
Sodium hydroxide	Fisher Scientific, # S/4920/53
Thapsigargin	Sigma-Aldrich, # T9033
Thiazolyl blue tetrazolium bromide (MTT)	Sigma- Aldrich, # M5655

N-[4-(2-chlorophenyl)-6,7-dimethyl-3-quinolinyl]-N'-(2,4-difluorophenyl)-urea (TMP-153)	Enzo Life Sciences, # BML-EI317-0020
TNF α (human)	Cell Signaling Technology, # 8902
Tris (hydroxymethyl) methylamine (Tris)	Fisher Scientific, # T/3710/60
Triton X-100	Sigma-Aldrich, # 282103
Tunicamycin	Merck Millipore, Calbiochem, # 645380
Tween®20	Sigma-Aldrich, # P1379

2.1.2. Tissue culture reagents

All reagents used for cell culture were sterile-filtered and only opened under sterile conditions in a microbiological safety cabinet. For prepared solutions, filter sterilisation was carried out using a 0.2 µm sterile filter and syringe.

Table 2.2. List of reagents used in tissue culture work.

Name	Company and catalogue number (cat. no.)
0.25% Trypsin-EDTA solution	Sigma-Aldrich, # T4049
DMEM high glucose, with phenol red	Sigma-Aldrich, # D5671
DMEM high glucose, w/o phenol red	ThermoFisher, # 31053-028
DMEM w/o glucose, with phenol red	Thermo Fisher, # 11966025
DMEM high glucose, w/o L-glutamine w/o sodium pyruvate	Biosera, # LM-D1112/500
Dulbecco's phosphate buffered saline	Biosera, # LM-S2041-1000 D857
Fetal bovine serum	Biosera, # S1830

Fetal calf serum	Biosera, CA-115
L-Glutamine	Biosera, # G7513
Penicillin-streptomycin, solution (10,000 U penicillin and 10 mg streptomycin/ml)	Sigma-Aldrich, # P4333
RPMI 1640	Sigma-Aldrich, #R0883
Trypan blue solution **(**0.4% w/v)	Sigma-Aldrich, # T8154

2.1.3. Enzymes and antibodies

Table 2.3.1. List of enzymes used in the study.

Enzyme	**Company, catalogue number (cat. no.)**
GoTaq® DNA polymerase	Promega, # M3001
GoTaq® hot start polymerase	Promega, # M5001
Superscript® III reverse transcriptase	Life Technologies, # 56575

Table 2.3.2. List of antibodies used in the study.

Primary antibody	**Dilution**	**Company, catalogue number (cat. no.)**
Anti-AKT	1:1000	Cell Signaling, # 4691
Anti-β-actin	1:20000	Sigma-Aldrich, # A2228
Anti-BiP	1:1000	Abcam, # ab-53068
Anti-CHOP	1:1000	Cell Signaling, # 2895
Anti-eIF2α	1:1000	Santa Cruz Biotechnology, # sc-11386
Anti-GAPDH	1:30000	Sigma-Aldrich, # G8795
Anti-HIF 1α	1:500	R&D Systems, # AF1935
Anti-JNK	1:1000	Cell Signaling, # 9252
Anti-phospho-eIF2α	1:1000	Santa Cruz Biotechnology, # sc-11386
Anti-phospho S473-AKT	1:1000	Cell Signaling, # 4060
Anti-phospho-JNK	1:1000	Cell Signaling, # 4668
Secondary antibodies	**Dilution**	**Company, catalogue number (cat. no.)**
Goat anti-rabbit-IgG (H+L)-horseradish peroxidase (HRP)-conjugated secondary	1: 20000	Cell Signaling, # 7074S
Goat anti mouse IgG (H+L)-HRP-conjugated antibody	1: 20000	Thermo Fisher Scientific, # 31432

2.1.4. Commercially available kits

Table 2.4. List of commercially available kits used in the study.

Name	Company and catalogue number (cat. no.)
Amersham™ ECL™ Western blotting detection reagents	GE Healthcare, # RPN2009
Criterion™ TGX™ precast gels 4-20%	BioRad, # 567-1094/95
DC™ protein assay kit I	BioRad, # 500-0111
EZ-RNA kit	Geneflow, # K1-0120
geNorm 6 reference genes (mouse)	PrimerDesign, # ge-SY-6
Pierce® ECL plus Western blotting substrate	ThermoScientific, # 32132
Precision 2 x real-time PCR MasterMix with SYBR green	PrimerDesign, Precision
Precision FAST 2xreal-time PCR MasterMix with SYBR Green	PrimerDesign, Precision-R
Restore™ Western Blot stripping buffer	Thermo Scientific, # 21059

2.1.5. Oligodeoxynucleotides

The oligodeoxynucleotides used in the study were synthesized by Sigma (liquid, 100 µM in water) or by Eurogentec Ltd (lyophilised). Lyophilised primers were resuspended in sterile water to a final concentration of 100 µM. All primers were stored at -20ºC. The oligonucleotides used in this study are listed in Table 2.5.

Table 2.5. Oligonucleotides sequences.

Name	Purpose	Sequence	Annealing temperature * (ºC)
Oligonucleotides for Mus musculus genes			
H8477	*GPAT3* PCR and RT-qPCR, forward primer	AGCCATTGTGGAGGATGAAG	60
H8478	*GPAT3* PCR and RT-qPCR, reverse primer	GGAAGCAATAGCGCACTAGG	60
H8677	*DGAT1* PCR and RT-qPCR, forward primer	TCATGGAAGAAGGCTGAGGT	60
H8678	*DGAT1* PCR and RT-qPCR, reverse primer	TCATGGAAGAAGGCTGAGGT	60
H8873	*PCYT1* PCR and RT-qPCR, forward primer	TGGGAGTCTGCAGTGATGAG	60
H8668	*Pcyt1* PCR and RT-qPCR, reverse primer	CTGCGTCCTTGATGTGCTTA	60

H8669	*HIF1α* PCR and RT-qPCR, forward primer	TCCATGTGACCATGAGGAAA	60
H8771	*HIF1α* PCR and RT-qPCR, reverse primer	AAAAAGCTCCGCTGTGTGTT	60
H8744	*RESISTIN*PCR and RT-qPCR, forward primer	TGGCTCGTGGGACATTCGTG	65
H8745	*RESISTIN* PCR and RT-qPCR, reverse primer	CCACGCTCACTTCCCCGACA	65
H8754	*MCP-1* PCR and RT-qPCR, forward primer	CACCAGCACCAGCCAACTCT	55
H8755	*MCP-1* PCR and RT-qPCR, reverse primer	GCCGGCAACTGTGAACAGCA	55
H8756	*IL-6* PCR and RT-qPCR, forward primer	ACAACCACGGCCTTCCCTAC	65
H8757	*IL-6* PCR and RT-qPCR, reverse primer	ACAGGTCTGTTGGGAGTGGT	65
H8877	*TNFα* PCR and RT-qPCR, forward primer	AGCCGATGGGTTGTACCTTG	60
H8878	*TNFα* PCR and RT-qPCR, reverse primer	ATAGCAAATCGGCTGACGGT	60
H8881	*Leptin* PCR and RT-qPCR, forward primer	TTTCACACACGCAGTCGGTA	62
H8882	*Leptin* PCR and RT-qPCR, reverse primer	GGGTGAAGCCCAGGAATGAA	62

H7961	*XBP1* PCR, forward primer	GATCCTGACGAGGTTCCAGA	Touchdown PCR
H7962	*XBP1* PCR, reverse primer	ACAGGGTCCAACTTGTCCAG	Touchdown PCR
H7994	*ACTB* PCR and RT-qPCR, forward primer	AGCCATGTACGTAGCCATCC	55
H7995	*ACTB* PCR and RT-qPCR, reverse primer	CTCTCAGCTGTGGTGGTGAA	55
H8553	*BiP* (*HSPA5*) RT-qPCR, forward primer	TTCGTGTCTCCTCCTGAC	55
H8554	*BiP* (*HSPA5*) RT-qPCR, reverse primer	ACAGTGAACTTCATCATGCC	55
H8660	*VEGFA* RT-qPCR, forward primer	AGAGCAACATCACCATGCAG	55
H8661	*VEGFA* RT-qPCR, reverse primer	TTTGACCCTTTCCCTTTCCT	55
H8736	*ERDJ4* (*DNAJB9*) RT-qPCR, forward primer	CTGTGGCCCTGACTTGGGTT	65
H8737	*ERDJ4* (*DNAJB9*) RT-qPCR, reverse primer	AGGGGCAAACAGCCAAAAGC	65
H8778	*CHOP* RT-qPCR, forward primer	TCTTGAGCCTAACACGTCGAT	55
H8779	*CHOP* RT-qPCR, reverse primer	CGTGGACCAGGTTCTGCTTT	55

H8796	*EDEM1* RT-qPCR, forward primer	TGGAAAGCTTCTTTCTCAGC	55
H8797	*EDEM1* RT-qPCR, reverse primer	ATTCCCGAAGACGTTTGTCC	55
H9106	*PERK* RT-qPCR, forward primer	CTCAAGTTTCCTCTACTGTTCACTC	60
H9107	*PERK* RT-qPCR, reverse primer	GCTGTCTCAGAACCGTTTTCCC	60
H9110	*IRE1α* RT-qPCR, forward primer	GCGCAAATTCAGAACCTACAAAGG	62
H9111	*IRE1α* RT-qPCR, reverse primer	GGAAGCGGGAAGTGAAGTAGC	62
Oligonucleotides for Homo sapiens genes			
H8287	*ACTB* PCR, forward primer	CTGAGCGTGGCTACTCCTTC	55
H8288	*ACTB* PCR, reverse primer	GGCATACAGGTCCTTCCTGA	55
H8289	*XBP1* PCR, forward primer	GAGTTAAGACAGCGCTTGGG	59
H8290	*XBP1* PCR, reverse primer	ACTGGGTCCAAGTTGTCCAG	59

* The primers were designed using NCBI's PrimerBlast software (http://www.ncbi.nlm.nih.gov/tools/primer-blast/) or Primer3 web tool using the parameters described by Santa Lucia et al [281]. The sequences were designed to have of 18-20 nucleotides, a guanine-cytosine (GC) content of 45-60 % and melting temperature (Tm) between 55 and 66 ºC (with less than 2 degree difference in between the primers pair).

Primers for murine *ACAT1* (acetyl-coenzyme A acetyltransferase 1), *SCD1* (stearoyl-CoA desaturase 1), *PLA1* (phospholipase A1), *PLA2* (Phospholipase A2) and *Pcyt2* (phosphate cytidyltransferase 2, ethanolamine) were ordered from Primer Design and the sequences are unknown. Murine *GAPDH* primers were included in the geNorm reference gene kit.

2.1.6. Buffers and solutions

All buffers and solutions were prepared using Nanopure H_2O according to the recipes listed in table below.

Table 2.6. Buffers and solutions used in the study.

Buffer /Solution	Composition	Quantity	Recipe
DEPC-H_2O	1 ml DEPC	1 l	Add 1 ml DEPC to 1 l Nanopure H_2O and stir vigorously for 30 min at room temperature. Autoclave the solution
dNTPs, 2 mM	2 mM dATP 2 mM dCTP 2 mM dGTP 2 mM dTTP 1 mM Tris·HCl (pH 8.0)	1 ml	Add 10 µl 100 mM Tris·HCl (pH 8.0) in 910 µl H_2O and mix the solution. Add the following to the solution: 20 µl 100 mM dATP, 20 µl 100 mM dCTP, 20 µl 100 mM dGTP, and 20 µl 100 mM dTTP.

EDTA, 0.5 M	93.1 g $Na_2EDTA \cdot 2H_2O$	500 ml	Dissolve 93.1 g $Na_2EDTA \cdot 2H_2O$ in ~ 350 ml H_2O and adjust pH to 8.0 with 10 M NaOH Add H_2O to 500 ml and autoclave
Isopropanol, 60 % (v/v)	100 % isopropanol		Mix 60 ml 100 % isopropanol with 40 ml H_2O
Oil red O stock solution	250 mg Oil red O	50 ml	Dissolve 250mg Oil Red O in 50 ml isopropanol by stirring continuously. Filter solution using a 0.45 µm filter and store at room temperature in a container protected from light.
Oil red O working solution		50 ml	Mix 30 ml Oil red O stock solution with 20 ml H_2O. Filter solution through a 0.22µm filter and store at room temperature in a contained protected from light. The solution should be made prior to the experiment as it is stable for max 1 week.
PBS, 10 X	1.37 M NaCl 26.8 mM KCl	4 l	Add 320 g NaCl, 8 g KCl, 57.6 g Na_2HPO_4 and 8 g KH_2PO_4 in

	101.4 mM Na_2HPO4 14.7 mM KH_2PO4		3 l of H2O. Stir until fully dissolved and add distilled water up to 4 l.
Ponceau Red S solution, 0.1% (w/v)	0.1 % (w/v) Ponceau Red S 20 % (v/v) acetic acid	500 ml	Mix 0.5g Ponceau Red S with 25 ml acetic acid and add water up to 500 ml. Stir well
RIPA buffer	50 mM Tris·HCl, pH 8.0 150 mM NaCl 1 % (v/v) Triton X-100 0.5 % (w/v) sodium deoxycholate 0.1 % (w/v) SDS	10 ml	Add 5 ml 1M Tris·HCl pH 8.0, 0.3 ml 5 M NaCl, 0.1 ml Triton X-100, 0.5 ml 10 % (w/v) sodium deoxycholate, and 0.1 ml 10 % (w/v) SDS in 8.5 ml H_2O. Mix well the solution and store at 4°C.
SDS-PAGE sample buffer, 6 X	350 mM Tris, (pH 6.8) 30 % (v/v) glycerol 10 % (w/v) SDS 0.5 g/l bromophenol blue	10 ml	Dissolve 3.78 g glycerol, 1.00 g SDS, 500 µl 10 g/l bromophenol blue, 3.50 ml 1 M Tris·HCl pH 6.8 and 200 µl β-mercaptoethanol in

	2 % (v/v) β-mercaptoethanol		10 ml H_2O on the shaker
SDS-PAGE buffer, 10 X	1.92 M glycine 0.248 M Tris 10 g/l SDS	1 l	Add 144.13 g glycine, 30.03 g Tris and 10.00 g SDS to 900 ml H_2O. Once completely dissolved, add H_2O to a final volume of 1 l
Semi-dry transfer buffer, 10 X	1 M Tris 1.52 M glycine	1 l	Dissolve 121.1g Tris base and 144.13g glycine in 600ml H2O and stir until fully dissolved.Add H_2O up to1l.
TAE, 50 X	2 M Tris·HOAc 0.1 M EDTA pH ~ 8.5	1 l	Add 242 g Tris, 57.1 ml HOAc and 37.2 g $Na_2EDTA·2H_2O$ to 1 l H_2O
TBS, 10 X	200 mM Tris 1.37 M NaCl	1 l	Dissolve 24.2g Tris base and 80g NaCl in 600ml H_2O and adjust the pH to 7.6 using HCl. Add H_2O up to 1 l.
TBST	200 mM Tris 1.37 M NaCl 0.1% Tween 20	1 l	Add the 24.2 g Tris and 80g NaCl in 800 ml H_2O and adjust the pH to 7.6 using HCl. Add 1 ml Tween 20 mix and adjust to 1 l with H_2O.

TE (pH 8.0), 10 X	100 mM Tris·HCl (pH 8.0) 10 mM EDTA	4 l	Add 400 ml 1 M Tris·HCl (pH 8.0) and 80 ml 0.5 M EDTA in 4l H_2O. Autoclave the solution.
Tris·HCl (pH 6.8), 1 M	1 M Tris	1 l	Dissolve 121.14 g Tris in 800 ml H2O and adjust the pH to 6.8 with concentrated HCl. Add H_2O to 1 l
Tris·HCl (pH 8.0), 1 M	1M Tris	1l	Dissolve 121.14 g Tris in 800 ml H2O and adjust the pH to 8.0 with conc. HCl. Add H2O to 1 l.

2.1.7. Special equipment

Table 2.7 Special equipment used in the study

Name	Company	Catalogue number (cat. no)
BD FACS Calibur Flow Cytometer	BD Biosciences	342975
Bioruptor	Diagenode	UCD-200TM-EX
Counting chamber	Marienfield Superior	0642010

Criterion ™ cell	BioRad	165-6001
Galaxy R+ CO2 incubator	RS Bioltech	170-300 PLUS
Gel doc 1000 mini transilluminator	BioRad	# 400-0065
Modular Incubator	Billups-Rotenberg	MIC-101
Mr Frosty™ Freezing Container	Thermo Scientific	5100-0001
PTC-200 Thermal Cycler	MJ Research	NA
Rotor-gene 6000	Corbett Life Science	9001560

2.1.8. Cell culture

General guidelines: All cell cultures were handled in a tissue culture designated room. For cell handling, culture and treatments Class II (HEPA-filtered) biological safety cabinets were used and the cells were maintained in a 37ºC, 5% (v/v) CO_2 and 95% air and humidity controlled incubator.

2.1.8.1. Cell lines

2.1.8.1.1. 3T3-F442A cell line

The 3T3-F442A [282, 283] murine preadipocytes used in this study were kindly provided by Prof. C. Hutchinson as subconfluent culture in Dulbecco's modified Eagle's medium (DMEM) 4.5 g/L D-glucose supplemented with 2 mM L-glutamine and 10% (v/v) fetal bovine serum.

2.1.8.1.2. 3T3-L1 cell line

The 3T3-L1[283, 284] murine preadipocytes used in this study were purchased from the ATCC collection (ATCC®-CL-173^{TM}) and cultured as instructed in Dulbecco's modified Eagle's medium (DMEM) 4.5 g/L D-glucose supplemented with 2 mM L-glutamine and 10 % bovine calf serum (complete growth medium).

2.1.8.1.3. THP-1 cell line

The THP-1 human monocytic cell line used in the study was kindly provided by Dr Adam Benham. The cells were cultured in RPMI-1640 growth medium supplemented with 2 mM L-glutamine and 10 % fetal bovine serum (complete growth medium).

2.2. Methods

2.2.1. Tissue culture methods

2.2.1.1. Subculture of adherent cell lines

To subculture adherent cell lines, the cells were washed with sterile PBS and incubated with 0.25 % trypsin-EDTA for 5 min at 37ºC in order to facilitate dispersion. After complete dispersion of the cells assessed by using an inverted microscope, serum supplemented growth medium was added (1:10 trypsin solution to medium ratio) to inactivate the trypsin. The cells were re-suspended and counted using a haemocytometer. In the counting process the number of viable cells was established using trypan blue exclusion protocol [285] and only the viable cell count was used for calculating the densities for the new cultures.

2.2.1.2. Subculture of non-adherent cell lines

For non-adherent cell lines (THP-1 cell line), the cell culture was gently mixed by pipetting up and down so that the cells will be evenly dispersed in the medium and viable cell density was measured using a haemocytometer and trypan blue dye. The culture was then centrifuged 5 minutes at 1200 rpm, room temperature (RT), and re-suspended in appropriate volume of fresh medium.

2.2.1.3. Counting cells using the haemocytometer

In order to prepare subcultures with a desired cell density, the viable cells were counted before plating using a haemocytometer and trypan blue solution. Prior to counting, the haemocytometer and coverslip were cleaned with 70 % ethanol and the coverslip attached to the haemocytometer in order to form the counting chamber. A small volume of the mixed suspension (~50 µl) was then carefully placed in the haemocytometer chamber avoiding overfilling and cells were counted using the 10 X objective of the microscope. The cell counting was performed using the trypan blue staining protocol for viable cells [285, 286] and the haemocytometer instructions.

2.2.1.4. Trypan blue staining

The trypan blue staining procedure followed the protocol described by Freshney et al [285]. In short, 100 µl of cell suspension was mixed with a 0.4% (w/v) trypan blue solution in a ratio of 1:1 (v/v).10 µl of the mixed suspension was loaded in the haemocytometer counting chamber and the cells were counted starting from the upper left corner. An area of 1 mm^2 square was counted avoiding counting the same cell twice. Only unstained, viable cells were counted. The same procedure was followed for a second and third square and the average number of cells was calculated.

The viable cell density per ml, the total number of viable cells and the viability percentage was determined using the following calculations:

No of cells per ml = the average count per square x dilution factor* x $10^{4\pm}$,

* dilution factor is the dilution factor of cell suspension in Trypan blue staining solution (in our case 2)

± conversion factor to 1 ml

Total no of cells = cells per ml x volume of original suspension

Cell viability (%) = (total viable cells (unstained) ÷ total cells (stained and unstained)) x 100

2.2.1.5. Cryopreservation

For cryopreservation freezing medium consisting in 90 % (v/v) FBS and 10 % (v/v) DMSO was used. Usually 80 - 90 % confluent cultures were used for the procedure as the cell density will allow a high number of cells to be stored and the cells are still in their growth phase. The cells were washed with warm (37ºC) sterile PBS and incubated with 0.25 % trypsin – EDTA at 37ºC until full detachment from the plate. Cells were then re-suspended in growth medium and the cell density was assessed using a haemocytometer. Appropriate volume of freezing medium was used to re-suspend the cells in order to obtain a 1-1.5 ml suspension (1x 10^5 cells/ml) per cryotube. The cryotubes were placed in Mr Frosty™ Freezing container, and were stored over night at -80ºC. The second day the cryotubes were transferred in liquid nitrogen for long time storage.

For THP-1 cells cryopreservation the same protocol was used with the only difference that the trypsin incubation step was removed as the cells are growing in suspension.

2.2.1.5. Revival of cryopreserved cells

The cells were revived by placing the cryotube in a 37ºC water bath until the cell suspension was thawed. The suspension was then re-suspended in 10 ml of complete growth medium and incubated for at least 2 days in a 37ºC, 95 % air and 5 % CO_2 incubator before changing the medium.

2.2.1.6. Adipocyte in vitro differentiation

For *in vitro* differentiation, the 3T3-F442A and 3T3-L1 murine preadipocytes were maintained in DMEM supplemented with 4.5 g/l D-glucose, 2 mM L-glutamine and 10 % (v/v) fetal bovine serum (FBS) until confluency. This step was shown to be extremely important due to a previously shown property of these cells to induce spontaneous growth arrest and differentiation upon very high density [283, 287].

Two days post confluency the medium was replaced with an induction medium containing complete growth medium supplemented with 1 μg/ml insulin, 0.5 mM IBMX, and 0.25 μM dexamethasone. The cells were maintained in this induction medium for three days and then for two more days in medium containing 1 μg/ml insulin. On day 5 of differentiation, the medium was replaced with complete growth medium and maintained for another 7 days,

while replacing the medium every 3 days. Adipocytes differentiation was assessed after 12 days of differentiation by staining with Oil red O or nile red as described below.

2.2.1.7. Oil Red O staining of neutral lipids

The Oil Red O staining of *in vitro* differentiated adipocytes was used as a method to evaluate the degree of differentiation of the cells 12 days after induction using an previously established protocol [288]

Reagents: 3.7 % (w/v) formaldehyde; 1 X sterile PBS; Oil Red O working solution (see Table 3.6); 60 % isopropanol.

Protocol

In vitro differentiated adipocytes as previously described were washed with warm PBS and incubated for 5 min with 3.7 % (w/v) formaldehyde. The formaldehyde was then replaced with fresh 3.7 % (w/v) formaldehyde and incubated for another hour to assure an optimal fixation of the cells. During the incubation the plates were wrapped in parafilm to prevent drying and covered with aluminum foil to protect from light. After incubation, the cells were washed with 60 % (v/v) isopropanol and left to dry completely. Oil red O working solution was added to each well and cells were incubated for 10 min at room temperature. The cells were washed four times with H_2O and photographed using a Nikon camera attached to the microscope.

2.2.1.8. Nile red fluorescent staining of lipids

Nile red fluorescent staining method was used to determine the percentage of differentiation in the 12 days *in vitro* differentiated adipocyte culture.

Reagents: Nile red working solution (100 ng/ml in PBS); 1 X sterile PBS

Protocol

In vitro differentiated adipocytes in day 12 of differentiation were trypsinised as previously described in section 2.2.1.1., re-suspended in fresh medium and then centrifuged for 5 minutes at 1200 g, RT. Cells were then re-suspended in sterile PBS and nile red working solution was added in a 1:100 ratio (100 ng/ml final concentration in PBS). The suspension was then incubated for 5 min at RT, protected by light. After the incubation, the **c**ells were centrifugated again for 5 min at 1200 g and washed once with fresh PBS to eliminate the excess dye**.** Cells were then re-suspended in fresh sterile PBS and immediately analysed by flow cytometry on a BD FACSCalibur Flow Cytometer at a low flow rate.

2.2.1.9. Flow cytometry

In the study, the nile red fluorescent staining of neutral lipids was used for characterisation of ~ 50,000 gated events/ sample with regard to size, granularity and fluorescence. Gates were set in order to exclude cellular debris and differentiate in between the two populations based on cell size (FCS) and cell granularity (SSC). Nile red fluorescence was excited at 488 nm and its fluorescence emission collected using the FL-1 (530/30 nm) band pass filter. The instrument settings used in the study are presented below.

For 3T3 F442A cells

Forward scatter (FSC , for cell size) – E-1 (lin, Amp gain = 4.50),

Side scatter (SSC, for granularity) – 280 V (lin, Amp gain = 1.00),

Fluorescence (FL1) – 275 V (log, Amp gain = 1.00).

For 3T3-L1 cells

Forward scatter (FSC, for cell size) – E-1 (lin, Amp gain = 4.50),

Side scatter (SSC, for granularity) – 326 V (lin, Amp gain = 1.00),

Fluorescence filter (FL1) – 275 V (log, Amp gain = 1.00).

Data were analysed in WinMDI 2.9 and graphs prepared in GraphPad Prism 6.04 (GraphPad Software). Three biological replicates were analysed for each sample.

2.2.1.10. THP-1 *in vitro* differentiation

The THP-1 monocytes were *in vitro* differentiated into macrophages by incubation with 50 nM phorbol-12-myristate 13-acetate (PMA) for 3 d, followed by 1 d incubation in growth medium [289]. The degree of differentiation of the cultures was visually assessed due to the adherent phenotype of differentiated macrophages. Renewal of the medium allowed that only the adherent differentiated macrophages were kept for the study.

2.2.2. Cell treatments

2.2.2.1. Palmitic acid treatment

In vitro differentiated 3T3-F442A and 3T3-L1 adipocytes were serum-starved overnight in DMEM containing 4.5 g/l D-glucose and 2 mM L-glutamine and then incubated in serum-free medium containing 2 % (w/v) fatty acid-free BSA and 0.05 - 1 mM palmitic acid. Palmitic acid to fatty acid-free BSA complexes were prepared as follows: the acid was dissolved in ethanol and diluted 1:100 in DMEM containing 4.5 g/l D-glucose and 2 % (w/v) fatty acid-free BSA. The solution containing the complexes was made fresh before the experiments and sterile filtered before addition to the cells. Control cells received ethanol diluted 1:100 into DMEM containing 4.5 g/l D-glucose and 2 % (w/v) fatty acid-free BSA. For the experiments investigating the effect of palmitic acid on insulin signalling in adipocytes and preadipocytes, the cells were incubated for 48 h with the treatment previously described before stimulation with 100 nM insulin for 15 min.

2.2.2.2. Cholesterol treatment

In vitro differentiated adipocytes were incubated for 48 hours in DMEM containing 4.5 g/l D-glucose, 2 mM L-glutamine and 100 μg/ml human acetylated LDL (AcLDL) in the presence or absence of the acyl-CoA:cholesterol acyltransferase (ACAT) inhibitor TMP-153 at a final concentration of 0.6 μM [290]. The same treatment was used on differentiated THP

cells but due to previously described induction of apoptosis in response to the cholesterol treatment [291], the incubation was limited to 16 h .

2.2.2.3. Proinflammatory cytokine treatments

In vitro differentiated adipocytes were incubated with 0 - 200 ng/ml tumour necrosis factor alpha (TNFα), interleukin 1 beta (IL-1β) or interleukin 6 (IL-6) for 0 - 24 hours in serum free DMEM 4.5 g/l D-glucose supplemented with 2 mM L-glutamine.

For experiments investigating the biological activity of the proinflammatory cytokines, preadipocytes were incubated for short periods of time (0 - 30 min) with 25 ng/ml TNF-α, 200 ng/ml IL-1β or 200 ng/ml IL-6.

2.2.2.4. D-Glucose starvation

For glucose starvation experiments, *in vitro* differentiated adipocytes were incubated for 6 - 48 hours in DMEM with or without D-glucose and supplemented with 2 mM L-glutamine.

2.2.2.5. Hypoxia treatment

Day 12 differentiated adipocytes were placed in a sealed hypoxia chamber and flushed with a pre-analysed gas mixture of 0.5 % (v/v) O_2, 5 % (v/v) CO_2 and nitrogen (BOC Industrial Gases), at a flow rate of 25 l/min for 5 min to completely replace air inside with the gas

mixture (time for complete replacement of air as recommended by the manufacturer). The modular chamber was then incubated at 37ºC for 0-8 hours.

2.2.2.6. Cell viability assay

The MTT assay protocol used in the present study was previously described by Tim Mosmann [292] and it is presented below.

Reagents: Phenol red free complete culture medium; isopropanol containing 4 mM HCl and 0.1% (v/v) Nonidet P-40

Protocol

After the desired treatment, the cells were incubated with 0.5 g/l MTT in phenol-red free medium for 4 h at 37°C, in order to allow formation of the insoluble purple formazan crystals. After 4 h the medium was discarded and the crystals were dissolved using isopropanol containing 4 mM HCl and 0.1% (v/v) Nonidet P-40. Absorbance of the obtained formazan solution was then read at 590 nm with a reference at 620 nm. The absorbance was expressed as the ratio of the absorbance at 590 nm to the absorbance at 620 nm.

2.3. Molecular methods

2.3.1. RNA extraction

Reagents: EZ RNA kit (Geneflow), ice-cold 100% isopropanol, 70% ethanol, DEPC water

Protocol

RNA from cells was isolated using the EZ RNA kit according to the manufacturer's instructions. Briefly, the cells were washed with sterile PBS and lysed directly in the culture dish using 0.5 ml denaturing solution containing guanidine thiocyanate (reagent A in kit). The lysates were homogenised by pipetting the solution up and down a few times and were incubated for 5 min at room temperature. Lysates were then transferred into 1.5 ml tubes and 0.5 ml extraction solution containing phenol-chloroform mix (reagent B in kit) was added. The tubes were shaken vigorously for 15 s and incubated at room temperature for 10 min. Samples were then centrifuged for 15 min at 12,000 g, 4ºC allowing formation of two phases: an aqueous upper phase that contains the RNA and an organic phase that contains the proteins and other cell components. The aqueous upper phase was transferred to a new tube and 0.5 ml ice-cold isopropanol was added to precipitate the RNA. The phase and isopropanol solution were mixed well by inverting the tube a few times and then incubated over night at -20ºC to allow the RNA to precipitate. Next day the samples were centrifuged for 10 min at 12,000 g, 4ºC and the supernatant was discarded. The pellet obtained was washed with 1 ml 75 % ethanol and centrifuged again for 5 min at 7,500 g, 4ºC. The supernatant was then removed and the pellet (RNA) was left to dry at room temperature for

10 min in order for the ethanol to completely evaporate. The RNA was then re-suspended in 30 µl DEPC-treated water and samples were stored at -80ºC.

2.3.2. RNA concentration quantification

The RNA concentration in the samples was assessed using an UV spectrophotometer. Each sample was diluted in DEPC-treated water in a ratio 1:50, and loaded in duplicate on an UV microtiter plate. The absorbance was measured at 230 nm (A_{230} for phenolic contaminants), 260 nm (A_{260} for nucleic acids) and 280 nm (A_{280} for protein contamination) in order to establish the concentration and purity of the RNA for each sample. The concentration of RNA was calculated using SoftMax Pro software, against a control made out of DEPC-treated water only. The purity of the RNA isolated was established using the ratios A_{260}/A_{230} (~2), A_{260}/A_{280} (~1.8).

2.3.2. Reverse transcription

The RNA obtained was reverse transcribed in a two steps reaction using SuperScriptIII Reverse Transcriptase (Invitrogen) and following the manufacturer's instructions. First strand cDNA synthesis was prepared in 20 µl total reaction volume in a nuclease-free tube as described below.

Table 2.8. Reverse transcription reaction reagents and conditions

Component / concentration	Volume (µl per sample)
oligo(dT)15, 50 µM	1.0
RNA, 5 µg	Calculated from concentration
dNTPs mix , 10mM	1.0
H_2O	Up to 13 µl

The components were mixed and incubated at 65°C for 5 minutes then placed on ice for 1 min. The following components were added to the reaction mix:

Component / concentration	Volume (µl per sample)
1^{st} Strand Buffer, 5X	4.0
DTT, 0.1M	1.0
RNaseOUT RNase Inhibitor, 40U/µL	1.0
SuperScript Reverse Transcriptase (Invitrogen), 200U/ml	1.0

The components were vortexed and heated to 50°C for 1 h followed by inactivation of the reverse transcriptase by heating to 70°C for 15 min. The cDNA obtained was stored at 4°C and used for the PCR and QPCR reactions.

2.3.3. Polymerase chain reaction (PCR)

Taq polymerase was used as a polymerase for *β-actin* amplification and Hot Start Taq polymerase, a modified Taq polymerase that is inactive at temperatures below 45ºC was used to investigate genes with lower expression.

Table 2.9. The general protocol of the PCR reaction

Component / concentration	Volume (µl per sample)
Green GoTaq flexi buffer, 5X	5
$MgCl_2$, 25 mM	1.5
dNTPs mix, 2 mM	1.25
Forward primer,10 µM	2.5
Reverse primer, 10 µM	2.5
cDNA	1.25
GoTaq (Hot Start) polymerase, 5U/µl	0.25
Sterile H_2O	10.75
Total volume	25

The fragments were amplified in a thermal cycler (PTC-200 Thermal cycler, MJ Research) using the following conditions:

Step	Temperature (ºC)	Time (seconds)	No of cycles
Initial denaturation	94	120	1
Denaturation	94	60	

Annealing	As presented in table 2.5	30	35
Extension	72	30	
Final extension	72	300	1

Table 2.10. PCR conditions for of *XBP1* mRNA splicing

Step	Temperature (°C)	Time (seconds)	No of cycles
Initial denaturation	95	300	22
Denaturation	94	30	
Annealing	72	30	
Decrease annealing temperature by 1.0°C each cycle			
Extension	72	15	35
Denaturation	94	30	
Annealing	50	30	
Extension	72	15	
Final extension	72	420	1

2.3.4. Preparation of agarose gels

The amplification products were run on an agarose gel in order to be investigated. Briefly, 1.5 g of agarose powder were mixed with 150 ml Tris-acetic acid-EDTA (TAE) buffer (1 % (w/v) agarose gel) and heated until the agarose was completely dissolved. The homogenised solution was then left to cool down until the solution was < 40ºC. 7 µl 10 mg/ml ethidium

bromide was then added and the solution was mixed thoroughly. The solution was poured in the agarose gel caster and left at room temperature until complete polymerisation. The gel was then submersed in 1 X TAE running buffer and the samples were run at a voltage of 2 V/cm^2.

For *XBP1* PCR products, due to the small difference in between the spliced and unspliced forms, the agarose gel used was 2 % (w/v) agarose in TAE buffer.

The gels were visualised in UV on a Gel Doc 1000 mini trans-illuminator and pictures were saved for further analysis. The images were quantified using Image J software and the percentage of splicing was calculated as described below.

2.3.5. Analysis of DNA samples on agarose gels

The percentage of *XBP1* splicing was calculated by dividing the signal for spliced *XBP1* cDNA by the sum of the signals for spliced and un-spliced *XBP1* mRNAs.

2.3.6. Quantitative PCR (qRT-PCR)

For the quantitative PCR (qRT-PCR) reactions, various kits were used during the study: 2xqPCR MasterMix (Primer Design), FAST 2xqPCR MasterMix (PrimerDesign) and qRT-PCR MasterMix (Promega), according to the manufacturer instructions. For all the kits, the detection was made on an Rotor-Gene thermo cycler (Corbett) using SYBR Green fluorescent dye and 40 amplification cycles.

Table 2.11. Reaction mix per sample using 2xqPCR MasterMix or FAST 2xqPCR MasterMix (Primer Design)

Component / concentration	Volume (µl per sample)
(FAST) 2xqPCR Master Mix	10
Forward primer, 10 µM	0.6
Reverse primer, 10 µM	0.6
cDNA (1:100 input cDNA from RT-PCR)	5
Sterile H_2O	3.8
Total volume	20

For primer pairs designed by Primer Design, the primer mixed added was 1 µl/sample and water was adjusted to a final volume of 20 µl.

Table 2.12. Cycling conditions for 2xqPCR Master Mix

Step	Temperature (ºC)	Time (seconds)	No of cycles
Initial denaturation	95	600	1
Denaturation	95	15	40
Annealing	As presented in table 2.5	30	
Extension	72	20	
Final extension	72	300	1
Melting curve	55-95	N/A	

Table 2.13. Cycling conditions for FAST 2xqPCR Master Mix

Step	Temperature (ºC)	Time (seconds)	No of cycles
Initial denaturation	94	300	1
Denaturation	94	15	
Annealing	55	20	
Extension	72	30	40
Final extension	72	300	1
Melting curve	55-95	N/A	

For all protocols amplification of a single qRT-PCR product was confirmed by recording the melting curves after each run. All amplification efficiencies were > 0.9. Calculation of C_T values (number of cycles required for the fluorescent signal to cross the threshold) was done with the RotorGene software using a manually set threshold. Each qRT-PCR experiment was repeated 3 times with independent biological samples. All qRT-PCR reactions were investigated using technical triplicate also in order to account for pipetting errors.

Relative quantitation of gene expression was used to quantify the difference in the expression of specific target gene between different samples. All values were normalised to *β-actin* housekeeping gene (reference gene) expression. Calculations were made using comparative Ct method [293]:

$$\Delta CT = \Delta CT_{target} - \Delta CT_{reference}$$

$$\Delta\Delta CT = \Delta CT_{target} - \Delta CT_{control}$$

$$\text{Ratio}_{\text{gene in sample vs gene in control}} = 2^{-\Delta\Delta CT}$$

where

CT target = CT value of the gene of interest in treated

CT reference = CT value of the housekeeping gene;

CT control = CT value of the gene of interest in untreated sample

2.4. Biochemical methods

2.4.1. Protein extraction

In order to analyse the protein expression profile in treated and un-treated cells, cell lysates were obtained. For adherent cell the reagents and protocol used were the following:

Reagents: Ice-cold RIPA buffer [50 mM Tris-HCl, pH 8.0, 150 mM NaCl, 0.5 % (w/v) sodium deoxycholate, 0.1 % (v/v) Triton X-100, 0.1 % (w/v) SDS]; protease and phosphatase inhibitors (Roche); ice-cold 1 X PBS

Protocol

Cells were washed 3 times with 4ºC 1X PBS and incubated with ice-cold RIPA buffer containing protease and phosphatase inhibitors. The culture was homogenised in the lysis buffer directly in the culture plate using the pipette tip or a cell scraper, and the lysate was transferred into 1.5 ml tubes and incubated for 10 min on ice to allow complete lysis. For differentiated adipocytes, in order to decrease their viscosity the lysates were briefly sonicated for 5 minutes using Bioruptor (Diagenode) at high power, with 10 s sonication bursts and 30 s pause intervals in between, according to the manufacturer instruction, Lysates

were then centrifuged for 5 minutes at 13,000 g, 4ºC in order to sediment the cell debris and separate the aqueous fraction containing the proteins. The supernatant was transferred to a fresh tube and the protein content was quantified using the DC Protein Assay kit (Lowry based method) according to the manufacturer instructions. After protein quantitation, the samples were stored for short term at -20ºC and for long term at -80ºC.

2.4.2. Protein quantification

Protein content of the lysates was quantified using DC Protein Assay according to the manufacturer instructions. In short, cell lysates were diluted 1:5 in distilled H_2O and 5 µl of the diluted lysate was loaded into a clean, dry microtiter plate. The lysate was then mixed with 25 µl reagent S+A mix (1:50 ratio reagent S to reagent A) and 200 µl reagent B. Similar to the samples, 5 µl of known BSA dilutions (0 to 2 mg/ml) used as standards were loaded onto the plate and mixed with the reaction reagents. All standards and samples were loaded in duplicate to minimise the possible pipetting errors. The plate was then incubated at RT, on a horizontal shaker for 15 minutes and the absorbance was read at 750 nm using a plate reader. A standard curve was made using the BSA standards readings and used for the sample protein concentrations.

2.4.3. Western Blotting

2.4.3.1. SDS-PAGE (sodium dodecyl sulphate polyacrylamide gel electrophoresis)

BioRad SDS-PAGE system and the 4-20% Criterion TGX precasted gels were used in the study according to the manufacturer instructions.

Reagents: 6XSDS-PAGE loading buffer; SDS-PAGE running buffer 4-20% Criterion TGX precast gels; prestained protein molecular marker

Protocol

The gel system was prepared according to the instructions and the wells of the precast gels were washed with the SDS-PAGE running buffer. For each sample 50 µg protein lysate was mixed with 6 X SDS-PAGE sample buffer and incubated for 5 min at 100ºC. Samples were then left to cool down at room temperature and loaded into the wells of the precast gel along with the prestained protein ladder. The gel was run at 240 V for ~ 30 min, until the bromphenol blue front in the sample loading buffer reached the bottom of the gel. The gel was then removed from the system and placed in TBST for few minutes.

2.4.3.2. Semi-dry transfer

In order to use immunological detection of investigated proteins, the proteins on the SDS-PAGE gel were transferred to a 0.45 µm polyvinylidene fluoride (PVDF) membrane that can be subjected to antibody incubation. The transfer was made using a semi-dry transfer system according to the manufacturer instructions.

Reagents: Semi-dry transfer buffer containing 5% (v/v) methanol; PVDF membrane; Whatman paper

Protocol

The PVDF membrane cut to the size of the gel was incubated for 1 minute in 100 % methanol. All the components of the semi-dry (PVDF membrane, SDS-PAGE gel and 8 Whatman papers) were then incubated for 10 minutes in 1X semi-dry transfer buffer containing 5 % methanol, on a shaking platform. Once the components were equilibrated in transfer buffer, the gel sandwich was assembled as following: 4 Whatman papers, the PVDF membrane, the SDS-PAGE gel, 4 Whatman papers, and the excess transfer buffer was removed. The transfer was made in a semi-dry unit at 2-3 mA /cm^2 for 70 minutes.

2.4.3.3. Ponceau S staining

Reagents: 0.1% (w/v) Ponceau Red S solution in 5% acetic acid; TBST; H_2O

Protocol

In order to evaluate if the protein transfer was efficient, the PVDF membrane was incubated immediately after the transfer in TBST for 10 minutes and then in 0.1% (w/v) Ponceau Red S solution in 5% acetic acid for another 10 minutes. The membrane was then washed with H_2O until the excess of the dye was removed allowing visualisation of the protein bands. After assessing the transfer efficiency, the membrane was washed several times in TBST in order to remove the Ponceau staining solution and was prepared for immunoblotting.

2.4.3.4. Immunoblotting

Reagents: TBST buffer; 5 % (w/v) skimmed milk in TBST; 5 % (w/v) BSA in TBST; antibodies (dilution as presented in table 2.3.2) Pierce ECL/ ECL Plus substrate; photographic film (CL-X Posure™ film, cat. no. 34091, Thermo Fisher Scientific)

Protocol

The PVDF membrane from the semi-dry transfer was incubated for 1 h in 5 % skimmed milk in TBST and then washed 5 times x 5 min with TBST. After the washing steps, the membrane was incubated with the desired primary antibody diluted as previously described in 5 % (w/v) skimmed milk in TBST or 5 % (w/v) BSA in TBST (for phosphorylated

proteins) over night at 4ºC, on a shaker. The next day, the membrane was washed 5 times x 5 min with TBST and incubated with the secondary antibody (HRP-linked) diluted 1:20,000 in 5 % (w/v) skimmed milk in TBST for 1 hour at room temperature, on a shaker. After the incubation, the membrane was washed again 5 times x 5 min with TBST and incubated with the chemiluminiscent ECL or ECL Plus substrate for 5 min in the dark. The excess of chemiluminiscent reagent was then removed and the membrane was placed in a cassette and exposed to a photographic film for appropriate lengths of time (1-10 min). The film was developed using an X-ray film developing machine according to the manufacturer's instructions.

2.4.3.5. Quantification of Western blotting bands

In order to quantify the bands resulted from the chemiluminiscent reaction between the HRP linked to the secondary antibody and the ECL substrate, the developed films were scanned on a CanoScan LiDE 600F scanner (Canon) and saved as tiff. files. The bands were quantitated using ImageJ as described under the heading "Gels Submenu" on the ImageJ web site (http://rsb.info.nih.gov/ij/docs/menus/analyze.html#plot).

In order to correct for differences in loading between individual lanes, the peak intensities for the used primary antibody were then divided by the peak intensities obtained with the antibody for the loading control in the corresponding lane. All loading control-corrected peak intensities obtained for one Western blot were then expressed relative to the loading control-corrected peak intensity of the 0 h sample.

Similarly, the GelDoc images of *XBP1* splicing were quantitated using ImageJ and following a similar protocol with the protein bands quantification. The percentage of splicing was calculated as described in subchapter 2.3.5.

CHAPTER 3

ADYPOCYTE *IN VITRO* DIFFERENTIATION

Obesity is the most common nutritional disorder in the developed world and a risk factor for associated diseases like type 2 diabetes mellitus, cardiovascular diseases and hypertension. As a key regulator of metabolic homeostasis the adipose tissue represents the main tissue affected by the pathological conditions in obesity. Though the cellular composition of the adipose tissue includes a variety of cell types as preadipocytes, adipocytes, macrophages and endothelial cells [46], alteration of adipocyte homeostasis has been shown to be the main cause of tissue dysfunction [149].

The aim of my study is to investigate whether physiological alterations in obesity, such as elevated plasma fatty acids, cholesterol levels, adipose tissue inflammation or remodelling can induce an endoplasmic reticulum stress response in adipocytes contributing to the lipotoxic and inflammatory drift of adipose tissue in obesity. In order to accomplish this aim, the first step was to obtain a cellular model of adipocytes that can be subjected to treatments without the interference from other tissue-related factors. For this, two established murine preadipocytes cell lines, 3T3-F442A and 3T3-L1 were selected due to previously described capacity to *in vitro* differentiate into adipocytes under controlled conditions [282, 294] Both cell lines originated from the 3T3 fibroblast cell line obtained by Todaro *et al* [295] from disaggregated Swiss mouse embryos. They are spontaneously immortalised lines capable of differentiating into adipocytes *in vitro* or *in vivo* [283]. The difference between the two cell lines resides in the ability to undergo adipose differentiation in the presence of serum adipogenic factors or growth hormones [294]. Compared to the L1 line, the F442A line presents a higher capacity of cell adipogenic cluster formation [283] and differentiation [296] under hormonal induction, the cell line being considered more "committed" to the adipogenic differentiation than the L1 line.

Due to their properties, both cell lines have been extensively used in studies investigating adipocyte physiology and pathology related to metabolic diseases. The *in vitro* differentiation process using adipogenic factors have been thoroughly described [297, 298]. In this study, both 3T3-F442A and 3T3-L1 cell lines were grown to confluency and maintained 2 d post confluency to induce cell growth arrest needed for differentiation induction as described by Green *et al* [287]. The cells were then differentiated for 12 d using an adipogenic cocktail according to the protocol described in the Materials and Methods chapter. Differentiation of the cells was assessed using lipid staining methods as cytoplasmic accumulation of lipid droplets has been previously shown to be increased directly proportional to the extent of adipocyte differentiation. Two lipid staining methods were used in the study: Oil red O staining that allowed a qualitative evaluation of the differentiation process and Nile red fluorescent staining using flow cytometry that allowed a quantitative evaluation of lipid accumulation. All experiments were done using adipocytes in day 12 of differentiation.

Microscopic evaluation of adipocyte differentiation after 12 d of induction using Oil red O staining revealed an increased accumulation of lipid droplets in the cells subjected to the adipogenic cocktail compared to the ones that did not receive the cocktail (Figure 3.1).

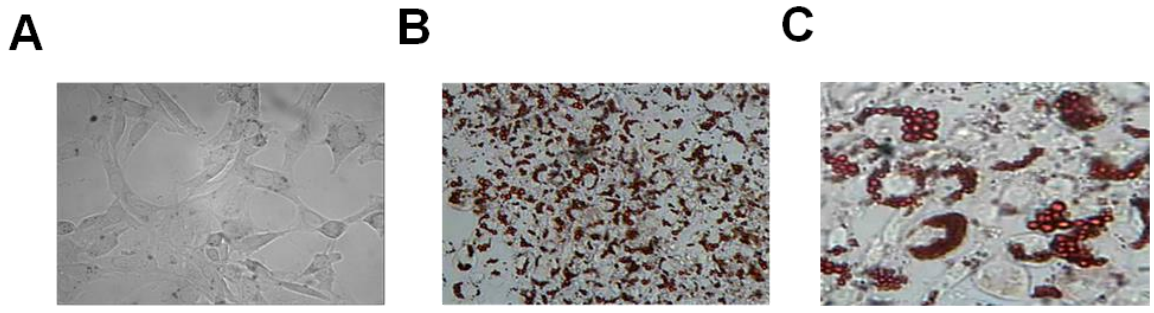

Figure 3.1. Oil Red O staining of neutral lipids in *in vitro* differentiated 3T3-F442A adipocytes
(A) Preadipocytes, 20X, **(B)** adipocytes day 12, 20X, and **(C)** adipocytes day 12, 10X.

The results show that the differentiation protocol used did induce accumulation of lipid droplets in 80 - 90 % of the cell population in 3T3- F442A cells as previously described [299, 300]. In order to accurately establish the percentage of cells presenting lipid droplets, the quantitative flow cytometry method using the fluorescent lipid probe nile red [301] was used. The flow cytometry experiments were set to investigate 50,000 cells/sample, comparing preadipocytes with adipocytes in day 12 of differentiation. Unstained preadipocytes and adipocytes were used as experimental controls for cell autofluorescence and gates were set in order to exclude cellular debris. Nile red fluorescence was used as an indicator of intracellular lipid accumulation.

Investigation of fluorescence in preadipocytes and adipocytes differentiated for 12 d revealed a mean fluorescence increase of 3.2 ± 0.2 fold upon differentiation of 3T3-L1 cells (Figure 3.2 A). For 3T3-F442A cells two distinguishable fluorescent populations were observed after 12 d, exhibiting 2.9 ± 0.1 fold and 25 ± 2 fold increase in nile red fluorescence compared to undifferentiated (0 d) cells (Figure 3.2 B).

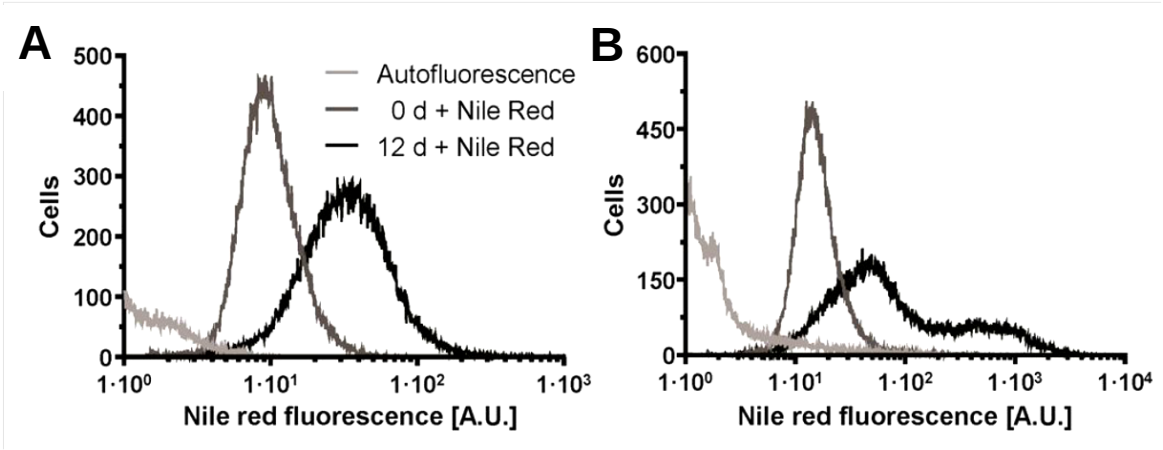

Figure 3.2. Nile red staining of lipids in adipocyte differentiation. Nile red fluorescence of **(A)** 3T3-L1 and **(B)** 3T3-F442A cells on day 0 (dark grey line) and 12 of differentiation (black line). The light grey line represents the autofluorescence of cells differentiated for 12 d without incubation with nile red. For each sample 50,000 gated cells were analysed. Results are representative for three biological repeats.

Quantitation of the nile red fluorescence data by constructing the probability distribution for the increase in nile red fluorescence upon differentiation and the constraint that the fluorescence of adipocytes has to be greater by at least two standard deviations then the mean nile red fluorescence of undifferentiated cells revealed that 72 ± 3 % of the 3T3-L1 and 80 ± 1 % of the 3T3-F442A cells acquired a lipid-loaded phenotype.

In order to better characterise the adipocyte-like phenotype of the increased fluorescent populations observed at day 12, I further looked for other parameters that could be used to discriminate between the undifferentiated and differentiated populations. The differentiation process has been previously shown to induce changes in the cellular phenotype due to accumulation of lipids in the cytoplasm [287]. These changes affect the size and granularity of the cell [302] and thus, the two parameters can be used in flow cytometry and plotted as side scatter (SSC-H) for granularity and forward scatter (FSC-H) for cell size. Investigation of the two parameters revealed increases in both the granularity and size of adipocytes (Figure 3.3 B, D) compared to preadipocytes (Figure 3.3 A, C) suggesting the previous described increased lipid accumulation in the cells [287, 302].

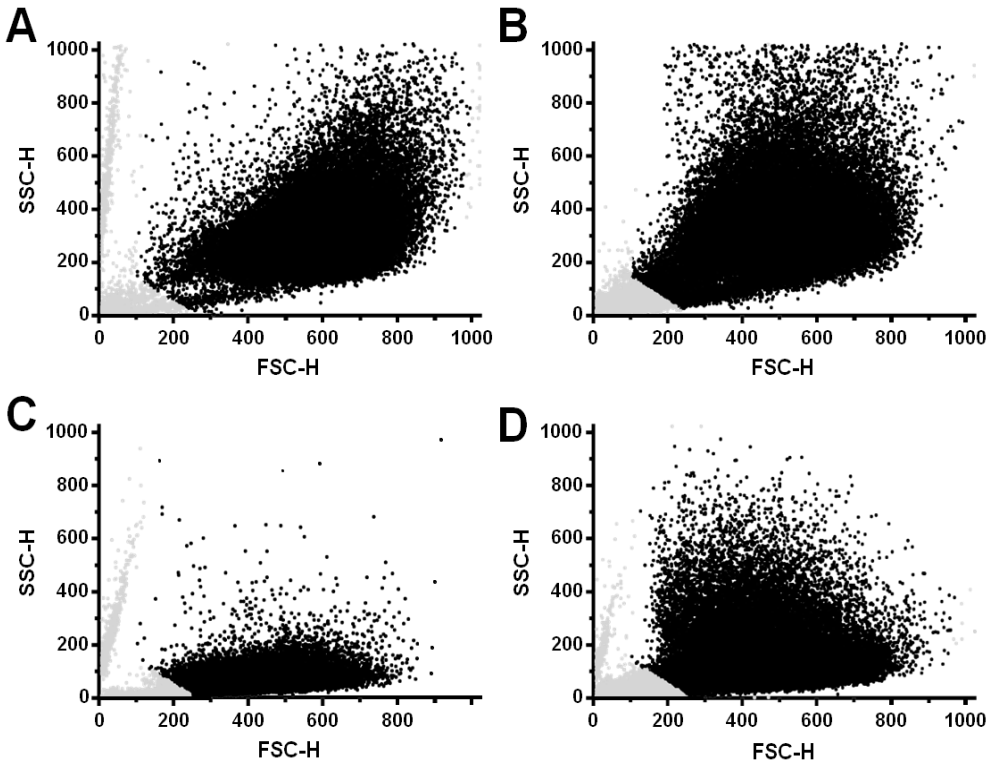

Figure 3.3. Dot plots of the side scatter (SSC-H) versus the forward scatter (FSC-H) for **(A, B)** 3T3-L1 and **(C, D)** 3T3-F442A cells before **(A, C)** and 12 d after induction of adipogenic differentiation **(B, D)**. Black dots are within the gated population that was analysed, grey dots are outside the gated population. The same gate was used to analyse all samples.

Further analysis to establish if there is a correlation between granularity (SSC-H) and fluorescence indicated a positive association between the two parameters, with a higher fluorescence in the population presenting increased SSC-H (≥ 300 A.U.) compared to the population with lower SSC-H (< 300 A.U.) (Figure 3.4 A, B).

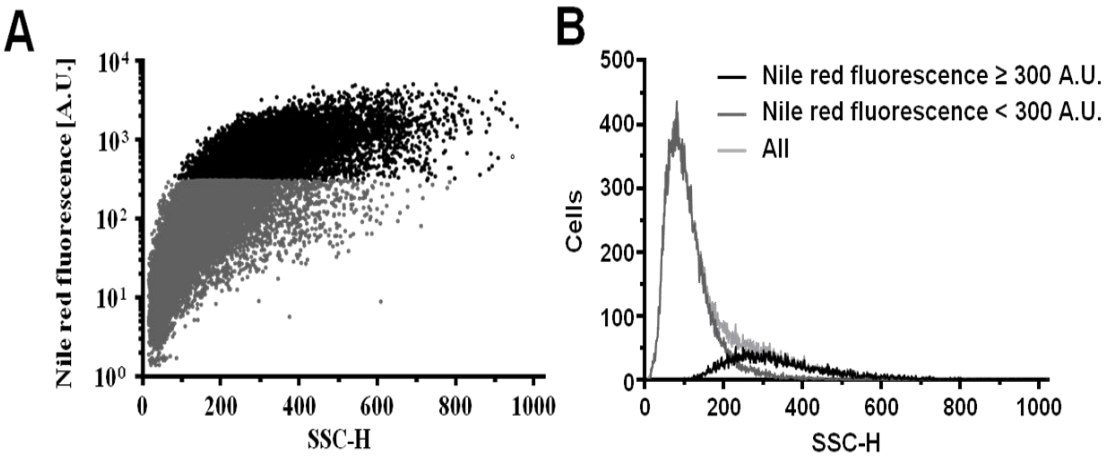

Figure 3.4. Increased nile red fluorescence correlates with granularity in differentiated 3T3-F442A adipocytes. (A) Dot plot of the Nile red fluorescence versus the side scatter SSC-H. The population with a nile red fluorescence of ≥ 300 arbitrary units (A.U.) represented by black dots, the population with a nile red fluorescence of < 300 A.U. by grey dots. **(B)** The histogram of the side scatter reveals that the population with a Nile red fluorescence of ≥ 300 A.U. displays increased side scatter.

Taken together, the data obtained suggest that, according to the correlated increase in size, granularity and fluorescence, the majority of the 3T3-L1 and 3T3-F442A cells at d 12 after the adipogenic induction have accumulated lipids presenting an adipocyte-like phenotype.

Discussion

The aim of this chapter was to investigate the degree of differentiation of both 3T3-F442A and 3T3-L1 cell lines exposed to adipogenic cocktail for 12 days as described in Material and methods chapter. Oil red O staining of neutral lipids revealed an 80 - 90 % increase in lipid accumulation upon differentiation (Figure 3.1), but the inherent difficulty of assigning lipid droplets to cells in this method precludes a quantitative analysis. To circumvent this problem flow cytometry using the fluorescent dye nile red was used and the cells were investigated using three previously established parameters for adipocyte differentiation: fluorescence, size and granularity [301-303]. Data obtained showed that 72 % of the L1 and 80 % of the F442A cells displayed increased lipid content after 12 d of differentiation (Figure 3.2). Both differentiated populations also showed an increase in granularity (Figure 3.3) and fluorescence (Figure 3.4). These results are comparable with previously data from Rubin *et al* [300] that showed a 80 - 90% differentiation of the 3T3-L1 population in response to a similar adipogenic stimulation. Their assessment of differentiation was also based on light microscopy observations of Oil red O stained cells but also on the measurement of triacylglycerol content of the heterogeneous differentiated population by extraction via saponification. The measurement of the percentage of differentiated cells by oil red O staining was similar to the ones I obtained using the same method and can be considered comparable to the 72 - 80 % differentiation rate I obtained using nile red fluorescent staining and flow cytometry as the method is much more accurate and quantitative.

An ~3 fold increase in nile red fluorescence in both 3T3-L1 and 3T3-F442A differentiated adipocytes is similar to the one obtained by Schaedlich *et al* [304] in adipogenic differentiation of the murine stem cell line CGR8. The increased fold fluorescence in F442A adipocytes can be explained by increased susceptibility of this cell line to differentiation

compared to the L1 line [296]. The observation of a second differentiated population in the F442A cell line that presents higher fluorescence and granularity (Figure 3.1 B and 3.4) is also in agreement with previous reports [305, 306]. Le *et al* [305] described heterogeneity in 3T3 cell populations in response to hormone stimulation during adipogenic differentiation. Their study showed that expression of adipogenic markers such as peroxisome proliferator-activated receptor γ (PPAR γ), CCAAT enhancer binding protein α (C/EBP α) and adipocyte protein 2 (aP2) is not sufficient for induction of the lipid-laden phenotype of adipocytes. In order for the cells to accumulate lipids, hormones as insulin, growth hormones or PPARγ ligands (thiazolidinediones, eg. Dexamethasone) are essential for lipid metabolism-related protein induction. The cell-to-cell variability and asynchrony in the response to these factors is responsible for the heterogeneity of the population in differentiation. Their observations are sustained also by Loo *et al* [306] that showed heterogeneity in the differentiating process, with multiple populations different both at molecular levels (expression of PPAR γ, perilipin A, C/EBP α) and phenotypic level (size of lipid droplets) in response to the adipogenic cocktail. Their study showed also formation of a small but highly differentiated population exhibiting numerous large lipid droplets that accumulate increased fluorescence similar to the one I have obtained. As the F442A cell line was shown to present a higher sensitivity to hormonal induction of adipogenesis [296] and considering the number of investigated cells per experiment, this could explain why the two distinct populations can be observed in the F442A compared to the L1. Experiments using fluorescence-activated cell sorting (FACS) and molecular analysis of the cells forming this population could provide more insight on the nature of this heterogeneity in the population.

My results indicate that the established *in vitro* differentiation treatment is inducing a change of the cell phenotype towards a lipid-laden one for 70 - 80 % of the 3T3-L1 and 3T3-F442A cell populations after 12 d of adipogenic induction. Taking into consideration the

observations made by Le *et al* [305] showing correspondence in increased lipid droplets accumulation, size and granularity of the cell and expression of adipogenic gene markers , my results suggest that the populations obtained are differentiated adipocytes.

CHAPTER 4

HIGH CONCENTRATIONS OF THE SATURATED FATTY ACID PALMITIC ACID DO NOT INDUCE ENDOPLASMIC RETICULUM STRESS IN *IN VITRO* DIFFERENTIATED ADIPOCYTES

Excess nutrient intake, elevated saturated fatty acids (SFA) and cholesterol blood levels commonly found in obese individuals have been previously linked to the profound physiological and metabolical alterations in adipocytes [157, 307-310]. Cellular hypertrophy, hyperplasia, mitochondrial and endoplasmic reticulum stress are some of the main phenotypical and physiological changes that occur in the adipose tissue during the onset of obesity. Obesity is the leading risk factor for type 2 diabetes, cardiovascular diseases and hypertension [2, 34] and it was linked to ER stress, inflammation and insulin resistance in adipose tissue [151, 251, 311]. Recent studies have shown that exposure to high concentrations of fatty acids, especially palmitate, leads to development of ER stress in different cell lines such as preadipocytes [221, 250], pancreatic β cells [248, 249]**,** podocytes [312] and hepatocytes [246, 247] but the physiological factors leading to ER stress and activation of the UPR in obese adipocytes are not well characterised. In order to investigate the role of high concentrations of saturated fatty acids in activation of the UPR in adipocytes, the results in this chapter address the following questions:

1. Do high concentrations of saturated fatty acids induce ER stress in adipocytes?

2. Is the differentiation process from preadipocytes to adipocyte affecting the cellular response to saturated free fatty acids?

4.1. The saturated fatty acid palmitic acid does not induce endoplasmic reticulum stress in adipocytes

In order to investigate the role of SFA in induction of ER stress in adipocytes, I evaluated the effect of palmitic acid on *in vitro* differentiated 3T3-F442A and 3T3-L1 cells. Palmitic acid was chosen for these experiments as it represents the most prevalent SFA in the normal diet [313] and also the most abundant SFA in circulating plasma [314, 315]. Moreover, palmitic acid has been shown to be the SFA with the highest cell toxicity due to the fact that acid represents a poor substrate for lipid metabolism and can represent a precursor for lipotoxic ceramide formation. The range of concentrations used in the experiment was in the physiological range reported for rodents and humans [314, 316].

The cells were maintained in serum free medium over night to avoid SFA contamination from serum and incubated with increasing concentrations (0 - 1 mM) of Palmitic acid complexed to fatty acid-free bovine serum albumin (BSA) for up to 48 h. Ethanol was used as no SFA: BSA control treatment as the alcohol served as solvent for the palmitic acid preparations. As a positive control for UPR induction 1 µM thapsigargin was used, as the compound is known to induce ER stress by depleting ER luminal Ca^{2+} stores [317].

Previous reports have indicated that high concentrations of palmitic acid can lead to apoptosis via lipotoxicity or induction of increased oxidative stress in preadipocytes [268], hepatocytes [247, 318] or pancreatic β-cells after 24 h treatment [319-322]. In order to ensure that the results obtained are determined by ER stress induction only, I first evaluated the effect of the proposed palmitic acid concentrations on cell viability. An MTT assay was used to assess cell viability for up to 48 h incubation with the treatment. Palmitic acid did not affect the viability of the 3T3-F442A adipocytes over a period of up to 48 h (Figure 4.1.1

and data not shown), while incubation with 1 μM thapsigargin decreased viability by ~37 % compared to the control.

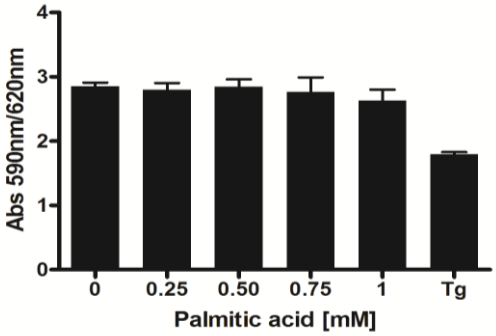

Figure 4.1.1. High concentrations of palmitic acid do not affect adipocyte viability. MTT assay on *in vitro* differentiated 3T3-F442A adipocytes incubated for 48 h with the indicated concentrations of BSA-complexed palmitic acid. 1 μM thapsigargin (Tg) was used as a positive control for induction of ER stress. Thapsigargin (Tg) - treated samples were compared to untreated (0) samples using a two-tailed, unpaired *t*-test.

In order to investigate the role of palmitate on ER stress induction, protein and mRNA levels for UPR markers were investigated. The activity of the PERK signalling branch of the UPR was assessed by Western blotting for CHOP protein, while activation of IRE1α was monitored by measuring the percentage of *XBP1* mRNA splicing.

Incubation of 3T3-F442A adipocytes for 6 - 8 h with increasing concentrations of palmitic acid did not show an quantifiable elevation of CHOP protein levels (Figure 4.1.2 A, B) or induce detectable levels of *XBP1* mRNA splicing (Figure 4.1.2 C, D) for any of the concentrations used.

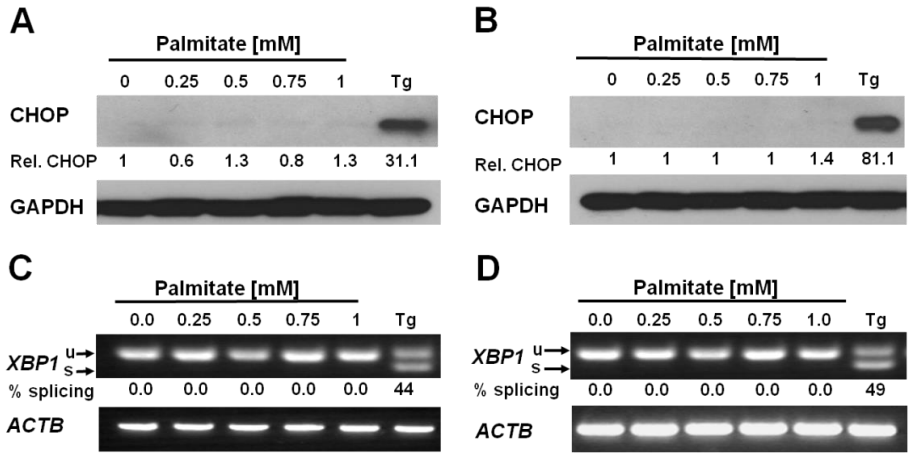

Figure 4.1.2. Palmitic acid does not induce CHOP protein expression (A, B) or *XBP1* splicing (C, D) in 3T3-F442A adipocytes after short term exposure. (A, C) 6 h incubation; (B, D) 8 h incubation; Relative (rel.) CHOP signals were corrected for the loading control GAPDH and the results from the quantitation are shown below the image. *XBP1* splicing was corrected for β-actin mRNA expression and the percentage of spliced *XBP1* mRNA is indicated below the image as % splicing; 1 μM thapsigargin (Tg) was used as a positive control for induction of ER stress; Images presented are representative for three independent biological repeats of the experiment. Abbreviations: u – unspliced *XBP1* mRNA, s – spliced *XBP1* mRNA.

Previous data from the literature indicate UPR activation in response to prolonged exposure (up to 24 h) to high concentrations of saturated fatty acids in variuos cell lines [221, 268, 312]. As the adipocyte main function represents lipids storage and trafficking, I decided to continue the investigatigation of palmitic acid high concentrations role on ER stress induction at longer time points than previously seen in other cell lines, respectively up to 48 h. Western blots analysis for CHOP protein expression in 3T3-F442A adipocytes incubated with palmitic acid for 12 or 24 h did not show any induction of the PERK branch of the UPR (Figure 4.1.3 A, B), results supported also by the lack of *XBP1* mRNA splicingby IRE1α in response to any of the concentrations of palmitate tested at any of the times investigated (Figure 4.1.3 C, D).

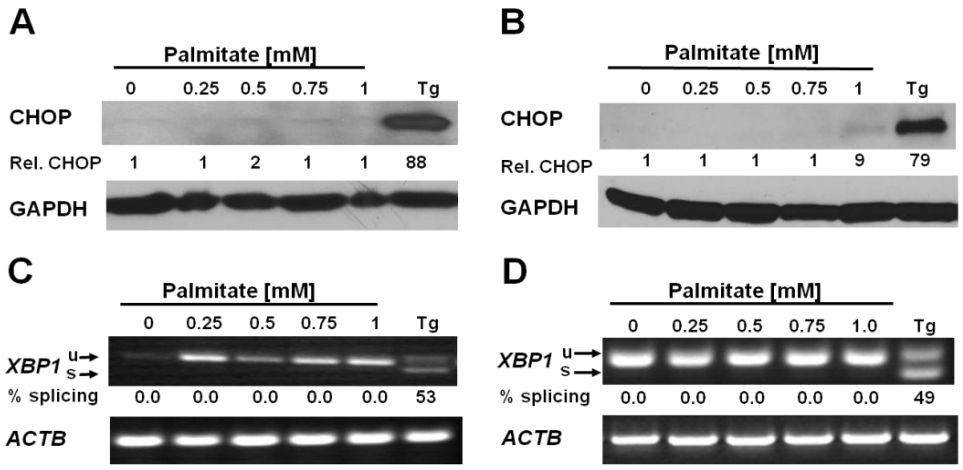

Figure 4.1.3. Palmitic acid does not induce CHOP (A, B) or *XBP1* splicing (C, D) in adipocytes after long term exposure. (A, C) 12 h and (B, D) 24 h exposure of 3T3-F442A adipocytes to various concentrations of palmitic acid. The images shown are representative for three independent biological repeats of the experiment.

Similar results were obtained after incubation with the SFA: BSA complex for 48 h (Figure 4.1.4 A, C).

In order to exclude the possibility that the results shown in Figures 4.1.2 - 4.1.4 are cell line specific, the 48 h incubation was repeated using the 3T3-L1 *in vitro* differentiated adipocytes (Figure 4.1.4 B, D). The results suggest that palmitic acid does not induce CHOP expression or *XBP1* splicing in any of the tested *in vitro* differentiated adipocytes, at any concentration and time point tested (Figure 4.1.4).

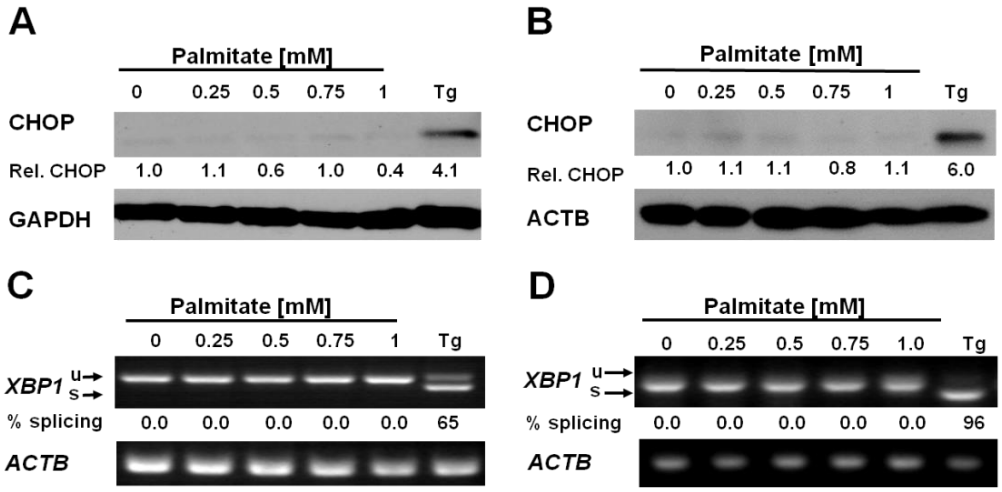

Figure 4.1.4. Palmitate does not induce CHOP protein expression or *XBP1* splicing in adipocytes. (A, B) CHOP expression in *in vitro* differentiated (A) 3T3-F442A adipocytes and (B) 3T3-L1 adipocytes exposed to the indicated concentrations of palmitate complexed to BSA for 48 h. Relative (rel.) CHOP signals were corrected for the loading controls GAPDH or ACTB. (C, D) *XBP1* splicing in *in vitro* differentiated (C) 3T3-F442A adipocytes and (D) 3T3-L1 adipocytes incubated for 48 h with the indicated concentrations of BSA-complexed palmitate. Images are representative for three biological repeats of the experiment.

In order to further validate the effect of high concentrations of palmitic acid on ER stress induction and consolidate the results obtained so far, I investigated also the mRNA levels for ER stress responsive genes such as *HSPA5 (BiP), GADD153 (CHOP)* and *ERDJ4* which are markers of downstream UPR activation [221, 224, 225, 268]. *HSPA5* encodes BiP (binding protein or GRP78), one of the most important ER chaperones involved in the proper folding of nascent proteins and prevention of aggregation of un- or misfolded proteins in the ER lumen that leads to activation of UPR [224, 247]. *GADD153* encodes CHOP (C/EBP homologous protein) protein, a bZIP transcription factor situated downstream in the PERK pathway. CHOP is induced early during ER stress [323] and its expression is maintained stable during activation of the UPR, making it a useful indicator of ER stress induction [224,

225]. *ERDJ4* encodes the DNAJ-like ERdj4 protein, an ER chaperone that acts as a co-factor for BiP in the ER-associated degradation of unfolded proteins [324]. All three genes have been previously shown to be highly induced by ER stress and play a key role in the outcome of the UPR, cell survival or apoptosis [224, 249, 323]. Expression levels of these genes were evaluated by quantitative PCR (RT-qPCR) in 3T3-F442A and 3T3-L1 adipocytes incubated for 48 h with increasing concentrations of palmitic acid. The high physiological concentrations of palmitate used in the experiments did not elevate the mRNA levels for any of the genes of interest: *BiP* (*HSPA5*, Figure 4.1.5 A), *CHOP* (*GADD153*, Figure 4.1.5 B) or *ERDJ4* (Figure 4.1.5 C) especially when compared to the large increases in mRNA levels of these genes in thapsigargin-treated adipocytes.

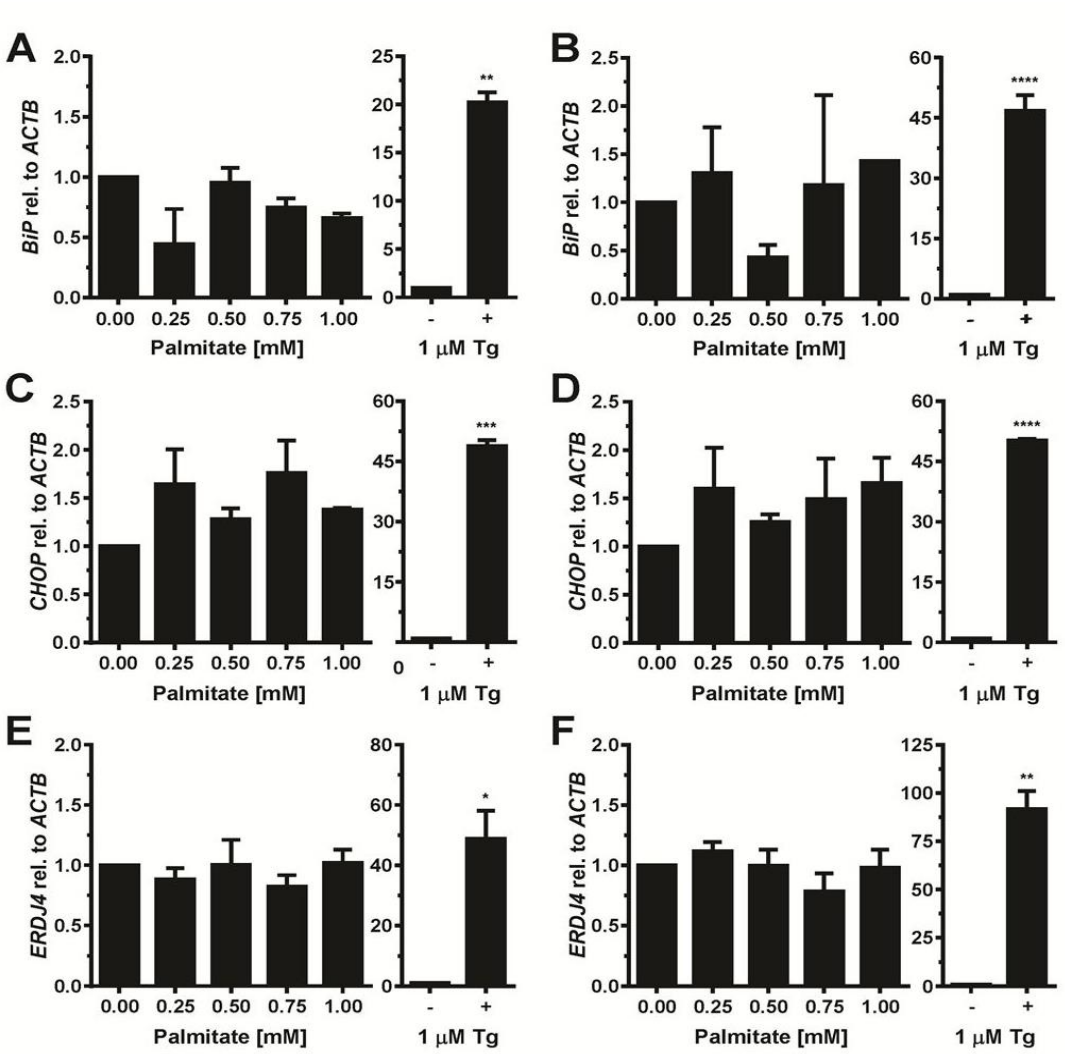

Figure 4.1.5. Palmitate does not induce *BiP*, *CHOP*, or *ERDJ4* transcription in adipocytes. (A, B) *BiP* mRNA, **(C, D)** *CHOP* mRNA, and **(E, F)** *ERDJ4* mRNA levels in *in vitro* differentiated (A, C, E) 3T3-F442A and (B, D, F) 3T3-L1 adipocytes incubated for 48 h with **the** indicated concentrations of BSA-complexed palmitate. The differences in *BiP* mRNA ($p = 0.10$ for 3T3-F442A adipocytes and $p = 0.34$ for 3T3-L1 adipocytes), *CHOP* mRNA ($p = 0.11$ for 3T3-F442A adipocytes and $p = 0.41$ for 3T3-L1 adipocytes), and *ERDJ4* mRNA ($p = 0.48$ for 3T3-F442A adipocytes and $p = 0.41$ for 3T3-L1 adipocytes) levels in the untreated and palmitate treated samples are not statistically significant. *p* values were calculated using ANOVA test and comparing treated and untreated samples after three biological repeats of the experiment. Thapsigargin-treated samples were compared to untreated samples using a two-tailed, paired *t*-test.

Taken together, the results presented in Figures 4.1.1 - 4.1.5 indicate that high concentrations of the SFA palmitic acid do not induce ER stress in adipocytes *in vitro*.

In order to make sure that the results were not artefacts resulting from technical problems regarding the palmitate:BSA complex formation, the complex biological activity was tested. Preadipocytes previously described in the literature to develop ER stress in response to high concentrations of palmitate [221] were incubated with the palmitate:BSA complexes (0 – 750 µM) for 6 - 24 hours [268] and ER stress was investigated via the *XBP1* splicing assay. The results presented in Figure 4.1.6 A, B indicated that palmitate concentrations $\geq$ 500 µM induce *XBP1* splicing starting 12 h, with even lower concentrations inducing *XBP1* splicing at higher time incubations (24 h). These data suggest that the palmitic acid-BSA complexes used in my experiments can induce ER stress as previously described in the literature and the results obtained in mature adipocytes are not a consequence of a technical problem.

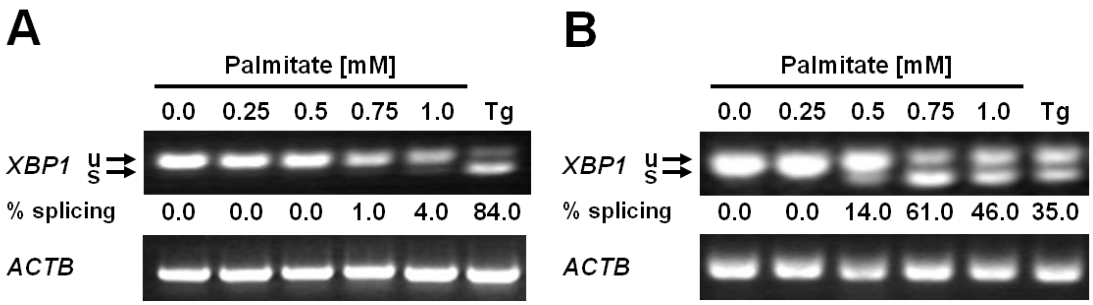

Figure 4.1.6. High concentrations of palmitic acid induce *XBP1* splicing in 3T3-F442A preadipocytes. *XBP1* mRNA splicing in preadipocytes incubated for (A) 12 h and (B) 24 h with the indicated concentrations of palmitic acid; percentage of spliced (s) vs unspliced (u) *XBP1* mRNA is indicated as *% splicing*. Images are representative for three biological repeats of the experiment.

Previous studies have suggested a positive association between ER stress and insulin resistance mainly through UPR-induced activation of proinflammatory signalling pathways such c-jun N-terminal kinase (JNK) and NFκB [206, 246, 247, 250, 311, 325, 326]. Ozcan

et al [311] and Karaskov *et al* [248] showed that chronic elevation of SFA characterising the obese status induces ER stress leading to JNK activation and impaired insulin signaling. The main proposed mechanism is that JNK activation in response to ER stress induces serine phosphorylation of IRS-1, making the substrate protein IRS-1 a poor substrate for the insulin receptor (IR). This results in reduced thyrosine activation of IRS-1 in response to IR activation and decreased insulin signaling transduction upon receptor stimulation [244, 252, 327]. Serine phosphorylation of IRS-1 also inhibits IRS-1/PI3-kinase interaction that is essential for insulin downstream signalling resulting furthermore in decreased signalling [328]. A second proposed mechanism is that upon stimuli or stresses, Akt activity can be modulated via interaction with cytosolic chaperones and in the case of ER stress via interaction with the chaperone BiP (GRP78) [252]. Whyle BiP is primarily an ER protein, it was shown that it can localise also at the plasma membrane under pathological conditions [329, 330] or in the cytosol, as GRP78va. The cytosolic form is results from alternative splicing (retention of intron 1) and is lacking the ER signalling peptide [331]. UPR activation induces BiP up-regulation and promotes the interaction between BiP and Akt that leads to inhibition of serine 473 (S473) phosphorylation in Akt and subsequently decreases its activity. Also, by inhibiting general translation ER stress decreases Akt levels leading to impaired insulin signaling and insulin resistance [253].

To investigate whether high concentrations of the SFA palmitic acid can affect insulin signaling in adipocytes, the murine 3T3-F442A adipocytes were preincubated overnight with the established concentrations of palmitatic acid and then incubated with 100 nM insulin for 15 min to stimulate the insulin signalling pathway. Akt phosphorylation at S473 and was investigated as a marker of impaired insulin signaling.

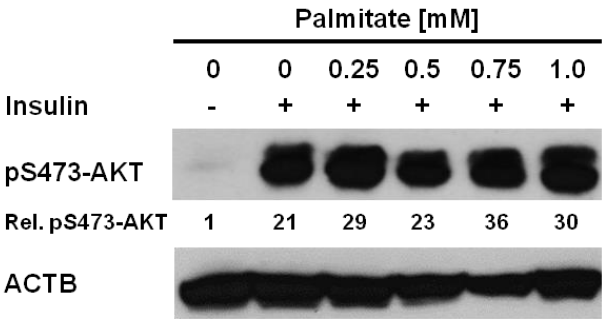

Figure 4.1.7. Palmitate does not inhibit insulin signalling in 3T3-F442A adipocytes. AKT S473 phosphorylation in serum-starved adipocytes incubated for 48 h with the indicated concentrations of BSA-complexed palmitic acid before stimulation with 100 nM insulin for 15 min. Phosphorylation of AKT at S473 (pS473-AKT) and total AKT levels were determined by Western blotting. Relative pS473-AKT signals were corrected to total AKT and values are presented below the pS473-AKT image. Actin (ACTB) was used as loading control. The image shown is representative for three independent biological repeats of the experiment.

The SFA palmitic acid did not inhibit insulin-stimulated AKT S473 phosphorylation in 3T3-F442A adipocytes as shown in Figure 4.1.7, which is consistent with several other reports [332-336], although it did induce a reduction of the AKT serine residue phosphorylation in preadipocytes even at lower concentrations (up to 0.75 mM palmitic acid) (Figure 4.1.8).

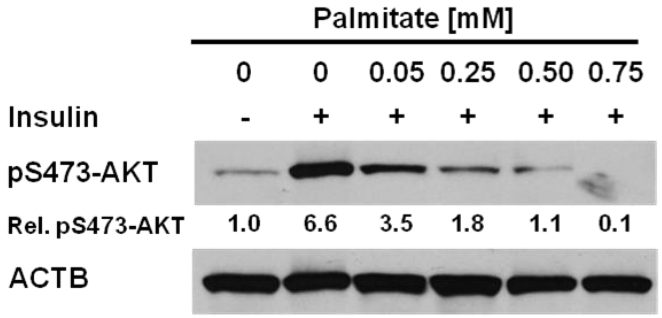

Fig 4.1.8. Palmitate inhibits insulin signalling in 3T3-F442A preadipocytes. AKT S473 phosphorylation in serum-starved preadipocytes incubated for 48 h with up to 0.75 mM BSA-complexed palmitic acid before stimulation with 100 nM insulin for 15 min. Relative pS473-AKT signals were corrected to total AKT and values are presented below the pS473-AKT image. The image presented is representative for three independent biological repeats of the experiment.

In conclusion, high concentrations of palmitic acid were not able to induce ER stress PERK pathway as shown via CHOP protein and mRNA levels investigation in Figures 4.1.2 to 4.1.4 (A,B) and 4.1.5 (B, C). Similar lack of induction was observed also for IRE1α pathway as none of the investigated downstream effectors *HSPA5* (BiP), *ERDJ4* mRNA (Figure 4.1.5 A,B, E, F) or *XBP1* mRNA splicing were induced. Taken together the results indicate that none of the investigated UPR pathways showed activation in response to high concentrations of palmitic acid in *in vitro* differentiated adipocytes.

Investigation of ER stress-induced insulin signalling alterations via AKT S473 phosphorylation as previoulsy described [248, 268, 311, 337], failed also to reveal any evidence that palmitic acid is able to induce ER stress in adipocytes or decreased insulin signalling.

In conclusion, my results indicate that high concentrations of the SFA palmitic acid do not induce an UPR in adipocytes even after up to 48 h incubation.

4.2. The cellular specialisation of adipocytes in lipid storage and metabolism may provide a protection mechanism against SFA-induced ER stress

Adipocytes represent the key modulator of lipid storage and metabolism in the body. In normal physiological states, during feeding, excess energy intake is stored in adipocytes in the form of triacylglycerol (TAG) and cholesteryl esters (CE) in lipid droplets. Postprandial or during fasting, adipocytes release lipids into the blood stream as free fatty acids (FA) and glycerol in order to meet the energy requirements of peripheral tissues. Excess accumulation of lipids in other tissues leads to lipotoxicity, inflammation and insulin resistance [34, 151]. This suggests that the high specialisation of adipocytes in lipid synthesis and breakdown may protect these cells against lipid injury. Taking into consideration the results presented in the first part of this chapter and the previously known data of ER stress induction by high levels of SFA in preadipocytes [268] and other cell lines [247, 248, 268, 318, 338], I hypothesised that cell specific mechanism(s) that protect adipocytes against SFA-induced injury exist. In order to identify possible components of this mechanism (s), I decided to investigate: (1) the basal mRNA levels of ER stress sensors in adipocytes *vs* preadipocytes and (2) the mRNA expression levels of several enzymes involved in SFA metabolism in adipocytes versus preadipocytes, respectively involved in TAG and phospholipid (PL) biosynthesis (described in detail in the *Introduction* chapter).

4.2.1 ER sensing protein basal levels are not involved in adipocyte protection mechanisms against SFA-induced ER stress

I have previously provided evidence that high concentrations of palmitic acid could not induce PERK (CHOP protein and mRNA expression) or IRE1α (*XBP1* mRNA splicing) pathways in adipocytes at any of the concentrations or time points investigated. Also, I have shown in Figure 4.6 that preadipocytes do exhibit *XBP1* splicing in response to palmitate similar to the previously published data by Guo *et al* [268] showing induction of both PERK and IRE1α pathways in response to SFA treatments. As the difference between the adipocyte and preadipocytes is based on the molecular and physiological changes during the differentiation process, I decided to investigate first if the basal levels of ER stress sensor proteins can be affected by this process. Increased basal levels of PERK or IRE1α in adipocytes *vs* preadipocytes could explain the protection against the SFA-induced ER stress investigated.

In order to investigate if this hypothetical mechanism is true, PERK and IRE1α mRNA levels were quantified via RT-qPCR and compared in adipocytes *vs.* preadipocytes.

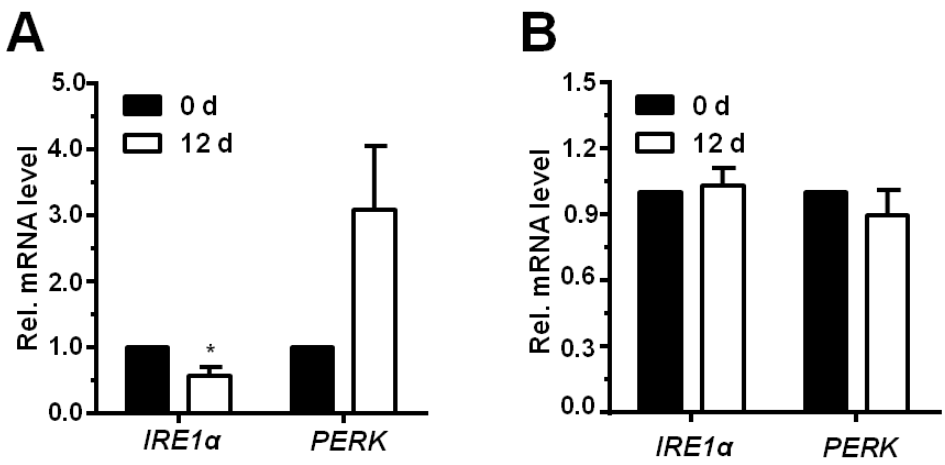

Figure 4.2.1. *IRE1a* and *PERK* mRNA in preadipocytes and *in vitro* differentiated adipocytes. **(A)** 3T3-F442A cells and **(B)** 3T3-L1 cells were differentiated for 12 d. mRNA levels were determined by RT-qPCR and standardised to *ACTB*. A two-tailed, unpaired *t*-test was used to compare the expression level in differentiated cells to the expression level in undifferentiated cells. Results are representative for three biological repeats of the experiment.

Results presented in Figure 4.2.1 panel A show a 40 ± 5 % decrease in *IRE1α* mRNA and a 50 ± 10 % increase in *PERK* levels in 3T3-F442A adipocytes *vs* preadipocytes. In 3T3-L1 cells no significant differences were observed in basal mRNA in adipocytes *vs* preadipocytes for *IRE1α* and respectively *PERK*.

The variation observed in the 3T3-F442A cells needs further addressing, as if the decrease in *IRE1α* mRNA basal levels observed is true, then the 3T3-F442A adipocytes should be more prone to develop ER stress and I have shown that it is not the case (Figures 4.1.2 to 4.1.4 C, D). Also, *PERK* mRNA levels do show a high increase but due to the large error bar the results are not statistically significant suggesting most probably technical variability in sample preparation. More repeats of the experiments are necessary in order to establish if the *PERK* mRNA basal levels are indeed increased in adipocytes *vs* preadipocytes in 3T3-F442A cell line and if this could contribute to the protection against SFA-induced ER stress.

The results obtained in the 3T3-L1 cell line showed no significant differences in the basal mRNA levels of the ER sensor proteins in adipocytes *vs* preadipocytes suggesting that the gene expression of the two investigated proteins is not part of the adipocyte protection mechanism hypothesised. Future repeats of the experiment in 3T3-F442A cells will provide more evidence if the gene expression for the two sensors is indeed altered by the differentiation process or the results obtained so far are generated by technical errors.

4.2.2. Changes in mRNA levels for enzymes involved in SFA metabolism during the differentiation process could confer protection against lipotoxicity in adipocytes

In adipocytes, the two major pathways involved in dietary SFA metabolism are represented by the TAG and phospholipids (PL) biosynthesis pathways. TAG biosynthesis allows the SFA to be stored in lipid droplets until physiologically demanded. TAGs represent the main cellular energy source. The phospholipid biosynthesis pathway leads to formation of phospholipids, essential components of biological membranes and cellular signalling.

In order to investigate if alteration of mRNA levels for enzymes involved in these pathways is conferring protection against dietary-induced SFA lipotoxicity in adipocytes, mRNA levels for some of the main enzymes involved in TAG and PL formation were investigated in adipocytes and preadipocytes.

One of the first steps in dietary SFA metabolism in the cell is desaturation to monounsaturated fatty acids (MUFA), which are the main components of PL, TAG and cholesterol esters [100, 112, 339]. This step is catalysed by stearoyl-CoA desaturase 1 (SCD1), a Δ^9 desaturase localised in the endoplasmic reticulum. In order to investigate if the desaturation capacity of the cell could be involved in the SFA-related injury, mRNA expression levels for *SCD1* desaturase were investigated in adipocytes *vs* preadipocytes.

Results shown in Figure 4.2.2 indicated a 4 ± 0.5 fold increase in *SCD1* desaturase mRNA levels in adipocytes suggesting that cellular specialisation of adipocytes during differentiation is indeed affecting their desaturation capacity.

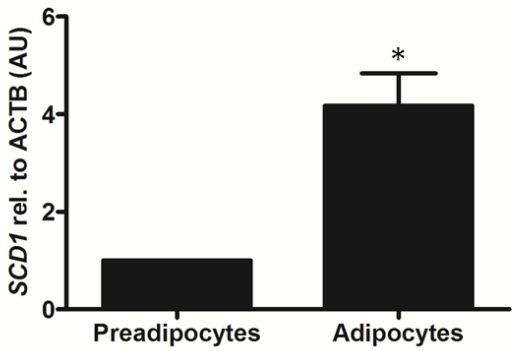

Figure 4.2.2. Basal levels of stearoyl-CoA desaturase 1 (*SCD1*) mRNA are increased in adipocytes versus preadipocytes. [P] preadipocytes versus [A] adipocytes. ***** $p < 0.05$, where the *p* value was obtained using a two-tailed paired *t* test. Results are representative for three biological results of the experiment.

For the TAG biosynthesis pathway, GPAT3 which catalyses acylation and formation of 1-acylglycerol-3-phosphate**,** lipin 1 which is a member of the PAP family involved in dephosphorylation of 1,2-diacylglycerol-3-phosphate to the intermediate 1,2-diacylglycerol and DGAT1 enzyme that catalyses acylation of 1,2-DAG to TAG mRNA levels were studied. Basal mRNA expression for all the investigated genes was shown to be significantly increased in adipocytes *vs* preadipocytes: *GPAT3* expression by 24 ± 2 fold, *lipin 1* by 3 ± 0.5 fold and *DGAT1* by 20 ± 2 fold, suggesting that adipocytes have indeed a higher basal expression of genes involved in SFA metabolism and TAG synthesis as hypothesised (Figure 4.2.3 A-C)

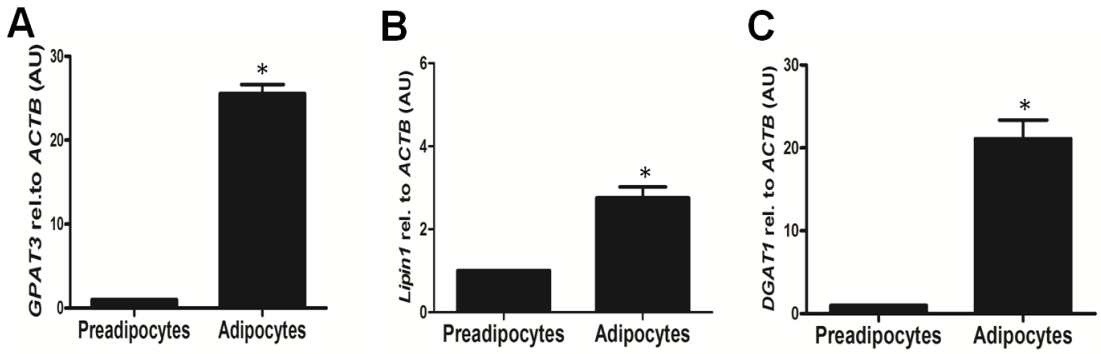

Figure 4.2.3. Basal levels of enzymes involved in TAG biosynthesis are increased in adipocytes versus preadipocytes. RT-qPCR results for genes involved in TAG formation, (A) *GPAT3* mRNA, **p* < 0.001, (B) *Lipin* 1 mRNA, **p* < 0.05, (C) *DGAT1* mRNA, **p* <0.05 in adipocytes [A] versus preadipocytes [P]. *p* values was obtained using a two-tailed paired *t* test. The results are representative of three biological repeats of the experiment.

For the PL biosynthesis pathway, CTP: phosphocholine cytidylyltransferase (CT), the rate-limiting enzyme of the CDP-choline pathway that leads to phosphatidylcholine (PC) formation and CTP: phosphoethanolamine cytidylyltransferase (ET) and the enzyme involved in phosphatidylethanolamine (PE) synthesis were chosen to be investigated in my study. mRNA levels for *CT* and respectively *ET* genes were investigated via RT-qPCR. The *CT* mRNA expression revealed a 5 ± 0.5 fold decrease in adipocytes compared to preadipocytes (Figure 4.2.4 A) while *ET* mRNA levels increased by 5 ± 1 fold (Figure 4.2.4 B) suggesting a possible shift in the PL biosynthesis ratio in differentiated adipocytes.

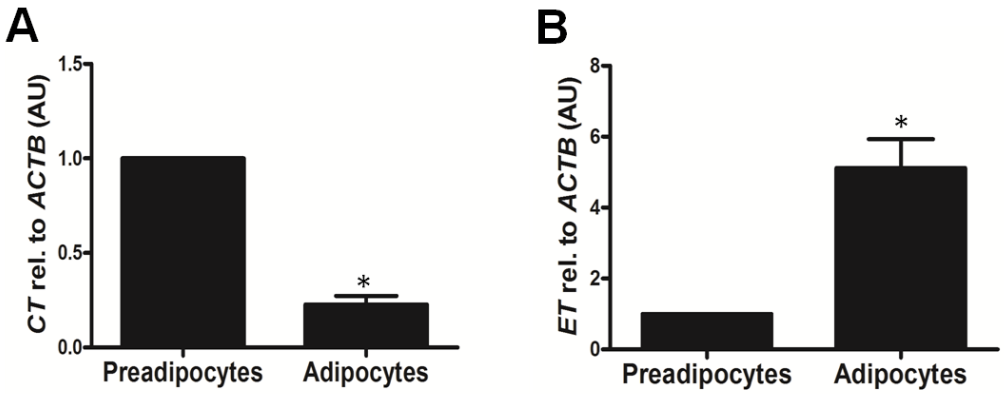

Figure 4.2.4. Basal levels of enzymes involved in PL biosynthesis in adipocytes versus preadipocytes. RT-qPCR results for mRNA levels of enzymes involved in PL formation (A) *CT* mRNA, **p*<0.005, (B) *ET* mRNA, **p*<0.05 in adipocytes versus preadipocytes. *p* values were obtained using a two-tailed paired *t* test. Results are representative for three biological repeats of the experiment.

Taken together my results show up-regulation of all the investigated genes involved in TAG biosynthesis, SFA desaturation and phosphatidylethanolamine synthesis suggesting that adipocyte differentiation process may protect the cells against SFA injury via up-regulation of lipid metabolism enzymes and storage of excess lipids.

Discussion

The SFA palmitic acid does not induce endoplasmic reticulum stress in adipocytes

The first aim of this study was to investigate whether high concentrations of the SFA acid are inducing ER stress in adipocytes. Previously it has been described that high concentrations of SFAs are able to activate the UPR in preadipocytes [221, 250], β pancreatic cells [248, 249], podocytes [312] and hepatocytes [246, 247] but limited data [266, 340] are available for adipocytes, the key players in obesity and metabolic diseases.

In the present chapter I have investigated the effect of up to 1 mM palmitic acid on *in vitro* differentiated 3T3-F442A and 3T3-L1 adipocytes, after short (0-8 h) or long (12-48 h) term incubations. Assessment of ER stress markers CHOP protein and *XBP1* mRNA splicing induction in response the SFA palmitic acid indicate that the SFA treatment was not able to induce either of the markers at any of the time points and concentrations investigated (Figure 4.1.2 to 4.1.4). Furthermore there was no evidence for increases in the basal mRNA levels for the ER stress-responsive genes encoding for BiP, CHOP and ERDJ4 (Figure 4.1.5). As no evidence of UPR was found in any of my experiments, in order to avoid possible negative results due to technical errors, I have also investigated if the palmitic acid: BSA complexes used in the cell treatment were able to induce ER stress in other cell lines as previously reported. For these experiments, 3T3-F442A preadipocytes were used as they were previously described by Guo *et. al* [268] to show ER stress induction in response to palmitic acid: BSA treatment. Induction of *XBP1* mRNA splicing in preadipocytes as shown in Figure 4.1.6 indicated that the designed treatment is biologically active but it does not induce ER stress in adipocytes.

Insulin resistance has been previously linked to ER stress in hepatocyte [332] via activation of proinflammatory pathways JNK or NFκB [244, 248, 251, 311, 332, 341]. As my results

showed no indication of ER stress induction, I have also investigated if palmitic acid is affecting insulin signalling in adipocytes. My results presented in Figure 4.1.7 show that that none of the SFA concentrations used was able to induce AKT S473 phosphorylation in adipocytes after 48 h incubation. SFA treatment control experiments in preadipocytes showed abolishment of AKT S473 phosphorylation in response to insulin stimulation at lower concentrations of palmitic acid (0.75mM) (Figure 4.1.8) as previously reported [268]. These results suggest that high concentrations of SFA palmitic acid do not induce ER stress or insulin resistance in adipocytes even after long term (48 h) incubation.

My results differ from ones previously presented by other groups but the studies vary greatly in the choice of the SFA or SFA mixes used and the adipocyte differentiation protocols. In 2007 Jiao *et al.*[342], using in vitro differentiated 3T3-L1 cells and mouse primary adipocytes, reported rapid induction (1-3 h incubation) of ER stress and possible insulin resistance in response to 0.5 mM mixture of SFAs. These results contradict not only my observations (Figure 4.1.2 to 4.1.5, and 4.1.7) but also several other papers investigating different FA role in ER stress induction. This is due to the fact that the SFA mix used was composed of myristic, lauric, arachidonic, oleic, and linoleic acids and previous studies have shown that unsaturated fatty acids oleic and linoleic acid protect cells from the negative effects of SFAs [343-348] while that the medium-chain fatty acids lauric and myristic acid do not induce insulin resistance [334]. Although the mix used by the group did not contain palmitic acid, palmitate is considered the most common saturated fatty acid reported to induce cell injury [320, 349] and I did not see any induction of ER stress markers or inhibition of AKT phosphorylation previously shown also by other groups [334]. A possible explanation for the results obtained by Jiao *et al* could be that the FA mixture used contains a high concentration of arachidonic acid (AA) and this could induce an intracellular Ca^{2+} mobilisation from the ER compartment towards the cytoplasm, as previously shown [350,

351]. Although AA represents one of the major components of plasma membrane phospholipids, 10 μM AA has been shown to induce Ca^{2+} mobilisation after few minutes incubation with a maximal effect after 30 min incubation [350]. Ca^{2+} release from the ER in response to 25 μM AA have been shown to also induce c-jun mRNA up-regulation (after 3 h incubation) and JNK phosphorylation [351]. These time points coincide with the induction of ER stress markers and JNK phosphorylation that Jiao *et al* describe in their study. PERK and IRE1α phosphorylation were shown to reach a peak at 30 min incubation, being maintained for up to 3 h. This overlap in the time of AA induced Ca^{2+} mobilisation from the ER and the time of ER stress markers induction suggests that AA-induced Ca^{2+} mobilisation from the ER could be the cause of ER stress.

Another study that reported SFA-induced ER stress comes from Kawasaki *et al*. [266] that reported induction of ER stress in 3T3-L1 adipocytes treated with 50 μg/ml of a free fatty acid mixture derived from human serum. Although the group showed induction mRNA levels for most of the ER-stress related genes (*Bip, Chop, Edem, Erdj4, Atf4*), the concentration used in the study is much lower than the one I have used in my experiments and the ones used in most of the published data related to FA effects in various cell lines (21, 22, 24, 93). Also, the described induction of ER stress in response to the FA mixture is very rapid (4 h) surpassing even the induction I could see in preadipocytes incubated with higher concentrations of palmitic acid (Figure 4.1.6). This contradiction between my results and their data could come from the difference in the SFA used, similar to the discrepancy observed in report to the data presented by Jiao et al [342], but the small concentration of fatty acid mixture used suggest also that compounds other than the SFAs present in the fatty acid mixture used by Kawasaki *et al.* seem to be causing ER stress in adipocytes.

Koh *et al.*[352] and Jeon *et al.*[340] have reported induction of eIF2α phosphorylation and downstream *ATF3* mRNA after 24 h incubation of 3T3-L1 adipocytes with 0.5 mM palmitic

acid. As eIF2α can be phosphorylated by other protein kinases that are not related to ER stress [353] and the groups did not show any other marker of ER stress induced, I concluded that the results obtained are not the result of ER stress as I could not see any induction of PERK-eIF2α downstream CHOP protein (Figure 4.1.1-4.1.4. A, B), *XBP1* mRNA splicing 4.1.2 C, D and 4.1.3 C, D) or mRNA for ER-stress related genes in response to even higher concentration of palmitic acid and for longer exposure.

The specialisation of adipocytes in lipid storage and metabolism may provide a protective mechanism against SFA-induced ER stress

The results discussed in the first part of this chapter indicate that high concentrations of the SFA palmitic acid do not induce ER stress or insulin resistance at any of the concentrations and time points used in the study. Palmitic acid is known to be able to induce ER stress in preadipocytes [268] and I have previously shown this effect in my results (Figure 4.1.6). This has raised the question of why the adipocytes are not injured. In order to find an answer to this question, I hypothesised the existence of a cell specific mechanism that protects adipocytes against SFA-induced ER stress. As the differential response to SFAs was observed after the differentiation process and it is known that adipocytes become highly specialised in lipid metabolism and storage [207], I decided to investigate two possible mechanisms that could protect the cell: (1) alteration in basal expression levels for genes encoding for ER-sensor proteins and (2) up-regulation of genes encoding for enzymes involved in SFA intracellular metabolism.

My results indicated no significant differences in the basal levels of *PERK* or *IRE1α* genes in adipocytes *vs* preadipocytes in 3T3-L1 cell line though the results obtained in the F442A line need further investigation to ensure the validity of the results (Figure 4.2.1). If the

variation between the basal mRNA levels of the two ER stress sensors in the F442A line will be proved to be correct and if the imbalance can be translated at protein level, this would suggest a cell line-specific unbalanced UPR response that could include different mechanisms of response to cellular stress and injury. If the results obtained are the consequence of technical errors in sample preparation then the results will be expected to be similar to the ones obtained in the L1 line. This would suggest that the basal level of genes for ER stress main sensor protein is not the reason behind the protection of adipocyte against lipotoxicity.

Investigation of the second proposed mechanism, revealed an up-regulation in mRNA levels for genes encoding for enzymes involved in desaturation (Figure 4.2.2), TAG biosynthesis (4.2.3) and PL-related ET gene (Figure 4.2.4 B) suggesting that this could be the protection mechanism against SFA-induced ER stress in adipocytes. This conclusion is in part sustained by recent evidence in the literature indicating key roles for SCD1 in protection against SFA-induced cell injury (SFAs accumulation and toxicity) in various cell lines such as β-cells [354-357], hepatocytes [358], human epithelial cells [359], human cancer cells [360], and adipocytes [106]. The mechanisms by which SCD1 levels are protecting against lipotoxicity are various. Collins et al. [106] show that in adipocytes SFA are inducing up-regulation of *de novo* lipogenesis and coordinate the up-regulation of elongation and desaturation pathways for disposal of saturated fatty acids and production of monosaturated fatty acids (MUFA) in order to protect the cells from saturated fatty acids toxicity. Dietary SFA such as palmitate and stearic acid have been shown to be substrates for SCD 1 [354, 356, 361] leading to formation of palmitoleate and oleate. Ariyama *et al.* [359] and Miyazaki *et al.* [362] show that *SCD1* knockdown decreases cellular MUFA and consequently increased SFA/MUFA ratio in membrane PLs leading to UPR induction *in vitro* and respectively *in vivo*, thus indicating the role of SCD1 in maintaining cell membrane fluidity and increase

cell survival in response to increase SFA intake. Up-regulation of TAG biosynthesis enzymes correlates positively with formation and enlargement of lipid droplets in adipocytes, the storage capacity of the cell not allowing accumulation of FAs that can cause cellular toxicity. Increased PL synthesis is also correlated with homeostasis of cellular membranes (plasma membrane, ER and mitochondrial) and lipid droplet membrane formation [363-365].

Listenberger *et al* [366] showed that overexpression of *SCD1* in CHO cells increases exogenous palmitate delivery to the TAG pool and protects against palmitate-induced lipoxicity. *SCD1* overexpression was directly correlated with increased desaturation of exogenous palmitic acid and also with increased deposition of palmitic acid in the TAG pool. Using deuterated palmitate, the group shows that in *scd1* overexpressing cells, the TAG fraction contains over 71 % of the deuterated fatty acid, 4.6 fold more than normal CHO cells. Interestingly, only ~ 25 % of the deuterated palmitate in TAG pool was associated with C16:1 while the majority was stored as saturated fatty acid. These data suggest that in case of increased unsaturated FAs levels in the cell due to the enzyme overexpression, *SCD1* can facilitate storage of the saturated FAs in the lipid droplet. Furthermore, the group brings evidence that resistance to palmitate-induced apoptosis is correlated in a dose-dependent manner with *SCD1* expression. They show that 25RA cells that have increased expression of *SCD1* (induced by overexpression of SREBP) but not as much as the *SCD1* CHO cells are moderately resistant to palmitate-induced lipotoxic cell death while the *SCD1* cells are completely protected. Furthermore, the study also establishes a correlation between TAG synthesis and palmitate and oleate induced lipotoxic apoptosis. Using *DGAT1*$^{-/-}$ fibroblasts they show that the deficient cells are similarly sensitive to palmitate as the WT but they exhibit apoptosis also in incubations with oleate whereas the WT cells exhibit only increased TAG synthesis. Taken together theses results show that the role of *SCD1* and TAG

biosynthesis in SFA-induced injury is essential. *Scd1* not only protects the cell against palmitate toxicity but is actively involved in both desaturation and storage of the SFA.

These results are in agreement with the hypothesis I formulated from my observations. During my PhD I have also designed genetic aproaches using lentiviral transduction in order to knockdown or over-express *SCD1* and *DGAT1* in adipocytes and preadipocytes in order to establish a clear correlation between the TAG synthesis and the protection against the palmitate toxicity. Due to technical problems though these experiments were not started. Further studies using the already set up lentiviral system will be able to show if indeed, up-regulation of the enzymes involved in TAG synthesis represents the adipocyte protection mechanism against palmitate lipotoxicity.

CHAPTER 5

INCREASED CONCENTRATIONS OF CHOLESTEROL DO NOT INDUCE UPR IN ADIPOCYTES

The results described in Chapter 4 provide evidence that obesity-related high concentrations of SFA are not able to induce ER stress in adipocytes. In this chapter I have continued to investigate other lipid factors in the obese individuals' blood that may affect homeostasis and lead to organelle dysfunction in adipocytes.

Hypercholesterolemia, or high blood cholesterol concentrations, is one of the hallmarks of obesity [269, 367, 368] and a major risk factors in development of cardiovascular and metabolic diseases [369-371]. In the adipose tissue, the second major tissue involved in cholesterol metabolism after the liver, excess cholesterol was shown to lead to abnormal cellular cholesterol distribution and organelle dysfunction [308, 372, 373] but the mechanisms involved are not fully elucidated. Recent studies have linked high cholesterol concentrations with mitochondrial and ER stress in macrophages [270, 374, 375] and smooth muscle cells [271]. The present chapter is investigating whether high concentrations of cholesterol are inducing the UPR in adipocytes and thus contributing to cellular dysfunction.

5.1. High cholesterol concentrations are not able to induce ER stress in adipocytes

Accumulation of excess unesterified (free) cholesterol (FC) in the cell has been previously shown to be cytotoxic due to an increased imbalance in the FC: phospholipid ratio in the cellular membrane leading to membrane rigidity and alteration of lipid raft dynamics [376]. This FC-induced cytotoxicity was described especially in cells that exhibit a low endogenous cholesterol biogenesis and rely on exogenous sources, such as adipocytes [377-379]. In humans, adipose tissue contains the largest pool of free cholesterol in the body, which is estimated at 25% of total body cholesterol [380, 381]. This amount of free cholesterol doubles in obese individuals [378, 382]. In the normal physiological state, most of the free cholesterol uptaken by the adipocytes is stored as cholesteryl esters in the lipid droplet but

during excess hyperlipidemic intake, the cell becomes overloaded with FC and this could lead to organelle dysfunction and cellular stress.

In order to investigate the role of high concentrations of cholesterol on ER stress induction in adipocytes, *in vitro* differentiated 3T3-F442A and 3T3-L1 adipocytes were incubated for 48 h with 100 µg/ml acetylated low density lipoprotein (AcLDL). UPR activation was assessed at the protein level - CHOP expression by Western blotting, and at the mRNA level - *XBP1* splicing by PCR (Figure 5.1.1). My results showed that AcLDL did not elevate of CHOP protein expression (Figure 5.1 A, B) or induce *XBP1* mRNA splicing (Figure 5.1.1 C, D).

One of the mechanisms involved in limitation of cellular FC-induced toxicity in adipocytes is cholesterol esterification that allows storage of cholesterol in the lipid droplets. This esterification is catalysed by the ER membrane acyl-coenzyme A: cholesterol acyltransferase (ACAT) enzyme [383], [384]. Inhibition of ACAT1 activity has been shown to increase the FC overloading in macrophages and muscle cells [271, 374, 383, 385] and has been associated with obesity and type 2 diabetes [386]. In order to investigate if ACAT activity is protecting against cholesterol overloading-induced ER stress in adipocytes, I have chemically inhibited esterification of cholesterol using the ACAT1 inhibitor TMP-153 [290]. Inhibition of ACAT with TMP-153 in the presence or absence of AcLDL did not induce elevation of CHOP protein levels or induce *XBP1* mRNA suggesting that cholesterol does not induce ER stress in adipocytes independently of the ACAT enzyme activity (Figure 5.1.1).

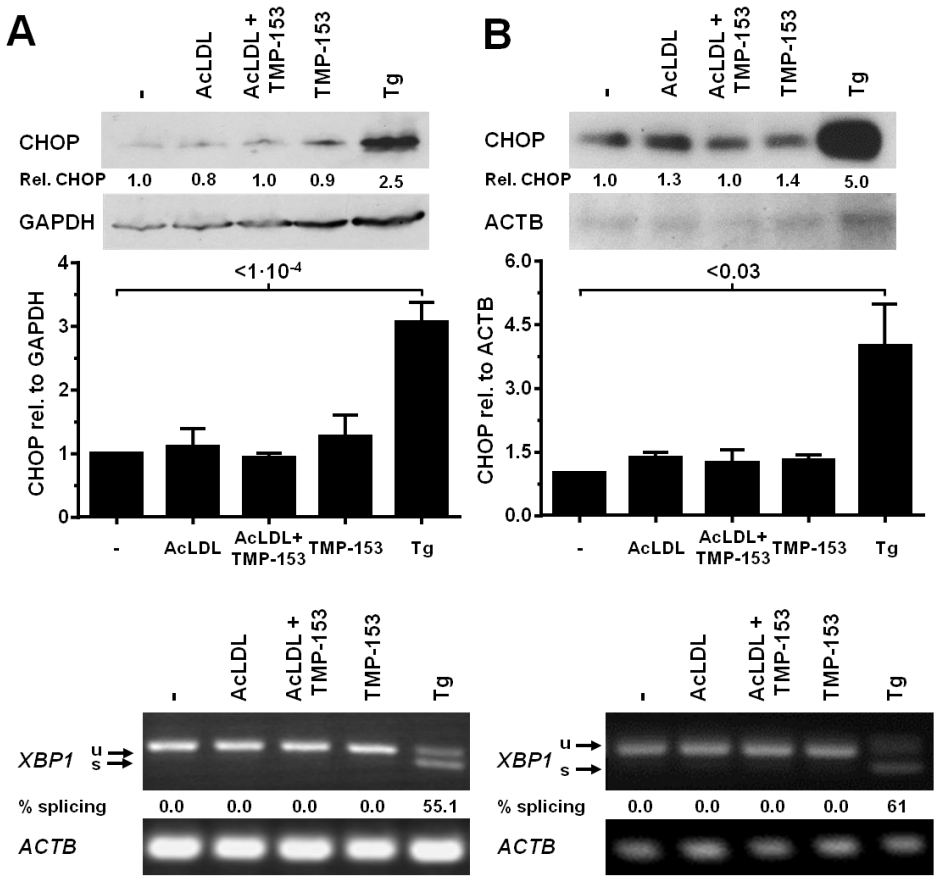

Figure 5.1.1. High cholesterol concentrations do not induce CHOP expression or *XBP1* splicing in adipocytes (A, B) CHOP protein levels and **(C, D)** *XBP1* splicing in *in vitro* differentiated (A, C) 3T3-F442A and (B, D) 3T3-L1 adipocytes incubated for 48 h with 100 µg/ml human acetylated LDL (AcLDL), AcLDL and 0.6 µM of the ACAT inhibitor TMP-153, 0.6 µM TMP-153, 1.0 µM Tg, or left untreated ('-'). The average and standard error of three independent experiments are shown in the bar graphs. Differences in CHOP protein levels between the untreated sample and the samples treated with AcLDL, AcLDL and 0.6 µM TMP-153, and 0.6 µM TMP-153 are not statistically significant (p = 0.26 for 3T3-F442A adipocytes and p = 0.35 for 3T3-L1 adipocytes in a repeated measures ANOVA test assuming equal variabilities of the differences).

To further validate these results, the next step was to investigate the mRNA levels of genes encoding for ER chaperones BiP and CHOP proteins in response to high concentrations of AcLDL. mRNA levels were quantitated using RT-QPCR and were normalised to β-actin mRNA. Results presented in Figure 5.1.2 show that cholesterol did not induce *BiP* or *CHOP*

m RNA levels in the presence or absence of ACAT1 inhibitor TMP-153 suggesting again that cholesterol does not induce ER stress in adipocytes.

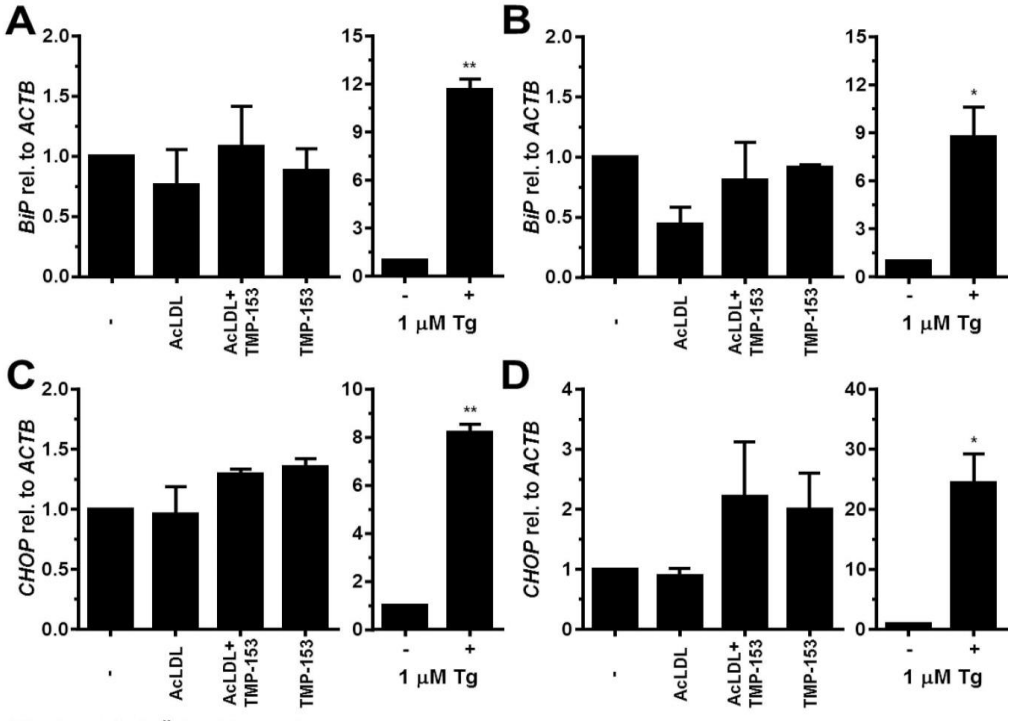

Figure 5.1.2. Cholesterol loading does not induce *BiP* or *CHOP* transcription in adipocytes.(A, B) *BiP* mRNA and **(C, D)** *CHOP* mRNA levels in *in vitro* differentiated (A, C) 3T3-F442A and (B, D) 3T3-L1 adipocytes incubated for 48 h with human acetylated LDL (AcLDL), AcLDL and 0.6 µM TMP-153, 0.6 µM TMP-153, 1.0 µM Tg, or left untreated ('-'). The average and standard error of three independent experiments are shown. Differences are not statistically significant (*BiP* mRNA: $p = 0.34$ for 3T3-F442A adipocytes and $p = 0.11$ for 3T3-L1 adipocytes; *CHOP* mRNA: $p = 0.09$ for 3T3-F442A adipocytes and $p = 0.11$ for 3T3-L1 adipocytes). *p* values were obtained from a repeated measures ANOVA test comparing the samples treated to the untreated (-) samples and assuming equal variabilities of the differences. Thapsigargin-treated samples were compared to untreated samples using a two-tailed, unpaired *t*-test.

In order to verify if my designed AcLDL treatment can induce ER stress, *in vitro* differentiated THP-1 macrophages were incubated with AcLDL for 16 h in the presence or absence of the ACAT inhibitor TMP-153. The macrophage cell line was chosen for this experiment due to previous data in the literature describing the THP-1 cells as prone to

develop ER stress in response to cholesterol overloading [291, 387]. The 16 h time point chosen was also in agreement with previous publications indicating elevation in apoptosis markers in macrophages after 18 h incubation with 100 µg/ml of acLDL [291, 374]. Evaluation of UPR induction was assessed as *XBP1* mRNA splicing and showed induction of splicing in both the presence and absence of the ACAT inhibitor TMP-153 (Figure 5.1.3). These results proved that the treatment used in the study is biologically active and has similar effects with the previous reported ones, supporting the validity of my findings.

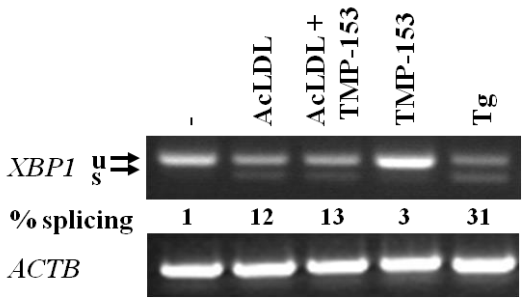

Figure 5.1.3. Cholesterol induces *XBP1* mRNA splicing in *in vitro* differentiated THP-1 macrophages. Cells were incubated for 16 h with either 100 µg/ml AcLDL , AcLDL and 0.6 µM TMP-153, 0.6 µM TMP-153 alone, 1.0 µM Tg or left untreated ('-'). Image presented is representative for three biological repeats of the experiment.

Taken together, my results indicate that high concentrations of cholesterol, although able to induce UPR in other cell lines (Figure 5.1.3 and ref [291, 374, 375]) are not able to induce ER stress in adipocytes.

Discussion

High plasma levels of cholesterol have been associated with obesity and cellular dysfunction. Accumulation of FC in various cell lines has been shown to result in plasma membrane stiffness [388, 389], formation of cholesterol needle-shaped crystals that damage organelle structure [390], accumulation of cytotoxic oxysterols [376], and activation of apoptotic pathways [385]. Recently, several groups have linked cholesterol overloading with ER stress both *in vitro* [270, 271, 374, 375] and *in vivo* [374] but few studies have investigated its effect in adipocytes, the only cells capable of storing large amounts of lipids in the organism and one of the main affected cell types in obesity.

In order to assess the impact of cholesterol overloading in adipocytes, I have investigated whether high concentrations of AcLDL can induce ER stress in *in vitro* differentiated adipocytes. My results indicate that in both 3T3-F442A and 3T3-L1 adipocytes treatment with high concentrations of cholesterol was not able to induce any of the UPR pathways investigated: CHOP protein and mRNA expression (Figure 5.1.1 A, B) (Figure 5.1.2 C, D) for PERK and *XBP1* mRNA splicing (Figure 5.1.1 C, D) or *BiP* mRNA (Figure 5.1.2 A, B) for IRE1α. These results suggest that high cholesterol concentrations do not induce ER stress in adipocytes.

My conclusion differ from the data reported by Chen *et al* [391] that shows induction of BiP and CHOP protein expression in response to increased concentrations of oxidised LDL (OxLDL) in 3T3-L1 adipocytes. The results though cannot be fully compared as the cholesterol-modified form used is different. Though both forms of LDL have similar cellular uptake [392], due to the presence of both oxidised protein and lipids, OxLDL can have multiple effects including impaired degradation [393-396] and enhanced inflammatory stimulation [395, 397, 398]. Also, the plasma AcLDL form is very reduced *in vivo* compared

to OxLDL, but used as a cholesterol substitute in *in vitro* experiments due to increased cellular uptake compared to the native form [399] and in order to specifically avoid cellular effects resulted from the oxidised components of molecule [400]. The *in vivo* oxidation of LDL was shown to be the results of various enzymes including NADPH oxidase, 15-lipoxygenase, myeloperoxidase and mitochondrial electron transport system enzymes [399] and takes place mainly in the vascular wall. The biological effects are though strongly influenced by the modification of the component proteins and lipids, with the degree of oxidation strongly influencing the cellular effects of the altered lipoprotein [401]. Even mild oxidation of LDL-coating phospholipids was shown to induce activation of proinflammatory pathways in vascular cells [401] and oxidative stress in endothelial cells [402, 403], human fibroblasts [404] and rat neurons [405]. Increasing degrees of oxidation were shown to be associated with increased biological cytotoxic effects leading to apoptosis in macrophages via activation of caspase-3 [406]. As my results did not show any induction of UPR markers at protein or mRNA level, and considering the above presented differences in the two modified forms of LDL, I consider that the ER stress induction showed by Chen *et al* [391] may be the result of the effect of oxidised components of LDL and not the cholesterol overloading.

As cholesterol loading did not show any effect on UPR induction in adipocytes, I have also investigated if cholesterol esterification via ACAT activity is the mechanism that protects adipocytes against this lipid overloading injury. Chemically-induced increase in intracellular FC levels via inhibition of ACAT1 using TMP-153 [290] revealed no changes in the UPR status in any of the cell lines investigated suggesting the existence of possible ACAT-independent cell-specific protection mechanisms against FC lipotoxicity in adipocytes. One of these mechanisms could be originating from lipid storage in adipocytes and metabolic functions of adipocytes. Previous studies have suggested that adipocytes are not only able to

store increased amounts of cholesterol, but they also use more FC in order to maintain the homeostasis and functionality of the lipid droplet (LD) [407, 408]. Therefore, adipocytes present an increased utilisation of uptaken cholesterol. LD biogenesis, though not fully understood, has been described as formation of neutral lipids within the ER membrane that leads to distension of the membrane and budding of LDs surrounded by a single ER-derived monolayer rich in FC and phosphatidylcholine [408-410]. Zechner *et al* [407] provided evidence that adipocyte differentiation, respectively LD formation, is linked to increased FC cellular storage. Similarly, Prattes *et al.* [411] have shown that expansion of the TAG pool is associated with increased cholesterol storage in both cholesteryl esters and FC form, with FC localised mainly in the LD membrane. Both studies have brought evidence that support the hypothesis that in case of cholesterol overloading the adipocyte can direct the FC into two possible pathways: esterification and storage in the pre-existing LD and incorporation into membranes of the new or enlarged LD. Up-regulation and increased translocation of the cholesterol trafficking protein caveolin 1 [412] to the surface of lipid droplets in response to cholesterol overloading [413] brings more evidence that this model may reflect the physiological response of the adipocyte to cholesterol overloading. Future experiments are needed though in order to provide better insight into this proposed protection mechanism. Due to time limitations, these questions could not be answered in my study but future investigations looking at the cellular fate of cholesterol taken-up by adipocytes will provide further insight if LD membrane biogenesis is indeed involved in protection against lipid-injury along with the increased storage capacity. In depth evidence are also needed to exclude the possibility that TMP-153 may not fully inhibit the ACAT enzymatic activity in adipocytes. Previous studies have indicated that TMP-153 concentrations similar to the one used in my treatments inhibit cholesterol esterification in other cell lines such as human colonic carcinoma LS180 (half maximal inhibitory concentration, IC_{50} = 150 nM) and human

hepatoma Hep G2 cells (IC_{50} = 330 nM) [414] or reduce plasma cholesterol in various animals such as hamsters and rats, with an IC_{50} of 5-10 nM [290]. This suggests that the 0.6 µM TMP-153 chosen for my experiments should be able to inhibit ACAT esterase activity and increase intracellular FC levels. However, more evidences are needed in order to reach this conclusion. These could be provided by constructing a TMP-153 dose-response curve in adipocytes in order to establish the exact IC50 needed to inhibit ACAT activity. Experiments using fluorescent labelled LDL could also elucidate the fate of the uptaken cholesterol in adipocytes via fluorescent microscopy while lipid extraction and fractionation by thin-layer chromatography could give an indication if the cholesterol is indeed stored in the lipid droplets as cholesteryl esters or used in membrane composition.

CHAPTER 6

THE PROINFLAMMATORY CYTOKINES TNF ALPHA, IL-6 AND IL-1 BETA DO NOT INDUCE AN UPR *IN VITRO* DIFFERENTIATED ADIPOCYTES

In the last decade, a number of studies have indicated that obesity is associated with chronic, low grade inflammation. It is characterized by abnormal cytokine production, increased acute-phase reactants, and activation of inflammatory signalling pathways [186]. A very important feature of this obesity-related inflammatory response is that it appears to be triggered and to reside predominantly in the adipose tissue [151, 415] due to two major events: macrophage infiltration and activation [153, 416], and dysfunctional hypertrophied adipocyte secretion of proinflammatory adipokines [155, 417]. Accumulation of proinflammatory cytokines in adipose tissue has been shown to contribute to a self-sustaining vicious inflammatory cycle leading to cellular dysfunction and obesity-related insulin resistance [418-421] but the molecular mechanisms involved are not yet fully understood. Recent data have shown that inflammatory cytokines such as TNFα, IL-6 and IL-1β elicit ER stress in L929 cells [255] hepatocytes and β-cells [272-274] and that activation of the UPR leads to subsequent activation of proinflammatory pathways [422, 423] and insulin resistance [167, 424-426]. Thus, I decided to investigate if proinflammatory cytokines in adipose tissue (TNFα, IL-6 and IL-β) can induce ER stress in adipocytes contributing to or directly inducing cellular dysfunction.

6.1. TNFα does not induce ER stress in adipocytes

TNFα is a dual proinflammatory cytokine involved in both host protective immune responses against infectious pathogens and in host damage in sepsis, tumour cachexia and autoimmune diseases [427, 428]. Due to its dual role, abnormal expression of TNFα has been extensively studied and has been linked to various immunological diseases. Recently, besides its immune roles, it has been shown that TNFα plays an important role in lipid [429-431] and glucose metabolism [418, 432, 433]. Kern *et al*.[434] and Hotamisligil *et al.* [424] have shown that,

though TNFα is mainly secreted by activated macrophages, the adipose tissue represents also a signifiant source of endogenous TNFα and that, its expression is elevated in this tissue in obesity in both human and animal models. Abnormal elevated TNFα levels in adipose tissue have been suggested to be the key mediator of insulin resistance via various mechanisms including: alteration in expression of glucose transporter 4 (GLUT4) gene [432, 433], inhibition of tyrosine phosphorylation of insulin receptor substrate 1(IRS-1) [418] and induction of oxidative stress [435-437]. It was shown to play an important role in inhibition of preadipocyte differentiation via down-regulation of adipogenic transcription factors such as PPARγ and C/EBPα and C/EBPδ [438-440], thus limiting the possibility of enhanced lipid clearance via storage of lipids in mature adipocyte in case of excess intake. Recently high concentrations of TNFα have been shown to activate the UPR in L929 cells [255], hepatocytes [441] and pancreatic β-cell [422]. Considering the fact that ER stress is known to mediate inflammation and insulin resistance in response to cellular dysfunction and the previous provided evidence of UPR induction in response to elevated TNFα, I decided to investigate the possibility that ER stress is the mediator of TNFα effects in obese dysfunctional adipocytes. In order to answer this objective, *in vitro* differentiated 3T3-F442A and 3T3-L1 adipocytes were exposed to 0-25 ng/ml TNFα for 0-24 h. Markers of ER stress were investigated at protein (CHOP expression) and mRNA level (*XBP1* mRNA splicing).

UPR induction in response to TNFα treatment was initially investigated during short-term exposure (0-6 h) as TNFα activation of proinflammatory molecular pathways is known to be rapid and transient. Also, Xue *et al*.[441] have described a possible transient activation of ATF6 and *XBP1* splicing induction in adipocytes after 4 h incubation with TNFα. My results, though, did not reveal any induction of any of the investigated UPR markers: CHOP

protein expression (Figure 6.1.1 A-C) or *XBP1*mRNA splicing (Figure 6.1.1 D-F) at any of the time points or the TNFα concentrations investigated.

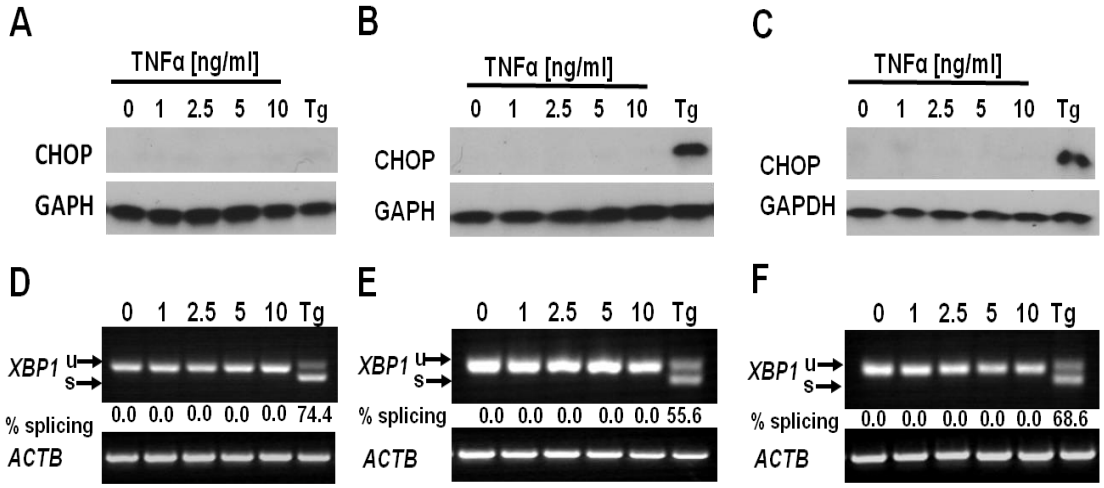

Figure 6.1.1. TNFα does not induce CHOP protein expression or *XBP1* splicing in adipocytes after short time incubation. (A-C) CHOP protein expression, (D-F) *XBP1* mRNA splicing in *in vitro* differentiated adipocytes incubated for (A, D) 2 h; (B, E) 4 h and (C, F) 6 h with the indicated concentrations of TNFα. Images are representative for three biological repeats of the experiments.

In order to further investigate if TNFα is involved in ER stress induction in adipocytes, the experiments were continued by exposing the *in vitro* differentiated cells to TNFα for longer periods of time (24 h) and higher concentrations of TNFα (25 ng/ml).

To avoid false results due to apoptosis resulted from TNFα-induced ROS accumulation as described in various cell lines [442, 443], before investigating the ER stress induction, the viability of the TNF treated cells was assessed using an MTT assay. The results shown in Figure 6.1.2 indicate that the concentrations used did not affect the cell viability even after 24 h incubation with TNFα.

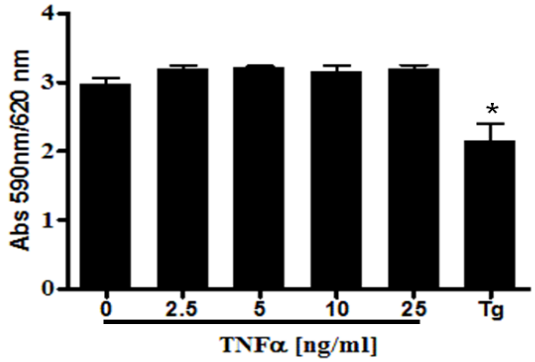

Figure 6.1.2. TNFα does not affect viability of adipocytes. MTT assay of *in vitro* differentiated adipocytes incubated with 0-25 ng/ml TNFα for 24 h. Tg, 1 µM thapsigargin. Differences between TNFα treated and untreated samples are not significant. * $p < 0.05$ for Tg compared to control "0". A repetead measures ANOVA test was used to compare treated and untreated samples. The data shown are representative for three biological repeats of the experiment.

The 24 h incubation of adipocytes with up to 25 ng/ml TNFα revealed that TNFα was not able to induce *XBP1* mRNA splicing (Figure 6.1.3) even at higher concentrations.

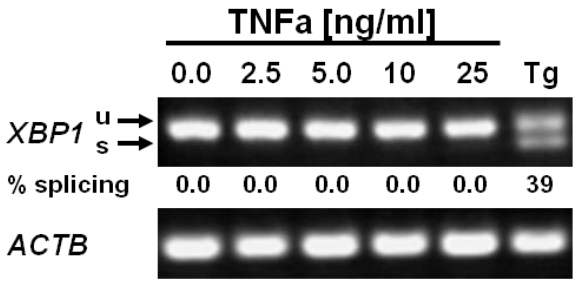

Figure 6.1.3. High concentrations of TNFα do not induce *XBP1* mRNA splicing in adipocytes. *XBP1* splicing in *in vitro* differentiated 3T3-F442A adipocytes incubated with the indicated concentrations of TNFα for 24 h. The results are representative for three biological repeats of the experiment.

In order to validate the TNF α activity, induction of JNK MAPK kinase was investigated as previously described in the literature [192, 444-446]. Preadipocytes were incubated with 25 ng/ml TNFα for 30 min and JNK phsophorylation was assessed via Western blotting. TNFα

strongly induced JNK phosphorylation in preadipocytes as presented in Figure 6.1.4 suggesting that the TNFα used in the experiment is active.

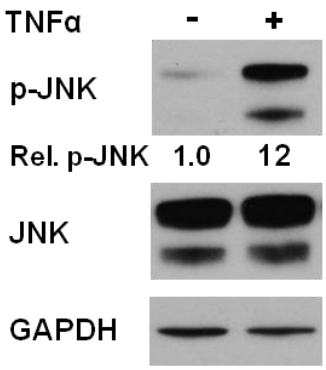

Figure 6.1.4. TNFα treatment induces JNK phosphorylation in preadipocytes. 3T3-F442A preadipocytes were incubated with 25 ng/ml TNFα for 30 min and JNK phosphorylation was assessed by Western blotting. Image is representative for three biological repeats of the experiment

Taken together, the absence of induction of any of the UPR markers investigated at protein level (CHOP) or mRNA level (*XBP1*) after short or long term incubation and for any of the investigated TNFα concentrations suggest that the cytokine does induce ER stress in *in vitro* differentiated 3T3-F442A and 3T3-L1 adipocytes.

6.2. The proinflammatory cytokines IL-6 and IL-1β do not induce ER stress in adipocytes

In part 1 of this chapter I have shown that high concentrations of the proinflammatory cytokine TNFα do not induce ER stress in *in vitro* differentiated 3T3-F442A and 3T3-L1 adipocytes. To further characterise the role of inflammation in ER stress induction in obesity, I continued my study with the investigation of two other possible cytokines involved in the adipose tissue proinflammatory process and known to be elevated in obese individuals: IL-6 [155, 417] and IL-1β [447]. Both interleukins are mediators of inflammatory responses and have been linked to insulin resistance *in vitro* and *in vivo* [417, 426, 448]. Also, circulating levels of IL-6 have been positively correlated with increase in the body mass index (BMI) [449] and general expansion and dysfunction of adipose tissue [450].

To study whether these two proinflammatory cytokines induce ER stress in adipocytes, I exposed *in vitro* differentiated 3T3-F442A adipocytes to various concentrations (0 – 200 ng/ml) of IL-6 or IL-1β for up to 24 h. The concentration range chosen for the experiment is higher than the circulating levels found in the blood of obese subjects (e.g. for BMI > 35, ~ 8 pg/ml IL-6 [451]) but within the concentrations used for *in vitro* models of obesity [452, 453].

Incubation for 24 h with high concentrations of IL-6 or IL-1β failed to induce *XBP1* mRNA splicing in adipocytes as presented in Figure 6.2.1.

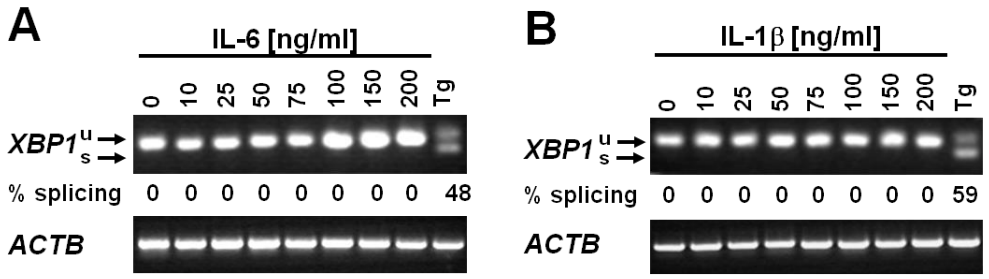

Figure 6.2.1. The proinflammatory cytokines IL-6 and IL-1β do not induce ER stress in adipocytes. *XBP1* mRNA splicing in *in vitro* differentiated 3T3-F442A adipocytes incubated for 24 h with the indicated concentrations of (A) IL-6 and (B) IL-1β. Results are representative for three biological repeats of the experiment.

To validate the activity of the two cytokines used, JNK activation was assessed in preadipocytes, in response to 200 ng/ml IL-6 or IL-1β. Short time incubation (0-30 min) of the cells in the presence of the cytokines preparations strongly induced JNK phosphorylation as shown in Figure 6.2.2 suggesting that the previous obtained results showing no induction of *XBP1* mRNA in response to the cytokine treatment are not the results of technical errors.

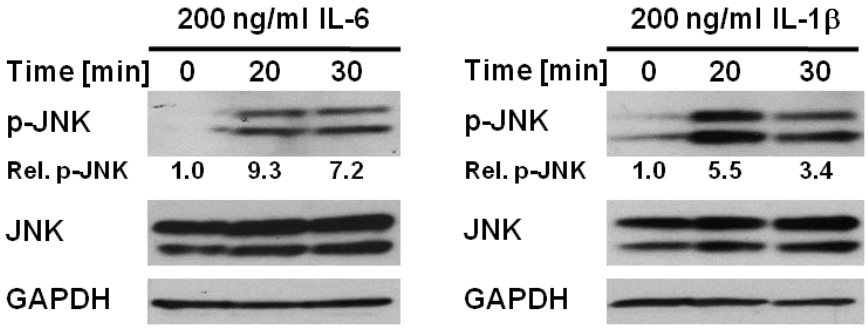

Figure 6.2.2. IL-6 and IL-1β induce JNK phosphorylation in 3T3-F442A preadipocytes. JNK phosphorylation in 3T3-F442A preadipocytes incubated for the indicated times with (A) 200 ng/ml IL-6 or (B) 200 ng/ml IL-1β. Results are representative for two biological results of the experiment.

Taken together, my results suggest that the proinflammatory cytokines IL-6 and IL-1β, similar to TNFα, do not induce ER stress in *in vitro* differentiated 3T3-F442A and –L1 adipocytes.

Discussion

TNFα does not induce ER stress in adipocytes

My results revealed no induction of any of the UPR markers for any of the time points or concentrations investigated suggesting that TNFα does not induce ER stress in *in vitro* differentiated 3T3 F442A or 3T3 L-1 adipocytes. My conclusions differ from the one drawn by Koh *et al* [352] that showed *XBP1* splicing and phosphorylation of eIF2α protein in response to TNFα treatment in adipocytes. This study shows that TNFα effects are mediated mainly via TNFα-induced down-regulation of mitochondrial biogenesis and mitochondrial injury rather than via direct ER stress activation. This suggests a possible connection but not a causal role for TNFα in UPR induction. As I could not see any ER stress induction in response to TNFα, I concluded that the experimental results obtained by Koh *et al* may be induced by other mechanisms than the UPR that were not fully described or investigated in the study. Besides down-regulation of mitochondrial biogenesis, there are two other mechanisms proposed for induction of UPR by TNFα. The first one is related to the TNFα-induced ROS formation [441], while the second is proposing that TNFα could induce ER stress via up-regulation of proinflammatory cytokines and increased ER burden.

In respect for the first mechanism proposed, Xue *et al* [441] study showed that TNFα activates ER stress pathways in a ROS-dependent fashion in L929 murine fibrosarcoma cells. They also show that the induction is very specific to the TNFα- induced ROS as oxidative stress inducers such as H_2O_2 and arsenite could not induce UPR though they were able to induce phosphorylation of eIF2α. Although the mechanism by which TNFα-induced ROS is activating the UPR is not fully addressed, the group proposed that BiP protein may play an important role in TNFα-mediated induction of ER stress. They hypothesise that increased formation of ROS in response to TNFα stimulation could dissociate BiP protein

from PERK and IRE1α and this dissociation would indirectly induce activation of the pathways via autophosphorylation. Though this proposed mechanism may be correct, there are still questions that can be raised from the data shown. For example, the TNFα-ROS-eIF2α signal transduction was not affected by PERK knock-down suggesting that another kinase may be responsible for the effects on the eIF2α transcription factor. This hypothesis is also supported by Denis *et al* [454] that show that TNFα was able to induce transient phosphorylation of PERK and IRE1α in hypothalamus but without activation of downstream effectors, suggesting that TNFα alone may not sufficient to induce ER stress. Also, the ER stress induction shown by Xue and collaborators [441] may be cell specific as L929 cells are known to be more sensitive to TNFα cytotoxicity [455, 456]. As I did not observe induction of any investigated ER stress markers, I believe that the observations and the mechanism proposed by [441] could be cell specific and resulted from an increased sensitivity of the cell line to TNFα.

Considering the second proposed mechanism of TNFα- induced ER stress, there is no evidence so far of a direct effect of TNFα-related transcriptional induction and increased protein folding burden in the ER. Although TNFα induces increased synthesis of proinflammatory cytokines [457] and pro-apoptotic molecules [458], it does also inhibit transcription of genes encoding for proteins involved in insulin signalling pathway [167], glucose [459] and FA transport [460], insulin-sensitising adipokines [461] and antioxidant enzymes [462]. Thus, the TNFα transcriptional regulation-induced protein burden mechanism is still under investigation.

Taking into consideration that the previous evidence shown to support the role of TNFα in ER stress induction may be cell specific or correlative but not direct causal evidence, and the fact that I could not see any induction of UPR at any of the time points and concentrations

used, I concluded that TNFα is not able to induce ER stress in my proposed *in vitro* adipocyte model.

The proinflammatory cytokines IL-6 and IL-1β do not induce ER stress in adipocytes

My results showed in the second part of this chapter that both IL-6 (Figure 6.2.1 A) and IL-1β (Figure 6.2.1 B) do not induce ER stress in *in vitro* differentiated 3T3 F442A and L1 adipocytes. As far as I am aware, this is the first study looking at the role of IL-6 and IL-1β in ER stress induction in adipocytes though an increasing number of data have shown their implications in insulin resistance and impaired glucose transport. There are only two studies that link the two cytokines to ER stress. The first one is coming from O'Neill *et al* [463] and is looking at the effect of the two cytokines on UPR induction in murine or human isolated pancreatic islets. Their results showed that overnight exposure of the islets to IL-6 and IL-β disrupt glucose-stimulated intracellular calcium response altering the Ca^{2+} homeostasis and inducing ER stress by limiting the intraluminal Ca2+ storage in a similar way to thapsigargin. Though the exact mechanism is still unknown, the effects were observed only when the cytokines were used simultaneous and not when the islets were incubated with each cytokine. Other observations in the study showed IL-6 does not seem to affect the islets function independently but its increasing the effects of IL-1β that is known to be increasingly detrimental to the β-cells [464]. This may suggest that the effects of the cytokine mix may be cell-specific due to increased sensitivity of the cells to IL-1β but further evidence is needed to confirm this hypothesis.

The second is the study of Zhang *et al* [243] that also described a possible mechanism of UPR induction in response to IL-6 and IL-1β, involving endoplasmic reticulum CREBH activation but the results were shown to be tissue-specific and the UPR induction could be

seen only in the liver, *in vivo*, but not in *in vitro* cultured hepatocytes suggesting that the ER stress induction seen may not be the result of the proinflammatory cytokine treatment itself. As I could not see induction of UPR response for any of the investigated cytokines, I consider the results obtained by O'Neill *et al* [463] may be also cell specific although future experiments may need to be made in order to investigate if the cytokines cumulated effect could also induce ER stress in adipocytes. The existence of a previously demonstrated sensitivity of the β-cells to IL-1β suggests though that the observations may not be applyed to adipocytes and the effects are restricted to the β-cell line.

CHAPTER 7

GLUCOSE STARVATION ACTIVATES THE UPR IN *IN VITRO* DIFFERENTIATED ADIPOCYTES

The adipose tissue is a highly active tissue subjected to continuous changes in size and composition throughout development and adult life [177]. This process of permanent remodelling is often discrete, reflecting the general turnover of adipose tissue cells in different depots and it is possible due to the high plasticity of the adipocytes and the well developed network of blood capillaries that ensure the cells an optimal exposure to nutrients and oxygen [176, 465]. In obesity, the remodelling process is pathologically accelerated and though it can be partially sustained by the hypertrophy and hyperplasia of the adipocytes, the angiogenesis process seems to be slower, the formation of new blood vessels acting as a limiting factor for the adipose tissue changes [154, 184]. Studies investigating the blood circulation have shown that the cardiac index and output remains constant in lean *vs* obese despite the different size of the adipose depots in both human and mice [177, 466] and that in obese subjects the postprandial blood flow per unit of adipocyte surface declines leading to suboptimal oxygen and nutrient delivery to the adipocytes [177, 467, 468]. In this context, the remodelling of the adipose tissue in obesity could be associated with nutrient starvation of cells in the newly over-expanded areas of the adipose tissue and this may contribute to cellular dysfunction and further metabolic implications.

As previous studies have linked glucose starvation to ER stress in cancer cells [275] and β-pancreatic cells [276], I have decided to investigate if the absence of glucose could also induce an UPR in adipocytes. In order to elucidate if glucose starvation can be one of the factors involved in ER stress induction, I incubated *in vitro* differentiated 3T3-F442A and 3T3-L1 cells in the presence or absence of glucose and induction ER stress markers was assessed. Cells were incubated for 24 h with serum free medium supplemented with 2 mM L-glutamine as energy source [469, 470] but no glucose. Western blot analysis of CHOP protein expression after 24 h incubation revealed a potent induction of the protein in both

lines, with a 3 ± 1 fold increase in 3T3-F442A and a 5 ± 0.2 fold increase in 3T3-L1 cells (Figure 7.1 A, B). Due to the fact that GAPDH expression is regulated by glucose [471], β-actin was used as the loading control.

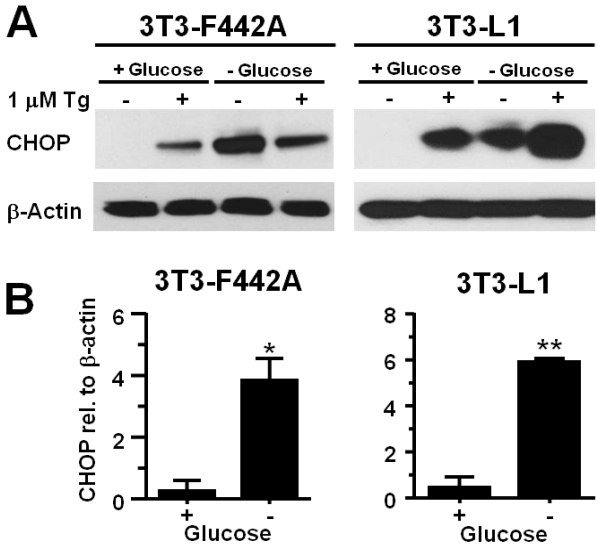

Figure 7.1. Glucose starvation induces CHOP in adipocytes. (A) CHOP protein levels in *in vitro* differentiated 3T3 F442A and 3T3-L1 adipocytes maintained for 24 h in the presence of 4.5 g/l D-glucose ("+ Glucose) or without glucose ("- Glucose). (B) Quantification of Western blots shown in panel (A). * $p < 0.05$, ** $p < 0.005$, with p values obtained using two-tailed, unpaired t-test. Images are representative for three biological repeats of the experiment.

Investigation of *XBP1* mRNA splicing revealed that induction of splicing in response to glucose starvation in 3T3-F442A *in vitro* differentiated adipocyte cell line. The induction started 12 h after glucose starvation when it recorded a 12 % splicing peak (Figure 7.2.A) and then decreased but maintained at 7 – 8 % splicing for up to 48 h (Figure 7.2 B). These data suggest that glucose starvation induces ER stress in *in vitro* differentiated 3T3-F442A and 3T3-L1 adipocytes.

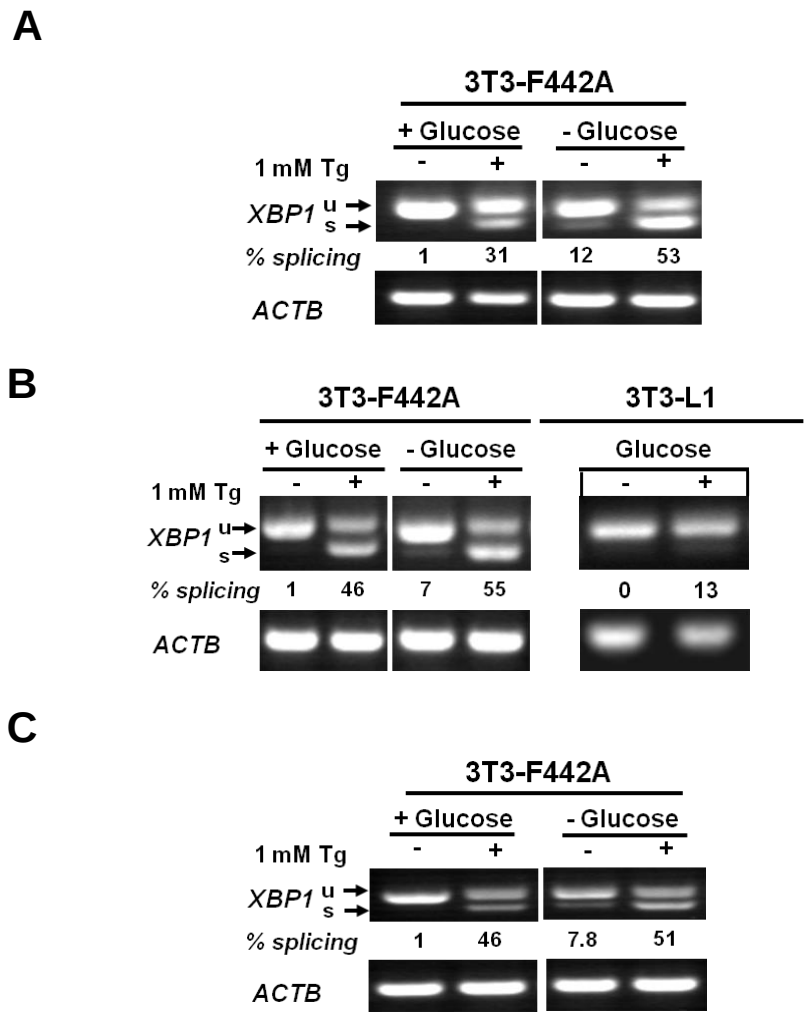

Figure 7.2. Glucose starvation induces *XBP*1 mRNA splicing in adipocytes. *In vitro* differentiated adipocytes incubated with or without glucose (A) 3T3-F442A for 12 h; (B) 3T3-F442A (with or without Tg) and 3T3-L1 (without Tg) for 24 h; (C) 3T3-F442A for 48 h. Results are representative of three repeats of the experiments.

To further confirm that glucose starvation induces ER stress in these two cell lines, I investigated the mRNA levels of some of the known UPR-induced genes after 24 h incubation with glucose free medium. A general increase in mRNA levels of all investigated markers was observed with: 5 ± 1 fold increase in *CHOP*, 16 ± 4 fold increase in *BiP*, 7 ± 1 fold increase in *ERDJ4* and 2 ± 0.5 fold increase in *EDEM1* mRNA compared to adipocytes maintained for 24 h in medium supplemented with 4.5 g/l D-glucose (Figure 7.3)

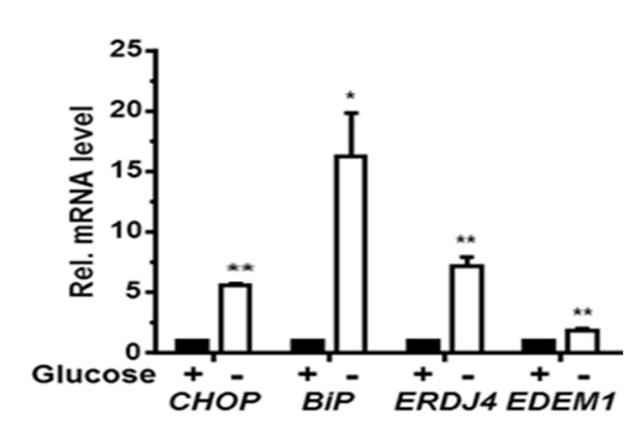

Figure 7.3. Glucose starvation induces an increase of mRNA levels for ER stress-related proteins. mRNA levels of *CHOP*, *BiP*, *ERDJ4* and *EDEM1* in *in vitro* differentiated 3T3-F422A adipocytes incubated for 24 h in the presence (+) or absence **(-)** of glucose. * $p < 0.05$, ** $p < 0.01$, were *p* values were obtained from two-tailed, unpaired *t*-tests.

Taken together these results suggest that glucose deprivation is inducing in ER stress at both protein and mRNA levels in *in vitro* differentiated 3T3-F442A adipocytes.

Recently, numerous studies have associated decreased levels or absence of glucose with increased vascular endothelial growth factor A (VEGFA) secretion in murine ovarian cancer cells [472], retinal epithelial cells [473] and human hepatoma cells [474, 475]. Ghosh *et al* [476] showed that ER stress activation plays an important role in *VEGFA* transcription and it is intimately correlated with induction of angiogenesis in response to nutrient deprivation. Similar evidence was described by Marjon *et al* [477] in human breast adenocarcinoma cell line (TSE) who showed that both low glucose and chemical (tunicamycin and brefeldin A) induction of ER stress markedly increased expression of *VEGFA* mRNA.

Angiogenic signalling was shown to be induced in the obese adipose tissue [478]. As I have previously shown that glucose starvation is inducing ER stress in *in vitro* differentiated adipocytes I decided to investigate also if glucose starvation is inducing *VEGFA* expression in adipocytes. Incubation of 3T3-F442A adipocytes for 24 h in the absence of glucose

revealed a 2 ± 0.5 fold induction of *VEGFA* mRNA (Figure 7.4) suggesting that adipocytes may play an important role in the continuously signalling for development of the vascular support in order to minimise the effects of the high nutrient intake in the rapidly expanding tissue in.

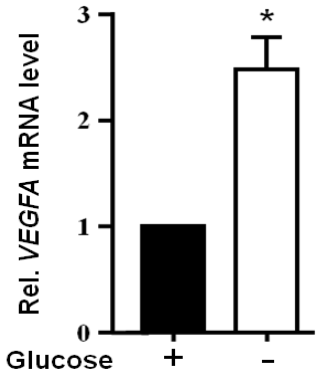

Figure 7.4. Glucose starvation induces *VEGFA* mRNA in adipocytes. RT-qPCR analysis of *VEGFA* mRNA levels in 3T3-F442A adipocytes incubated for 24 h in the presence or absence of glucose. Results are representative for three biological repeats of the experiment.

Discussion

An increasing number of studies suggest that in obesity, the adipose tissue remodelling may be imbalanced, with the adipocytes rapid expansion surpassing the angiogenesis rate [154, 176]. This imbalance was observed as reduced blood flow in the obese tissue [479] resulting in possible local deprivation of nutrients and ER stress induction in adipocytes.

ER stress has been shown to be closely linked to the nutrient status in various cell lines [480]13,14], with glucose as the main regulator of glucose-regulated ER chaperones (GRP78/BiP, GRP 94, GRP 170) gene expression [481] and PERK-mediated signalling being involved in maintenance of glucose homeostasis [482]. Low levels of glucose have been shown to induce UPR via multiple mechanisms including defects in N-glycosylation that could lead to protein misfolding [481] and decrease in ATP cellular levels and inhibition of SERCA pump activity in the ER membrane resulting in decreased Ca^{2+} levels in the ER lumen and PERK activation [276].These mechanisms have been described by Xi *et al* [483] and Palorini *et al* [275] in cancer cells and Moore *et al* [276] in pancreatic β-cells and showed that the ER stress induction in response to glucose deprivation is not a cell type-specific response. In order to investigate if glucose starvation can induce UPR in adipocytes, *in vitro* differentiated 3T3-F442A and 3T3-L1 adipocytes were subjected to glucose starvation for various periods of time (12 to 48 h) and the expression of ER stress markers was assessed at both the protein and mRNA levels. Western blot experiments for CHOP protein expression revealed protein induction after 24 h incubation of adipocytes with medium without glucose (Figure 7.1), suggesting activation of ER stress PERK. Induction of *XBP1* mRNA splicing was observed starting 12 h and was maintained up to 48 h incubation (Figure 7.2) showing activation of the second UPR branch, IRE1α. Transcriptional data investigating the mRNA levels of the UPR downstream *CHOP*, *BiP*,

ERDJ4 and *EDEM1* proteins consolidated the previous results and validated the conclusion that glucose starvation is inducing ER stress in adipocytes.

My results are in agreement with data previously reported by Wasef *et al* [267] who showed *CHOP* mRNA induction in 3T3-L1 cells after 4 h exposure to medium without glucose and increase in CHOP protein expression after overnight glucose starvation. As this is the only study I am aware of that is looking at glucose starvation-induced ER stress in adipocytes, my results provide further evidence that UPR is indeed induced by glucose deprivation in adipocytes and this could contribute to the cellular dysfunction of the adipocyte in the obese adipose tissue.

In the last part of this chapter I have continued my investigation by addressing a question related to the potential physiological implications of glucose starvation- induced ER stress in adipocytes. As adipocytes are known to secrete vasoactive factors as VEGFA in response to glucose starvation [484], and I showed that glucose starvation is inducing ER stress in *in vitro* differentiated adipocytes, I have hypothesised that the UPR may represent a mechanism of the stressed cells to try to alleviate the low glucose stress by inducing angiogenic signalling and formation of blood vessels in the affected tissue areas. In support of this hypothesis are the observations made by Ghosh *et al* [476] that showed that chemically-induced ER stress increase *VEGFA* mRNA levels in PC3, HepG2 and Ins1 832/13 cells. Using deficient mouse embryonic fibroblasts (MEFs) for PERK (*perk*$^{-/-}$) and IRE1α (*ire1α*$^{-/-}$) they showed that the *VEGFA* mRNA expression in response to chemical ER stress induction is reduced in these cells compared to the wild-type and that the phenotype can be restored by lentiviral transduction with the human IRE1α or PERK protein. Via Ire1α and *XBP1* siRNA experiments they also provided evidence of IRE1α and downstream effector XBP1 involvement in VEGFA induction in HepG2 cells. As I could see induction of both PERK and IRE1α pathways in response to glucose starvation, I decided to investigate if

VEGFA is induced in adipocytes at the same time point as the ER stress pathways. Incubation of 3T3-F442A adipocytes in the absence of glucose for 24 h, the time point when all UPR markers were observed to be induced, revealed a 2 ± 0.5 fold increase in *VEGFA* mRNA. Though I could see induction of *VEGFA* at the same time point and in the same conditions with ER stress induction, a direct connection between the two could not be established with the present evidence. Direct investigation of ER stress pathways in VEGFA induction in adipocytes using chemically designed inhibitors or genetically modified cell lines is required in order to establish causality between glucose starvation induction of UPR and angiogenic signalling. This causality could not be addressed in this study due to time limitations but will hopefully be addressed in detail in future projects.

CHAPTER 8

HYPOXIA INDUCES ER STRESS IN *IN VITRO* DIFFERENTIATED ADIPOCYTES

As discussed in the previous chapter, the adipose tissue remodeling process in obesity can play an important role in the pathological progress of the disease via formation of poor vascularised areas where the adipocytes are subjected to low blood supply. Along with the lack of nutrient supply, the cells could also to be subjected to low oxygen conditions that could further affect the homeostasis and induce dysfunction. In the last decade, increasing numbers of studies have brought evidence of hypoxic conditions in obese adipose tissue. The unchanged cardiac output [180] and postprandial blood flow [485] in the adipose tissue of obese *vs* lean subjects or the decreased oxygen partial pressure in adipose tissue of *ob*/*ob* or dietary obese mice compared to the lean control [278, 486] are some of the evidence presented. The increased size of the obese adipocytes is also supporting the existence of hypoxia in obese adipose tissue, as the hypertrophic cells can reach 150-200 nm diameter [181], exceeding the normal O_2 diffusion rate of 100-200 nm [487]

Investigation of hypoxia effects in adipocytes have shown a positive correlation between the low oxygen conditions and increased secretion of proinflammatory adipokines both in *in vitro* [277, 278] and *in vivo* [278, 488]. Insulin signaling was also shown to be disrupted by hypoxia via attenuation of glucose transport [279, 280] and inhibition of IR and IRS-1 phosphorylation [280]. As ER stress in adipocyte has been strongly associated with both induction of proinflammatory cytokine and insulin resistance in obesity, in this chapter I have investigated if hypoxia could trigger ER stress in adipocytes.

To fulfill this objective, *in vitro* differentiated 3T3-F442A and 3T3-L1adipocytes were cultured in 0.5 % O_2 for up to 8 h and markers of ER stress induction were analyzed at the protein and mRNA level. Induction of hypoxia was evaluated by investigation of protein level of hypoxia inducible factor 1 α (HIF-1α), a key regulator of cell response in O_2 restriction [489, 490]. In normal O_2 conditions HIF-1α protein is constantly synthesized in the cell but rapidly degraded as a result of post-translational modifications made by prolyl

hydroxylase enzymes (PHDs) [491]. The PHDs use oxygen to hydroxylate proline residues in the oxygen-dependent degradation domain of HIF-1α and make the protein accessible to the von Hippel-Lindau tumor suppressor protein which initiates ubiquitination and degradation via the 26S proteasome complex [492, 493]. In low oxygen conditions, the prolyl hydroxylases are inactive and HIF-1α is stabilised as the degradation complex cannot bind to it [491]. The strict regulation of the protein in response to oxygen levels, makes HIF-1α protein levels a good indicator of oxygen conditions that can be used to identify hypoxic conditions [494, 495].

Investigation of HIF-1α protein in the *in vitro* 3T3-F442A and 3T3-L1 differentiated adipocytes revealed an increase in the protein levels within 2 h of incubation in 0.5 % O_2. The increase further was maintained for up to 8 h in both cell lines (Figure 8.1 A). As hypoxia was previously shown to induce HIF-1α also at transcriptional level [496, 497], mRNA levels of *HIF-1α* were investigated by RT-qPCR. The increase in mRNA levels observed followed a similar pattern to the one described by the protein expression (Figure 8.1 C) and further validated the experimental hypoxia induction.

PERK activation in response to hypoxia was investigated as induction of eukaryotic translation initiation factor 2 α (eIF2α) phosphorylation and revealed increase in phosphorylation of the eIF2α protein corresponding with the HIF-1α protein expression (Figure 8.1 A, B). These results suggest that hypoxia may induce PERK activation but further investigations are needed to ensure that PERK kinase is responsible for the eIF2α protein phosphorylation. This is due to the fact that eIF2α protein can also be phosphorylated by two other kinases: general control non-derepressible 2 (GCN2) [498] and protein kinase R (PKR) [499]. GCN2 is a serin/threonine protein kinase that senses amino acid deficiency and it is involved in regulation of amino acid metabolism [498] while PKR is induced by double-stranded RNA (dsRNA), cytokines and mechanical stressors and is signalling for

inflammation. Involvement of two kinases in hypoxia induction of eIF2α phosphorylation have been previously investigated but the data are contradictory and vary largely with the model used [500-502]. Investigation of CHOP protein expression could not be used as evidence of PERK induction as CHOP protein expression could not be detected in the Western blotting experiments (data not shown). Multiple repeats of the experiments suggested that the lack of protein induction was not the result of a technical error as initially believed from the eIF2α phosphorylation observations. The explanation could reside in the fact that CHOP protein may be induced by hypoxia at longer time points than the ones investigated in my study although the mRNA levels showed increased transcription starting 6 h exposure to hypoxia (Figure 8.3 C). This explanation is supported also by the observations of Lopez-Hernandez *et al* [503] that show CHOP induction starting 9 h incubation with chemical hypoxia inducer $CoCl_2$.

Taken together, these data suggest that hypoxia could induce PERK activation in adipocytes but there is no sufficient evidence to conclude that induction of eIF2α phosphorylation is strictly PERK-mediated.

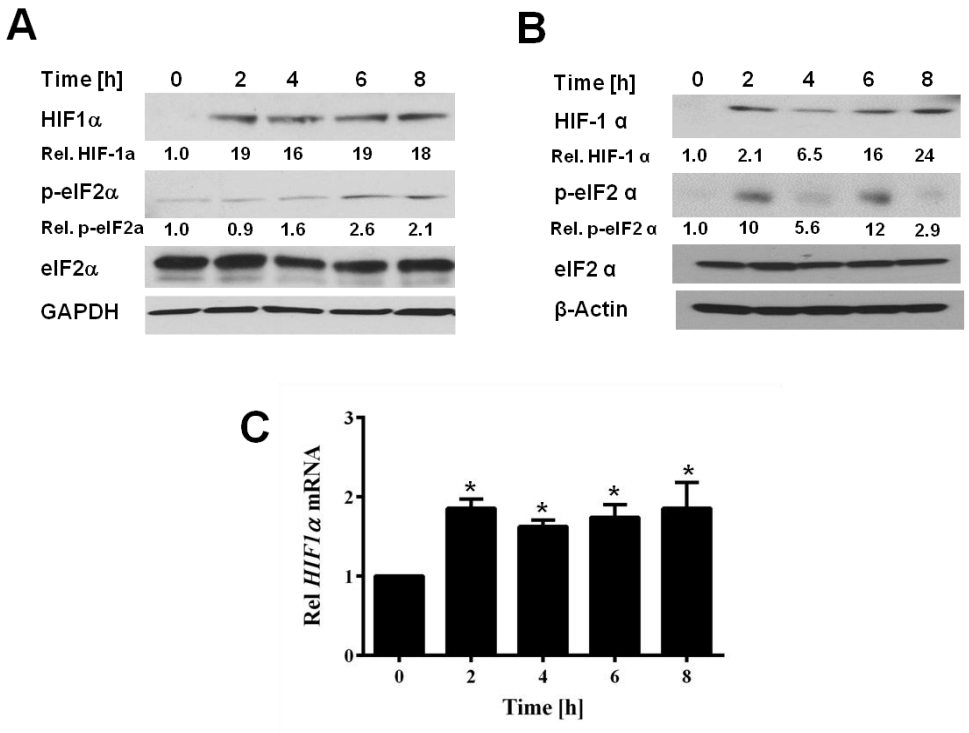

Figure 8.1. Hypoxia induces increased phosphorylation of eIF2α in adipocytes (A,B) Induction of HIF 1α protein and eIF2 α phosphorylation at serine 51 in *in vitro* differentiated (A) 3T3-F442A and (B) 3T3-L1 adipocytes, and (C) *HIF-1α* mRNA expression in 3T3-L1 adipocytes incubated for the indicated times under 0.5 % (v/v) O_2. Results are representative for three biological repeats of the experiment. * $p < 0.05$ was calculated using ANOVA test comparing the 2-8 h samples to the control (0 h).

Activation of the Ire1α branch of the ER stress response in response to hypoxia was investigated as *XBP1* mRNA splicing induction and revealed significant splicing starting after 2 h exposure to low O_2 conditions. The splicing induction was maintained up to 8 h of hypoxia incubation and followed a similar pattern with HIF-1α and induction of eIF2α phosphorylation (Figure 8.2)

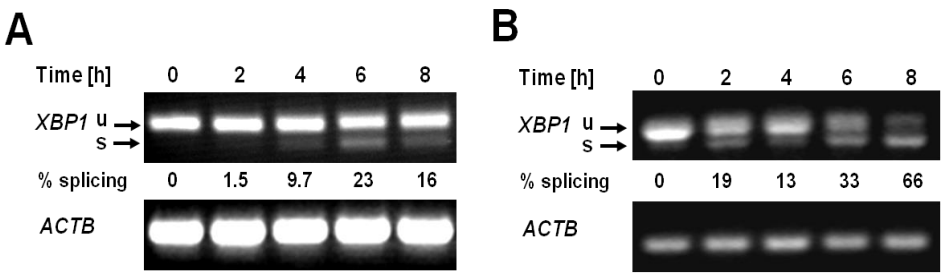

Figure 8.2. Low oxygen conditions induce *XBP 1* mRNA splicing in *in vitro* differentiated adipocytes. *XBP1* mRNA splicing levels in *in vitro* differentiated **(A)** 3T3-F442A and **(B)** 3T3-L1 adipocytes incubated for the indicated times under hypoxic conditions. Results are representative for three biological repeats of the experiment.

In order to further investigate ER stress induction in response to low oxygen conditions, I have also assessed the mRNA levels of the UPR downstream genes *BiP*, *CHOP* and *ERDJ4* in adipocytes incubated under hypoxic conditions. Elevated mRNA levels for *BiP*, *CHOP* and *ERDJ4* mRNA were observed in adipocytes incubated in hypoxic conditions compared to normal O_2 ones (Figure 8.3). The increase in mRNA levels followed a similar pattern with the one observed in *HIF-1α* mRNA, *XBP1* mRNA splicing and eIF2α phosphorylation.

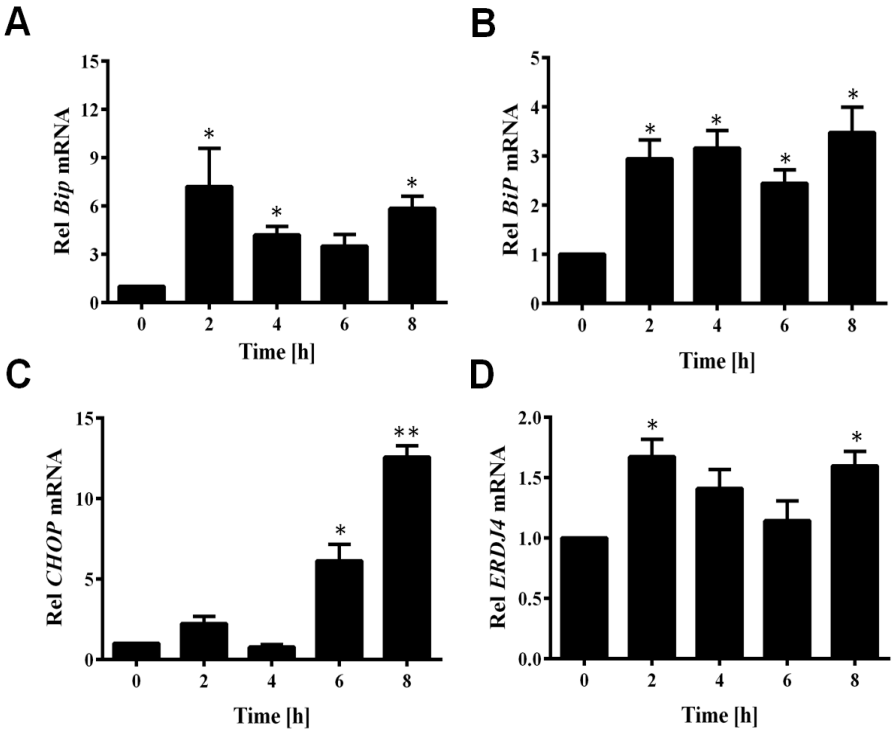

Figure 8.3. Hypoxia induces ER-stress related genes in *in vitro* differentiated adipocytes. mRNA levels of *BiP* in **(A)** 3T3-F442A, **(B)** 3T3-L1 and of **(C)** *CHOP and* **(D)** *ERDJ4* in *in vitro* differentiated 3T3-L1 adipocytes incubated for up to 8 h in 0.5% (v/v) O_2. * $p< 0.5$, ** $p< 0.05$. *p* values were calculated using ANOVA test.

Taken together, these results suggest that hypoxic conditions validated by HIF-1α expression, induce ER stress in *in vitro* differentiated adipocytes although further experiments are needed to conclude that PERK induction is the only kinase responsible for the eIF2α phosphorylation observed.

Discussion

Adipose tissue remodelling in obesity has been associated with formation of poor vascularised areas where adipocytes are subjected to nutrient and oxygen starvation. These cells have been previously shown to exhibit markers of cellular stress and alterations in proinflammatory adipokines secretion and insulin signalling. In Chapter 7 I have provided evidence that glucose starvation induces ER stress in *in vitro* differentiated adipocytes. The present chapter continues the investigation of the factors associated with adipose tissue remodelling, by addressing the question if hypoxia can also induce ER stress in adipocytes.

Incubation of 3T3-F442A and 3T3-L1 adipocytes in hypoxic conditions (0.5 % O_2) revealed induction of eIF2α phosphorylation (Figure 8.1 A, B) and IRE1α- induced *XBP1* mRNA splicing (Figure 8.2) starting 2 h incubation. The induction was correlated with increase in O_2 sensing HIF-1α protein and mRNA expression indicating hypoxia (Figure 8.1 A-C). Quantitation of mRNA levels for ER stress-related genes *BiP*, *CHOP* and *ERDJ4* showed up-regulation of the gene expression in response to low O_2 conditions (Figure 8.3). The induction was observed at similar time points as the induction of HIF-1α expression (and Figure 8.1) supporting the previous results suggesting that hypoxia is inducing ER stress in the *in vitro* differentiated model of adipocytes. Although my experiments could not conclude that phosphorylation of eIF2α is induced by PERK only, the cumulating results from the IRE1α branch of UPR and the mRNA induction of ER-downstream indicate without doubt that hypoxia is inducing ER stress in the differentiated adipocytes.

My observations are similar to the ones described by Hosogai *et al* [277] that showed induction of eIF2α phosphorylation after 2 h incubation of 3T3-L1 adipocytes in 1 % O_2 conditions. Induction of *XBP1* mRNA splicing was also observed in Hosogai's study but at a later time point (6 h) probably due to the sensitivity of the method used for evaluation (*Pst*I digestion of PCR products) and maybe the stringency of the hypoxic conditions.

Similar to my data regarding eIF2α phosphorylation in response to hypoxic conditions, Koumenis *et al* [500] described induction of eIF2α phosphorylation in lung carcinoma A549 cells, human fibroblasts AG1522 and HeLa cervical carcinoma cells after 2 h exposure to 0.02 % O_2 chemically-induced hypoxia. Using cells expressing a dominant-negative PERK allele or $PERK^{-/-}$ mouse embryo fibroblasts (MEFs), they have also shown that PERK is the only kinase responsible for phosphorylation of eIF2α in response to hypoxia. Interestingly, using $PERK^{-/-}$ cells maintained for 24 h in stringent hypoxic conditions (0.05 % O_2), they have also showed that PERK activation is very important in survival of the cells in hypoxic conditions, a decreased viability of PERK the deficient cells being observed compared to the control. In agreement with their results and previously described effects of PERK induction, the authors formulated the hypothesis that PERK protection in hypoxia is based on the transcriptional arrest induced by eIF2α phosphorylation, helping the cell to minimize the energetic needs and use the resources left for the basic functions that can ensure survival. They also suggest that extended hypoxia becomes negative towards the cell homeostasis either directly via induction of HIF-1α and expression of proinflammatory genes [490, 495, 504] or indirectly via prolonged translational arrest. The indirect effects include induction of NFκB due to degradation of IκB inhibitor as a results of the short half-life of the protein [27] and alteration of adipokines expression[277]. Although the proposed mechanism could explain some of the protective effects of PERK induction, it does not seem to correlate with induction time frame of eIF2α phosphorylation and HIF-1α observed in my experiments. Though eIF2α phosphorylation was detected within 2 h of hypoxia, absence of CHOP induction after 8 h of hypoxia in my experiments or the late induction of CHOP protein observed by [503] suggest that the PERK-mediated signaling is not rapid. Also, if HIF-1α accumulation is detrimental to the cell then the observed increase in HIF-1α protein and mRNA levels starting 2 h exposure to hypoxia would induce detrimental effects before

PERK induction can exert the protective effects. This suggests that although both studies show PERK induction by hypoxia, the role and kinetics of PERK activation may differ due to cell-specific mechanisms or different type of hypoxia induction used. Future experiments using longer exposure of adipocytes to hypoxic conditions and different type of hypoxia (chemically induced or low O_2 conditions) may provide a better insight in the kinetics of ER induction in adipocytes and the role of different UPR components in the cellular response to hypoxia. Another important aspect that could be investigated in future experiments is the role of hypoxia-induced ER stress in angiogenesis induction. Previous observations have shown that ER stress induces expression of pro-angiogenic VEGFA factor via PERK-ATF4 and IRE1α-XBP1 induction in cancer cells exposed to low O_2 conditions [31,32]. HIF-1α has been also shown to induce *VEGFA* expression in adipocytes [505] and cancer cells [506]. Taken together, these observations could suggest that the ER stress induced by hypoxia may play an important role in stimulation of angiogenesis together with HIF-1α independent effects.

CHAPTER 9

DISCUSSION

The data presented in this thesis provides an insight into the role of several obesity-related factors in ER stress induction in murine adipocytes. Although some of the investigated factors have been previously shown to be correlated with insulin resistance, inflammation and lipotoxicity, few data are available about the role that they play in ER stress induction. My work provides some evidence that glucose starvation and hypoxia resulted from the adipose tissue remodelling in obesity, but not palmitate, cholesterol or several proinflammatory cytokines (TNFα, IL-6 and IL-1β) induce ER stress in two *in vitro* adipocyte models, 3T3-F442A and 3T3-L1.

Two murine 3T3 preadipocyte cell lines, 3T3-F442A and 3T3-L1 were chosen as model for *in vitro* differentiation of adipocytes. The choice of the cell lines was made according to the few advantages provided: (1) the cells are known to be committed to the adipogenic lineage and undergo differentiation into adipocytes under established adipogenic stimulation [283, 287], (2) the cell cultures presents continuous replication capacity compared to the primary cells [282] and (3) the cell lines are well characterised and present less heterogeneity than the primary cultures providing a more accurate observation of the cellular responses [287]. Evidence for the *in vitro* differentiation of the two cell lines were presented in Chapter 3 showing a 70-80 % differentiation of the cultures 12 d after the adipogenic induction.

In chapter 4, I have shown that palmitate does not induce ER stress or impair insulin signalling in adipocytes. Although the effects of palmitate on insulin signalling have been previously investigated [334], this is the first study to show that the saturated fatty acid palmitic acid does not induce ER stress in *in vitro* differentiated adipocytes. Considering that palmitate induces UPR in preadipocytes as I have also shown, my results suggest the existence of an adipocyte-specific mechanism(s) that protects the cell against fatty acid induced-ER stress. Therefore, I have hypothesised and investigated two possible mechanisms: (1) alteration of mRNA basal levels of ER stress components PERK and IRE1α

in adipocytes *vs* preadipocytes and (2) up-regulation of gene expression for enzymes involved in FA and TAG metabolism during the differentiation process due adipocyte specialisation in lipid storage. The mRNA expression for the two ER stress sensor proteins IRE α and PERK was found to be similar in preadipocytes and adipocytes for the 3T3-L1 cell line suggesting that increased basal activity of ER stress signalling pathways is not the mechanism protecting the cells against palmitate-induced ER stress. In 3T3-F442A, due to possible technical errors, PERK basal levels are up-regulated in adipocytes *vs* preadipocytes whereas IRE1α levels were decreased after differentiation.

The observed up-regulation of genes encoding for enzymes involved in FA metabolism and TAG synthesis was in accordance with literature data showing induction of lipid metabolism enzymes during adipocytes differentiation [297, 507] and supported the protection mechanism hypothesised. Increased levels of stearoyl-CoA desaturase observed could also explain, in accordance with the proposed mechanism, the ability of the cell to avoid saturated fatty acid lipotoxicity and dispose the excess palmitate in the triacylglycerol pools. Data provided in Chapter 5 shows that cholesterol does not induce ER stress in the two *in vitro* differentiated adipocyte cell lines. The results obtained could be linked to the protection mechanism formulated in the previous chapter as the expansion of the triacylglycerol pool would also affect the storage capacity for cholesterol, more than a third of the total cholesterol in the adipocyte cell being stored in the lipid droplets [411] Therefore, cholesterol storage and utilisation in lipid droplet formation may explain why high concentrations of cholesterol do not induce ER stress in adipocytes.

Proinflammatory cytokines TNFα, IL-6 and IL-1β were also shown to be unable to induce ER stress in my model of adipocytes (Chapter 6). Though few other studies proposed possible mechanisms for TNFα induction of ER stress, my data did not found any evidence to support proposed the role of TNFα in UPR induction. The role of IL-6 and IL-1β in ER

stress induction in adipocytes was not studied before, my data showing for the first time that the two proinflammatory cytokines do not induce UPR in *in vitro* differentiated adipocytes, Chapter 7 and 8 have addressed the obese adipose tissue remodelling process-induces factors: the low nutrient and oxygen supply. My results showed that both glucose starvation and hypoxia are inducing ER stress activation in *in vitro* differentiated adipocytes and could contribute to cellular dysfunction and inflammation. Also, due to large overlap of the known effects of hypoxia and ER stress on the adipose tissue, including inflammation [251, 278, 509], insulin resistance [207, 510], my results suggest that ER stress may contribute to or mediate the effects of hypoxia on adipocytes.

My conclusions differ from the ones drawn in other studies, which suggest that free fatty acids [266, 340, 511], cholesterol [391] and TNF α [352] induce ER stress in *in vitro* differentiated adipocytes. Kawasaki *et al*. [266] reported induction of *XBP1* mRNA splicing, *ATF4*, *BiP*, *CHOP*, *EDEM*, *ERDJ4*, and *PDI* mRNA in 3T3-L1 adipocytes in response to 50 μg/ml of a free fatty acid mixture derived from human serum. Although the composition of the fatty acid mixture used in the study is unknown, palmitic acid should be one the components as it was previously shown to be the most abundant SFA in human serum composition. Also, palmitic acid is considered to be the SFA with the highest potential for cell injury as palmitate-CoA represent a poor substrate for DGAT enzyme [512] contributing to accumulation of potential toxic ceramide. High concentrations of palmitate were shown to also induce synthesis of 1,2-dipalmitate-phosphatidilglycerol, a cardiolipin precursor that inhibits the cardiolipin synthase activity and can induce apoptosis [513]. But, if their mixture contains palmitic acid, the FA was shown to only elicit ER stress, insulin resistance or cell injury at much higher concentrations in different cell lines [268, 316, 514], and my results did not show any induction of ER stress markers in 3T3-F442A or 3T3-L1 adipocytes in response to concentrations up to 20 times higher than the ones used in their study. Therefore,

I consider that compounds other than the saturated fatty acids present in the fatty acid mixture used by Kawasaki *et al* [266] may cause the ER stress in adipocytes described by the group. Jiao *et al* [342] reported that a mixture of lauric, myristic, oleic, linoleic and arachidonic acids induces ER stress and potently inhibits insulin-stimulated AKT serine 473 and threonine 308 phosphorylation in *in vitro* differentiated 3T3-L1 adipocytes. These results contradict not only my observations but also several other papers which have reported that the unsaturated fatty acids oleic and linoleic acid protect cells from the negative effects of saturated fatty acids [345, 346, 348] and that the medium-chain fatty acids lauric and myristic acid do not induce insulin resistance [334]. The explanation could reside in the concentration of the arachidonic acid present in the used mixture, as the polyunsaturated FA was shown to be able to induce Ca^{2+} release from the ER and induce ER stress [350, 351].

Chen *et al* [391] reported that oxLDL induces BiP and CHOP in 3T3-L1 adipocytes and suggested that intracellular cholesterol overload may be partially responsible for this ER stress response. Though both AcLDL and oxLDL are taken up by adipocytes via the scavenger receptor A [399], the oxidised components of oxLDL have been previously shown to induce enhanced degradation [393] and inflammation [397]. As I have not observed induction of *XBP1* splicing in 3T3-F442A or 3T3-L1 adipocytes exposed to AcLDL I concluded that an oxidized lipid or protein component of oxLDL [515], but not cholesterol was responsible for the ER stress induction described by the group.

Koh *et al.*[352] and Jeon *et al.*[340] have reported that TNF-α and palmitate elevate phosphorylation of eIF2α, induce *ATF3* mRNA and activate JNK in 3T3-L1 adipocytes and, on the basis of these changes, concluded that TNF-α and palmitate cause ER stress in adipocytes. eIF2α phosphorylation and the increase in *ATF3* mRNA downstream of eIF2α phosphorylation are controlled by four protein kinases [353] of which only PERK directly responds to ER stress [516]. JNK is activated by many stresses [192]. As my data show

absence of *XBP1* splicing that is a more specific marker for ER stress, I concluded that other stresses are responsible for the increase in the stress markers monitored by the two studies.

In conclusion, some of my work shows that glucose and oxygen deprivation rather than elevated saturated fatty acids, cholesterol or proinflammatory cytokines (TNFα, IL-6 and IL-1β) levels cause ER stress in adipocytes *in vitro*, suggesting that the adipose tissue remodelling in obesity may play a more central role in adipocyte dysfunction then initially believed. My observations open new perspectives in understanding the factors inducing adipocyte dysfunction in obesity and their role and succession in the pathological progress of the disease. If the reduced blood supply will be identified as one of the first ER stress inducers in the overloaded adipocytes, then increased vascularisation of the obese adipose tissue may alleviate the ER stress effects on adipocytes. Future experiments investigating hypoxia, glucose starvation and ER stress markers co-localisation (e.g. via immunofluorescence) in animal models of obesity could provide evidence of *in vivo* ER stress induction in response to the two proposed factors. Assessment of ER stress induction in obese adipose tissue exhibiting genetically or chemically induced angiogenesis could provide more insight in the role of imbalanced expansion of the tissue in obesity.

My data and the hypothesis of adipocyte-specific mechanism of protection against saturated fatty acid and cholesterol lipotoxicity also set the premises for future studies that could provide more evidence to support the hypotheses proposed. Genetic approaches using knockdown or over-expression of the genes for enzymes involved in the FA metabolism could be used to indicate the role of these enzymes in the adipocyte protection against FA-injury. Experiments using fluorescent conjugated palmitate or fluorescent fatty acids analogs (e.g. BODIPY-conjugated palmitate, BODIPY fatty acid analogs) [517, 518] could allow intracellular tracing of the fatty acid and establish if the excess FA is indeed metabolised and

stored in the triacylglycerol pool as hypothesised. Similar methodology using fluorescent or radiolabeled cholesterol [519] could be used to investigate the intracellular trafficking and localisation of up-taken excess cholesterol in adipocytes. Genetic approaches using ACAT1 shRNA could also elucidate the role of the enzyme in the cholesterol loading-induced lipotoxicity.

All these approaches will provide a better insight into the mechanisms that underlie the ER stress induction in adipocytes and the role that the UPR activation plays in cellular dysfunction in obesity. Identifying the obesity-related factors that induce ER stress and promote the pathological progress of the disease could provide new prevention strategies and help to formulate more targeted therapeutic approaches of the disease.

APPENDIX

RESEARCH PAPER

Adipocyte 4:3, 188–202; July/August/September 2015; © 2015 Taylor & Francis Group, LLC

Glucose starvation and hypoxia, but not the saturated fatty acid palmitic acid or cholesterol, activate the unfolded protein response in 3T3-F442A and 3T3-L1 adipocytes

Adina D Mihai[1,2,3] and Martin Schröder[1,2,3,*]

[1]School of Biological and Biomedical Sciences; Durham University; Durham, United Kingdom; [2]Biophysical Sciences Institute; Durham University; Durham, United Kingdom; [3]North East England Stem Cell Institute (NESCI); Life Bioscience Center; International Center for Life; Central Parkway; Newcastle Upon Tyne, United Kingdom

Keywords: adipocyte, diabetes, glucose starvation, hypoxia, obesity, unfolded protein response

Obesity is associated with endoplasmic reticulum (ER) stress and activation of the unfolded protein response (UPR) in adipose tissue. In this study we identify physiological triggers of ER stress and of the UPR in adipocytes in vitro. We show that two markers of adipose tissue remodelling in obesity, glucose starvation and hypoxia, cause ER stress in 3T3-F442A and 3T3-L1 adipocytes. Both conditions induced molecular markers of the IRE1α and PERK branches of the UPR, such as splicing of *XBP1* mRNA and CHOP, as well as transcription of the ER stress responsive gene *BiP*. Hypoxia also induced an increase in phosphorylation of the PERK substrate eIF2α. By contrast, physiological triggers of ER stress in many other cell types, such as the saturated fatty acid palmitic acid, cholesterol, or several inflammatory cytokines including TNF-α, IL-1β, and IL-6, do not cause ER stress in 3T3-F442A and 3T3-L1 adipocytes. Our data suggest that physiological changes associated with remodelling of adipose tissue in obesity, such as hypoxia and glucose starvation, are more likely physiological ER stressors of adipocytes than the lipid overload or hyperinsulinemia associated with obesity.

Introduction

Obesity is the leading risk factor for type 2 diabetes, cardiovascular disease, and hypertension.[1,2] Obesity affects the homeostasis of the whole body but mainly the liver and the adipose tissue, and is characterized by low grade inflammation, hyperlipidemia, and insulin resistance in surrounding and peripheral tissues.[1,2] Adipose tissue is exposed to several stresses in obesity, including inflammation, hypoxia, and endoplasmic reticulum (ER) stress.[3] Limited angiogenesis, adipocyte hypertrophy and hyperplasia cause hypoxia in obese adipose tissue.[4] Secretion of MCP-1 by dysfunctional adipocytes attracts circulating monocytes into adipose tissue,[5,6] while a change in the adipokine profile, including decreased adiponectin and increased leptin secretion,[5] may contribute to the replacement of adipose tissue resident alternatively activated (M2) macrophages with classically activated (M1) macrophages.[6] While physiological causes of inflammation and hypoxia in adipose tissue have been characterized, little is known about the physiological triggers of ER stress in obese adipose tissue. At the molecular level, ER stress is caused by the build-up of misfolded proteins in the ER and activation of a signaling network called the unfolded protein response (UPR).[7] The UPR attempts to restore ER homeostasis by inducing expression of genes encoding molecular chaperones and protein foldases, lipid biosynthetic enzymes, and proteins involved in ER-associated protein degradation. If the ER stress cannot be resolved, the UPR promotes apoptosis. ER stress also plays key roles in both inflammation and insulin resistance in obesity and type 2 diabetes.[8,9]

In mammalian cells, three UPR signaling cascades are initiated by the ER transmembrane proteins PERK, IRE1α, and ATF6. Phosphorylation of the translation initiation factor eIF2α by the protein kinase PERK inhibits general translation, but also stimulates translation of mRNAs harbouring several short upstream open reading frames in their 5' untranslated regions. This mechanism of translational activation results in induction of the transcription factors ATF4 and C/EBP homologous protein (CHOP).[10,11] CHOP reactivates protein synthesis and oxidation in the ER.[12] IRE1α up-regulates ER chaperone genes and genes involved in ER-associated protein degradation via endoribonuclease domain-induced splicing of X-box protein 1 (XBP1) mRNA.[13,14] The transcription factor ATF6 translocates to the nucleus after proteolytic release from the Golgi membrane by the Golgi proteases S1P and S2P[15] and induces expression of genes encoding ER resident molecular chaperones and proteins functioning in ER-associated protein degradation.[16,17] Upon prolonged or irremediable ER stress the UPR induces apoptosis via activation of JNK[18] by IRE1α and TRB3 by CHOP.[19]

*Correspondence to: Martin Schröder; Email: martin.schroeder@durham.ac.uk
Submitted: 06/05/2014; Revised: 11/08/2014; Accepted: 11/14/2014
http://dx.doi.org/10.4161/21623945.2014.989728

The physiological factors leading to ER stress and activation of the UPR in obese adipocytes are not well characterized. For several other cell types, including hepatocytes, pancreatic β cells, and macrophages physiological ER stressors have been reported. Saturated fatty acids (SFAs) or cholesterol loading induce an UPR in several cell types such as hepatocytes,[20,21] pancreatic β cells,[22] macrophages,[23] and preadipocytes.[24] Inflammatory cytokines such as TNF-α, IL-6 and IL-1β, which are secreted by stressed adipocytes or macrophages recruited into inflamed adipose tissue,[25] elicit an ER stress response in L929 myoblast cells and hepatocytes.[26,27] Glucose starvation is the earliest identified physiological ER stressor,[28,29] while the hypoxic environment of tumors induces an UPR in tumor cells.[30-32]

The purpose of this study was to identify obesity-related physiological inducers of ER stress and the UPR in adipocytes by exposing in vitro differentiated 3T3-F442A adipocytes to several physiological ER stressors, including the SFA palmitic acid, cholesterol, inflammatory cytokines, glucose starvation, and hypoxia. We report that potent physiological ER stressors in other cell types, such as palmitic acid, cholesterol, or the inflammatory cytokines TNF-α, IL-1β, and IL-6, do not induce an ER stress response in in vitro differentiated 3T3-F442A and 3T3-L1 adipocytes. Glucose starvation and hypoxia, however, induce markers of ER stress, such as splicing of *XBP1* mRNA, transcriptional activation of ER stress responsive genes including *BiP* and *ERDJ4*, CHOP and phosphorylation of eIF2α. Our results suggest that hypoxia and glucose starvation are likely physiological ER stressors for adipocytes in vivo.

Results

Palmitate does not induce ER stress in adipocytes

To identify which obesity-related physiological factors trigger the UPR in adipocytes, we exposed in vitro differentiated 3T3-F442A and 3T3-L1 adipocytes to several compounds whose plasma levels are elevated in obesity,[33-39] including palmitic acid, cholesterol, and the inflammatory cytokines TNF-α, IL-1β, and IL-6. 3T3-F442A adipocytes were chosen because these cells form normal adipose tissue without the addition of exogenous inducers when implanted subcutaneously into athymic mice.[40,41] 3T3-L1 adipocytes were included to provide a second source of adipocytes. Both cell lines were differentiated for 12 d and the percentage of cells with an increased lipid content determined by flow cytometry with the fluorescent lipid probe nile red.[42] Flow cytometry revealed a mean fluorescence increase of 3.2 ± 0.2 fold upon differentiation of 3T3-L1 cells (**Fig. 1A**). In differentiated 3T3-F442A cells 2 populations with 2.9 ± 0.1 fold and 25 ± 2 fold increases in nile red fluorescence were distinguishable (**Fig. 1B**). A ~3-fold increase in nile red fluorescence in differentiated 3T3-L1 adipocytes and the larger population of differentiated 3T3-F442A adipocytes is in good agreement with previously published increases in nile red fluorescence during differentiation of human adipocytes[43] and adipogenic differentiation of the murine embryonic stem cell line CGR8.[44] Quantitation of the histograms for the nile red fluorescence by constructing the probability distribution for the increase in nile red fluorescence upon differentiation and the constraint that the nile red fluorescence of adipocytes has to be greater by at least two standard deviations of the mean nile red fluorescence of undifferentiated cells than the nile red fluorescence of undifferentiated cells reveals that 72 ± 3% of the 3T3-L1 and 80 ± 1% of the 3T3-F442A cells acquired a lipid-laden phenotype. These degrees of differentiation are comparable to previously published data.[45]

The granularity of cells increases during differentiation into adipocytes because of the accumulation of lipid droplets.[46] This increase in granularity is reflected by an increase in the side scatter of the exciting laser beam[47] and is also seen after differentiation of both 3T3-L1 and 3T3-F442A cells for 12 d (**Fig. 1C and D**). The side scatter of the highly fluorescent 3T3-F442A adipocyte population (≥ 300 A.U. in **Fig. 1B**) is significantly higher than the side scatter of the weaker fluorescent population (<300 A. U., **Fig. S2**), suggesting that the highly fluorescent cells contain more lipid droplets than the weaker fluorescing population. Forward scatter, which is affected by cell size and shape,[47] decreases in 3T3-L1 cells and becomes more heterogeneous in 3T3-F442A cells (**Fig. 1E and F**). Taken together, these data suggest that the majority of the 3T3-L1 and 3T3-F442A cells have acquired a lipid-laden phenotype 12 d after initiation of adipogenic differentiation.

To determine whether palmitic acid causes ER stress in adipocytes in vitro, 3T3-L1 and 3T3-F442A adipocytes were incubated with different concentrations (0–1 mM) of palmitate complexed to fatty acid-free bovine serum albumin (BSA) for up to 48 h. The activity of the PERK branch of the UPR was assessed by Western blotting for CHOP, while activation of IRE1α was monitored by measuring splicing of *XBP1* mRNA. Exposure of adipocytes to up to 1 mM palmitate for 48 h did not elevate CHOP levels (**Fig. 2A and B**), induce detectable levels of *XBP1* splicing (**Fig. 2C and D**, S3–7), or elevate mRNA levels for the ER stress responsive genes *BiP* (**Fig. 3A and B**), *CHOP* (**Fig. 3C and D**), or *ERDJ4* (**Fig. 3E and F**) especially when compared to the large increases in mRNA levels of these genes and CHOP protein levels in thapsigargin-treated adipocytes (**Figs. 2A and B** and **3**). Treatment with palmitate complexed to BSA for 8 or 24 h did also not induce *XBP1* splicing in 3T3-F442A adipocytes (**Figs. S5–7**). Palmitate did also not affect the viability of 3T3-F442A adipocytes over a period of up to 48 h, while incubation with 1 μM thapsigargin, which causes ER stress by depleting ER luminal Ca^{2+} stores,[48] for 48 h decreased viability by ~37% (**Fig. 2E**). Palmitate did also not inhibit insulin-stimulated AKT serine 473 phosphorylation in 3T3-F442A adipocytes (**Fig. 4A**), which is consistent with several other reports.[49–56] To validate that our BSA-palmitate complexes induce ER stress, we characterized *XBP1* splicing in undifferentiated preadipocytes exposed to palmitate complexed to BSA. Exposure of preadipocytes to palmitate complexed to BSA induces *XBP1* splicing in these cells.[24] Indeed, palmitate induced *XBP1* splicing in undifferentiated preadipocytes (**Figs. 2F** and **S8**) and also inhibited insulin action in these cells (**Fig. 4B**). Collectively, these results show

that the SFA palmitic acid does not induce ER stress in adipocytes.

Cholesterol does not induce an UPR in adipocytes

To characterize whether cholesterol elicits ER stress in adipocytes we exposed differentiated 3T3-F442A and 3T3-L1 adipocytes to 100 μg/ml human acetylated low density lipoprotein (AcLDL) for 48 h. AcLDL did not elevate CHOP levels (**Fig. 5A and B**), induce *XBP1* splicing (**Figs. 5C and D** and **S9A and B**), or elevate *BiP* or *CHOP* mRNA levels (**Fig. 6**). We, therefore, repeated these experiments in the presence of the acyl-CoA:cholesterol acyltransferase (ACAT) inhibitor TMP-153 to inhibit cholesterol esterification and to elevate intracellular free cholesterol levels. After 24 h no changes in expression of CHOP or in *XBP1* splicing were observed (data not shown). 48 h of treatment with AcLDL and TMP-153 did not increase CHOP protein levels (**Fig. 5A and B**), induce *XBP1* splicing (**Fig. 5C and D**), or elevate the mRNA levels for *BiP* (**Fig. 6A and B**) or *CHOP* (**Fig. 6C and D**). To validate that AcLDL can, in principle, activate the UPR, we repeated these experiments with in vitro differentiated THP-1 macrophages which are known to develop ER stress in response to cholesterol overloading.[57] In differentiated THP-1 macrophages AcLDL induced *XBP1* splicing both in the presence and absence of TMP-153 (**Figs. 5E** and **S9C**). Treatment of THP-1 macrophages with TMP-153 alone also increased *XBP1* splicing ~2.6 fold (**Figs. 5E** and **S9C**). These results suggest that exposure of adipocytes to AcLDL does not cause ER stress.

Proinflammatory cytokines do not induce ER stress in adipocytes

To study whether inflammatory cytokines induce ER stress in adipocytes we exposed differentiated 3T3-F442A adipocytes to various concentrations of TNF-α, IL-6, or IL-1β for up to 24 h. Incubation of adipocytes with increasing concentrations of TNF-α for 24 h did not affect the viability of these cells (**Fig. 7A**), but also failed to induce *XBP1* splicing (**Figs. 7B** and **S10**). Various concentrations of IL-6 and IL-1β also failed to induce *XBP1* splicing over a period of 24 h (**Figs. 7D and E** and **S11–12**). To validate that the cytokines possess biological activity we characterized activation of the MAPK kinase JNK in preadipocytes. All three cytokines stimulated phosphorylation of JNK (**Fig. 7C and F**), thus providing evidence that the cytokine preparations we utilized possess biological activity. Taken together, these data suggest that the inflammatory cytokines TNF-α, IL-6, and IL-1β do not cause ER stress in adipocytes.

Glucose starvation induces ER stress in adipocytes

Prolonged exposure of cells to glucose concentrations of <0.2 g/l induces the ER resident chaperones BiP and GRP94,[28,58] whose expression is controlled by XBP1 and ATF6. To characterize whether glucose starvation, which may be caused by the poor vascularization of the expanding adipose tissue in obesity, can induce ER stress in adipocytes, we maintained in

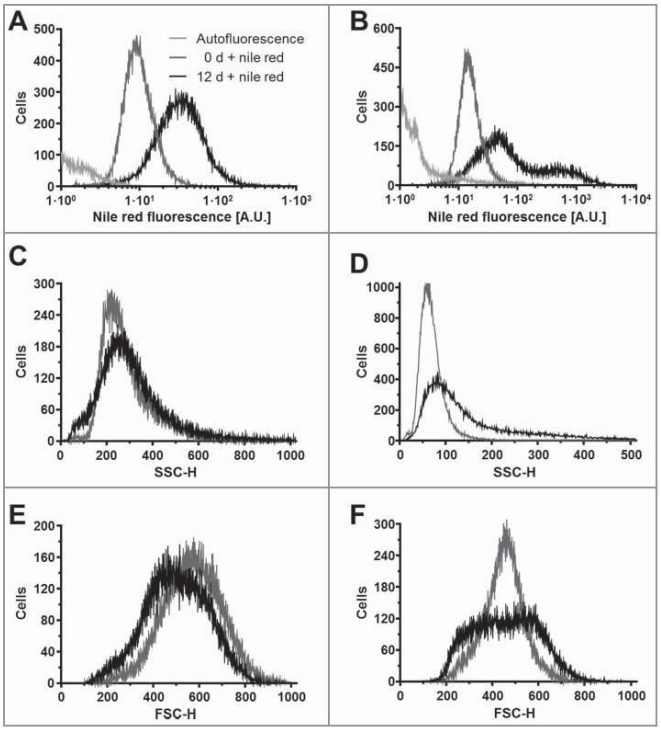

Figure 1. Adipocyte differentiation of 3T3-L1 and 3T3-F442A cells. (A and B) Nile red fluorescence, **(C and D)** side scatter (SSC-H), and **(E and F)** forward scatter (FSC-H) of **(A, C, E)** 3T3-L1 and **(B, D, F)** 3T3-F442A cells before (0 d, gray lines) and 12 d after induction of adipocyte differentiation (black lines). The light gray lines represent the autofluorescence of cells differentiated for 12 d. Dot plots of the side scatter SSC-H versus the forward scatter SSC-H for 3T3-L1 and 3T3-F442A cells before and 12 d after differentiation are shown in **Figure S1**. The mean nile red fluorescence of preadipocytes is significantly different from the mean nile red fluorescence of differentiated adipocytes in a one way analysis of variance (ANOVA) test with Dunnett's correction for multiple comparisons[112,113] ($P < 0.0001$ for both 3T3-L1 and 3T3-F442A cells).

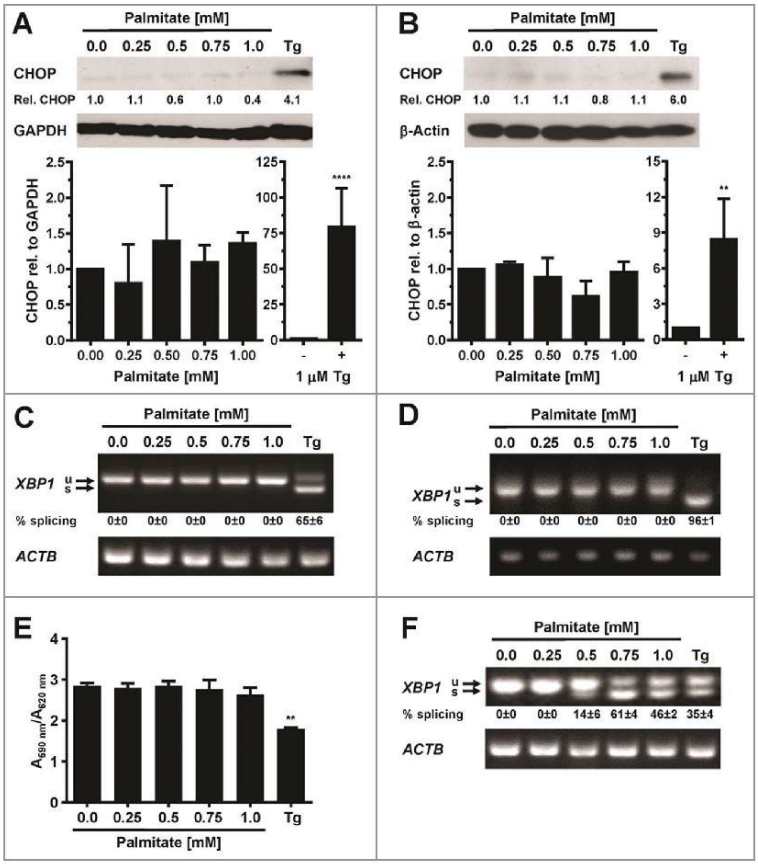

Figure 2. Palmitate does not induce CHOP protein expression or *XBP1* splicing in adipocytes. **(A and B)** CHOP expression in in vitro differentiated (**A**) 3T3-F442A adipocytes and (**B**) 3T3-L1 adipocytes exposed to the indicated concentrations of palmitate complexed to BSA for 48 h. Relative (rel.) CHOP signals were corrected for the loading controls GAPDH or β-actin. The bar graphs show the average and standard error of three independent repeats. Differences are not statistically significant ($p = 0.42$ for 3T3-F442A adipocytes and $p = 0.10$ for 3T3-L1 adipocytes in a repeated measures ANOVA test that compares the treated samples to the untreated sample. Equal variabilities of the differences were assumed for the treated and untreated samples and Dunnett's correction for multiple comparisons[112,113] was used). 1 μM thapsigargin (Tg) was used as a positive control for induction of ER stress. Thapsigargin-treated samples were compared to untreated samples using a two-tailed, unpaired *t*-test. **(C and D)** *XBP1* splicing in in vitro differentiated (**C**) 3T3-F442A adipocytes and (**D**) 3T3-L1 adipocytes incubated for 48 h with the indicated concentrations of BSA-complexed palmitate. % splicing indicates the percentage of spliced *XBP1* mRNA, for which the average and standard error of three independent experiments are shown. Abbreviations: u—unspliced *XBP1* mRNA, s—spliced *XBP1* mRNA. (**E**) MTT assay on in vitro differentiated 3T3-F442A adipocytes incubated for 48 h with the indicated concentrations of BSA-complexed palmitate. A repeated measures ANOVA test was used to compare the treated samples to the untreated sample. Equal variabilities of the differences were assumed for the treated and untreated samples and Dunnett's correction for multiple comparisons[112,113] was applied. (**F**) *XBP1* splicing in 3T3-F442A preadipocytes incubated for 12 h with the indicated concentrations of BSA-complexed palmitate. Abbreviations: * – $P < 0.05$, ** – $P < 0.01$, *** – $P < 0.001$, and **** – $P < 0.0001$.

vitro differentiated 3T3-F442A and 3T3-L1 adipocytes for up to 24 h in serum free medium supplemented with 2 mM L-glutamine but completely lacking glucose. Glutaminolysis serves as an energy source in this medium.[59,60] Glucose starvation for 24 h induced CHOP potently in both 3T3-F442A and 3T3-L1 adipocytes (**Fig. 8A and B**). *XBP1* splicing peaked 12 h after induction of glucose starvation (**Fig. S13A**) and remained elevated for the next 36 h in 3T3-F442A-adipocytes (**Figs. 8C and D** and **S13B**). 24 h of glucose starvation also induced *XBP1* splicing in 3T3-L1 adipocytes and elevated the steady-state mRNA levels of *CHOP*, *BiP*, and *ERDJ4*, and, to a lesser extent, *EDEM1* and *VEGFA* mRNAs in 3T3-F442A adipocytes (**Fig. 8E**). Thus, glucose starvation causes ER stress in adipocytes which coincides with increased expression of the pro-angiogenic factor *VEGFA*.

Hypoxia causes ER stress in adipocytes

We characterized whether hypoxia causes ER stress in in vitro differentiated 3T3-F442A adipocytes, because hypoxia is another physiological alteration in poorly vascularized obese adipose tissue.[3] In vitro differentiated 3T3-F442A adipocytes were cultured in 0.5% O_2 for up to 8 h before protein extraction and characterization of ER stress markers and the hypoxia marker HIF1α[61] by Western blotting. Hypoxia increased HIF1α levels

within 2 h (**Fig. 9A and B**) and also led to an increase in eIF2α phosphorylation (**Fig. 9A and B**), *XBP1* splicing (**Fig. 9C and D**), and *BiP* mRNA levels (**Fig. 9E and F**). The increases in *XBP1* splicing, *BiP* mRNA levels, and eIF2α phosphorylation, once manifested, persisted throughout the time course of the experiment. Collectively, these data show that hypoxia induces ER stress in adipocytes.

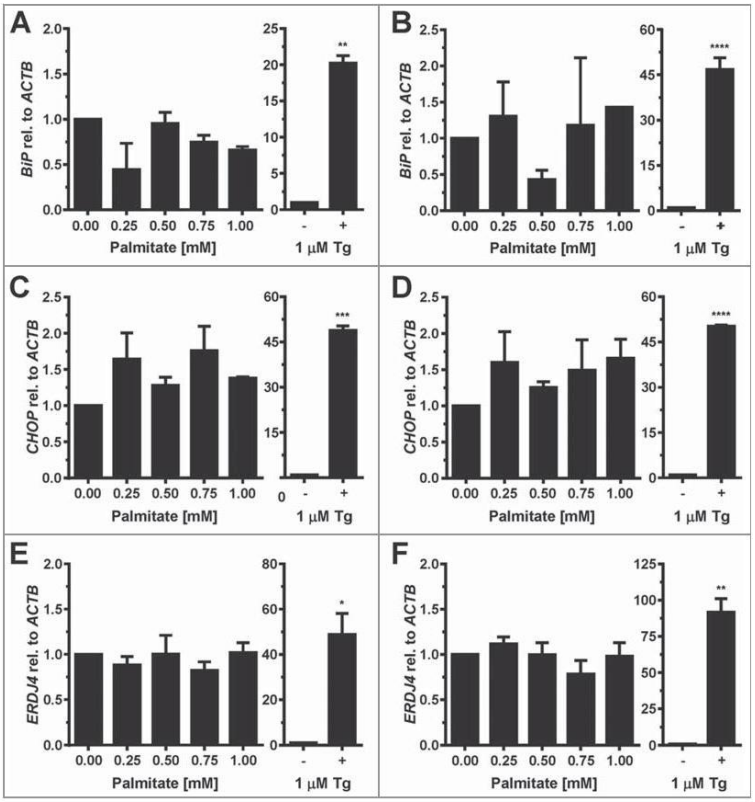

Figure 3. Palmitate does not induce *BiP*, *CHOP*, or *ERDJ4* transcription in adipocytes. **(A and B)** *BiP* mRNA, **(C and D)** *CHOP* mRNA, and **(E and F)** *ERDJ4* mRNA levels in in vitro differentiated **(A, C, E)** 3T3-F442A and **(B, D, F)** 3T3-L1 adipocytes incubated for 48 h with the indicated concentrations of BSA-complexed palmitate. The differences in *BiP* mRNA ($p = 0.10$ for 3T3-F442A adipocytes and $p = 0.34$ for 3T3-L1 adipocytes), *CHOP* mRNA ($p = 0.11$ for 3T3-F442A adipocytes and $p = 0.41$ for 3T3-L1 adipocytes), and *ERDJ4* mRNA ($p = 0.48$ for 3T3-F442A adipocytes and $p = 0.41$ for 3T3-L1 adipocytes) levels in the untreated and palmitate treated samples are not statistically significant. A repeated measures ANOVA test with Dunnett's correction for multiple comparisons[112,113] and assuming equal variabilities of the differences was used to compare the palmitate-treated samples to the untreated sample. Thapsigargin-treated samples were compared to untreated samples using a two-tailed, unpaired *t*-test.

Discussion

We present evidence that glucose starvation and hypoxia (**Figs. 8** and **9**), but not palmitate (**Figs. 2, 3** and **S3–7**), cholesterol (**Figs. 5, 6,** and **S9**), or several inflammatory cytokines (**Fig. 7** and **S10–12**) cause ER stress in two in vitro adipocyte models, 3T3-F442A and 3T3-L1. These data suggest that the poor vascularization of adipose tissue in obesity causes ER stress in adipocytes, because adipose tissue expansion in obesity leads to formation of poorly vascularized, hypoxic areas.[3,4] Glucose starvation may contribute to the adverse effects of hypoxia on adipose tissue, because obese adipocytes reach diameters that are comparable to the maximum distance of diffusive glucose supply from a blood vessel.[62–64] The large overlap of the effects of hypoxia and ER stress on adipose tissue, including inflammation,[4] insulin resistance,[65] changes in adiponectin secretion,[66] and increased angiogenesis,[67-69] suggests that ER stress may contribute to or mediate the effects of hypoxia on adipocytes.

Our work also suggests that palmitate, cholesterol, and inflammatory cytokines do not elicit an ER stress response in adipocytes. The mRNA expression for two ER stress sensors, IRE1α and PERK, is similar in preadipocytes and adipocytes (**Fig. S14**), which suggests that increased basal activity of these ER stress signaling pathways cannot explain the protection of adipocytes from palmitate- or cholesterol-induced ER stress. A dominant feature of adipocyte differentiation is the induction of nearly all enzymes of fatty acid and triacylglycerol synthesis, including stearoyl-CoA desaturases and diacylglycerol acyltransferases.[70,71] Hence, adipocytes may be protected from palmitate-induced ER stress because of their greatly increased ability to dispose of excess palmitate in their triacylglycerol pool.[72] The expansion of the triacylglycerol pool will also increase the storage capacity of adipocytes for cholesterol[73,74] and thus may explain why cholesterol does not induce ER stress in adipocytes. Increased cholesterol

no. I5879), insulin (cat. no. I0516), palmitic acid (cat. no. P5585), fatty acid free bovine serum albumin (BSA, cat. no. A3803), BSA (cat. no. A2153), and thiazolyl blue tetrazolium bromide (MTT, cat. no. M5655), and 9-diethylamino-5*H*-benzo[α]phenoxazine-5-one (nile red, cat. no. N3013) were purchased from Sigma-Aldrich. TMP-153 was purchased from Enzo Life Sciences. AcLDL (cat. no. 5685–3404) was purchased from AbD Serotec, IL-1β (cat. no. RIL1BI) from Thermo Fisher Scientific, IL-6 (cat. no. PHC0066) from Life Technologies, and human TNF-α (cat. no. 8902) from Cell Signaling Technology Inc.

Cell culture

3T3-L1 murine preadipocytes[103] were obtained from the ATCC and were maintained as subconfluent cultures in Dulbecco's modified Eagle's medium (DMEM) supplemented with 4.5 g/l D-glucose, 2 mM L-glutamine and 10% (v/v) bovine calf serum. 3T3-F442A murine preadipocytes[104] were maintained in DMEM supplemented with 4.5 g/l D-glucose, 2 mM L-glutamine and 10% (v/v) foetal bovine serum (FBS). For differentiation,[45] both cell lines were grown to confluence. Two days post-confluency, differentiation was induced by addition of 1 μg/ml insulin, 0.5 mM IBMX, and 0.25 μM dexamethasone. The cells were maintained in this medium for 3 d and then for 2 more days in medium containing 1 μg/ml insulin. After five days of differentiation insulin was omitted from the medium and the cells were maintained for another 7 d. In all experiments both 3T3-F442A and 3T3-L1 adipocytes were used 12 d after induction of differentiation. The THP-1 human monocytic leukemia cell line[105] was maintained in RPMI 1640 medium containing 10% (v/v) foetal bovine serum (FBS) and 2 mM L-glutamine. The cells were

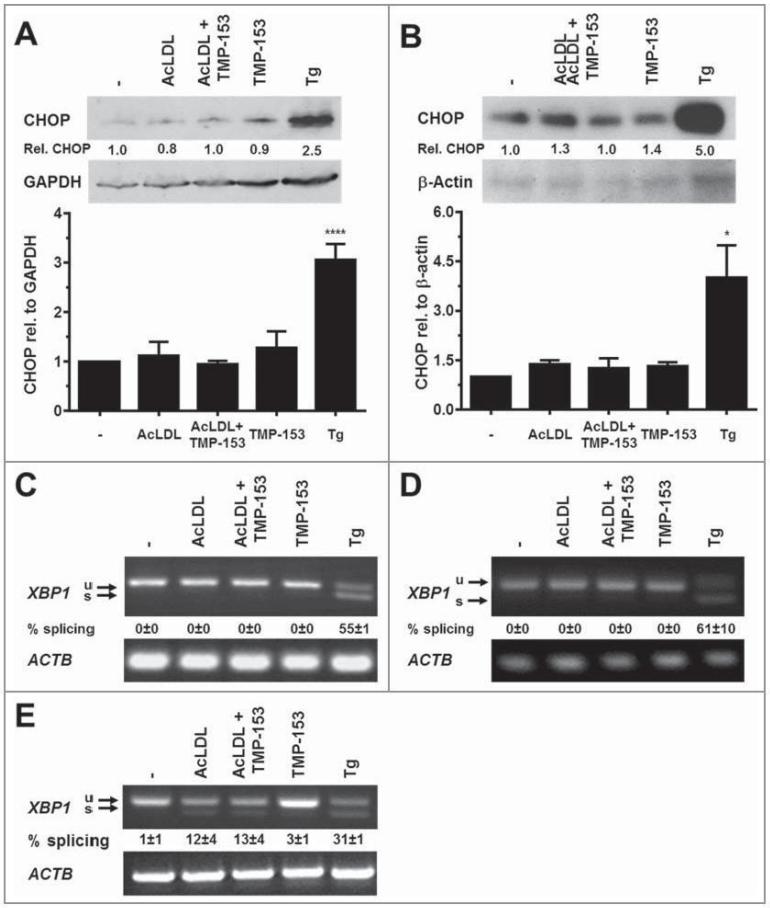

Figure 5. Cholesterol loading does not induce CHOP protein expression or *XBP1* splicing in adipocytes. **(A and B)** CHOP protein levels and **(C and D)** *XBP1* splicing in in vitro differentiated (**A and C**) 3T3-F442A and (**B and D**) 3T3-L1 adipocytes incubated for 48 h with human acetylated LDL (AcLDL), AcLDL and 0.6 μM of the ACAT inhibitor TMP-153, 0.6 μM TMP-153, 1.0 μM Tg, or left untreated ('-'). The average and standard error of 3 independent experiments are shown in the bar graphs. Differences in CHOP protein levels between the untreated sample and the samples treated with AcLDL, AcLDL and 0.6 μM TMP-153, and 0.6 μM TMP-153 are not statistically significant ($p = 0.26$ for 3T3-F442A adipocytes and $p = 0.35$ for 3T3-L1 adipocytes in a repeated measures ANOVA test with Dunnett's correction for multiple comparisons[112,113] comparing the treated samples to the untreated samples and assuming equal variabilities of the differences). (**E**) *XBP1* splicing in untreated in vitro differentiated human THP-1 macrophages and macrophages incubated for 16 h with AcLDL, AcLDL + 0.6 μM TMP-153, 0.6 μM TMP-153, or 1.0 μM Tg.

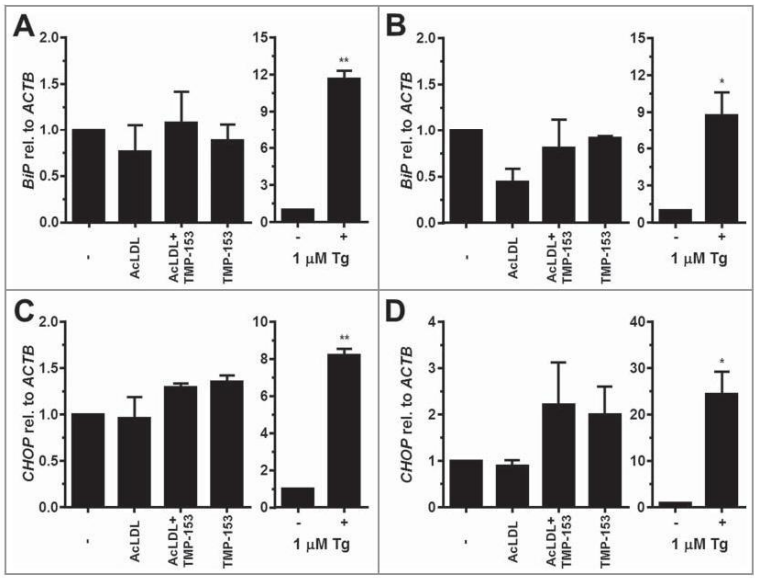

Figure 6. Cholesterol loading does not induce *BiP* or *CHOP* transcription in adipocytes. **(A and B)** *BiP* mRNA and **(C and D)** *CHOP* mRNA levels in in vitro differentiated **(A and C)** 3T3-F442A and **(B and D)** 3T3-L1 adipocytes incubated for 48 h with human acetylated LDL (AcLDL), AcLDL and 0.6 μM of the ACAT inhibitor TMP-153, 0.6 μM TMP-153, 1.0 μM Tg, or left untreated ('-'). The average and standard error of three independent experiments are shown. Differences are not statistically significant (*BiP* mRNA: $p = 0.34$ for 3T3-F442A adipocytes and $p = 0.11$ for 3T3-L1 adipocytes; *CHOP* mRNA: $p = 0.09$ for 3T3-F442A adipocytes and $p = 0.11$ for 3T3-L1 adipocytes). p values were obtained from a repeated measures ANOVA test comparing the samples treated with AcLDL, AcLDL and 0.6 μM TMP-153, and 0.6 μM TMP-153 to the untreated samples and assuming equal variabilities of the differences. Dunnett's correction for multiple comparisons[112,113] was applied. Thapsigargin-treated samples were compared to untreated samples using a two-tailed, unpaired *t*-test.

differentiated into macrophages by incubation with 50 nM phorbol-12-myristate 13-acetate (PMA) for 3 d, followed by incubation for 1 d without PMA.[106] Before addition of AcLDL or TMP-153 the cells were serum-starved for 7 h.

Flow cytometry

Cells were stained with nile red and analyzed by flow cytometry essentially as described before.[42] In brief, cells were trypsinized, washed once with DMEM supplemented with 4.5 g/l D-glucose, 2 mM L-glutamine and 10% (v/v) bovine calf serum, and then with phosphate-buffered saline (PBS, 4.3 mM Na_2HPO_4, 1.47 mM KH_2PO_4, 27 mM KCl, 137 mM NaCl, pH 7.4), stained for 5 min with 100 ng/ml nile red in PBS, washed once with PBS and immediately analyzed by flow cytometry on a BD FACSCalibur Flow Cytometer (BD Biosciences) at a LO flow rate. For each sample ~50,000 gated events were collected. Nile red fluorescence was excited at 488 nm and its fluorescence emission collected using the FL-1 (530/30 nm) band pass filter set. The instrument settings for 3T3-L1 cells were FSC—E-1 (lin, Amp gain = 4.50), SSC—326 V (lin, Amp gain = 1.00), and FL1—275 V (log, Amp gain = 1.00), and for 3T3-F442A cells FSC—E-1 (lin, Amp gain = 4.50), SSC—280 V (lin, Amp gain = 1.00), and FL1—275 V (log, Amp gain = 1.00). No thresholds were applied. Data were analyzed in WinMDI 2.9 and graphs prepared in GraphPad Prism 6.04 (GraphPad Software). Three biological replicates were analyzed for each sample and results are represented as the average and standard error of these three repeats.

Cell viability was determined using the MTT assay.[107] In short, after TNF-α or palmitate treatment cells were incubated for 4 h at 37°C with 0.5 g/l MTT in phenol-red free DMEM containing 4.5 g/l D-glucose, and 2 mM L-glutamine or 2% (w/v) BSA, respectively. Insoluble formazan crystals were dissolved for 15 min in isopropanol containing 4 mM HCl and 0.1% (v/v) Nonidet P-40. The absorbance of the formazan solution was read at a wavelength of 590 nm and a reference wavelength of 620 nm and the formazan absorbance expressed as the ratio of the absorbance at 590 nm to the absorbance at 620 nm.

Palmitate treatment

In vitro differentiated 3T3-F442A adipocytes were serum-starved overnight in DMEM containing 4.5 g/l D-glucose, and 2 mM L-glutamine and then incubated in serum-free medium containing 2% (w/v) fatty acid-free BSA and 0.05—1 mM palmitic acid. These palmitate concentrations are in the physiological range reported for rodents and humans.[108] Palmitic acid was complexed to fatty acid-free BSA as follows. In brief, palmitic acid was dissolved in ethanol and diluted 1:100 in DMEM containing 4.5 g/l D-glucose and 2% (w/v) fatty acid-free BSA before addition to the cells. Control cells received ethanol diluted 1:100 into DMEM containing 4.5 g/l D-glucose and 2% (w/v) fatty acid-free BSA.[109]

Cholesterol and cytokine treatments

In vitro differentiated adipocytes were incubated in DMEM containing 4.5 g/l D-glucose, 2 mM L-glutamine, and 100 μg/ml AcLDL in the presence or absence of the ACAT inhibitor TMP-153 at a final concentration of 0.6 μM. The cells were incubated with cytokines in serum-free medium.

D-Glucose starvation experiments were performed by incubating the cells for the indicated times in D-glucose-free DMEM supplemented with 2 mM L-glutamine. Control cells '+ D-glucose' were incubated for the same time in DMEM containing 4.5 g/l D-glucose and 2 mM L-glutamine.

Hypoxia experiments were performed using a Billups-Rotenberg hypoxia chamber. A pre-analyzed gas mixture of 0.5% (v/v) O_2, 5% (v/v) CO_2 and nitrogen (BOC Industrial Gases) was flushed through the chamber at a flow rate of 25 l/min for 5 min to completely replace air inside the chamber with the gas mixture. The hypoxia chamber was incubated at 37°C for the indicated times. Cells were rapidly harvested and lysed at 4°C using degassed buffers as described before.[110]

RNA analysis

RNA was extracted and analyzed by reverse transcriptase (RT) PCR as described before.[110] Primers for quantitative PCR (qPCR) are listed in **Table 1**. RT-qPCR data were standardized to *ACTB* as loading control. The percentage of *XBP1* splicing was calculated by dividing the signal for spliced *XBP1* mRNA by the sums of the signals for spliced and unspliced *XBP1* mRNAs. Band intensities were quantitated using ImageJ.

Protein extraction and Western blotting

Cells were washed 3 times with ice-cold PBS and lysed in RIPA buffer [50 mM Tris-HCl, pH 8.0, 150 mM NaCl, 0.5% (w/v) sodium deoxycholate, 0.1% (v/v) Triton X-100, 0.1% (w/v) SDS] containing Roche complete protease inhibitors (cat. no. 11836153001, Roche Applied Science) and phosphatase inhibitors (cat. no. 04 906 837 001, Roche Applied Science) as described before.[110]

Proteins were separated by SDS-PAGE on 4–20% Criterion TGX Precast gels (cat. no. 567–1094, Bio-Rad Laboratories) and transferred to polyvinylidene difluoride (PVDF) membranes (Amersham HyBond™-P, pore size 0.45 μm, cat. no. RPN303F, GE Healthcare) by semi-dry

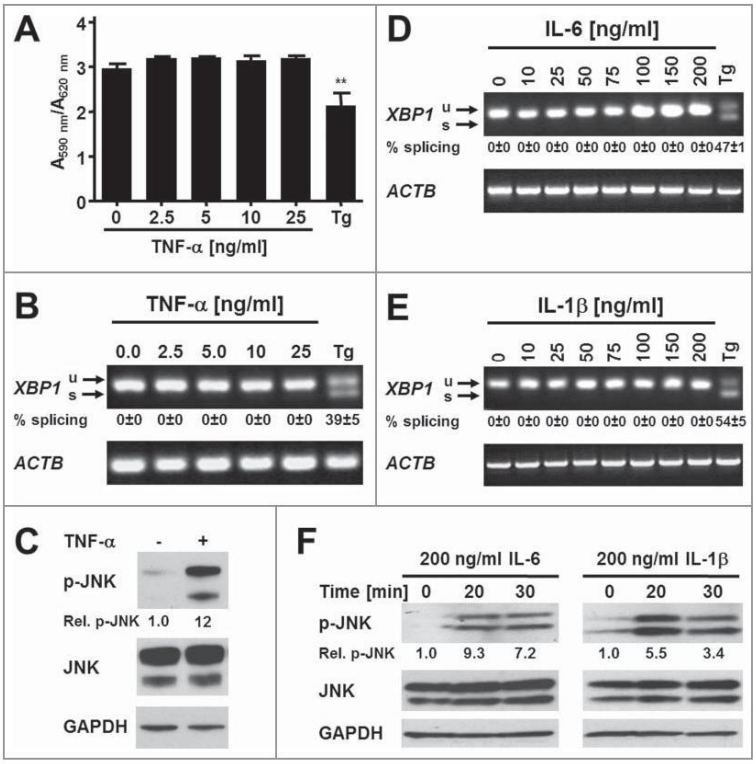

Figure 7. The proinflammatory cytokines TNF-α, IL-6, and IL-1β do not induce ER stress in adipocytes. (**A**) MTT assay on in vitro differentiated 3T3-F442A adipocytes incubated for 24 h with the indicated concentrations of TNF-α. A repeated measures ANOVA test was used to compare the treated samples to the untreated sample. Equal variabilities of the differences were assumed for the treated and untreated samples and Dunnett's correction for multiple comparisons[112,113] was applied. (**B**) *XBP1* splicing in in vitro differentiated 3T3-F442A adipocytes incubated for 24 h with the indicated concentrations of TNF-α or 1.0 μM Tg. The average and standard error from three independent experiments are shown. (**C**) JNK phosphorylation in 3T3-F442A preadipocytes incubated for 30 min with 25 ng/ml TNF-α. (**D** and **E**) *XBP1* splicing in in vitro differentiated 3T3-F442A adipocytes incubated for 24 h with the indicated concentrations of (**D**) IL-6 and (**E**) IL-1β. The average and standard error of two independent experiments are shown. (**F**) JNK phosphorylation in 3T3-F442A preadipocytes incubated for the indicated times with 200 ng/ml IL-6 or 200 ng/ml IL-1β.

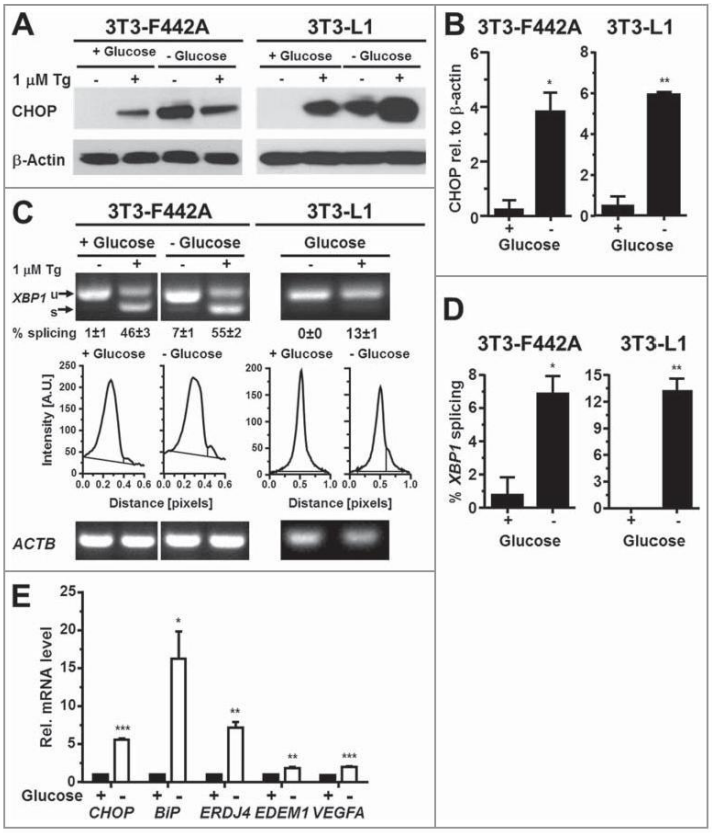

Figure 8. Glucose starvation induces ER stress in adipocytes. (**A**) CHOP protein levels in in vitro differentiated 3T3-F442A and 3T3-L1 adipocytes maintained for 24 h in the presence of 4.5 g/l D-glucose ('+ Glucose') or without any glucose ('- Glucose'). β-Actin was used as a loading control. (**B**) Quantitation of the Western blots shown in panel (**A**). (**C**) *XBP1* splicing in in vitro differentiated 3T3-F442A and 3T3-L1 adipocytes maintained for 24 h in the presence of 4.5 g/l D-glucose or without any glucose. Below the images of the agarose gels the intensity of the ethidium bromide fluorescence was plotted vs. the migration distance of the PCR products. (**D**) Quantitation of XBP1 splicing shown in panel (**C**). For both cell lines the average and standard error of three independent repeats are shown. (**E**) Steady-state mRNA levels of *CHOP, BiP, ERDJ4, EDEM1, and VEGFA* mRNAs in 3T3-F442A adipocytes maintained for 24 h in the presence of 4.5 g/l D-glucose or without any glucose. *p* values were obtained from two-tailed, unpaired *t*-tests.

electrotransfer in 0.1 M Tris, 0.192 M glycine, and 5% (v/v) methanol at 2 mA/cm^2 for 60–75 min. Membranes were then blocked for 1 h in 5% (w/v) skimmed milk powder in TBST [20 mM Tris-HCl, pH 7.6, 137 mM NaCl, and 0.1% (v/v) Tween-20] for antibodies against non-phosphorylated proteins and 5% BSA in TBST for antibodies against phosphorylated proteins. Incubations with antibodies were performed over night at 4°C with gentle agitation. Blots were washed three times with TBST and then probed with secondary antibody for 1 hour at room temperature. The rabbit anti-AKT, anti-phospho-S473-AKT, anti-phospho-S51-eIF2α, anti-JNK and anti-phospho-JNK antibodies were used at a 1:1,000 dilution in TBST + 5% (w/v) BSA. The rabbit anti-eIF2α antibody was used at a 1:500 dilution in TBST + 5% (w/v) skimmed milk powder. Membranes were developed with goat anti-rabbit-IgG (H+L)-horseradish peroxidase (HRP)-conjugated secondary antibody at a 1:1,000 dilution in TBST + 5% (w/v) skimmed milk powder for 1 h at room temperature. The mouse anti-CHOP antibody and anti-β-actin antibodies were used at a 1:1,000 dilution in TBST + 5% (w/v) skimmed milk powder, and the mouse anti-GAPDH antibody at a 1:30,000 dilution in TBST + 5% (w/v) skimmed milk powder. These antibodies were developed with goat anti-mouse IgG (H+L)-horseradish peroxidase (HRP)-conjugated secondary antibody at a 1:20,000 dilution in TBST +5% (w/v) skimmed milk powder for 1 h at room temperature. The goat anti-HIF1α antibody was used at a dilution of 1:500 in TBST + 5% (w/v) skimmed milk powder and developed with mouse anti-goat IgG (H+L)-HRP-conjugated antibody at a dilution of 1:30,000 in TBST + 5% (w/v) skimmed milk powder for 1 h at room temperature. To reprobe blots for detection of nonphosphorylated proteins, membranes were stripped using Restore Western Blot Stripping Buffer (Thermo Fisher Scientific, Loughborough, UK, cat. no. 21059) and blocked with 5% (w/v) skimmed milk powder in TBST.

For signal detection, Pierce ECL Western Blotting Substrate (cat. no. 32209) or Pierce ECL Plus Western Blotting

Substrate (cat. no. 32132) from Thermo Fisher Scientific were used. Blots were exposed to CL X Posure™ film (cat. no. 34091, Thermo Fisher Scientific). Exposure times were adjusted on the basis of previous exposures to obtain exposures in the linear range of the film. Films were scanned on a CanoScan LiDE 600F scanner (Canon) and saved as tif files. Bands were quantified using ImageJ exactly as described under the heading "Gels Submenu" on the ImageJ web site (http://rsb.info.nih.gov/ij/docs/menus/analyze.html#plot). Peak intensities for the experimental antibody were then divided by the peak intensities obtained with the antibody for the loading control in the corresponding lane to correct for differences in loading between individual lanes. All loading control-corrected peak intensities obtained for one Western blot were then expressed relative to the loading control-corrected peak intensity of the 0 h sample.

Statistical analysis

All data are presented as the average and standard error of three independently differentiated adipocyte cultures. Errors were propagated using the law of error propagation for random, independent errors.[111] Statistical analyses were performed in GraphPad Prism 6.04. The statistical tests and corrections for multiple comparison used to analyze the data are described in detail in the figure legends.

Disclosure of Potential Conflicts of Interest

No potential conflicts of interest were disclosed.

Acknowledgments

ADM and MS devised the study, analyzed the data, designed the experiments and wrote the manuscript. We thank A Benham (Durham University) for providing the human THP-1 cells and C. Hutchison (Durham University) for providing the 3T3-F442A preadipocytes. We thank O Alainis and C Manning for help with the flow cytometry, and N Hole for use of the hypoxia chamber.

Supplemental Material

Supplemental data for this article can be accessed on the publisher's website.

Funding

This work was supported by Diabetes UK BDA 09/0003949 grant.

References

1. Hotamisligil GS. Inflammation and metabolic disorders. Nature 2006; 444:860-7; PMID:17167474; http://dx.doi.org/10.1038/nature05485
2. Van Gaal LF, Mertens IL, De Block CE. Mechanisms linking obesity with cardiovascular disease. Nature 2006; 444:875-80; PMID:17167476; http://dx.doi.org/10.1038/nature05487
3. Sun K, Kusminski CM, Scherer PE. Adipose tissue remodeling and obesity. J Clin Invest 2011; 121:2094-101; PMID:21633177; http://dx.doi.org/10.1172/JCI45887
4. Ye J, Gao Z, Yin J, He Q. Hypoxia is a potential risk factor for chronic inflammation and adiponectin reduction in adipose tissue of *ob/ob* and dietary obese mice. Am J Physiol Endocrinol Metab 2007; 293:E1118-28; PMID:17666485; http://dx.doi.org/10.1152/ajpendo.00435.2007
5. Coenen KR, Gruen ML, Chait A, Hasty AH. Diet-induced increases in adiposity, but not plasma lipids, promote macrophage infiltration into white adipose tissue. Diabetes 2007; 56:564-73; PMID:17327423; http://dx.doi.org/10.2337/db06-1375
6. Lumeng CN, Bodzin JL, Saltiel AR. Obesity induces a phenotypic switch in adipose tissue macrophage polarization. J Clin Invest 2007; 117:175-84; PMID:17200717; http://dx.doi.org/10.1172/JCI29881
7. Schröder M. Endoplasmic reticulum stress responses. Cell Mol Life Sci 2008; 65:862-94; PMID:18038217; http://dx.doi.org/10.1007/s00018-007-7383-5
8. Zhang K, Kaufman RJ. From endoplasmic-reticulum stress to the inflammatory response. Nature 2008; 454:455-62; PMID:18650916; http://dx.doi.org/10.1038/nature07203
9. Samuel VT, Shulman GI. Mechanisms for insulin resistance: common threads and missing links. Cell 2012; 148:852-71; PMID:22385956; http://dx.doi.org/10.1016/j.cell.2012.02.017
10. Gregor MF, Hotamisligil GS. Adipocyte stress: the endoplasmic reticulum and metabolic disease. J Lipid Res 2007; 48:1905-14; PMID:17699733; http://dx.doi.org/10.1194/jlr.R700007-JLR200
11. Schröder M, Kaufman RJ. ER stress and the unfolded protein response. Mutat Res 2005; 569:29-63; PMID:15603751; http://dx.doi.org/10.1016/j.mrfmmm.2004.06.056
12. Marciniak SJ, Yun CY, Oyadomari S, Novoa I, Zhang Y, Jungreis R, Nagata K, Harding HP, Ron D. CHOP induces death by promoting protein synthesis and oxidation in the stressed endoplasmic reticulum. Genes Dev 2004; 18:3066-77; PMID:15601821; http://dx.doi.org/10.1101/gad.1250704
13. Calfon M, Zeng H, Urano F, Till JH, Hubbard SR, Harding HP, Clark SG, Ron D. IRE1 couples endoplasmic reticulum load to secretory capacity by processing the *XBP-1* mRNA. Nature 2002; 415:92-6; PMID:11780124; http://dx.doi.org/10.1038/415092a
14. Yoshida H, Matsui T, Yamamoto A, Okada T, Mori K. XBP1 mRNA is induced by ATF6 and spliced by IRE1 in response to ER stress to produce a highly active transcription factor. Cell 2001; 107:881-91; PMID:11779464; http://dx.doi.org/10.1016/S0092-8674(01)00611-0
15. Ye J, Rawson RB, Komuro R, Chen X, Dave UP, Prywes R, Brown MS, Goldstein JL. ER stress induces cleavage of membrane-bound ATF6 by the same proteases that process SREBPs. Mol Cell 2000; 6:1355-64; PMID:11163209; http://dx.doi.org/10.1016/S1097-2765(00)00133-7
16. Wu J, Rutkowski DT, Dubois M, Swathirajan J, Saunders T, Wang J, Song B, Yau GD-Y, Kaufman RJ. ATF6α optimizes long-term endoplasmic reticulum function to protect cells from chronic stress. Dev Cell 2007; 13:351-64; PMID:17765679; http://dx.doi.org/10.1016/j.devcel.2007.07.005
17. Yamamoto K, Sato T, Matsui T, Sato M, Okada T, Yoshida H, Harada A, Mori K. Transcriptional induction of mammalian ER quality control proteins is mediated by single or combined action of ATF6α and XBP1. Dev Cell 2007; 13:365-76; PMID:17765680; http://dx.doi.org/10.1016/j.devcel.2007.07.018
18. Nishitoh H, Matsuzawa A, Tobiume K, Saegusa K, Takeda K, Inoue K, Hori S, Kakizuka A, Ichijo H. ASK1 is essential for endoplasmic reticulum stress-induced neuronal cell death triggered by expanded polyglutamine repeats. Genes Dev 2002; 16:1345-55; PMID:12050113; http://dx.doi.org/10.1101/gad.992302
19. Ohoka N, Yoshii S, Hattori T, Onozaki K, Hayashi H. *TRB3*, a novel ER stress-inducible gene, is induced via ATF4-CHOP pathway and is involved in cell death. EMBO J 2005; 24:1243-55; PMID:15775988; http://dx.doi.org/10.1038/sj.emboj.7600596
20. Özcan U, Cao Q, Yilmaz E, Lee A-H, Iwakoshi NN, Ozdelen E, Tuncman G, Görgün C, Glimcher LH, Hotamisligil GS. Endoplasmic reticulum stress links obesity, insulin action, and type 2 diabetes. Science 2004; 306:457-61; PMID:15486293; http://dx.doi.org/10.1126/science.1103160
21. Wei Y, Wang D, Topczewski F, Pagliassotti MJ. Saturated fatty acids induce endoplasmic reticulum stress and apoptosis independently of ceramide in liver cells. Am J Physiol Endocrinol Metab 2006; 291:E275-81; PMID:16492686; http://dx.doi.org/10.1152/ajpendo.00644.2005
22. Laybutt DR, Preston AM, Åkerfeldt MC, Kench JG, Busch AK, Biankin AV, Biden TJ. Endoplasmic reticulum stress contributes to beta cell apoptosis in type 2 diabetes. Diabetologia 2007; 50:752-63; PMID:17268797; http://dx.doi.org/10.1007/s00125-006-0590-z
23. DeVries-Seimon T, Li Y, Yao PM, Stone E, Wang Y, Davis RJ, Flavell R, Tabas I. Cholesterol-induced macrophage apoptosis requires ER stress pathways and engagement of the type A scavenger receptor. J Cell Biol 2005; 171:61-73; PMID:16203857; http://dx.doi.org/10.1083/jcb.200502078
24. Guo W, Wong S, Xie W, Lei T, Luo Z. Palmitate modulates intracellular signaling, induces endoplasmic reticulum stress, and causes apoptosis in mouse 3T3-L1 and rat primary preadipocytes. Am J Physiol Endocrinol Metab 2007; 293:E576-86; PMID:17519282; http://dx.doi.org/10.1152/ajpendo.00523.2006
25. Antuna-Puente B, Feve B, Fellahi S, Bastard J-P. Adipokines: the missing link between insulin resistance and obesity. Diabetes Metab 2008; 34:2-11; PMID:18093861; http://dx.doi.org/10.1016/j.diabet.2007.09.004

26. Zhang K, Shen X, Wu J, Sakaki K, Saunders T, Rutkowski DT, Back SH, Kaufman RJ. Endoplasmic reticulum stress activates cleavage of CREBH to induce a systemic inflammatory response. Cell 2006; 124:587-99; PMID:16469704; http://dx.doi.org/10.1016/j.cell.2005.11.040
27. Xue X, Piao J-H, Nakajima A, Sakon-Komazawa S, Kojima Y, Mori K, Yagita H, Okumura K, Harding H, Nakano H. Tumor necrosis factor α (TNFα) induces the unfolded protein response (UPR) in a reactive oxygen species (ROS)-dependent fashion, and the UPR counteracts ROS accumulation by TNFα. J Biol Chem 2005; 280:33917-25; PMID:16107336; http://dx.doi.org/10.1074/jbc.M505818200
28. Shiu RP, Pouyssegur J, Pastan I. Glucose depletion accounts for the induction of two transformation-sensitive membrane proteins in Rous sarcoma virus-transformed chick embryo fibroblasts. Proc Natl Acad Sci U S A 1977; 74:3840-4; PMID:198809; http://dx.doi.org/10.1073/pnas.74.9.3840
29. Lin AY, Lee AS. Induction of two genes by glucose starvation in hamster fibroblasts. Proc Natl Acad Sci U S A 1984; 81:988-92; PMID:6583707; http://dx.doi.org/10.1073/pnas.81.4.988
30. Romero-Ramirez L, Cao H, Nelson D, Hammond E, Lee A-H, Yoshida H, Mori K, Glimcher LH, Denko NC, Giaccia AJ, et al. XBP1 is essential for survival under hypoxic conditions and is required for tumor growth. Cancer Res 2004; 64:5943-7; PMID:15342372; http://dx.doi.org/10.1158/0008-5472.CAN-04-1606
31. Koumenis C, Naczki C, Koritzinsky M, Rastani S, Diehl A, Sonenberg N, Koromilas A, Wouters BG. Regulation of protein synthesis by hypoxia via activation of the endoplasmic reticulum kinase PERK and phosphorylation of the translation initiation factor eIF2α. Mol Cell Biol 2002; 22:7405-16; PMID:12370288; http://dx.doi.org/10.1128/MCB.22.21.7405-7416.2002
32. Bi MX, Naczki C, Koritzinsky M, Fels D, Blais J, Hu NP, Harding H, Novoa I, Varia M, Raleigh J, et al. ER stress-regulated translation increases tolerance to extreme hypoxia and promotes tumor growth. EMBO J 2005; 24:3470-81; PMID:16148948; http://dx.doi.org/10.1038/sj.emboj.7600777
33. Hotamisligil GS, Arner P, Caro JF, Atkinson RL, Spiegelman BM. Increased adipose tissue expression of tumor necrosis factor-α in human obesity and insulin resistance. J Clin Invest 1995; 95:2409-15; PMID:7738205; http://dx.doi.org/10.1172/JCI117936
34. Kern PA, Ranganathan S, Li C, Wood L, Ranganathan G. Adipose tissue tumor necrosis factor and interleukin-6 expression in human obesity and insulin resistance. Am J Physiol Endocrinol Metab 2001; 280:E745-51; PMID:11287357
35. Misaki Y, Miyauchi R, Mochizuki K, Takabe S, Shimada M, Ichikawa Y, Goda T. Plasma interleukin-1β concentrations are closely associated with fasting blood glucose levels in healthy and prediniical middle-aged nonoverweight and overweight Japanese men. Metabolism 2010; 59:1465-71; PMID:20170929; http://dx.doi.org/10.1016/j.metabol.2010.01.011
36. Spranger J, Kroke A, Möhlig M, Hoffmann K, Bergmann MM, Ristow M, Boeing H, Pfeiffer AFH. Inflammatory cytokines and the risk to develop type 2 diabetes: results of the prospective population-based European Prospective Investigation into Cancer and Nutrition (EPIC)-Potsdam Study. Diabetes 2003; 52:812-7; PMID:12606524; http://dx.doi.org/10.2337/diabetes.52.3.812
37. Tremblay AJ, Després JP, Piché ME, Nadeau A, Bergeron J, Alméras N, Tremblay A, Lemieux S. Associations between the fatty acid content of triglyceride, visceral adipose tissue accumulation, and components of the insulin resistance syndrome. Metabolism 2004; 53:310-7; PMID:15015142; http://dx.doi.org/10.1016/j.metabol.2003.10.011
38. Sorensen TI, Andersen B, Kam-Hansen L. Total plasma cholesterol in obesity after jejunoileal bypass with 3:1 or 1:3 jejunoileal ratio. A randomized trial. Scand J Gastroenterol 1979; 14:865-8; PMID:395631; http://dx.doi.org/10.3109/00365527909181417
39. Dobrea GM, Wieland RG, Johnson MW. The effect of rapid weight loss due to jejunoileal bypass on total cholesterol and high-density lipoprotein. Am J Clin Nutr 1981; 34:1994-6; PMID:7293931
40. Green H, Kehinde O. Formation of normally differentiated subcutaneous fat pads by an established preadipose cell line. J Cell Physiol 1979; 101:169-71; PMID:541350; http://dx.doi.org/10.1002/jcp.1041010119
41. Mandrup S, Loftus TM, MacDougald OA, Kuhajda FP, Lane MD. Obese gene expression at in vivo levels by fat pads derived from s.c. implanted 3T3-F442A preadipocytes. Proc Natl Acad Sci U S A 1997; 94:4300-5; PMID:9113984; http://dx.doi.org/10.1073/pnas.94.9.4300
42. Greenspan P, Mayer EP, Fowler SD. Nile red: a selective fluorescent stain for intracellular lipid droplets. J Cell Biol 1985; 100:965-73; PMID:3972906; http://dx.doi.org/10.1083/jcb.100.3.965
43. Crandall DL, Quinet EM, Morgan GA, Busler DE, McHendry-Rinde B, Kral JG. Synthesis and secretion of plasminogen activator inhibitor-1 by human preadipocytes. J Clin Endocrinol Metab 1999; 84:3222-7; PMID:10487691; http://dx.doi.org/10.1210/jcem.84.9.5987
44. Schaedlich K, Knelangen JM, Santos AN, Fischer B. A simple method to sort ESC-derived adipocytes. Cytometry A 2010; 77:990-5; PMID:21290474; http://dx.doi.org/10.1002/cyto.a.20953
45. Rubin CS, Hirsch A, Fung C, Rosen OM. Development of hormone receptors and hormonal responsiveness in vitro. Insulin receptors and insulin sensitivity in the preadipocyte and adipocyte forms of 3T3-L1 cells. J Biol Chem 1978; 253:7570-8; PMID:81205.
46. Lee YH, Chen SY, Wiesner RJ, Huang YF. Simple flow cytometric method used to assess lipid accumulation in fat cells. J Lipid Res 2004; 45:1162-7; PMID:14993237; http://dx.doi.org/10.1194/jlr.D300028-JLR200
47. Rothe G. Technical background and methodological principles of flow cytometry. In: Sack U, Tárnok A, Rothe G, eds. Cellular Diagnostics Basics, Methods and Clinical Applications of Flow Cytometry. Basel: Karger, 2009:53-88.
48. Back SH, Schröder M, Lee K, Zhang K, Kaufman RJ. ER stress signaling by regulated splicing: IRE1/HAC1/XBP1. Methods 2005; 35:395-416; PMID:15804613; http://dx.doi.org/10.1016/j.ymeth.2005.03.001
49. Yang L, Qian Z, Ji H, Yang R, Wang Y, Xi L, Sheng L, Zhao B, Zhang X. Inhibitory effect on protein kinase Cθ by crocetin attenuates palmitate-induced insulin insensitivity in 3T3-L1 adipocytes. Eur J Pharmacol 2010; 642:47-55; PMID:20541543; http://dx.doi.org/10.1016/j.ejphar.2010.05.061
50. Dasgupta S, Bhattacharya S, Biswas A, Majumdar SS, Mukhopadhyay S, Ray S, Bhattacharya S. NF-κB mediates lipid-induced fetuin-A expression in hepatocytes that impairs adipocyte function effecting insulin resistance. Biochem J 2010; 429:451-62; PMID:20482516; http://dx.doi.org/10.1042/BJ20100330
51. Xi L, Qian Z, Xu G, Zhou C, Sun S. Crocetin attenuates palmitate-induced insulin insensitivity and disordered tumor necrosis factor-α and adiponectin expression in rat adipocytes. Br J Pharmacol 2007; 151:610-7; PMID:17471172; http://dx.doi.org/10.1038/sj.bjp.0707276
52. Chavez JA, Summers SA. Characterizing the effects of saturated fatty acids on insulin signaling and ceramide and diacylglycerol accumulation in 3T3-L1 adipocytes and C2C12 myotubes. Arch Biochem Biophys 2003; 419:101-9; PMID:14592453; http://dx.doi.org/10.1016/j.abb.2003.08.020
53. Usui I, Haruta T, Takata Y, Iwata M, Uno T, Takano A, Ueno E, Ishibashi O, Ishihara H, Wada T, et al. Differential effects of palmitate on glucose uptake in rat-1 fibroblasts and 3T3-L1 adipocytes. Horm Metab Res 1999; 31:546-52; PMID:10596963; http://dx.doi.org/10.1055/s-2007-978793
54. Hunnicutt JW, Hardy RW, Williford J, McDonald JM. Saturated fatty acid-induced insulin resistance in rat adipocytes. Diabetes 1994; 43:540-5; PMID:8138059; http://dx.doi.org/10.2337/diab.43.4.540
55. Van Epps-Fung M, Williford J, Wells A, Hardy RW. Fatty acid-induced insulin resistance in adipocytes. Endocrinology 1997; 138:4338-45; PMID:9322948
56. Lundgren M, Eriksson JW. No in vitro effects of fatty acids on glucose uptake, lipolysis or insulin signaling in rat adipocytes. Horm Metab Res 2004; 36:203-9; PMID:15114517; http://dx.doi.org/10.1055/s-2004-814446
57. Tao J-L, Ruan X-Z, Li H, Li X-M, Moorhead JF, Varghese Z, Li X-W. Endoplasmic reticulum stress is involved in acetylated low-density lipoprotein induced apoptosis in THP-1 differentiated macrophages. Chin Med J (Engl) 2009; 122:1794-9; PMID:19781328
58. Kasimbalides EJ, Lanks KW. Effects of low molecular weight nutrients on the pattern of proteins synthesized by non-proliferating murine L cells. Exp Cell Res 1981; 132:31-9; PMID:7202562; http://dx.doi.org/10.1016/0014-4827(81)90079-3
59. Kowalchuk JM, Curi R, Newsholme EA. Glutamine metabolism in isolated incubated adipocytes of the rat. Biochem J 1988; 249:705-8; PMID:2895633
60. Yoo H, Antoniewicz MR, Stephanopoulos G, Kelleher JK. Quantifying reductive carboxylation flux of glutamine to lipid in a brown adipocyte cell line. J Biol Chem 2008; 283:20621-7; PMID:18364355; http://dx.doi.org/10.1074/jbc.M706494200
61. Semenza GL. HIF-1: mediator of physiological and pathophysiological responses to hypoxia. J Appl Physiol 2000; 88:1474-80; PMID:10749844
62. Kallinowski F, Runkel S, Fortmeyer HP, Förster H, Vaupel P. L-glutamine: a major substrate for tumor cells in vivo? J Cancer Res Clin Oncol 1987; 113:209-15; PMID:3584211; http://dx.doi.org/10.1007/BF00396375
63. Chandramouli V, Carter JR Jr. Metabolic effects of 2-deoxy-D-glucose in isolated fat cells. Biochim Biophys Acta 1977; 496:278-91; PMID:836900; http://dx.doi.org/10.1016/0304-4165(77)90310-5
64. Skurk T, Alberti-Huber C, Herder C, Hauner H. Relationship between adipocyte size and adipokine expression and secretion. J Clin Endocrinol Metab 2007; 92:1023-33; PMID:17164304; http://dx.doi.org/10.1210/jc.2006-1055
65. Yin J, Gao Z, He Q, Zhou D, Guo Z, Ye J. Role of hypoxia in obesity-induced disorders of glucose and lipid metabolism in adipose tissue. Am J Physiol Endocrinol Metab 2009; 296:E333-42; PMID:19066318; http://dx.doi.org/10.1152/ajpendo.90760.2008
66. Hosogai N, Fukuhara A, Oshima K, Miyata Y, Tanaka S, Segawa K, Furukawa S, Tochino Y, Komuro R, Matsuda M, et al. Adipose tissue hypoxia in obesity and its impact on adipocytokine dysregulation. Diabetes 2007; 56:901-11; PMID:17395738; http://dx.doi.org/10.2337/db06-0911
67. Michailidou Z, Turban S, Miller E, Zou X, Schrader J, Ratcliffe PJ, Hadoke PW, Walker BR, Iredale JP, Morton NM, et al. Increased angiogenesis protects against adipose hypoxia and fibrosis in metabolic disease-resistant 11β-hydroxysteroid dehydrogenase type 1 (HSD1)-deficient mice. J Biol Chem 2012; 287:4188-97; PMID:22158867; http://dx.doi.org/10.1074/jbc.M111.259325
68. Sung H-K, Doh K-O, Son JE, Park JG, Bae Y, Choi S, Nelson SM, Cowling R, Nagy K, Michael IP, et al.

Adipose vascular endothelial growth factor regulates metabolic homeostasis through angiogenesis. Cell Metab 2013; 17:61-72; PMID:23312284; http://dx.doi.org/10.1016/j.cmet.2012.12.010

69. Sun K, Wernstedt Asterholm I, Kusminski CM, Bueno AC, Wang ZV, Pollard JW, Brekken RA, Scherer PE. Dichotomous effects of VEGF-A on adipose tissue dysfunction. Proc Natl Acad Sci U S A 2012; 109:5874-9; PMID:22451920; http://dx.doi.org/10.1073/pnas.1200447109
70. Cornelius P, MacDougald OA, Lane MD. Regulation of adipocyte development. Annu Rev Nutr 1994; 14:99-129; PMID:7946535; http://dx.doi.org/10.1146/annurev.nu.14.070194.000531
71. Gregoire FM, Smas CM, Sul HS. Understanding adipocyte differentiation. Physiol Rev 1998; 78:783-809; PMID:9674695
72. Bosma M, Dapito DH, Drosatos-Tampakaki Z, Huiping-Son N, Huang L-S, Kersten S, Drosatos K, Goldberg IJ. Sequestration of fatty acids in triglycerides prevents endoplasmic reticulum stress in an in vitro model of cardiomyocyte lipotoxicity. Biochim Biophys Acta 2014; 1841:1648-55; PMID:25251292; http://dx.doi.org/10.1016/j.bbalip.2014.09.012
73. Kovanen PT, Nikkilä EA, Miettinen TA. Regulation of cholesterol synthesis and storage in fat cells. J Lipid Res 1975; 16:211-23; PMID:1127358
74. Prattes S, Hörl G, Hammer A, Blaschitz A, Graier WF, Sattler W, Zechner R, Steyrer E. Intracellular distribution and mobilization of unesterified cholesterol in adipocytes: triglyceride droplets are surrounded by cholesterol-rich ER-like surface layer structures. J Cell Sci 2000; 113:2977-89; PMID:10934037
75. Ross SE, Erickson RL, Gerin I, DeRose PM, Bajnok L, Longo KA, Misek DE, Kuick R, Hanash SM, Atkins KB, et al. Microarray analyses during adipogenesis: understanding the effects of Wnt signaling on adipogenesis and the roles of liver X receptor a in adipocyte metabolism. Mol Cell Biol 2002; 22:5989-99; PMID:12138207; http://dx.doi.org/10.1128/MCB.22.16.5989-5999.2002
76. Burton GR, Nagarajan R, Peterson CA, McGehee RE Jr. Microarray analysis of differentiation-specific gene expression during 3T3-L1 adipogenesis. Gene 2004; 329:167-85; PMID:15033539; http://dx.doi.org/10.1016/j.gene.2003.12.012
77. Higuchi M, Dusting GJ, Peshavariya H, Jiang F, Hsiao ST, Chan EC, Liu GS. Differentiation of human adipose-derived stem cells into fat involves reactive oxygen species and Forkhead box O1 mediated upregulation of antioxidant enzymes. Stem Cells Dev 2013; 22:878-88; PMID:23025577; http://dx.doi.org/10.1089/scd.2012.0306
78. Qiang L, Farmer SR. C/EBPa-dependent induction of glutathione *S*-transferase ζ/maleylacetoacetate isomerase (GSTζ/MAAI) expression during the differentiation of mouse fibroblasts into adipocytes. Biochem Biophys Res Commun 2006; 340:845-51; PMID:16376852; http://dx.doi.org/10.1016/j.bbrc.2005.12.067
79. Jowsey IR, Smith SA, Hayes JD. Expression of the murine glutathione *S*-transferase α3 (GSTA3) subunit is markedly induced during adipocyte differentiation: activation of the *GSTA3* gene promoter by the pro-adipogenic eicosanoid 15-deoxy-$\Delta^{12,14}$-prostaglandin J_2. Biochem Biophys Res Commun 2003; 312:1226-35; PMID:14652005; http://dx.doi.org/10.1016/j.bbrc.2003.11.068
80. Si Y, Yoon J, Lee K. Flux profile and modularity analysis of time-dependent metabolic changes of de novo adipocyte formation. Am J Physiol Endocrinol Metab 2007; 292:E1637-46; PMID:17284573; http://dx.doi.org/10.1152/ajpendo.00670.2006
81. Oyadomari S, Takeda K, Takiguchi M, Gotoh T, Matsumoto M, Wada I, Akira S, Araki E, Mori M. Nitric oxide-induced apoptosis in pancreatic β cells is mediated by the endoplasmic reticulum stress pathway. Proc Natl Acad Sci U S A 2001; 98:10845-50; PMID:11526215; http://dx.doi.org/10.1073/pnas.191207498
82. Chambers KT, Unverferth JA, Weber SM, Wek RC, Urano F, Corbett JA. The role of nitric oxide and the unfolded protein response in cytokine induced β-cell death. Diabetes 2008; 57:124-32; PMID:17928398; http://dx.doi.org/10.2337/db07-0944
83. Koh EH, Park J-Y, Park H-S, Jeon MJ, Ryu JW, Kim M, Kim SY, Kim M-S, Kim S-W, Park IS, et al. Essential role of mitochondrial function in adiponectin synthesis in adipocytes. Diabetes 2007; 56:2973-81; PMID:17827403; http://dx.doi.org/10.2337/db07-0510
84. Alhusaini S, McGee K, Schisano B, Harte A, McTernan P, Kumar S, Tripathi G. Lipopolysaccharide, high glucose and saturated fatty acids induce endoplasmic reticulum stress in cultured primary human adipocytes: salicylate alleviates this stress. Biochem Biophys Res Commun 2010; 397:472-8; PMID:20515657; http://dx.doi.org/10.1016/j.bbrc.2010.05.138
85. Jeon MJ, Leem J, Ko MS, Jang JE, Park H-S, Kim HS, Kim M, Kim EH, Yoo HJ, Lee C-H, et al. Mitochondrial dysfunction and activation of iNOS are responsible for the palmitate-induced decrease in adiponectin synthesis in 3T3L1 adipocytes. Exp Mol Med 2012; 44:562-70; PMID:22809900; http://dx.doi.org/10.3858/emm.2012.44.9.064
86. Kawasaki N, Asada R, Saito A, Kanemoto S, Imaizumi K. Obesity-induced endoplasmic reticulum stress causes chronic inflammation in adipose tissue. Sci Rep 2012; 2:799; PMID:23150771; http://dx.doi.org/10.1038/srep00799
87. Jiao P, Ma J, Feng B, Zhang H, Alan Diehl J, Eugene Chin Y, Yan W, Xu H. FFA-induced adipocyte inflammation and insulin resistance: involvement of ER stress and IKKβ pathways. Obesity (Silver Spring) 2011; 19:483-91; PMID:20829802; http://dx.doi.org/10.1038/oby.2010.200
88. Chen Y, Chen M, Wu Z, Zhao S. Ox-LDL induces ER stress and promotes the adipokines secretion in 3T3-L1 adipocytes. PLoS One 2013; 8:e81379; PMID:24278099; http://dx.doi.org/10.1371/journal.pone.0081379
89. Dever TE, Chen JJ, Barber GN, Cigan AM, Feng L, Donahue TF, London IM, Katze MG, Hinnebusch AG. Mammalian eukaryotic initiation factor 2α kinases functionally substitute for *GCN2* protein kinase in the *GCN4* translational control mechanism of yeast. Proc Natl Acad Sci U S A 1993; 90:4616-20; PMID:8099443; http://dx.doi.org/10.1073/pnas.90.10.4616
90. Harding HP, Zhang Y, Ron D. Protein translation and folding are coupled by an endoplasmic-reticulum-resident kinase. Nature 1999; 397:271-4; PMID:9930704; http://dx.doi.org/10.1038/16729
91. Kyriakis JM, Banerjee P, Nikolakaki E, Dai T, Rubie EA, Ahmad MF, Avruch J, Woodgett JR. The stress-activated protein kinase subfamily of c-Jun kinases. Nature 1994; 369:156-60; PMID:8177321; http://dx.doi.org/10.1038/369156a0
92. Li LO, Klett EL, Coleman RA. Acyl-CoA synthesis, lipid metabolism and lipotoxicity. Biochim Biophys Acta 2010; 1801:246-51; PMID:19818872; http://dx.doi.org/10.1016/j.bbalip.2009.09.024
93. Hassan RH, Hainault I, Vilquin J-T, Samama C, Lasnier F, Ferré P, Foufelle F, Hajduch E. Endoplasmic reticulum stress does not mediate palmitate-induced insulin resistance in mouse and human muscle cells. Diabetologia 2012; 55:204-14; PMID:22006247; http://dx.doi.org/10.1007/s00125-011-2328-9
94. Weigert C, Brodbeck K, Staiger H, Kausch C, Machicao F, Haring HU, Schleicher ED. Palmitate, but not unsaturated fatty acids, induces the expression of interleukin-6 in human myotubes through proteasome-dependent activation of nuclear factor-κB. J Biol Chem 2004; 279:23942-52; PMID:15028733; http://dx.doi.org/10.1074/jbc.M312692200
95. Miller TA, LeBrasseur NK, Cote GM, Trucillo MP, Pimentel DR, Ido Y, Ruderman NB, Sawyer DB. Oleate prevents palmitate-induced cytotoxic stress in cardiac myocytes. Biochem Biophys Res Commun 2005; 336:309-15; PMID:16126172; http://dx.doi.org/10.1016/j.bbrc.2005.08.088
96. Diakogiannaki E, Welters HJ, Morgan NG. Differential regulation of the endoplasmic reticulum stress response in pancreatic β-cells exposed to long-chain saturated and monounsaturated fatty acids. J Endocrinol 2008; 197:553-63; PMID:18492819; http://dx.doi.org/10.1677/JOE-08-0041
97. Katsoulieris E, Mabley JG, Samai M, Green IC, Chatterjee PK. α-Linolenic acid protects renal cells against palmitic acid lipotoxicity via inhibition of endoplasmic reticulum stress. Eur J Pharmacol 2009; 623:107-12; PMID:19765573; http://dx.doi.org/10.1016/j.ejphar.2009.09.015
98. Akazawa Y, Cazanave S, Mott JL, Elmi N, Bronk SF, Kohno S, Charlton MR, Gores GJ. Palmitoleate attenuates palmitate-induced Bim and PUMA up-regulation and hepatocyte lipoapoptosis. J Hepatol 2010; 52:586-93; PMID:20206402; http://dx.doi.org/10.1016/j.jhep.2010.01.003
99. Salvadó L, Coll T, Gómez-Foix AM, Salmerón E, Barroso E, Palomer X, Vázquez-Carrera M. Oleate prevents saturated-fatty-acid-induced ER stress, inflammation and insulin resistance in skeletal muscle cells through an AMPK-dependent mechanism. Diabetologia 2013; 56:1372-82; PMID:23460021; http://dx.doi.org/10.1007/s00125-013-2867-3
100. Sommerweiß D, Gorski T, Richter S, Garten A, Kiess W. Oleate rescues INS-1E β-cells from palmitate induced apoptosis by preventing activation of the unfolded protein response. Biochem Biophys Res Commun 2013; 441:770-6; PMID:24189472; http://dx.doi.org/10.1016/j.bbrc.2013.10.130
101. Steinberg D. Low density lipoprotein oxidation and its pathobiological significance. J Biol Chem 1997; 272:20963-6; PMID:9261091; http://dx.doi.org/10.1074/jbc.272.34.20963
102. Schroepfer GJ Jr. Oxysterols: modulators of cholesterol metabolism and other processes. Physiol Rev 2000; 80:361-554; PMID:10617772
103. Green H, Kehinde O. Sublines of mouse 3T3 cells that accumulate lipid. Cell 1974; 1:113-6; http://dx.doi.org/10.1016/0092-8674(74)90126-3
104. Green H, Kehinde O. Spontaneous heritable changes leading to increased adipose conversion in 3T3 cells. Cell 1976; 7:105-13; PMID:949738; http://dx.doi.org/10.1016/0092-8674(76)90260-9
105. Tsuchiya S, Yamabe M, Yamaguchi Y, Kobayashi Y, Konno T, Tada K. Establishment and characterization of a human acute monocytic leukemia cell line (THP-1). Int J Cancer 1980; 26:171-6; PMID:6970727; http://dx.doi.org/10.1002/ijc.2910260208
106. Daigneault M, Preston JA, Marriott HM, Whyte MK, Dockrell DH. The identification of markers of macrophage differentiation in PMA-stimulated THP-1 cells and monocyte-derived macrophages. PLoS One 2010; 5:e8668; PMID:20084270; http://dx.doi.org/10.1371/journal.pone.0008668
107. Mosmann T. Rapid colorimetric assay for cellular growth and survival: application to proliferation and cytotoxicity assays. J Immunol Methods 1983; 65:55-63; PMID:6606682; http://dx.doi.org/10.1016/0022-1759(83)90303-4
108. Bradley RL, Fisher FF, Maratos-Flier E. Dietary fatty acids differentially regulate production of TNF-α and IL-10 by murine 3T3-L1 adipocytes. Obesity (Silver Spring) 2008; 16:938-44; PMID:18356844; http://dx.doi.org/10.1038/oby.2008.39
109. Chavez JA, Knotts TA, Wang LP, Li G, Dobrowsky RT, Florant GL, Summers SA. A role for ceramide, but not diacylglycerol, in the antagonism of insulin signal transduction by saturated fatty acids. J Biol

Chem 2003; 278:10297-303; PMID:12525490; http://dx.doi.org/10.1074/jbc.M212307200
110. Cox DJ, Strudwick N, Ali AA, Paton AW, Paton JC, Schröder M. Measuring signaling by the unfolded protein response. Methods Enzymol 2011; 491:261-92; PMID:21329805; http://dx.doi.org/10.1016/B978-0-12-385928-0.00015-8
111. Ku HH. Notes on use of propagation of error formulas. J Res Nat Bureau Standards Sect C — Eng Instrumentat 1966; 70:263-73; http://dx.doi.org/10.6028/jres.070C.025
112. Dunnett CW. New tables for multiple comparisons with control. Biometrics 1964; 20:482-91; http://dx.doi.org/10.2307/2528490
113. Dunnett CW. A multiple comparison procedure for comparing several treatments with a control. J Am Stat Assoc 1955; 50:1096-121; PMID:9252830; http://dx.doi.org/10.1080/01621459.1955.10501294

BIBLIOGRAPHY

1. Calle, E.E., et al., *Overweight, obesity, and mortality from cancer in a prospectively studied cohort of US adults.* New England Journal of Medicine, 2003. **348**(17): p. 1625-1638.
2. Van Gaal, L.F., I.L. Mertens, and C.E. De Block, *Mechanisms linking obesity with cardiovascular disease.* Nature, 2006. **444**(7121): p. 875-80.
3. Lovren, F., H. Teoh, and S. Verma, *Obesity and atherosclerosis: mechanistic insights.* Can J Cardiol, 2015. **31**(2): p. 177-83.
4. WHO, *Obesity and oveweight fact sheets.* 2015.
5. Public Health England, P., *Lifestyle and behaviours* http://www.noo.org.uk/NOO_about_obesity/lifestyle.
6. Collins, S., et al., *Genetic vulnerability to diet-induced obesity in the C57BL/6J mouse: physiological and molecular characteristics.* Physiology & behavior, 2004. **81**(2): p. 243-248.
7. Nilsson, C., et al., *Laboratory animals as surrogate models of human obesity.* Acta Pharmacol Sin, 2012. **33**(2): p. 173-181.
8. Knudsen, N., et al., *Small differences in thyroid function may be important for body mass index and the occurrence of obesity in the population.* J Clin Endocrinol Metab, 2005. **90**(7): p. 4019-24.
9. Barahona, M.a.-J., et al., *Persistent body fat mass and inflammatory marker increases after long-term cure of Cushing's syndrome.* J Clin Endocrinol Metab, 2009. **94**(9): p. 3365-71.
10. Sam, S., *Obesity and Polycystic Ovary Syndrome.* Obesity management, 2007. **3**(2): p. 69-73.
11. Harley, I.T.W. and C.L. Karp, *Obesity and the gut microbiome: Striving for causality.* Molecular Metabolism, 2012. **1**(1–2): p. 21-31.
12. Ruth E. Ley , et al., *Obesity alters gut microbial ecology.* PNAS, 2005. **102** (31): p. 11070–11075.
13. F., B., et al., *The gut microbiota as an environmental factor that regulates fat storage.* PNAS, 2004. **101**: p. 15718–15723.
14. Amos-Landgraf, J.M., et al., *Chromosome breakage in the Prader-Willi and Angelman syndromes involves recombination between large, transcribed repeats at proximal and distal breakpoints.* Am J Hum Genet, 1999. **65**(2): p. 370-86.
15. Butler, M.G., *Prader-Willi Syndrome: Obesity due to Genomic Imprinting.* Current Genomics, 2011. **12**(3): p. 204-215.
16. Chen, D. and A. Garg, *Monogenic disorders of obesity and body fat distribution.* Journal of lipid research, 1999. **40**(10): p. 1735-1746.
17. Olshansky, S.J., et al., *A potential decline in life expectancy in the United States in the 21st century.* New England Journal of Medicine, 2005. **352**(11): p. 1138-1145.
18. Clement, K., et al., *A mutation in the human leptin receptor gene causes obesity and pituitary dysfunction.* Nature, 1998. **392**(6674): p. 398-401.
19. Jackson, R.S., et al., *Obesity and impaired prohormone processing associated with mutations in the human prohormone convertase 1 gene.* Nat Genet, 1997. **16**(3): p. 303-6.

20. Krude, H., et al., *Severe early-onset obesity, adrenal insufficiency and red hair pigmentation caused by POMC mutations in humans.* Nat Genet, 1998. **19**(2): p. 155-7.
21. Vaisse, C., et al., *A frameshift mutation in human MC4R is associated with a dominant form of obesity.* Nat Genet, 1998. **20**(2): p. 113-114.
22. Montague, C.T., et al., *Congenital leptin deficiency is associated with severe early-onset obesity in humans.* Nature, 1997. **387**(6636): p. 903-8.
23. Yeo, G.S., et al., *A frameshift mutation in MC4R associated with dominantly inherited human obesity.* Nat Genet, 1998. **20**(2): p. 111-2.
24. Lutz, T.A. and S.C. Woods, *Overview of Animal Models of Obesity.* Curr Protoc Pharmacol, 2012 (Unit5.61.).
25. Mynatt, R., et al., *Combined effects of insulin treatment and adipose tissue-specific agouti expression on the development of obesity.* Proceedings of the National Academy of Sciences, 1997. **94**(3): p. 919-922.
26. Zhang, Y., et al., *Positional cloning of the mouse obese gene and its human homologue.* Nature, 1994. **372**(6505): p. 425-432.
27. Andreas Nygaard Madsen, et al., *Long-term characterization of the diet-induced obese and diet-resistant rat model: a polygenetic rat model mimicking the human obesity syndrome.* J Endocrinol September 2010. **1**(206): p. 287-296
28. Ng, M., et al., *Global, regional, and national prevalence of overweight and obesity in children and adults during 1980-2013: a systematic analysis for the Global Burden of Disease Study 2013.* The Lancet, 2013. **384**(9945): p. 766-781.
29. CDC, *Overweight and obesity data and statistics.* Center for Disease Control and Prevention, Division of Nutrition, Physical Activity and Obesity, 2015.
30. HSCIC, *Health and Social care information Center - Statistics on Obesity, Physical Activity and Diet* http://www.hscic.gov.uk/catalogue/PUB16988/obes-phys-acti-diet-eng-2015.pdf, 2015.
31. Health Survey for England, H., *Health Survey for England - 2013.* http://www.hscic.gov.uk/catalogue/PUB16076, 2013.
32. Lim, S.S., et al., *A comparative risk assessment of burden of disease and injury attributable to 67 risk factors and risk factor clusters in 21 regions, 1990-2010: a systematic analysis for the Global Burden of Disease Study 2010.* The Lancet, 2010. **380**(9859): p. 2224-2260.
33. Kahn, S.E., R.L. Hull, and K.M. Utzschneider, *Mechanisms linking obesity to insulin resistance and type 2 diabetes.* Nature, 2006. **444**(7121): p. 840-846.
34. Hotamisligil, G.k.S., *Inflammation and metabolic disorders.* Nature, 2006. **444**(7121): p. 860-7.
35. Hajer, G.R., T.W. van Haeften, and F.L.J. Visseren, *Adipose tissue dysfunction in obesity, diabetes, and vascular diseases*. Vol. 29. 2008. 2959-2971.
36. Guilherme, A., et al., *Adipocyte dysfunctions linking obesity to insulin resistance and type 2 diabetes.* Nature reviews Molecular cell biology, 2008. **9**(5): p. 367-377.
37. Renehan, A.G., et al., *Body-mass index and incidence of cancer: a systematic review and meta-analysis of prospective observational studies.* The Lancet, 2008. **371**(9612): p. 569-578.
38. Luppino, F.S., et al., *Overweight, obesity, and depression: a systematic review and meta-analysis of longitudinal studies.* Archives of general psychiatry, 2010. **67**(3): p. 220-229.
39. Naderali, E.K., S.H. Ratcliffe, and M.C. Dale, *Review: obesity and Alzheimer's disease: a link between body weight and cognitive function in old age.* American journal of Alzheimer's disease and other dementias, 2009. **24**(6): p. 445-449.

40. Schwartz, A.R., et al., *Obesity and Obstructive Sleep Apnea: Pathogenic Mechanisms and Therapeutic Approaches.* Proceedings of the American Thoracic Society, 2008. **5**(2): p. 185-192.
41. Grotle, M., et al., *Obesity and osteoarthritis in knee, hip and/or hand: an epidemiological study in the general population with 10 years follow-up.* BMC musculoskeletal disorders, 2008. **9**(1): p. 132.
42. Pandey, S., et al., *The impact of female obesity on the outcome of fertility treatment.* Journal of Human Reproductive Sciences, 2010. **3**(2): p. 62-67.
43. MGI, M.G.I., *Overcoming obesity: an initial economic analysis.* 2014.
44. Butland B, J.S., Kopelman P, *Tackling obesities: future choices – project report (2nd Ed).* London: Foresight Programme of the Government Office for Science, 2007.
45. Cinti, S., *The adipose organ.* Prostaglandins Leukot Essent Fatty Acids, 2005. **73**(1): p. 9-15.
46. Wronska, A. and Z. Kmiec, *Structural and biochemical characteristics of various white adipose tissue depots.* Acta Physiol (Oxf), 2012. **205**(2): p. 194-208.
47. Cannon, B. and J. Nedergaard, *Brown adipose tissue: function and physiological significance.* Physiol Rev, 2004. **84**(1): p. 277-359.
48. Schulz, T.J. and Y.-H. Tseng, *Brown adipose tissue: development, metabolism and beyond.* Biochem J, 2013. **453**(2): p. 167-78.
49. Nedergaard, J., T. Bengtsson, and B. Cannon, *Unexpected evidence for active brown adipose tissue in adult humans.* Am J Physiol Endocrinol Metab, 2007. **293**(2): p. E444-52.
50. Gesta, S., Y.-H. Tseng, and C.R. Kahn, *Developmental Origin of Fat: Tracking Obesity to Its Source.* Cell, 2007. **131**(2): p. 242-256.
51. Enerback, S., *Human Brown Adipose Tissue.* Cell metabolism, 2010. **11**(4): p. 248-252.
52. Marta, G. and V. Francesc, *White, Brown, Beige/Brite: Different Adipose Cells for Different Functions?* Endocrinology, 2013. **154**(9): p. 2992-3000.
53. Dawkins, M.J.R. and J.W. Scopes, *Non-shivering thermogenesis and brown adipose tissue in the human new-born infant.* 1965.
54. Cypess, A.M., et al., *Identification and importance of brown adipose tissue in adult humans.* N Engl J Med, 2009. **360**(15): p. 1509-17.
55. Virtanen, K.A., et al., *Functional brown adipose tissue in healthy adults.* New England Journal of Medicine, 2009. **360**(15): p. 1518-1525.
56. van Marken Lichtenbelt, W.D., et al., *Cold-activated brown adipose tissue in healthy men.* New England Journal of Medicine, 2009. **360**(15): p. 1500-1508.
57. Paul, L., M.S. Michael, and K.Y.H. Ken, *Brown Adipose Tissue in Adult Humans: A Metabolic Renaissance.* Endocrine Reviews, 2013. **34**(3): p. 413-438.
58. Rothwell, N.J. and M.J. Stock, *A role for brown adipose tissue in diet-induced thermogenesis.* Nature, 1979. **281**(5726): p. 31-35.
59. Lowell, B.B., et al., *Development of obesity in transgenic mice after genetic ablation of brown adipose tissue.* Nature, 1993. **366**(6457): p. 740-2.
60. Feldmann, H.M., et al., *UCP1 ablation induces obesity and abolishes diet-induced thermogenesis in mice exempt from thermal stress by living at thermoneutrality.* Cell metabolism, 2009. **9**(2): p. 203-209.
61. van Marken Lichtenbelt, W.D., et al., *Cold-Activated Brown Adipose Tissue in Healthy Men.* New England Journal of Medicine, 2009. **360**(15): p. 1500-1508.
62. Vijgen, G.H., et al., *Brown adipose tissue in morbidly obese subjects.* PloS one, 2011. **6**(2): p. e17247.

63. Yoneshiro, T., et al., *Recruited brown adipose tissue as an antiobesity agent in humans.* The Journal of Clinical Investigation, 2013. **123**(8): p. 3404-3408.
64. Geisler, J.G., *Targeting energy expenditure via fuel switching and beyond.* Diabetologia, 2011. **54**(2): p. 237-44.
65. Wu, C., et al., *Brown Adipose Tissue Can Be Activated or Inhibited within an Hour before (18)F-FDG Injection: A Preliminary Study with MicroPET.* Journal of Biomedicine and Biotechnology, 2011. **2011**: p. 159834.
66. Harms, M. and P. Seale, *Brown and beige fat: development, function and therapeutic potential.* Nat Med, 2012. **19**(10): p. 1252-1263.
67. Bartness, T.J. and C.K. Song, *Brain-Adipose Tissue Neural Crosstalk.* Physiology & behavior, 2007. **91**(4): p. 343-351.
68. Arbuthnott, E., *Brown adipose tissue: structure and function.* Proceedings of the Nutrition Society, 1989. **48**(02): p. 177-182.
69. Deveaud, C., et al., *Regional differences in oxidative capacity of rat white adipose tissue are linked to the mitochondrial content of mature adipocytes.* Mol Cell Biochem, 2004. **267**(1-2): p. 157-66.
70. Ouchi, N., et al., *Adipokines in inflammation and metabolic disease.* Nat Rev Immunol, 2011. **11**(2): p. 85-97.
71. Driskell, R., et al., *Defining dermal adipose tissue.* Experimental dermatology, 2014. **23**(9): p. 629-631.
72. Wojciechowicz, K., et al., *Development of the Mouse Dermal Adipose Layer Occurs Independently of Subcutaneous Adipose Tissue and Is Marked by Restricted Early Expression of FABP4.* PLoS One, 2013. **8**(3).
73. Tchkonia, T., et al., *Identification of depot-specific human fat cell progenitors through distinct expression profiles and developmental gene patterns.* Am J Physiol Endocrinol Metab, 2007. **292**(1): p. E298-307.
74. Gealekman, O., et al., *Depot-specific differences and insufficient subcutaneous adipose tissue angiogenesis in human obesity.* Circulation, 2011. **123**(2): p. 186-194.
75. Tchernof, A., et al., *Regional differences in adipose tissue metabolism in women: minor effect of obesity and body fat distribution.* Diabetes, 2006. **55**(5): p. 1353-60.
76. Drolet, R., et al., *Fat depot-specific impact of visceral obesity on adipocyte adiponectin release in women.* Obesity (Silver Spring), 2009. **17**(3): p. 424-30.
77. Van Harmelen, V., et al., *Leptin secretion from subcutaneous and visceral adipose tissue in women.* Diabetes, 1998. **47**(6): p. 913-917.
78. Virtanen, K.A., et al., *Glucose uptake and perfusion in subcutaneous and visceral adipose tissue during insulin stimulation in nonobese and obese humans.* The Journal of Clinical Endocrinology & Metabolism, 2002. **87**(8): p. 3902-3910.
79. Hannukainen, J.C., et al., *Higher free fatty acid uptake in visceral than in abdominal subcutaneous fat tissue in men.* Obesity, 2010. **18**(2): p. 261-265.
80. Fontana, L., et al., *Visceral fat adipokine secretion is associated with systemic inflammation in obese humans.* Diabetes, 2007. **56**(4): p. 1010-1013.
81. Glatz, J.F.C., J.J.F.P. Luiken, and A. Bonen, *Membrane fatty acid transporters as regulators of lipid metabolism: implications for metabolic disease.* Physiological reviews, 2010. **90**(1): p. 367-417.
82. Zhang, L., et al., *Role of fatty acid uptake and fatty acid beta-oxidation in mediating insulin resistance in heart and skeletal muscle.* Biochim Biophys Acta, 2010. **1801**(1): p. 1-22.
83. Sumida, C., R. Graber, and E. Nunez, *Role of fatty acids in signal transduction: modulators and messengers.* Prostaglandins Leukot Essent Fatty Acids, 1993. **48**(1): p. 117-22.

84. Graber, R., C. Sumida, and E.A. Nunez, *Fatty acids and cell signal transduction.* J Lipid Mediat Cell Signal, 1994. **9**(2): p. 91-116.
85. Griffin, M.E., et al., *Free fatty acid-induced insulin resistance is associated with activation of protein kinase C theta and alterations in the insulin signaling cascade.* Diabetes, 1999. **48**(6): p. 1270-1274.
86. Boden, G. and G.I. Shulman, *Free fatty acids in obesity and type 2 diabetes: defining their role in the development of insulin resistance and β-cell dysfunction.* European Journal of Clinical Investigation, 2002. **32**: p. 14-23.
87. Berg JM, Tymoczko JL, and S. L., *Biochemistry 5th edition.* WH Freeman, 2002. **5**: p. Chapter 22.4.
88. Lowe, M.E., *The triglyceride lipases of the pancreas.* J Lipid Res, 2002. **43**(12): p. 2007-16.
89. Rosen, E.D. and B.M. Spiegelman, *Adipocytes as regulators of energy balance and glucose homeostasis.* Nature, 2006. **444**(7121): p. 847-853.
90. Karpe, F., J.R. Dickmann, and K.N. Frayn, *Fatty Acids, Obesity, and Insulin Resistance: Time for a Reevaluation.* Diabetes, 2011. **60**(10): p. 2441-2449.
91. Weiss, S.B., E.P. Kennedy, and J.Y. Kiyasu, *The enzymatic synthesis of triglycerides.* J Biol Chem, 1960. **235**: p. 40-4.
92. Coleman, R.A., T.M. Lewin, and D.M. Muoio, *Physiological and nutritional regulation of enzymes of triacylglycerol synthesis.* Annu Rev Nutr, 2000. **20**: p. 77-103.
93. Lehner, R. and A. Kuksis, *Biosynthesis of triacylglycerols.* Prog Lipid Res, 1996. **35**(2): p. 169-201.
94. Packer, L., et al., *Phosphatidic Acid Phosphohydrolase: Its Role in Cell Signalling*, in *Signalling Mechanisms from Transcription Factors to Oxidative Stress*. 1995, Springer Berlin Heidelberg. p. 57-64.
95. Yen, C.-L.E., et al., *DGAT enzymes and triacylglycerol biosynthesis.* Journal of lipid research, 2008. **49**(11): p. 2283-2301.
96. Yen, C.-L.E., et al., *Thematic Review Series: Glycerolipids. DGAT enzymes and triacylglycerol biosynthesis.* Journal of lipid research, 2008. **49**(11): p. 2283-2301.
97. Gurr Mi.I, H.J.L., FraynK.N, *Lipid biochemistry- an introduction, 5th Edition.* Blackwell Publishing, 2002.
98. Man, W.C., et al., *Colocalization of SCD1 and DGAT2: implying preference for endogenous monounsaturated fatty acids in triglyceride synthesis.* Journal of lipid research, 2006. **47**(9): p. 1928-1939.
99. Enoch, H.G., A. Catala, and P. Strittmatter, *Mechanism of rat liver microsomal stearyl-CoA desaturase. Studies of the substrate specificity, enzyme-substrate interactions, and the function of lipid.* Journal of Biological Chemistry, 1976. **251**(16): p. 5095-5103.
100. Paton, C.M. and J.M. Ntambi, *Biochemical and physiological function of stearoyl-CoA desaturase.* American Journal of Physiology-Endocrinology and Metabolism, 2009. **297**(1): p. E28-E37.
101. Bernlohr, D.A., et al., *Evidence for an increase in transcription of specific mRNAs during differentiation of 3T3-L1 preadipocytes.* Journal of Biological Chemistry, 1985. **260**(9): p. 5563-5567.
102. Hu, C.C., K. Qing, and Y. Chen, *Diet-induced changes in stearoyl-CoA desaturase 1 expression in obesity-prone and -resistant mice.* Obes Res, 2004. **12**(8): p. 1264-70.

103. Gutierrez-Juarez, R., et al., *Critical role of stearoyl-CoA desaturase-1 (SCD1) in the onset of diet-induced hepatic insulin resistance.* J Clin Invest, 2006. **116**(6): p. 1686-95.
104. Dobrzyn, A. and J.M. Ntambi, *The Role of Stearoyl-CoA Desaturase in Body Weight Regulation.* Trends in cardiovascular medicine, 2004. **14**(2): p. 77-81.
105. Schaffer, J.E., *Lipotoxicity: when tissues overeat.* Current opinion in lipidology, 2003. **14**(3): p. 281-287.
106. Collins, J.M., et al., *De novo lipogenesis and stearoyl-CoA desaturase are coordinately regulated in the human adipocyte and protect against palmitate-induced cell injury.* Journal of Biological Chemistry, 2011. **285**(9): p. 6044-6052.
107. Lands, W.E.M. and C.G. Crawford, *Enzymes of membrane phospholipid metabolism in animals*, in *The Enzymes of Bioligical Membranes*. 1976, Springer. p. 3-85.
108. Ntambi, J.M., et al., *Loss of stearoyl-CoA desaturase-1 function protects mice against adiposity.* Proceedings of the National Academy of Sciences, 2002. **99**(17): p. 11482-11486.
109. Ntambi, J.M. and M. Miyazaki, *Recent insights into stearoyl-CoA desaturase-1*. Current opinion in lipidology, 2003. **14**(3): p. 255-261.
110. Dobrzyn, A., et al., *Stearoyl-CoA desaturase-1 deficiency reduces ceramide synthesis by downregulating serine palmitoyltransferase and increasing beta-oxidation in skeletal muscle.* Am J Physiol Endocrinol Metab, 2005. **288**(3): p. E599-607.
111. Kim, E., et al., *Inhibition of stearoyl-CoA desaturase1 activates AMPK and exhibits beneficial lipid metabolic effects in vitro.* European journal of pharmacology, 2011. **672**(1-3): p. 38-44.
112. Miyazaki, M. and J.M. Ntambi, *Role of stearoyl-coenzyme A desaturase in lipid metabolism.* Prostaglandins, Leukotrienes and Essential Fatty Acids, 2003. **68**(2): p. 113-121.
113. Gibbons, G.F., K. Islam, and R.J. Pease, *Mobilisation of triacylglycerol stores.* Biochim Biophys Acta, 2000. **1483**(1): p. 37-57.
114. Lafontan, M. and D. Langin, *Lipolysis and lipid mobilization in human adipose tissue.* Progress in Lipid Research, 2009. **48**(5): p. 275-297.
115. Zimmermann, R., et al., *Fat mobilization in adipose tissue is promoted by adipose triglyceride lipase.* Science, 2004. **306**(5700): p. 1383-6.
116. Langin, D., et al., *Adipocyte lipases and defect of lipolysis in human obesity.* Diabetes, 2005. **54**(11): p. 3190-7.
117. Lafontan, M., et al., *Recent developments on lipolysis regulation in humans and discovery of a new lipolytic pathway.* International journal of obesity and related metabolic disorders: journal of the International Association for the Study of Obesity, 2000. **24**: p. S47-52.
118. Zhang, H.H., et al., *Lipase-selective functional domains of perilipin A differentially regulate constitutive and protein kinase A-stimulated lipolysis.* J Biol Chem, 2003. **278**(51): p. 51535-42.
119. Meijssen, S., et al., *Insulin Mediated Inhibition of Hormone Sensitive Lipase Activity in Vivo in Relation to Endogenous Catecholamines in Healthy Subjects.* The Journal of Clinical Endocrinology & Metabolism, 2001. **86**(9): p. 4193-4197.
120. Engfeldt, P., et al., *Effects of insulin on adrenoceptor binding and the rate of catecholamine-induced lipolysis in isolated human fat cells.* Journal of Biological Chemistry, 1988. **263**(30): p. 15553-15560.
121. Wang, S.P., et al., *The adipose tissue phenotype of hormone-sensitive lipase deficiency in mice.* Obes Res, 2001. **9**(2): p. 119-28.

122. Jenkins, C.M., et al., *Identification, cloning, expression, and purification of three novel human calcium-independent phospholipase A2 family members possessing triacylglycerol lipase and acylglycerol transacylase activities.* J Biol Chem, 2004. **279**(47): p. 48968-75.
123. Villena, J.A., et al., *Desnutrin, an adipocyte gene encoding a novel patatin domain-containing protein, is induced by fasting and glucocorticoids: ectopic expression of desnutrin increases triglyceride hydrolysis.* J Biol Chem, 2004. **279**(45): p. 47066-75.
124. Haemmerle, G., et al., *Defective lipolysis and altered energy metabolism in mice lacking adipose triglyceride lipase.* Science, 2006. **312**(5774): p. 734-7.
125. Kershaw, E.E., et al., *Adipose Triglyceride Lipase: Function, Regulation by Insulin, and Comparison With Adiponutrin.* Diabetes, 2006. **55**(1): p. 148.
126. Friedman, J.M. and J.L. Halaas, *Leptin and the regulation of body weight in mammals.* Nature, 1998. **395**(6704): p. 763-70.
127. Kern, P.A., et al., *Adiponectin expression from human adipose tissue relation to obesity, insulin resistance, and tumor necrosis factor-kB expression.* Diabetes, 2003. **52**(7): p. 1779-1785.
128. Cook, K.S., et al., *Adipsin: a circulating serine protease homolog secreted by adipose tissue and sciatic nerve.* Science, 1987. **237**(4813): p. 402-5.
129. Kershaw, E.E. and J.S. Flier, *Adipose tissue as an endocrine organ.* J Clin Endocrinol Metab, 2004. **89**(6): p. 2548-56.
130. Huang-Doran, I., et al., *Lipodystrophy: metabolic insights from a rare disorder.* Journal of Endocrinology, 2010. **207**(3): p. 245-255.
131. Fain, J.N., et al., *Comparison of the release of adipokines by adipose tissue, adipose tissue matrix, and adipocytes from visceral and subcutaneous abdominal adipose tissues of obese humans.* Endocrinology, 2004. **145**(5): p. 2273-2282.
132. Fried, S.K., et al., *Regulation of Leptin Production in Humans.* The Journal of nutrition, 2000. **130**(12): p. 3127S-3131S.
133. Li, H., M. Matheny, and P.J. Scarpace, *beta 3-Adrenergic-mediated suppression of leptin gene expression in rats.* American Journal of Physiology - Endocrinology and Metabolism, 1997. **272**(6): p. E1031-E1036.
134. Shintani, M., et al., *Downregulation of leptin by free fatty acids in rat adipocytes: effects of triacsin C, palmitate, and 2-bromopalmitate.* Metabolism, 2000. **49**(3): p. 326-30.
135. Fonseca-Alaniz, M.H., et al., *Adipose tissue as an endocrine organ: from theory to practice.* Jornal de Pediatria, 2007. **83**(5): p. S192-S203.
136. Shimomura, I., et al., *Leptin reverses insulin resistance and diabetes mellitus in mice with congenital lipodystrophy.* Nature, 1999. **401**(6748): p. 73-6.
137. Fogteloo, J., et al., *The decline in plasma leptin in response to calorie restriction predicts the effects of adjunctive leptin treatment on body weight in humans.* Eur J Intern Med, 2003. **14**(7): p. 415-418.
138. Klok, M.D., S. Jakobsdottir, and M.L. Drent, *The role of leptin and ghrelin in the regulation of food intake and body weight in humans: a review.* Obes Rev, 2007. **8**(1): p. 21-34.
139. Bjorbaek, C. and B.B. Kahn, *Leptin signaling in the central nervous system and the periphery.* Recent progress in hormone research, 2004. **59**: p. 305-332.
140. Hileman, S.M., D.D. Pierroz, and J.S. Flier, *Leptin, nutrition, and reproduction: timing is everything.* The Journal of clinical endocrinology and metabolism, 2000. **85**(2): p. 804.

141. Lord, G.M., et al., *Leptin modulates the T-cell immune response and reverses starvation-induced immunosuppression.* Nature, 1998. **394**(6696): p. 897-901.
142. Margetic, S., et al., *Leptin: a review of its peripheral actions and interactions.* International journal of obesity and related metabolic disorders: journal of the International Association for the Study of Obesity, 2002. **26**(11): p. 1407-1433.
143. Chandran, M., et al., *Adiponectin: more than just another fat cell hormone?* Diabetes Care, 2003. **26**(8): p. 2442-50.
144. Ouchi, N., et al., *Obesity, adiponectin and vascular inflammatory disease.* Current opinion in lipidology, 2003. **14**(6): p. 561-566.
145. Fruebis, J., et al., *Proteolytic cleavage product of 30-kDa adipocyte complement-related protein increases fatty acid oxidation in muscle and causes weight loss in mice.* Proc Natl Acad Sci U S A, 2001. **98**(4): p. 2005-10.
146. Gil-Campos, M., R.R. Canete, and A. Gil, *Adiponectin, the missing link in insulin resistance and obesity.* Clin Nutr, 2004. **23**(5): p. 963-74.
147. Lang, H.-F., et al., *Weight loss increased serum adiponectin but decreased lipid levels in obese subjects whose body mass index was lower than 30 kg/m².* Nutr Res, 2011. **31**(5): p. 378-86.
148. Maeda, N., et al., *Diet-induced insulin resistance in mice lacking adiponectin/ACRP30.* Nat Med, 2002. **8**(7): p. 731-7.
149. Sun, K., C.M. Kusminski, and P.E. Scherer, *Adipose tissue remodeling and obesity.* J Clin Invest, 2011. **121**(6): p. 2094-101.
150. Gregor, M.F. and G.S. Hotamisligil, *Thematic review series: Adipocyte Biology. Adipocyte stress: the endoplasmic reticulum and metabolic disease.* Journal of lipid research, 2007. **48**(9): p. 1905.
151. Wellen, K.E. and G.S. Hotamisligil, *Inflammation, stress, and diabetes.* J Clin Invest, 2005. **115**(5): p. 1111-9.
152. Weisberg, S.P., et al., *Obesity is associated with macrophage accumulation in adipose tissue.* Journal of Clinical Investigation, 2003. **112**(12): p. 1796.
153. Strissel, K.J., et al., *Adipocyte death, adipose tissue remodeling, and obesity complications.* Diabetes, 2007. **56**(12): p. 2910-2918.
154. Lee, M.-J., Y. Wu, and S.K. Fried, *Adipose tissue remodeling in pathophysiology of obesity.* Current opinion in clinical nutrition and metabolic care, 2010. **13**(4): p. 371-376.
155. Antuna-Puente, B., et al., *Adipokines: the missing link between insulin resistance and obesity.* Diabetes Metab, 2008. **34**(1): p. 2-11.
156. Weisberg, S.P., et al., *Obesity is associated with macrophage accumulation in adipose tissue.* J Clin Invest, 2003. **112**(12): p. 1796-808.
157. Lionetti, L., et al., *From chronic overnutrition to insulin resistance: the role of fat-storing capacity and inflammation.* Nutr Metab Cardiovasc Dis, 2009. **19**(2): p. 146-52.
158. Sun, K. and P.E. Scherer, *Adipose tissue dysfunction: a multistep process*, in *Novel Insights into Adipose Cell Functions*. 2010, Springer. p. 67-75.
159. Lumeng, C.N., et al., *Increased inflammatory properties of adipose tissue macrophages recruited during diet-induced obesity.* Diabetes, 2007. **56**(1): p. 16-23.
160. Kanda, H., et al., *MCP-1 contributes to macrophage infiltration into adipose tissue, insulin resistance, and hepatic steatosis in obesity.* Journal of Clinical Investigation, 2006. **116**(6): p. 1494-1505.
161. Cinti, S., et al., *Adipocyte death defines macrophage localization and function in adipose tissue of obese mice and humans.* Journal of lipid research, 2005. **46**(11): p. 2347-2355.

162. Pajvani, U.B., et al., *Fat apoptosis through targeted activation of caspase 8: a new mouse model of inducible and reversible lipoatrophy.* Nature medicine, 2005. **11**(7): p. 797-803.
163. Trujillo, M.E., U.B. Pajvani, and P.E. Scherer, *Apoptosis Through Targeted Activation of Caspase8 (ATTAC-mice): Novel Mouse Models of Inducible and Reversible Tissue Ablation.* Cell Cycle, 2005. **4**(9): p. 1141-1145.
164. Lumeng, C.N., J.L. Bodzin, and A.R. Saltiel, *Obesity induces a phenotypic switch in adipose tissue macrophage polarization.* Journal of Clinical Investigation, 2007. **117**(1): p. 175.
165. Jetten, N., et al., *Anti-inflammatory M2, but not pro-inflammatory M1 macrophages promote angiogenesis in vivo.* Angiogenesis, 2014. **17**(1): p. 109-18.
166. Fujisaka, S., et al., *Regulatory mechanisms for adipose tissue M1 and M2 macrophages in diet-induced obese mice.* Diabetes, 2009. **58**(11): p. 2574-2582.
167. Uysal, K.T., et al., *Protection from obesity-induced insulin resistance in mice lacking TNF-α function.* Nature, 1997. **389**(6651): p. 610-614.
168. Weisberg, S.P., et al., *CCR2 modulates inflammatory and metabolic effects of high-fat feeding.* Journal of Clinical Investigation, 2006. **116**(1): p. 115.
169. Kawanishi, N., et al., *Exercise training inhibits inflammation in adipose tissue via both suppression of macrophage infiltration and acceleration of phenotypic switching from M1 to M2 macrophages in high-fat-diet-induced obese mice.* Exerc Immunol Rev, 2010. **16**: p. 105-18.
170. Aron-Wisnewsky, J., et al., *Human adipose tissue macrophages: m1 and m2 cell surface markers in subcutaneous and omental depots and after weight loss.* The Journal of Clinical Endocrinology & Metabolism, 2009. **94**(11): p. 4619-4623.
171. Shi, H., et al., *TLR4 links innate immunity and fatty acid-induced insulin resistance.* Journal of Clinical Investigation, 2006. **116**(11): p. 3015.
172. Schaeffler, A., et al., *Fatty acid-induced induction of Toll-like receptor-4/nuclear factor-kB pathway in adipocytes links nutritional signalling with innate immunity.* Immunology, 2009. **126**(2): p. 233-245.
173. Lee, J.Y., et al., *Saturated fatty acids, but not unsaturated fatty acids, induce the expression of cyclooxygenase-2 mediated through Toll-like receptor 4.* J Biol Chem, 2001. **276**(20): p. 16683-9.
174. Wong, A.L., et al., *Tie2 expression and phosphorylation in angiogenic and quiescent adult tissues.* Circulation research, 1997. **81**(4): p. 567-574.
175. Rupnick, M.A., et al., *Adipose tissue mass can be regulated through the vasculature.* Proceedings of the National Academy of Sciences, 2002. **99**(16): p. 10730-10735.
176. Nishimura, S., et al., *Adipogenesis in obesity requires close interplay between differentiating adipocytes, stromal cells, and blood vessels.* Diabetes, 2007. **56**(6): p. 1517-1526.
177. Crandall, D.L., et al., *Adipocyte blood flow: influence of age, anatomic location, and dietary manipulation.* American Journal of Physiology - Regulatory, Integrative and Comparative Physiology, 1984. **247**(1): p. R46-R51.
178. Sierra-Honigmann, M.R.Ì.o., et al., *Biological action of leptin as an angiogenic factor.* Science, 1998. **281**(5383): p. 1683-1686.
179. Claffey, K.P., W.O. Wilkison, and B.M. Spiegelman, *Vascular endothelial growth factor. Regulation by cell differentiation and activated second messenger pathways.* Journal of Biological Chemistry, 1992. **267**(23): p. 16317-16322.
180. Kabon, B., et al., *Obesity decreases perioperative tissue oxygenation.* Anesthesiology, 2004. **100**(2): p. 274.

181. Skurk, T., et al., *Relationship between adipocyte size and adipokine expression and secretion.* The Journal of Clinical Endocrinology & Metabolism, 2007. **92**(3): p. 1023-1033.
182. Semenza, G.L., *Hypoxia-inducible factor 1: master regulator of O 2 homeostasis.* Current opinion in genetics & development, 1998. **8**(5): p. 588-594.
183. He, Q., et al., *Regulation of HIF-1a activity in adipose tissue by obesity-associated factors: adipogenesis, insulin, and hypoxia.* American Journal of Physiology - Endocrinology and Metabolism, 2011. **300**(5): p. E877-E885.
184. Liekens, S., E. de Clercq, and J. Neyts, *Angiogenesis: regulators and clinical applications.* Biochemical Pharmacology, 2001. **61**(3): p. 253-270.
185. Schenk, S., M. Saberi, and J.M. Olefsky, *Insulin sensitivity: modulation by nutrients and inflammation.* The Journal of clinical investigation, 2008. **118**(9): p. 2992.
186. Hotamisligil, G.S., N.S. Shargill, and B.M. Spiegelman, *Adipose expression of tumor necrosis factor-alpha: direct role in obesity-linked insulin resistance.* Science, 1993. **259**(5091): p. 87-91.
187. Itoh, M., et al., *Adipose tissue remodeling as homeostatic inflammation.* Int J Inflam. **2011**: p. 720926.
188. Ohmura, K., et al., *Natural killer T cells are involved in adipose tissues inflammation and glucose intolerance in diet-induced obese mice.* Arteriosclerosis, thrombosis, and vascular biology, 2010. **30**(2): p. 193-199.
189. Hayden, M.S. and S. Ghosh, *Signaling to NF-kB.* Genes & development, 2004. **18**(18): p. 2195-2224.
190. Oeckinghaus, A., M.S. Hayden, and S. Ghosh, *Crosstalk in NF-[kappa] B signaling pathways.* Nature immunology, 2011. **12**(8): p. 695-708.
191. Moynagh, P.N., *The NF-kB pathway.* Journal of cell science, 2005. **118**(20): p. 4589-4592.
192. Kyriakis, J.M., et al., *The stress-activated protein kinase subfamily of c-Jun kinases.* Nature, 1994. **369**(6476): p. 156-160.
193. Tournier, C., et al., *Mitogen-activated protein kinase kinase 7 is an activator of the c-Jun NH2-terminal kinase.* Proceedings of the National Academy of Sciences, 1997. **94**(14): p. 7337-7342.
194. Gupta, S., et al., *Selective interaction of JNK protein kinase isoforms with transcription factors.* The EMBO journal, 1996. **15**(11): p. 2760.
195. Ameyar, M., M. Wisniewska, and J.B. Weitzman, *A role for AP-1 in apoptosis: the case for and against.* Biochimie, 2003. **85**(8): p. 747-752.
196. Yudkin, J.S., et al., *Inflammation, obesity, stress and coronary heart disease: is interleukin-6 the link?* Atherosclerosis, 2000. **148**(2): p. 209-14.
197. Xu, H., et al., *Chronic inflammation in fat plays a crucial role in the development of obesity-related insulin resistance.* Journal of Clinical Investigation, 2003. **112**(12): p. 1821.
198. Pietsch, J., et al., *Toll-Like Receptor Expression and Response to Specific Stimulation in Adipocytes and Preadipocytes.* Annals of the New York Academy of Sciences, 2006. **1072**(1): p. 407-409.
199. Bes-Houtmann, S., et al., *Presence of functional TLR2 and TLR4 on human adipocytes.* Histochem Cell Biol, 2007. **127**(2): p. 131-7.
200. Zuany-Amorim, C., J. Hastewell, and C. Walker, *Toll-like receptors as potential therapeutic targets for multiple diseases.* Nat Rev Drug Discov, 2002. **1**(10): p. 797-807.
201. Akira, S., K. Takeda, and T. Kaisho, *Toll-like receptors: critical proteins linking innate and acquired immunity.* Nat Immunol, 2001. **2**(8): p. 675-680.

202. Fresno, M., R. Alvarez, and N. Cuesta, *Toll-like receptors, inflammation, metabolism and obesity.* Archives of physiology and biochemistry, 2011. **117**(3): p. 151-164.
203. Caricilli, A.a.M., et al., *Inhibition of toll-like receptor 2 expression improves insulin sensitivity and signaling in muscle and white adipose tissue of mice fed a high-fat diet.* Journal of Endocrinology, 2008. **199**(3): p. 399-406.
204. Triantafilou, M., et al., *Membrane sorting of toll-like receptor (TLR)-2/6 and TLR2/1 heterodimers at the cell surface determines heterotypic associations with CD36 and intracellular targeting.* Journal of Biological Chemistry, 2006. **281**(41): p. 31002-31011.
205. Ehses, J.A., et al., *Toll-like receptor 2-deficient mice are protected from insulin resistance and beta cell dysfunction induced by a high-fat diet.* Diabetologia, 2010. **53**(8): p. 1795-1806.
206. Jiao, P., et al., *FFA-Induced Adipocyte Inflammation and Insulin Resistance: Involvement of ER Stress and IKK Pathways.* Obesity.
207. Gregor, M.F. and G.k.S. Hotamisligil, *Thematic review series: Adipocyte Biology. Adipocyte stress: the endoplasmic reticulum and metabolic disease.* J Lipid Res, 2007. **48**(9): p. 1905-14.
208. Furukawa, S., et al., *Increased oxidative stress in obesity and its impact on metabolic syndrome.* The Journal of Clinical Investigation, 2004. **114**(12): p. 1752-1761.
209. Gao, Z., et al., *Inhibition of insulin sensitivity by free fatty acids requires activation of multiple serine kinases in 3T3-L1 adipocytes.* Mol Endocrinol, 2004. **18**(8): p. 2024-34.
210. Patti, M.-E. and S. Corvera, *The role of mitochondria in the pathogenesis of type 2 diabetes.* Endocr Rev, 2010. **31**(3): p. 364-95.
211. Bhandary, B., et al., *An involvement of oxidative stress in endoplasmic reticulum stress and its associated diseases.* International journal of molecular sciences, 2012. **14**(1): p. 434-456.
212. Deng, J., et al., *Translational repression mediates activation of nuclear factor kappa B by phosphorylated translation initiation factor 2.* Molecular and cellular biology, 2004. **24**(23): p. 10161-10168.
213. Hu, P., et al., *Autocrine tumor necrosis factor alpha links endoplasmic reticulum stress to the membrane death receptor pathway through IRE1 {alpha}-mediated NF-{kappa} B activation and down-regulation of TRAF2 expression.* Molecular and cellular biology, 2006. **26**(8): p. 3071.
214. Urano, F., A. Bertolotti, and D. Ron, *IRE1 and efferent signaling from the endoplasmic reticulum.* Journal of cell science, 2000. **113**(21): p. 3697-3702.
215. Guo, S., et al., *Role of A20 in cIAP-2 protection against tumor necrosis factor Îα (TNF-Îα)-mediated apoptosis in endothelial cells.* Int J Mol Sci. **15**(3): p. 3816-33.
216. Faustman, D. and M. Davis, *TNF receptor 2 pathway: drug target for autoimmune diseases.* Nat Rev Drug Discov, 2010. **9**(6): p. 482-493.
217. Juge-Aubry, C.E., et al., *Adipose Tissue Is a Major Source of Interleukin-1 Receptor Antagonist: Upregulation in Obesity and Inflammation.* Diabetes, 2003. **52**(5): p. 1104-1110.
218. Seckinger, P., et al., *A urine inhibitor of interleukin 1 activity that blocks ligand binding.* The Journal of Immunology, 1987. **139**(5): p. 1546-9.
219. Culver, C., et al., *Mechanism of hypoxia-induced NF-kappaB.* Mol Cell Biol, 2010. **30**(20): p. 4901-21.
220. Koong, A.C., E.Y. Chen, and A.J. Giaccia, *Hypoxia causes the activation of nuclear factor kappa B through the phosphorylation of I kappa B alpha on tyrosine residues.* Cancer Res, 1994. **54**(6): p. 1425-30.

221. Zhang, K. and R.J. Kaufman, *From endoplasmic-reticulum stress to the inflammatory response.* Nature, 2008. **454**(7203): p. 455-462.
222. Yoshida, H., *ER stress and diseases.* FEBS journal, 2007. **274**(3): p. 630-658.
223. Harding, H.P., et al., *An integrated stress response regulates amino acid metabolism and resistance to oxidative stress.* Molecular cell, 2003. **11**(3): p. 619-633.
224. Schroeder, M. and R.J. Kaufman, *ER stress and the unfolded protein response.* Mutation Research/Fundamental and Molecular Mechanisms of Mutagenesis, 2005. **569**(1): p. 29-63.
225. Kaufman, R.J., et al., *The unfolded protein response in nutrient sensing and differentiation.* Nature reviews Molecular cell biology, 2002. **3**(6): p. 411-421.
226. Schröder, M. and R.J. Kaufman, *The mammalian unfolded protein response.* Annu. Rev. Biochem., 2005. **74**: p. 739-789.
227. Hershey, J.W.B., *Translational control in mammalian cells.* Annual review of biochemistry, 1991. **60**(1): p. 717-755.
228. Jackson, R.J., C.U.T. Hellen, and T.V. Pestova, *The mechanism of eukaryotic translation initiation and principles of its regulation.* Nature Reviews molecular cell biology. **11**(2): p. 113-127.
229. Schroder, M. and R.J. Kaufman, *ER stress and the unfolded protein response.* Mutation Research/Fundamental and Molecular Mechanisms of Mutagenesis, 2005. **569**(1-2): p. 29-63.
230. Vattem, K.M. and R.C. Wek, *Reinitiation involving upstream ORFs regulates ATF4 mRNA translation in mammalian cells.* Proceedings of the National Academy of Sciences of the United States of America, 2004. **101**(31): p. 11269.
231. Tirasophon, W., A.A. Welihinda, and R.J. Kaufman, *A stress response pathway from the endoplasmic reticulum to the nucleus requires a novel bifunctional protein kinase/endoribonuclease (Ire1p) in mammalian cells.* Genes & development, 1998. **12**(12): p. 1812.
232. Urano, F., A. Bertolotti, and D. Ron, *IRE1 and efferent signaling from the endoplasmic reticulum.* Journal of cell science, 2000. **113**(21): p. 3697.
233. Bertolotti, A., et al., *Increased sensitivity to dextran sodium sulfate colitis in IRE1beta-deficient mice.* Journal of Clinical Investigation, 2001. **107**(5): p. 585-594.
234. Uemura, A., et al., *Unconventional splicing of XBP1 mRNA occurs in the cytoplasm during the mammalian unfolded protein response.* Journal of cell science, 2009. **122**(16): p. 2877-2886.
235. Nguyen, M.T., et al., *JNK and tumor necrosis factor- mediate free fatty acid-induced insulin resistance in 3T3-L1 adipocytes.* Journal of Biological Chemistry, 2005. **280**(42): p. 35361.
236. Thuerauf, D.J., et al., *Effects of the isoform-specific characteristics of ATF6 alpha and ATF6 beta on endoplasmic reticulum stress response gene expression and cell viability.* J Biol Chem, 2007. **282**(31): p. 22865-78.
237. DeBose-Boyd, R.A., et al., *Transport-Dependent Proteolysis of SREBP: Relocation of Site-1 Protease from Golgi to ER Obviates the Need for SREBP Transport to Golgi.* Cell, 1999. **99**(7): p. 703-712.
238. Tu, B.P. and J.S. Weissman, *The FAD-and O 2-dependent reaction cycle of Ero1-mediated oxidative protein folding in the endoplasmic reticulum.* Molecular cell, 2002. **10**(5): p. 983-994.
239. Deniaud, A., *Endoplasmic reticulum stress induces calcium-dependent permeability transition, mitochondrial outer membrane permeabilization and apoptosis.* Oncogene, 2007. **27**(3): p. 285-299.

240. Pahl, H.L. and P.A. Baeuerle, *The ER-overload response: activation of NF-[kappa] B.* Trends in biochemical sciences, 1997. **22**(2): p. 63-67.
241. Deng, J., et al., *Translational repression mediates activation of nuclear factor kappa B by phosphorylated translation initiation factor 2.* Molecular and cellular biology, 2004. **24**(23): p. 10161.
242. Jiang, H.Y., et al., *Phosphorylation of the {alpha} subunit of eukaryotic initiation factor 2 is required for activation of NF-{kappa} B in response to diverse cellular stresses.* Molecular and cellular biology, 2003. **23**(16): p. 5651.
243. Zhang, K., et al., *Endoplasmic reticulum stress activates cleavage of CREBH to induce a systemic inflammatory response.* Cell, 2006. **124**(3): p. 587-599.
244. Hirosumi, J., et al., *A central role for JNK in obesity and insulin resistance.* Nature, 2002. **420**(6913): p. 333-336.
245. Sabio, G., et al., *A stress signaling pathway in adipose tissue regulates hepatic insulin resistance.* Science, 2008. **322**(5907): p. 1539.
246. Wei, Y., et al., *Saturated fatty acids induce endoplasmic reticulum stress and apoptosis independently of ceramide in liver cells.* American Journal of Physiology-Endocrinology And Metabolism, 2006. **291**(2): p. E275.
247. Gu, X., et al., *Bip overexpression, but not CHOP inhibition, attenuates fatty acid-induced endoplasmic reticulum stress and apoptosis in HepG2 liver cells.* Life sciences, 2010. **87**(21-26): p. 724-32.
248. Karaskov, E., et al., *Chronic palmitate but not oleate exposure induces endoplasmic reticulum stress, which may contribute to INS-1 pancreatic {beta}-cell apoptosis.* Endocrinology, 2006. **147**(7): p. 3398.
249. Laybutt, D.R., et al., *Endoplasmic reticulum stress contributes to beta cell apoptosis in type 2 diabetes.* Diabetologia, 2007. **50**(4): p. 752-63.
250. Guo, W., et al., *Palmitate modulates intracellular signaling, induces endoplasmic reticulum stress, and causes apoptosis in mouse 3T3-L1 and rat primary preadipocytes.* American Journal of Physiology-Endocrinology And Metabolism, 2007. **293**(2): p. E576.
251. Hotamisligil, G.S., *Role of endoplasmic reticulum stress and c-Jun NH2-terminal kinase pathways in inflammation and origin of obesity and diabetes.* Diabetes, 2005. **54 Suppl 2**: p. S73-8.
252. Yung, H.W., D.S. Charnock-Jones, and G.J. Burton, *Regulation of AKT Phosphorylation at Ser473 and Thr308 by Endoplasmic Reticulum Stress Modulates Substrate Specificity in a Severity Dependent Manner.*PLoS One, 2011. **6**(3): e17894.
253. Yung, H., et al., *Endoplasmic reticulum stress exacerbates ischemia-reperfusion-induced apoptosis through attenuation of Akt protein synthesis in human choriocarcinoma cells.* The FASEB Journal, 2007. **21**(3): p. 872.
254. Antuna-Puente, B., et al., *Adipokines: the missing link between insulin resistance and obesity.* Diabetes & metabolism, 2008. **34**(1): p. 2-11.
255. Xue, X., et al., *Tumor necrosis factor (TNF) induces the unfolded protein response (UPR) in a reactive oxygen species (ROS)-dependent fashion, and the UPR counteracts ROS accumulation by TNF.* Journal of Biological Chemistry, 2005. **280**(40): p. 33917.
256. Müller, S., et al., *Impaired glucose tolerance is associated with increased serum concentrations of interleukin 6 and co-regulated acute-phase proteins but not TNF-a or its receptors.* Diabetologia, 2002. **45**(6): p. 805-812.
257. Xu, H., et al., *Altered tumor necrosis factor- (TNF-) processing in adipocytes and increased expression of transmembrane TNF- in obesity.* Diabetes, 2002. **51**(6): p. 1876.

258. Liu, L.S., et al., *Tumor necrosis factor-alpha acutely inhibits insulin signaling in human adipocytes: implication of the p80 tumor necrosis factor receptor.* Diabetes, 1998. **47**(4): p. 515.
259. Rotter, V., I. Nagaev, and U. Smith, *Interleukin-6 (IL-6) induces insulin resistance in 3T3-L1 adipocytes and is, like IL-8 and tumor necrosis factor- , overexpressed in human fat cells from insulin-resistant subjects.* Journal of Biological Chemistry, 2003. **278**(46): p. 45777.
260. Peraldi, P. and B. Spiegelman, *TNF- and insulin resistance: summary and future prospects.* Molecular and cellular biochemistry, 1998. **182**(1): p. 169-175.
261. Kanety, H., et al., *Tumor necrosis factor-induced phosphorylation of insulin receptor substrate-1 (IRS-1).* Journal of Biological Chemistry, 1995. **270**(40): p. 23780.
262. Hotamisligil, G.S., et al., *IRS-1-mediated inhibition of insulin receptor tyrosine kinase activity in TNF- -and obesity-induced insulin resistance.* Science, 1996. **271**(5249): p. 665.
263. Stephens, J.M. and P.H. Pekala, *Transcriptional repression of the GLUT4 and C/EBP genes in 3T3-L1 adipocytes by tumor necrosis factor-alpha.* Journal of Biological Chemistry, 1991. **266**(32): p. 21839.
264. Stephens, J.M., J. Lee, and P.F. Pilch, *Tumor necrosis factor- -induced insulin resistance in 3T3-L1 adipocytes is accompanied by a loss of insulin receptor substrate-1 and GLUT4 expression without a loss of insulin receptor-mediated signal transduction.* Journal of Biological Chemistry, 1997. **272**(2): p. 971.
265. Senn, J.J., et al., *Suppressor of cytokine signaling-3 (SOCS-3), a potential mediator of interleukin-6-dependent insulin resistance in hepatocytes.* Journal of Biological Chemistry, 2003. **278**(16): p. 13740.
266. Kawasaki, N., et al., *Obesity-induced endoplasmic reticulum stress causes chronic inflammation in adipose tissue.* Scientific reports, 2012. **2**.
267. Yacoub Wasef, S.Z., et al., *Glucose, dexamethasone, and the unfolded protein response regulate TRB3 mRNA expression in 3T3-L1 adipocytes and L6 myotubes.* American Journal of Physiology - Endocrinology and Metabolism, 2006. **291**(6): p. E1274-E1280.
268. Guo, W., et al., *Palmitate modulates intracellular signaling, induces endoplasmic reticulum stress, and causes apoptosis in mouse 3T3-L1 and rat primary preadipocytes.* Am J Physiol Endocrinol Metab, 2007. **293**(2): p. E576-86.
269. Montoye, H.J., F.H. Epstein, and M.O. Kjelsberg, *Relationship Between Serum Cholesterol and Body Fatness An Epidemiologic Study.* The American journal of clinical nutrition, 1966. **18**(6): p. 397-406.
270. Devries-Seimon, T., et al., *Cholesterol-induced macrophage apoptosis requires ER stress pathways and engagement of the type A scavenger receptor.* J Cell Biol, 2005. **171**(1): p. 61-73.
271. Kedi, X., et al., *Free cholesterol overloading induced smooth muscle cells death and activated both ER-and mitochondrial-dependent death pathway.* Atherosclerosis, 2009. **207**(1): p. 123-130.
272. Song, B., et al., *Chop deletion reduces oxidative stress, improves beta cell function, and promotes cell survival in multiple mouse models of diabetes.* The Journal of Clinical Investigation, 2008. **118**(10): p. 3378.
273. Wang, Q., et al., *IL-1beta caused pancreatic beta-cells apoptosis is mediated in part by endoplasmic reticulum stress via the induction of endoplasmic reticulum Ca2+ release through the c-Jun N-terminal kinase pathway.* Mol Cell Biochem, 2009. **324**(1-2): p. 183-90.

274. Cardozo, A.K., et al., *Cytokines downregulate the sarcoendoplasmic reticulum pump Ca2+ ATPase 2b and deplete endoplasmic reticulum Ca2+, leading to induction of endoplasmic reticulum stress in pancreatic beta-cells.* Diabetes, 2005. **54**(2): p. 452-461.
275. Palorini, R., et al., *Glucose starvation induces cell death in K-ras-transformed cells by interfering with the hexosamine biosynthesis pathway and activating the unfolded protein response.* Cell Death Dis, 2013. **4**: p. e732.
276. Moore, C.E., et al., *PERK Activation at Low Glucose Concentration Is Mediated by SERCA Pump Inhibition and Confers Preemptive Cytoprotection to Pancreatic Î²-Cells.* Molecular Endocrinology, 2010. **25**(2): p. 315-326.
277. Hosogai, N., et al., *Adipose tissue hypoxia in obesity and its impact on adipocytokine dysregulation.* Diabetes, 2007. **56**(4): p. 901-911.
278. Ye, J., et al., *Hypoxia is a potential risk factor for chronic inflammation and adiponectin reduction in adipose tissue of ob/ob and dietary obese mice.* American Journal of Physiology-Endocrinology and Metabolism, 2007. **293**(4): p. E1118-E1128.
279. Regazzetti, C., et al., *Hypoxia decreases insulin signaling pathways in adipocytes.* Diabetes, 2009. **58**(1): p. 95-103.
280. Yin, J., et al., *Role of hypoxia in obesity-induced disorders of glucose and lipid metabolism in adipose tissue.* American Journal of Physiology-Endocrinology and Metabolism, 2009. **296**(2): p. E333-E342.
281. SantaLucia, J., *A unified view of polymer, dumbbell, and oligonucleotide DNA nearest-neighbor thermodynamics.* Proceedings of the National Academy of Sciences, 1998. **95**(4): p. 1460-1465.
282. Green, H. and O. Kehinde, *An established preadipose cell line and its differentiation in culture. II. Factors affecting the adipose conversion.* Cell, 1975. **5**(1): p. 19-27.
283. Green, H. and O. Kehinde, *Spontaneous heritable changes leading to increased adipose conversion in 3T3 cells.* Cell, 1976. **7**(1): p. 105-13.
284. Mandrup, S., et al., *Obese gene expression at in vivo levels by fat pads derived from s.c. implanted 3T3-F442A preadipocytes.* Proc Natl Acad Sci U S A, 1997. **94**(9): p. 4300-5.
285. Freshney, R.I., *Subculture and cell lines.* Culture of Animal Cells, 1987.
286. Strober, W., *Trypan blue exclusion test of cell viability.* Curr Protoc Immunol, 2001. **Appendix 3**: p. Appendix 3B.
287. Green H, K.O., *Sublines of mouse 3T3 cells that accumulate lipid.* Cell 1974. **1**(113-6).
288. Hansen JB, P.R., Larsen BM, Bartkova J, Alsner J, Kristiansen K, *Activation of peroxisome proliferator-activated receptor g bypasses the function of the retinoblastoma protein in adipocyte differentiation.* J Biol Chem, 1999. **274**(4): p. 2386-2393.
289. Daigneault, M., et al., *The identification of markers of macrophage differentiation in PMA-stimulated THP-1 cells and monocyte-derived macrophages.* PloS one, 2010. **5**(1): p. e8668.
290. Sugiyama, Y., et al., *TMP-153, a novel ACAT inhibitor, inhibits cholesterol absorption and lowers plasma cholesterol in rats and hamsters.* Atherosclerosis, 1995. **113**(1): p. 71-78.
291. Tao, J.-l., et al., *Endoplasmic reticulum stress is involved in acetylated low-density lipoprotein induced apoptosis in THP-1 differentiated macrophages.* Chinese medical journal, 2009. **122**(15): p. 1794-1799.

292. Mosmann, T., *Rapid colorimetric assay for cellular growth and survival: application to proliferation and cytotoxicity assays.* Journal of immunological methods, 1983. **65**(1): p. 55-63.
293. Qiagen, *Introduction to Real-Time Quantitative PCR (qPCR).* http://www.sabiosciences.com/manuals/seminars/qPCR%20Introduction_April%202012.pdf.
294. Watt, F.M., *Cell culture models of differentiation.* The FASEB journal, 1991. **5**(3): p. 287-294.
295. Todaro, G.J. and H. Green, *Quantitative studies of the growth of mouse embryo cells in culture and their development into established lines.* The Journal of cell biology, 1963. **17**(2): p. 299-313.
296. Salazar-Olivo, L.A., F. Castro-Munozledo, and W. Kuri-Harcuch, *A preadipose 3T3 cell variant highly sensitive to adipogenic factors and to human growth hormone.* J Cell Sci, 1995. **108 (Pt 5)**: p. 2101-7.
297. O'Shea Alvarez, M.S., *3T3 cells in adipocytic conversion.* Arch Invest Med (Mex), 1991. **22**(2): p. 235-44.
298. Kuri-Harcuch, W. and H. Green, *Adipose conversion of 3T3 cells depends on a serum factor.* Proc Natl Acad Sci U S A, 1978. **75**(12): p. 6107-9.
299. Ramirez-Zacarias, J.L., F. Castro-Munozledo, and W. Kuri-Harcuch, *Quantitation of adipose conversion and triglycerides by staining intracytoplasmic lipids with Oil red O.* Histochemistry, 1992. **97**(6): p. 493-497.
300. Rubin, C.S., et al., *Development of hormone receptors and hormonal responsiveness in vitro. Insulin receptors and insulin sensitivity in the preadipocyte and adipocyte forms of 3T3-L1 cells.* J Biol Chem, 1978. **253**(20): p. 7570-8.
301. Greenspan, P., E.P. Mayer, and S.D. Fowler, *Nile red: a selective fluorescent stain for intracellular lipid droplets.* The Journal of cell biology, 1985. **100**(3): p. 965-973.
302. Lee, Y.-H., et al., *Simple flow cytometric method used to assess lipid accumulation in fat cells.* J Lipid Res, 2004. **45**(6): p. 1162-7.
303. Greenspan, P. and S.D. Fowler, *Spectrofluorometric studies of the lipid probe, nile red.* Journal of lipid research, 1985. **26**(7): p. 781-789.
304. Schaedlich, K., et al., *A simple method to sort ESC-derived adipocytes.* Cytometry Part A, 2010. **77A**(10): p. 990-995.
305. Le, T.T. and J.-X. Cheng, *Single-Cell Profiling Reveals the Origin of Phenotypic Variability in Adipogenesis.* PloS one, 2009. **4**(4): p. e5189.
306. Loo, L.-H., et al., *Heterogeneity in the physiological states and pharmacological responses of differentiating 3T3-L1 preadipocytes.* The Journal of cell biology, 2009. **187**(3): p. 375-384.
307. Capurso, C. and A. Capurso, *From excess adiposity to insulin resistance: the role of free fatty acids.* Vascul Pharmacol, 2012. **57**(2-4): p. 91-7.
308. Yu, B.L., S.P. Zhao, and J.R. Hu, *Cholesterol imbalance in adipocytes: a possible mechanism of adipocytes dysfunction in obesity.* Obes Rev, 2010. **11**(8): p. 560-7.
309. de Ferranti, S. and D. Mozaffarian, *The perfect storm: obesity, adipocyte dysfunction, and metabolic consequences.* Clinical chemistry, 2008. **54**(6): p. 945-955.
310. Qatanani, M. and M.A. Lazar, *Mechanisms of obesity-associated insulin resistance: many choices on the menu.* Genes & development, 2007. **21**(12): p. 1443-1455.
311. Özcan, U., et al., *Endoplasmic reticulum stress links obesity, insulin action, and type 2 diabetes.* Science, 2004. **306**(5695): p. 457.
312. Sieber, J., et al., *Regulation of podocyte survival and endoplasmic reticulum stress by fatty acids*. Vol. 299. 2010. F821-F829.

313. Ma, J., et al., *Plasma fatty acid composition as an indicator of habitual dietary fat intake in middle-aged adults. The Atherosclerosis Risk in Communities (ARIC) Study Investigators.* The American journal of clinical nutrition, 1995. **62**(3): p. 564-571.
314. Raatz, S.K., et al., *Total fat intake modifies plasma fatty acid composition in humans.* The Journal of nutrition, 2001. **131**(2): p. 231-234.
315. Chavez, J.A., et al., *A role for ceramide, but not diacylglycerol, in the antagonism of insulin signal transduction by saturated fatty acids.* J Biol Chem, 2003. **278**(12): p. 10297-303.
316. Bradley, R.L., F.F.M. Fisher, and E. Maratos-Flier, *Dietary fatty acids differentially regulate production of TNF-alpha and IL-10 by murine 3T3-L1 adipocytes.* Obesity (Silver Spring), 2008. **16**(5): p. 938-44.
317. Back, S.H., et al., *ER stress signaling by regulated splicing: IRE1/HAC1/XBP1.* Methods, 2005. **35**(4): p. 395-416.
318. Wei, Y., et al., *Saturated fatty acids induce endoplasmic reticulum stress and apoptosis independently of ceramide in liver cells.* Am J Physiol Endocrinol Metab, 2006. **291**(2): p. E275-81.
319. Lai, E., et al., *Differential activation of ER stress and apoptosis in response to chronically elevated free fatty acids in pancreatic -cells.* American Journal of Physiology-Endocrinology And Metabolism, 2008. **294**(3): p. E540.
320. Shimabukuro, M., et al., *Fatty acid-induced beta cell apoptosis: A link between obesity and diabetes.* Proceedings of the National Academy of Sciences, 1998. **95**(5): p. 2498-2502.
321. Ilham, K., et al., *Free Fatty Acids and Cytokines Induce Pancreatic Beta-Cell Apoptosis by Different Mechanisms: Role of Nuclear Factor-kB and Endoplasmic Reticulum Stress.* Endocrinology, 2004. **145**(11): p. 5087-5096.
322. Lupi, R., et al., *Prolonged exposure to free fatty acids has cytostatic and pro-apoptotic effects on human pancreatic islets evidence that beta-cell death is caspase mediated, partially dependent on ceramide pathway, and bcl-2 regulated.* Diabetes, 2002. **51**(5): p. 1437-1442.
323. Wang, X.-Z., et al., *Signals from the stressed endoplasmic reticulum induce C/EBP-homologous protein (CHOP/GADD153).* Molecular and cellular biology, 1996. **16**(8): p. 4273-4280.
324. Lai, C.W., et al., *ERdj4 Protein Is a Soluble Endoplasmic Reticulum (ER) DnaJ Family Protein That Interacts with ER-associated Degradation Machinery.* The Journal of Biological Chemistry, 2012. **287**(11): p. 7969-7978.
325. Ozcan, U., et al., *Chemical chaperones reduce ER stress and restore glucose homeostasis in a mouse model of type 2 diabetes.* Science, 2006. **313**(5790): p. 1137-40.
326. Nakatani, Y., et al., *Involvement of endoplasmic reticulum stress in insulin resistance and diabetes.* Journal of Biological Chemistry, 2005. **280**(1): p. 847.
327. Dresner, A., et al., *Effects of free fatty acids on glucose transport and IRS-1-associated phosphatidylinositol 3-kinase activity.* Journal of Clinical Investigation, 1999. **103**: p. 253-260.
328. Aguirre, V., et al., *Phosphorylation of Ser307 in Insulin Receptor Substrate-1 Blocks Interactions with the Insulin Receptor and Inhibits Insulin Action.* Journal of Biological Chemistry, 2002. **277**(2): p. 1531-1537.
329. Gonzalez-Gronow, M., et al., *GRP78: a multifunctional receptor on the cell surface.* Antioxid Redox Signal, 2009. **11**(9): p. 2299-306.

330. Zhang, Y., et al., *Cell surface relocalization of the endoplasmic reticulum chaperone and unfolded protein response regulator GRP78/BiP.* J Biol Chem, 2010. **285**(20): p. 15065-75.
331. Ni, M., et al., *Regulation of PERK Signaling and Leukemic Cell Survival by a Novel Cytosolic Isoform of the UPR Regulator GRP78/BiP.* PloS one, 2009. **4**(8): p. e6868.
332. Dasgupta, S., et al., *NF-kappaB mediates lipid-induced fetuin-A expression in hepatocytes that impairs adipocyte function effecting insulin resistance.* Biochem. J, 2010. **429**: p. 451-462.
333. Xi, L., et al., *Crocetin attenuates palmitate-induced insulin insensitivity and disordered tumor necrosis factor-alpha and adiponectin expression in rat adipocytes.* British journal of pharmacology, 2007. **151**(5): p. 610-617.
334. Chavez, J.A. and S.A. Summers, *Characterizing the effects of saturated fatty acids on insulin signaling and ceramide and diacylglycerol accumulation in 3T3-L1 adipocytes and C2C12 myotubes.* Archives of biochemistry and biophysics, 2003. **419**(2): p. 101-109.
335. Hunnicutt, J.W., et al., *Saturated fatty acid-induced insulin resistance in rat adipocytes.* Diabetes, 1994. **43**(4): p. 540-545.
336. Van Epps-Fung, M., et al., *Fatty Acid-Induced Insulin Resistance in Adipocytes 1.* Endocrinology, 1997. **138**(10): p. 4338-4345.
337. Nguyen, M.T.A., et al., *JNK and tumor necrosis factor-alpha mediate free fatty acid-induced insulin resistance in 3T3-L1 adipocytes.* J Biol Chem, 2005. **280**(42): p. 35361-71.
338. Bosma, M., et al., *Sequestration of fatty acids in triglycerides prevents endoplasmic reticulum stress in an in vitro model of cardiomyocyte lipotoxicity.* Biochimica et Biophysica Acta (BBA)-Molecular and Cell Biology of Lipids, 2014. **1841**(12): p. 1648-1655.
339. Ahmadian, M., et al., *Triacylglycerol metabolism in adipose tissue.* Future lipidology, 2007. **2**(2): p. 229-237.
340. Jeon, M.J., et al., *Mitochondrial dysfunction and activation of iNOS are responsible for the palmitate-induced decrease in adiponectin synthesis in 3T3L1 adipocytes.* Experimental & molecular medicine, 2012. **44**(9): p. 562-570.
341. Kennedy, A., et al., *Saturated fatty acid-mediated inflammation and insulin resistance in adipose tissue: mechanisms of action and implications.* The Journal of nutrition, 2009. **139**(1): p. 1-4.
342. Jiao, P., et al., *FFA-Induced Adipocyte Inflammation and Insulin Resistance: Involvement of ER Stress and IKKb Pathways.* Obesity, 2011. **19**(3): p. 483-491.
343. Weigert, C., et al., *Palmitate, but not unsaturated fatty acids, induces the expression of interleukin-6 in human myotubes through proteasome-dependent activation of nuclear factor-kB.* Journal of Biological Chemistry, 2004. **279**(23): p. 23942-23952.
344. Miller, T.A., et al., *Oleate prevents palmitate-induced cytotoxic stress in cardiac myocytes.* Biochemical and biophysical research communications, 2005. **336**(1): p. 309-315.
345. Diakogiannaki, E., H.J. Welters, and N.G. Morgan, *Differential regulation of the endoplasmic reticulum stress response in pancreatic beta-cells exposed to long-chain saturated and monounsaturated fatty acids.* J Endocrinol, 2008. **197**(3): p. 553-63.
346. Katsoulieris, E., et al., *Alpha-Linolenic acid protects renal cells against palmitic acid lipotoxicity via inhibition of endoplasmic reticulum stress.* European journal of pharmacology, 2009. **623**(1): p. 107-112.

347. Akazawa, Y., et al., *Palmitoleate attenuates palmitate-induced Bim and PUMA up-regulation and hepatocyte lipoapoptosis.* Journal of hepatology, 2010. **52**(4): p. 586-593.
348. Salvado, L., et al., *Oleate prevents saturated-fatty-acid-induced ER stress, inflammation and insulin resistance in skeletal muscle cells through an AMPK-dependent mechanism.* Diabetologia, 2013. **56**(6): p. 1372-1382.
349. Reynoso, R.a., L.M. Salgado, and V.c. Calderon, *High levels of palmitic acid lead to insulin resistance due to changes in the level of phosphorylation of the insulin receptor and insulin receptor substrate-1*, in *Vascular Biochemistry*. 2003, Springer. p. 155-162.
350. Wolf, B., et al., *Intracellular Ca2+ mobilization by arachidonic acid.* Journal of Biological Chemistry, 1986. **261**(8): p. 3501-3511.
351. Rizzo, M., et al., *Arachidonic acid induces mobilisation of calcium stores and c-jun gene expression: evidence that intracellular calcium release is associated with c-jun activation.* Prostaglandins Leukot Essent Fatty Acids, 1999. **60**(3): p. 187-198.
352. Koh, E.H., et al., *Essential role of mitochondrial function in adiponectin synthesis in adipocytes.* Diabetes, 2007. **56**(12): p. 2973-2981.
353. Dever, T.E., et al., *Mammalian eukaryotic initiation factor 2 alpha kinases functionally substitute for GCN2 protein kinase in the GCN4 translational control mechanism of yeast.* Proceedings of the National Academy of Sciences, 1993. **90**(10): p. 4616-4620.
354. Green, C.D. and L.K. Olson, *Modulation of palmitate-induced endoplasmic reticulum stress and apoptosis in pancreatic beta-cells by stearoyl-CoA desaturase and Elovl6.* American Journal of Physiology-Endocrinology and Metabolism, 2011. **300**(4): p. E640-E649.
355. Busch, A.K., et al., *Increased fatty acid desaturation and enhanced expression of stearoyl coenzyme A desaturase protects pancreatic beta-cells from lipoapoptosis.* Diabetes, 2005. **54**(10): p. 2917-2924.
356. Hellemans, K.H., et al., *Susceptibility of pancreatic beta cells to fatty acids is regulated by LXR/PPARalpha-dependent stearoyl-coenzyme A desaturase.* PloS one, 2009. **4**(9): p. e7266.
357. Flowers, J.B., et al., *Loss of stearoyl-CoA desaturase-1 improves insulin sensitivity in lean mice but worsens diabetes in leptin-deficient obese mice.* Diabetes, 2007. **56**(5): p. 1228-1239.
358. Silbernagel, G., et al., *High hepatic SCD1 activity is associated with low liver fat content in healthy subjects under a lipogenic diet.* The Journal of Clinical Endocrinology & Metabolism, 2012. **97**(12): p. E2288-E2292.
359. Ariyama, H., et al., *Decrease in membrane phospholipid unsaturation induces unfolded protein response.* Journal of Biological Chemistry, 2010. **285**(29): p. 22027-22035.
360. Minville-Walz, M., et al., *Inhibition of stearoyl-CoA desaturase 1 expression induces CHOP-dependent cell death in human cancer cells.* PloS one, 2010. **5**(12): p. e14363.
361. Yee, J.K., et al., *Compartmentalization of stearoyl-CoA desaturase enzyme-1 activity in HepG2 cells.* J Lipid Res, 2008. **49**: p. 2124–2134.
362. Miyazaki, M., W.C. Man, and J.M. Ntambi, *Targeted disruption of stearoyl-CoA desaturase1 gene in mice causes atrophy of sebaceous and meibomian glands and depletion of wax esters in the eyelid.* The Journal of nutrition, 2001. **131**(9): p. 2260-2268.

363. Lagace, T.A. and N.D. Ridgway, *The role of phospholipids in the biological activity and structure of the endoplasmic reticulum.* Biochimica et Biophysica Acta (BBA)-Molecular Cell Research, 2013. **1833**(11): p. 2499-2510.
364. Penno, A., G. Hackenbroich, and C. Thiele, *Phospholipids and lipid droplets.* Biochimica et Biophysica Acta (BBA)-Molecular and Cell Biology of Lipids, 2013. **1831**(3): p. 589-594.
365. Leamy, A.K., et al., *Enhanced synthesis of saturated phospholipids is associated with ER stress and lipotoxicity in palmitate treated hepatic cells.* Journal of lipid research, 2014. **55**(7): p. 1478-1488.
366. Listenberger, L.L., et al., *Triglyceride accumulation protects against fatty acid-induced lipotoxicity.* Proceedings of the National Academy of Sciences, 2003. **100**(6): p. 3077-3082.
367. Denke, M.A., C.T. Sempos, and S.M. Grundy, *Excess body weight: an underrecognized contributor to high blood cholesterol levels in white American men.* Archives of Internal Medicine, 1993. **153**(9): p. 1093-1103.
368. Brown, C.D., et al., *Body mass index and the prevalence of hypertension and dyslipidemia.* Obesity research, 2000. **8**(9): p. 605-619.
369. Wang, Z. and J. Ge, *Managing hypercholesterolemia and preventing cardiovascular events in elderly and younger Chinese adults: focus on rosuvastatin.* Clinical interventions in aging, 2014. **9**: p. 1.
370. Kannel, W.B., et al., *Serum cholesterol, lipoproteins, and the risk of coronary heart disease: the Framingham Study.* Annals of Internal Medicine, 1971. **74**(1): p. 1-12.
371. Cui, Y., et al., *Non-high-density lipoprotein cholesterol level as a predictor of cardiovascular disease mortality.* Archives of Internal Medicine, 2001. **161**(11): p. 1413-1419.
372. Aguilar, D. and M.L. Fernandez, *Hypercholesterolemia Induces Adipose Dysfunction in Conditions of Obesity and Nonobesity.* Advances in Nutrition: An International Review Journal, 2014. **5**(5): p. 497-502.
373. Guerre-Millo, M.l., et al., *Alteration in membrane lipid order and composition in metabolically hyperactive fatty rat adipocytes.* Lipids, 1994. **29**(3): p. 205-209.
374. Feng, B., et al., *The endoplasmic reticulum is the site of cholesterol-induced cytotoxicity in macrophages.* Nature cell biology, 2003. **5**(9): p. 781-792.
375. Li, Y., et al., *Enrichment of Endoplasmic Reticulum with Cholesterol Inhibits Sarcoplasmic-Endoplasmic Reticulum Calcium ATPase-2b Activity in Parallel with Increased Order of Membrane Lipids IMPLICATIONS FOR DEPLETION OF ENDOPLASMIC RETICULUM CALCIUM STORES AND APOPTOSIS IN CHOLESTEROL-LOADED MACROPHAGES.* Journal of Biological Chemistry, 2004. **279**(35): p. 37030-37039.
376. Tabas, I., *Consequences of cellular cholesterol accumulation: basic concepts and physiological implications.* The Journal of Clinical Investigation, 2002. **110**(7): p. 905-911.
377. Murphy, A.J. and L. Yvan-Charvet, *Adipose Modulation of ABCG1 Uncovers an Intimate Link Between Sphingomyelin and Triglyceride Storage.* Diabetes, 2015. **64**(3): p. 689-692.
378. Krause, B.R., et al., *Adipocyte cholesterol storage: effect of experimental hypercholesterolemia in the rat.* J Nutr, 1979. **109**(12): p. 2213-25.
379. Fazio, S. and M.F. Linton, *Unique pathway for cholesterol uptake in fat cells.* Arteriosclerosis, thrombosis, and vascular biology, 2004. **24**(9): p. 1538-1539.
380. Edgel, K.A., et al., *Obesity and weight loss result in increased adipose tissue ABCG1 expression in db/db mice.* Biochim Biophys Acta, 2012. **1821**(3): p. 425-34.

381. Farkas, J., A. Angel, and M.I. Avigan, *Studies on the compartmentation of lipid in adipose cells. II. Cholesterol accumulation and distribution in adipose tissue components.* Journal of lipid research, 1973. **14**(3): p. 344-356.
382. Krause, B.R. and A.D. Hartman, *Adipose tissue and cholesterol metabolism.* Journal of lipid research, 1984. **25**(2): p. 97-110.
383. Kellner-Weibel, G., et al., *Effects of Intracellular Free Cholesterol Accumulation on Macrophage Viability A Model for Foam Cell Death.* Arteriosclerosis, thrombosis, and vascular biology, 1998. **18**(3): p. 423-431.
384. Rogers, M.A., et al., *Acyl-CoA:cholesterol acyltransferases (ACATs/SOATs): Enzymes with multiple sterols as substrates and as activators.* J Steroid Biochem Mol Biol, 2015. **151**: p. 102-107.
385. Yao, P.M. and I. Tabas, *Free cholesterol loading of macrophages induces apoptosis involving the fas pathway.* Journal of Biological Chemistry, 2000. **275**(31): p. 23807-23813.
386. Dharuri, H., et al., *Downregulation of the acetyl-CoA metabolic network in adipose tissue of obese diabetic individuals and recovery after weight loss.* Diabetologia, 2014. **57**(11): p. 2384-2392.
387. Yao, S., et al., *Minimally modified low-density lipoprotein induces macrophage endoplasmic reticulum stress via toll-like receptor 4.* Biochimica et Biophysica Acta (BBA)-Molecular and Cell Biology of Lipids, 2012. **1821**(7): p. 954-963.
388. Simons, K. and R. Ehehalt, *Cholesterol, lipid rafts, and disease.* The Journal of Clinical Investigation, 2002. **110**(110 (5)): p. 597-603.
389. Tabas, I., *Free cholesterol-induced cytotoxicity: a possible contributing factor to macrophage foam cell necrosis in advanced atherosclerotic lesions.* Trends in cardiovascular medicine, 1997. **7**(7): p. 256-263.
390. Kellner-Weibel, G., et al., *Crystallization of free cholesterol in model macrophage foam cells.* Arteriosclerosis, thrombosis, and vascular biology, 1999. **19**(8): p. 1891-1898.
391. Chen, Y., et al., *Ox-LDL induces ER stress and promotes the adipokines secretion in 3T3-L1 adipocytes.* PloS one, 2013. **8**(10): p. e81379.
392. Kunjathoor, V.V., et al., *Scavenger receptors class AI/II and CD36 are the principal receptors responsible for the uptake of modified low density lipoprotein leading to lipid loading in macrophages.* Journal of Biological Chemistry, 2002. **277**(51): p. 49982-49988.
393. Roma, P., et al., *Defective catabolism of oxidized LDL by J774 murine macrophages.* Journal of lipid research, 1992. **33**(6): p. 819-829.
394. Dhaliwal, B.S. and U.P. Steinbrecher, *Cholesterol delivered to macrophages by oxidized low density lipoprotein is sequestered in lysosomes and fails to efflux normally.* Journal of lipid research, 2000. **41**(10): p. 1658-1665.
395. Wang, M.-D., et al., *Different cellular traffic of LDL-cholesterol and acetylated LDL-cholesterol leads to distinct reverse cholesterol transport pathways.* Journal of lipid research, 2007. **48**(3): p. 633-645.
396. Lougheed, M., et al., *Uptake of oxidized LDL by macrophages differs from that of acetyl LDL and leads to expansion of an acidic endolysosomal compartment.* Arteriosclerosis, thrombosis, and vascular biology, 1999. **19**(8): p. 1881-1890.
397. Chen, T., et al., *MicroRNA-125a-5p partly regulates the inflammatory response, lipid uptake, and ORP9 expression in oxLDL-stimulated monocyte/macrophages.* Cardiovascular research, 2009. **83**(1): p. 131-139.
398. Daub, K., et al. *Oxidized LDL-activated platelets induce vascular inflammation*. in *Seminars in thrombosis and hemostasis*. 2010.

399. Steinberg, D., *Low density lipoprotein oxidation and its pathobiological significance.* Journal of Biological Chemistry, 1997. **272**(34): p. 20963-20966.
400. Berlett, B.S. and E.R. Stadtman, *Protein Oxidation in Aging, Disease, and Oxidative Stress.* Journal of Biological Chemistry, 1997. **272**(33): p. 20313-20316.
401. Berliner, J.A., et al., *Atherosclerosis: Basic Mechanisms: Oxidation, Inflammation, and Genetics.* Circulation, 1995. **91**(9): p. 2488-2496.
402. O'Donnell, R.W., et al., *Endothelial NADPH oxidase: mechanism of activation by low-density lipoprotein.* Endothelium, 2003. **10**(6): p. 291-297.
403. Galle, J., et al., *Lp (a) and LDL induce apoptosis in human endothelial cells and in rabbit aorta: role of oxidative stress.* Kidney international, 1999. **55**(4): p. 1450-1461.
404. Maziere, C., et al., *Oxidized LDL induces an oxidative stress and activates the tumor suppressor p53 in MRC5 human fibroblasts.* Biochemical and biophysical research communications, 2000. **276**(2): p. 718-723.
405. Vincent, A.M., et al., *Dyslipidemia-Induced Neuropathy in Mice The Role of oxLDL/LOX-1.* Diabetes, 2009. **58**(10): p. 2376-2385.
406. Wintergerst, E.S., et al., *Apoptosis induced by oxidized low density lipoprotein in human monocyte-derived macrophages involves CD36 and activation of caspase-3.* European Journal of Biochemistry, 2000. **267**(19): p. 6050-6059.
407. Zechner, R., et al., *Apolipoprotein E gene expression in mouse 3T3-L1 adipocytes and human adipose tissue and its regulation by differentiation and lipid content.* Journal of Biological Chemistry, 1991. **266**(16): p. 10583-10588.
408. Martin, S. and R.G. Parton, *Lipid droplets: a unified view of a dynamic organelle.* Nature reviews Molecular cell biology, 2006. **7**(5): p. 373-378.
409. Tauchi-Sato, K., et al., *The surface of lipid droplets is a phospholipid monolayer with a unique fatty acid composition.* Journal of Biological Chemistry, 2002. **277**(46): p. 44507-44512.
410. Ozeki, S., et al., *Rab18 localizes to lipid droplets and induces their close apposition to the endoplasmic reticulum-derived membrane.* Journal of cell science, 2005. **118**(12): p. 2601-2611.
411. Prattes, S., et al., *Intracellular distribution and mobilization of unesterified cholesterol in adipocytes: triglyceride droplets are surrounded by cholesterol-rich ER-like surface layer structures.* Journal of cell science, 2000. **113**(17): p. 2977-2989.
412. Ikonen, E., S. Heino, and S. Lusa, *Caveolins and membrane cholesterol.* Biochem Soc Trans, 2004. **32**(Pt 1): p. 121-3.
413. Le Lay, S., et al., *Cholesterol-Induced Caveolin Targeting to Lipid Droplets in Adipocytes: A Role for Caveolar Endocytosis.* Traffic, 2006. **7**(5): p. 549-561.
414. Sugiyama, Y., et al., *TMP-153, a novel ACAT inhibitor, lowers plasma cholesterol through its hepatic action in Golden hamsters.* Atherosclerosis, 1995. **118**(1): p. 145-153.
415. Wellen, K.E. and G.k.S. Hotamisligil, *Obesity-induced inflammatory changes in adipose tissue.* Journal of Clinical Investigation, 2003. **112**(12): p. 1785.
416. Murano, I., et al., *Dead adipocytes, detected as crown-like structures, are prevalent in visceral fat depots of genetically obese mice.* Journal of lipid research, 2008. **49**(7): p. 1562-1568.
417. Bastard, J.-P., et al., *Adipose tissue IL-6 content correlates with resistance to insulin activation of glucose uptake both in vivo and in vitro.* The Journal of Clinical Endocrinology & Metabolism, 2002. **87**(5): p. 2084-2089.

418. Hotamisligil, G.S., et al., *Reduced tyrosine kinase activity of the insulin receptor in obesity-diabetes. Central role of tumor necrosis factor-alpha.* Journal of Clinical Investigation, 1994. **94**(4): p. 1543.
419. Hotamisligil, G.S. and B.M. Spiegelman, *Tumor necrosis factor alpha: a key component of the obesity-diabetes link.* Diabetes, 1994. **43**(11): p. 1271.
420. Weisberg, S.P., et al., *Obesity is associated with macrophage accumulation in adipose tissue.* Journal of Clinical Investigation, 2003. **112**(12): p. 1796-1808.
421. Liang, B., et al., *Involvement of TR3/Nur77 translocation to the endoplasmic reticulum in ER stress-induced apoptosis.* Exp Cell Res, 2007. **313**(13): p. 2833-44.
422. Kharroubi, I., et al., *Free fatty acids and cytokines induce pancreatic beta-cell apoptosis by different mechanisms: role of nuclear factor-kB and endoplasmic reticulum stress.* Endocrinology, 2004. **145**(11): p. 5087-5096.
423. Zhang, Y., et al., *Stimulation of Interleukin-6 mRNA Levels by Tumor Necrosis Factor and Interleukin-1.* Annals of the New York Academy of Sciences, 1989. **557**(1): p. 548-549.
424. Hotamisligil, G.S., et al., *Increased adipose tissue expression of tumor necrosis factor-alpha in human obesity and insulin resistance.* Journal of Clinical Investigation, 1995. **95**(5): p. 2409.
425. Rotter, V., I. Nagaev, and U. Smith, *Interleukin-6 (IL-6) induces insulin resistance in 3T3-L1 adipocytes and is, like IL-8 and tumor necrosis factor-α, overexpressed in human fat cells from insulin-resistant subjects.* Journal of Biological Chemistry, 2003. **278**(46): p. 45777-45784.
426. Lagathu, C., et al., *Long-term treatment with interleukin-1b induces insulin resistance in murine and human adipocytes.* Diabetologia, 2006. **49**(9): p. 2162-2173.
427. Pfeffer, K., *Biological functions of tumor necrosis factor cytokines and their receptors.* Cytokine and Growth Factor Reviews, 2003. **14**(3): p. 185-191.
428. Beutler, B. and A. Cerami, *The biology of cachectin/TNF--a primary mediator of the host response.* Annual review of immunology, 1989. **7**(1): p. 625-655.
429. Feingold, K.R., et al., *Stimulation of lipolysis in cultured fat cells by tumor necrosis factor, interleukin-1, and the interferons is blocked by inhibition of prostaglandin synthesis.* Endocrinology, 1992. **130**(1): p. 10-16.
430. Grunfeld, C. and K.R. Feingold, *The metabolic effects of tumor necrosis factor and other cytokines.* Biotherapy, 1991. **3**(2): p. 143-158.
431. Grunfeld, C., et al., *Endotoxin and cytokines induce expression of leptin, the ob gene product, in hamsters.* Journal of Clinical Investigation, 1996. **97**(9): p. 2152.
432. Stephens, J.M. and P.H. Pekala, *Transcriptional repression of the C/EBP-alpha and GLUT4 genes in 3T3-L1 adipocytes by tumor necrosis factor-alpha. Regulations is coordinate and independent of protein synthesis.* Journal of Biological Chemistry, 1992. **267**(19): p. 13580-13584.
433. Stephens, J.M., J. Lee, and P.F. Pilch, *Tumor necrosis factor-alpha-induced insulin resistance in 3T3-L1 adipocytes is accompanied by a loss of insulin receptor substrate-1 and GLUT4 expression without a loss of insulin receptor-mediated signal transduction.* J Biol Chem, 1997. **272**(2): p. 971-6.
434. Kern, P.A., et al., *The expression of tumor necrosis factor in human adipose tissue. Regulation by obesity, weight loss, and relationship to lipoprotein lipase.* Journal of Clinical Investigation, 1995. **95**(5): p. 2111.
435. Rudich, A., et al., *Oxidant stress reduces insulin responsiveness in 3T3-L1 adipocytes.* American Journal of Physiology-Endocrinology and Metabolism, 1997. **272**(5): p. E935-E940.

436. Rudich, A., et al., *Prolonged oxidative stress impairs insulin-induced GLUT4 translocation in 3T3-L1 adipocytes.* Diabetes, 1998. **47**(10): p. 1562-1569.
437. Tirosh, A., et al., *Oxidative Stress Disrupts Insulin-induced Cellular Redistribution of Insulin Receptor Substrate-1 and Phosphatidylinositol 3-Kinase in 3T3-L1 Adipocytes A putative cellular mechanism for impaired protein kinase B activation and GLUT 4 translocation.* Journal of Biological Chemistry, 1999. **274**(15): p. 10595-10602.
438. Kudo, M., et al., *Transcription suppression of peroxisome proliferator-activated receptor gamma2 gene expression by tumor necrosis factor alpha via an inhibition of CCAAT/ enhancer-binding protein delta during the early stage of adipocyte differentiation.* Endocrinology, 2004. **145**(11): p. 4948-56.
439. Palacios-Ortega, S., et al., *Effect of TNF-Alpha on Caveolin-1 Expression and Insulin Signaling During Adipocyte Differentiation and in Mature Adipocytes.* Cell Physiol Biochem, 2015. **36**(4): p. 1499-1516.
440. Wei, Y.-T., et al., *Secretion of adipocytes and macrophages under conditions of inflammation and/or insulin resistance and effect of adipocytes on preadipocytes under these conditions.* Biochemistry (Moscow), 2014. **79**(7): p. 663-671.
441. Xue, X., et al., *Tumor necrosis factor α (TNFα) induces the unfolded protein response (UPR) in a reactive oxygen species (ROS)-dependent fashion, and the UPR counteracts ROS accumulation by TNFα.* Journal of Biological Chemistry, 2005. **280**(40): p. 33917-33925.
442. Binder, C., et al., *Induction of inducible nitric oxide synthase is an essential part of tumor necrosis factor-alpha-induced apoptosis in MCF-7 and other epithelial tumor cells.* Laboratory investigation; a journal of technical methods and pathology, 1999. **79**(12): p. 1703-1712.
443. Gottlieb, E., M.G. Vander Heiden, and C.B. Thompson, *Bcl-xL prevents the initial decrease in mitochondrial membrane potential and subsequent reactive oxygen species production during tumor necrosis factor alpha-induced apoptosis.* Molecular and cellular biology, 2000. **20**(15): p. 5680-5689.
444. Kyriakis, J.M. and J. Avruch, *Sounding the alarm: protein kinase cascades activated by stress and inflammation.* Journal of Biological Chemistry, 1996. **271**(40): p. 24313-24316.
445. Hirosumi, J., et al., *A central role for JNK in obesity and insulin resistance.* Nature, 2002. **420**(6913): p. 333-336.
446. Souza, S.C., et al., *TNF-α induction of lipolysis is mediated through activation of the extracellular signal related kinase pathway in 3T3-L1 adipocytes.* Journal of Cellular Biochemistry, 2003. **89**(6): p. 1077-1086.
447. Coppack, S.W., *Pro-inflammatory cytokines and adipose tissue.* Proc Nutr Soc, 2001. **60**(3): p. 349-56.
448. Kern, P.A., et al., *Adipose tissue tumor necrosis factor and interleukin-6 expression in human obesity and insulin resistance*. Vol. 280. 2001. E745-E751.
449. Mohamed-Ali, V., et al., *Subcutaneous Adipose Tissue Releases Interleukin-6, But Not Tumor Necrosis Factor-alpha, in Vivo 1.* The Journal of Clinical Endocrinology & Metabolism, 1997. **82**(12): p. 4196-4200.
450. Vozarova, B., et al., *Circulating interleukin-6 in relation to adiposity, insulin action, and insulin secretion.* Obesity research, 2001. **9**(7): p. 414-417.
451. Roytblat, L., et al., *Raised Interleukin-6 Levels in Obese Patients.* Obesity research, 2000. **8**(9): p. 673-675.

452. Maria, E.T., et al., *Interleukin-6 Regulates Human Adipose Tissue Lipid Metabolism and Leptin Production in Vitro.* The Journal of Clinical Endocrinology & Metabolism, 2004. **89**(11): p. 5577-5582.
453. Jager, J., et al., *Interleukin-1 beta-induced insulin resistance in adipocytes through down-regulation of insulin receptor substrate-1 expression.* Endocrinology, 2007. **148**(1): p. 241-51.
454. Denis, R.G., et al., *TNF-α transiently induces endoplasmic reticulum stress and an incomplete unfolded protein response in the hypothalamus.* Neuroscience, 2010. **170**(4): p. 1035-1044.
455. Schulze-Osthoff, K., et al., *Cytotoxic activity of tumor necrosis factor is mediated by early damage of mitochondrial functions. Evidence for the involvement of mitochondrial radical generation.* Journal of Biological Chemistry, 1992. **267**(8): p. 5317-5323.
456. Shiau, M.-Y., et al., *Establishment of a consistent L929 bioassay system for TNF-α quantitation to evaluate the effect of lipopolysaccharide, phytomitogens and cytodifferentiation agents on cytotoxicity of TNF-α secreted by adherent human mononuclear cells.* Mediators of inflammation, 2001. **10**(4): p. 199-208.
457. Cawthorn, W.P. and J.K. Sethi, *TNF-alpha and adipocyte biology.* FEBS Letters, 2008. **582**(1): p. 117-131.
458. Sethi, J.K. and G.S. Hotamisligil. *The role of TNFα in adipocyte metabolism*. in *Seminars in cell & developmental biology*. 1999. Elsevier.
459. Stephens, J.M. and P.H. Pekala, *Transcriptional repression of the GLUT4 and C/EBP genes in 3T3-L1 adipocytes by tumor necrosis factor-alpha.* J Biol Chem, 1991. **266**(32): p. 21839-45.
460. Memon, R.A., et al., *Regulation of fatty acid transport protein and fatty acid translocase mRNA levels by endotoxin and cytokines.* American Journal of Physiology-Endocrinology and Metabolism, 1998. **274**(2): p. E210-E217.
461. Kita, A., et al., *Identification of the promoter region required for human adiponectin gene transcription: Association with CCAAT/enhancer binding protein-beta and tumor necrosis factor-α.* Biochemical and biophysical research communications, 2005. **331**(2): p. 484-490.
462. Dahlman, I., et al., *Downregulation of electron transport chain genes in visceral adipose tissue in type 2 diabetes independent of obesity and possibly involving tumor necrosis factor-alpha.* Diabetes, 2006. **55**(6): p. 1792-1799.
463. O'Neill, C.M., et al., *Circulating Levels of IL-1B+IL-6 Cause ER Stress and Dysfunction in Islets From Prediabetic Male Mice.* Endocrinology, 2013. **154**(9): p. 3077-3088.
464. Maedler, K., et al., *Interleukin-1 targeted therapy for type 2 diabetes.* Expert Opin Biol Ther., 2009. **9**: p. 1177-1188.
465. Hausman, G.J. and R.L. Richardson, *Adipose tissue angiogenesis.* J Anim Sci, 2004. **82**(3): p. 925-34.
466. Nishimura, S., et al., *In vivo imaging in mice reveals local cell dynamics and inflammation in obese adipose tissue.* The Journal of clinical investigation, 2008. **118**(2): p. 710.
467. Summers, L.K.M., et al., *Subcutaneous Abdominal Adipose Tissue Blood Flow: Variation within and between Subjects and Relationship to Obesity.* Clinical Science, 1996. **91**(6): p. 679-683.
468. Blaak, E.E., et al., *Beta-adrenergic stimulation and abdominal subcutaneous fat blood flow in lean, obese, and reduced-obese subjects.* Metabolism, 1995. **44**(2): p. 183-7.

469. Kowalchuk, J.M., R. Curi, and E.A. Newsholme, *Glutamine metabolism in isolated incubated adipocytes of the rat.* Biochemical Journal, 1988. **249**(3): p. 705-708.
470. Yoo, H., et al., *Quantifying Reductive Carboxylation Flux of Glutamine to Lipid in a Brown Adipocyte Cell Line.* The Journal of Biological Chemistry, 2008. **283**(30): p. 20621-20627.
471. Chao, C.C., W.C. Yam, and S. Lin-Chao, *Coordinated induction of two unrelated glucose-regulated protein genes by a calcium ionophore: human BiP/GRP78 and GAPDH.* Biochemical and biophysical research communications, 1990. **171**(1): p. 431-438.
472. Zhang, L., et al., *Different Effects of Glucose Starvation on Expression and Stability of VEGF mRNA Isoforms in Murine Ovarian Cancer Cells.* Biochemical and biophysical research communications, 2002. **292**(4): p. 860-868.
473. Sone, H., et al., *Vascular Endothelial Growth Factor Is Induced by Long-Term High Glucose Concentration and Up-Regulated by Acute Glucose Deprivation in Cultured Bovine Retinal Pigmented Epithelial Cells.* Biochemical and biophysical research communications, 1996. **221**(1): p. 193-198.
474. Park, S.H., et al., *Hypoglycemia-induced VEGF expression is mediated by intracellular Ca2+ and protein kinase C signaling pathway in HepG2 human hepatoblastoma cells.* Int J Mol Med, 2001. **7**(1): p. 91-6.
475. Yun, H., et al., *Glucose deprivation increases mRNA stability of vascular endothelial growth factor through activation of AMP-activated protein kinase in DU145 prostate carcinoma.* Journal of Biological Chemistry, 2005. **280**(11): p. 9963-9972.
476. Ghosh, R., et al., *Transcriptional Regulation of VEGF-A by the Unfolded Protein Response Pathway.* PloS one, 2010. **5**(3): p. e9575.
477. Marjon, P.L., E.V. Bobrovnikova-Marjon, and S.F. Abcouwer, *Expression of the pro-angiogenic factors vascular endothelial growth factor and interleukin-8/CXCL8 by human breast carcinomas is responsive to nutrient deprivation and endoplasmic reticulum stress.* Mol Cancer, 2004. **3**(4): p. 5670-5674.
478. Cao, Y., *Adipose tissue angiogenesis as a therapeutic target for obesity and metabolic diseases.* Nature reviews Drug discovery, 2010. **9**(2): p. 107-115.
479. West, D.B., et al., *Adipocyte blood flow is decreased in obese Zucker rats.* American Journal of Physiology-Regulatory, Integrative and Comparative Physiology, 1987. **253**(2): p. R228-R233.
480. Priebe, A., et al., *Glucose deprivation activates AMPK and induces cell death through modulation of Akt in ovarian cancer cells.* Gynecologic Oncology, 2011. **122**(2): p. 389-395.
481. Lee, A.S., *The glucose-regulated proteins: stress induction and clinical applications.* Trends in biochemical sciences, 2001. **26**(8): p. 504-510.
482. Hotamisligil, G.S. and E. Erbay, *Nutrient sensing and inflammation in metabolic diseases.* Nat Rev Immunol, 2008. **8**(12).
483. Xi, H., et al., *Endoplasmic reticulum stress induced by 2-deoxyglucose but not glucose starvation activates AMPK through CaMKKb leading to autophagy.* Biochemical Pharmacology, 2013. **85**(10): p. 1463-1477.
484. Mick, G.J., X. Wang, and K. McCormick, *White adipocyte vascular endothelial growth factor: regulation by insulin.* Endocrinology, 2002. **143**(3): p. 948-53.
485. Karpe, F., et al., *Impaired postprandial adipose tissue blood flow response is related to aspects of insulin sensitivity.* Diabetes, 2002. **51**(8): p. 2467-2473.
486. Trayhurn, P., *Hypoxia and Adipose Tissue Function and Dysfunction in Obesity.* Physiological reviews, 2013. **93**(1): p. 1-21.

487. Brahimi-Horn, M.C. and J. Pouyssegur, *Oxygen, a source of life and stress.* FEBS Letters, 2007. **581**(19): p. 3582-3591.
488. Rausch, M.E., et al., *Obesity in C57BL/6J mice is characterized by adipose tissue hypoxia and cytotoxic T-cell infiltration.* International journal of obesity, 2008. **32**(3): p. 451-463.
489. Wang, G.L. and G.L. Semenza, *General involvement of hypoxia-inducible factor 1 in transcriptional response to hypoxia.* Proceedings of the National Academy of Sciences, 1993. **90**(9): p. 4304-4308.
490. Semenza, G.L., *HIF-1: mediator of physiological and pathophysiological responses to hypoxia.* Journal of applied physiology, 2000. **88**(4): p. 1474-1480.
491. Ivan, M., et al., *HIF-alpha Targeted for VHL-Mediated Destruction by Proline Hydroxylation: Implications for O2 Sensing.* Science, 2001. **292**(5516): p. 464-468.
492. Masson, N., et al., *Independent function of two destruction domains in hypoxia-inducible factor-alpha chains activated by prolyl hydroxylation.* The EMBO journal, 2001. **20**(18): p. 5197-5206.
493. Jaakkola, P., et al., *Targeting of HIF-alpha to the von Hippel-Lindau Ubiquitylation Complex by O2-Regulated Prolyl Hydroxylation.* Science, 2001. **292**(5516): p. 468-472.
494. Salceda, S. and J. Caro, *Hypoxia-inducible factor 1alpha (HIF-1alpha) protein is rapidly degraded by the ubiquitin-proteasome system under normoxic conditions. Its stabilization by hypoxia depends on redox-induced changes.* J Biol Chem, 1997. **272**(36): p. 22642-7.
495. Ke, Q. and M. Costa, *Hypoxia-Inducible Factor-1 (HIF-1).* Molecular Pharmacology, 2006. **70**(5): p. 1469-1480.
496. BelAiba, R.S., et al., *Hypoxia up-regulates hypoxia-inducible factor-alpha transcription by involving phosphatidylinositol 3-kinase and nuclear factor kB in pulmonary artery smooth muscle cells.* Molecular biology of the cell, 2007. **18**(12): p. 4691-4697.
497. Conde, E., et al., *Hypoxia Inducible Factor 1-Alpha (HIF-1 Alpha) Is Induced during Reperfusion after Renal Ischemia and Is Critical for Proximal Tubule Cell Survival.* PloS one, 2012. **7**(3): p. e33258.
498. Zhang, P., et al., *The GCN2 eIF2a kinase is required for adaptation to amino acid deprivation in mice.* Molecular and Cellular Biology, 2002. **22**(19): p. 6681-6688.
499. Dar, A., T.E. Dever, and F. Sicheri, *Higher-order substrate recognition of eIF2alpha by the RNA-dependent protein kinase PKR.* Cell, 2005. **122**(6): p. 887-900.
500. Koumenis, C., et al., *Regulation of protein synthesis by hypoxia via activation of the endoplasmic reticulum kinase PERK and phosphorylation of the translation initiation factor eIF2alpha.* Mol Cell Biol, 2002. **22**(21): p. 7405-16.
501. Liu, Y., et al., *Regulation of G1 arrest and apoptosis in hypoxia by PERK and GCN2-mediated eIF2alpha phosphorylation.* Neoplasia, 2010. **12**(1): p. 61-68.
502. Papadakis, A., et al., *eIF2alpha kinase PKR modulates the hypoxic response by STAT-dependent transcriptional suppression of HIF-1a.* Molecular and Cellular Pathobiology, 2010. **70**(20).
503. Lopez-Hernandez, B., V. Cena, and I. Posadas, *The endoplasmic reticulum and HIF-1 signalling pathways are involved in the neuronal damage caused by chemical hypoxia.* British Journal of Pharmacology, 2015. **172**: p. 2838-2851.
504. Choi, S.J., et al., *Hypoxia Antagonizes Glucose Deprivation on Interleukin 6 Expression in an Akt Dependent, but HIF-1/2a Independent Manner.* PloS one, 2013. **8**(3): p. e58662.

505. Lolmede, K., et al., *Effects of hypoxia on the expression of proangiogenic factors in differentiated 3T3-F442A adipocytes.* Int J Obes Relat Metab Disord, 2003. **27**(10): p. 1187-95.
506. May, D., et al., *Ero1-L[alpha] plays a key role in a HIF-1-mediated pathway to improve disulfide bond formation and VEGF secretion under hypoxia: implication for cancer.* Oncogene, 2004. **24**(6): p. 1011-1020.
507. Gregoire, F.M., C.M. Smas, and H.S. Sul, *Understanding adipocyte differentiation.* Physiological reviews, 1998. **78**(3): p. 783-809.
509. Wood, I.S., et al., *Cellular hypoxia and adipose tissue dysfunction in obesity.* Proc Nutr Soc, 2009. **68**(4): p. 370-7.
510. Chen, B., et al., *Hypoxia dysregulates the production of adiponectin and plasminogen activator inhibitor-1 independent of reactive oxygen species in adipocytes.* Biochemical and biophysical research communications, 2006. **341**(2): p. 549-556.
511. Si, Y., J. Yoon, and K. Lee, *Flux profile and modularity analysis of time-dependent metabolic changes of de novo adipocyte formation.* American Journal of Physiology-Endocrinology and Metabolism, 2007. **292**(6): p. E1637-E1646.
512. Coleman, R. and R. Bell, *Triacylglycerol synthesis in isolated fat cells. Studies on the microsomal diacylglycerol acyltransferase activity using ethanol-disperse diacylglycerols.* J Biol Chem, 1976. **251**(15): p. 4537-4543.
513. McMillin, J. and W. Dowhan, *Cardiolipin and apoptosis.* Biochem Biophys Acta, 2002. **1585**(2-3): p. 97-107.
514. Lai, E., et al., *Differential activation of ER stress and apoptosis in response to chronically elevated free fatty acids in pancreatic beta-cells.* American Journal of Physiology-Endocrinology and Metabolism, 2008. **294**(3): p. E540-E550.
515. Schroepfer, G.J., *Oxysterols: modulators of cholesterol metabolism and other processes.* Physiological reviews, 2000. **80**(1): p. 361-554.
516. Harding, H.P., Y. Zhang, and D. Ron, *Protein translation and folding are coupled by an endoplasmic-reticulum-resident kinase.* Nature, 1999. **397**(6716): p. 271-274.
517. Palanivel, R. and G. Sweeney, *Regulation of fatty acid uptake and metabolism in L6 muscle cells by resistin.* FEBS Letters, 2005. **579**(22): p. 5049-5054.
518. Thumser, A. and J. Storch, *Characterisation of BODIPY-labeled fluorescent fatty acid analogue. Binding to fatty acid-binding proteins, intracellular localisation and metabolism.* Mol Cell Biochem, 2007. **299**(1-2): p. 67-73.
519. Maxfield, F.R. and D. Wustner, *Analysis of cholesterol trafficking with fluorescent probes* Methods Cell Biol, 2012. **108**: p. 367-393.